ELECTROPHYSIOLOGICAL CORRELATES OF SELF-MOTION PERCEPTION

THE ELECTROPHYSIOLOGICAL CORRELATES OF MULTISENSORY SELF-MOTION PERCEPTION

By BEN TOWNSEND, B.A. (hons.), M.A.

A Thesis Submitted to the School of Graduate Studies in Partial Fulfillment of the Requirements for the Degree Doctor of Philosophy

McMaster University

DOCTOR OF PHILOSOPHY (2022) McMaster University (Psychology)

TITLE: The electrophysiological correlates of multisensory self-motion perception

AUTHOR: Ben Townsend, B.A. (hons.) (University of Guelph), M.A. (Carleton University)

SUPERVISOR: Professor Judith M. Shedden

NUMBER OF PAGES: xx; 252

Lay Abstract

As we move through the environment, either by walking, or operating a vehicle, our senses collect many different kinds of information that allow us to perceive factors such as, how fast we are moving, which direction we are headed in, or how other objects are moving around us. Many of our senses take in very different information, for example, the vestibular system processes information about our head movements, while our visual system processes information about incoming light waves. Despite how different all of this self-motion information can be, we still manage to have one smooth perception of our bodies moving through the environment. This smooth perception of self-motion is due to our senses sharing information with one another, which is called multisensory integration. Two of the most important senses for collecting information about self-motion are the visual and vestibular systems. To this point, very little is known about the biological processes in the brain while the visual and vestibular systems integrate information about self-motion. Understanding this process is limited because until recently, we have not had the technology or the methodology to adequately record the brain while physically moving people in a virtual environment. Our team developed a ground-breaking set of methodologies to solve this issue, and discovered key insights into brainwave patterns that take place in order for us to perceive ourselves in motion. There were two critical insights from our line of research. First, we identified a specific brainwave frequency (beta oscillations) that indexes integration between the visual and vestibular systems. Second, we demonstrated another brainwave frequency (theta oscillation) that is associated with perceiving which direction we are headed in, regardless of which sense this direction information is coming from. Our research lays the foundation for our understanding of biological processes of self-motion perception and can be applied to diagnosing vestibular disorders or improving pilot simulator training.

Abstract

The perception of self-motion draws on inputs from the visual, vestibular and proprioceptive systems. Decades of behavioural research has shed light on constructs such as multisensory weighting, heading perception, and sensory thresholds, that are involved in self-motion perception. Despite the abundance of knowledge generated by behavioural studies, there is a clear lack of research exploring the neural processes associated with full-body, multisensory self-motion perception in humans. Much of what is known about the neural correlates of self-motion perception comes from either the animal literature, or from human neuroimaging studies only administering visual self-motion stimuli. The goal of this thesis was to bridge the gap between understanding the behavioural correlates of full-body self-motion perception, and the underlying neural processes of the human brain. We used a high-fidelity motion simulator to manipulate the interaction of the visual and vestibular systems to gain insights into cognitive processes related to self-motion perception. The present line of research demonstrated that theta, alpha and beta oscillations are the underlying electrophysiological oscillations associated with self-motion perception. Specifically, the three empirical chapters combine to contribute two main findings to our understanding of self-motion perception. First, the beta band is an index of visual-vestibular weighting. We demonstrated that beta event-related synchronization power is associated with visual weighting bias, and beta event-related desynchronization power is associated with vestibular weighting bias. Second, the theta band is associated with direction processing, regardless of whether direction information is provided through the visual or vestibular system. This research is the first of its kind and has opened the door for future research to further develop our understanding of biomarkers related to self-motion perception.

Acknowledgments

My journey through graduate school will likely be the most influential and character-developing experience of my life. I have had the privilege of working in some of the most unique and technologically-advanced labs in the world, with some of the most talented people I have ever met. Having access to high-fidelity motion simulators to study the brain is unfathomably rare, and I was fortunate enough to stumble upon two different labs that offered me this opportunity. It is difficult for me to put into words how appreciative I am for these opportunities, but there are so many people who deserve thanks for the existence of this thesis, so I will try.

I remember being a fourth-year undergrad at the University of Guelph, and applying to eight different master's programs because I was so anxious about not getting accepted (I would like to thank and apologize to my referees for having to write so many letters of recommendation!). The wait between sending in my applications and hearing back from graduate programs was excruciating. I didn't know how I compared to all of the other applicants, and I didn't know which city I would be living in within the next few months. The wait finally ended after four months, when I received an acceptance email, and I felt like I could finally breathe again.

My graduate journey, and introduction into this unique field of research began at Carleton University, under the supervision of Dr. Chris Herdman. This was the most impressive research facility I had ever seen. There were so many multimillion-dollar flight simulators, and the lab was in partnership with organizations such as the Canadian Space Agency, Canada Search and Rescue, and the like. I was incredibly intimidated. These feelings of intimidation did not last long however, as Chris' calm demeanor influenced me (as it does with all of his graduate students) to realize that I actually was capable of working with such high-tech equipment, and

that I was not an imposter. I want to thank Chris for helping me believe in myself, and laying the foundation of my knowledge that would ultimately lead to me achieving this Ph.D. I also need to thank Chris for landing me the coolest job listed on my resume: Research Student for the Canadian Space Agency.

I absolutely loved my time at Carleton, but by the end of my master's program, I found myself most interested in the biological processes going on in my participants' brains when they were completing tasks in our simulated environments. I cannot express how few laboratories in the world are capable of exploring that question. This is when blind luck played a major component in my journey. I applied to two labs at McMaster University for my Ph.D., neither of which were the lab I ultimately ended up joining. Fortunately for me, I was invited to McMaster's recruitment weekend, where I had the honour of meeting many professors in the PNB department. I was primarily there to visit Dr. Hong Jin Sun, as his lab was my main interest. During the interview segment of that weekend, I met with Dr. Judy Shedden, who showed me her motion simulator lab. A lab I had not applied to, nor was I aware of. Her team had just started a new research program exploring the EEG correlates of self-motion perception. This was literally the perfect fit for my research interests and I didn't even have to move to a different country (I was considering it). I remember feeling guilty for not joining Dr. Sun's lab, as I enjoyed my visit with him, and was really excited about the research possibilities that would come with joining his lab. I would like to thank Dr. Sun for handling that situation with such grace, and agreeing to be a part of my graduate committee. Your research was what drew me to McMaster in the first place, and you have contributed invaluable guidance during my time as a Ph.D. student.

Once again, this new line of research that I had just committed to was intimidating, and my sense of imposter syndrome had returned. I had no previous experience recording the brain, and now I was tasked with developing a research program that recorded the brain while physically moving people around in a motion simulator; a challenge that only a handful of labs around the world had accomplished. Our core research team included Dr. Judy Shedden, Dr. Martin von Mohrenschildt, Joey Legere, Dr. Shannon O'Malley, and myself. I could not have asked for a more supportive, team-oriented, and brilliant group of scientists to belong to. We worked together cohesively to accomplish something truly special, and we need to celebrate that.

Each team member played a unique and critical role in this line of research. Shannon, you were the leader of our office space. You were a perfect role model for every graduate and undergraduate student who worked in our lab. I cannot thank you enough for showing me what professionalism looks like behind the scenes, and for taking the time to bounce ideas off of one another. It meant a lot to me and it contributed to the quality of our research. Martin, working with you taught me so much about how to communicate with someone from a different field of study. I have taken this lesson and applied it to my positions in industry, and it has helped me tremendously in working with multidisciplinary teams, and just being an overall better communicator. You are the brains behind our simulator, and bring our ideas to life, without you none of this research would be possible. Joey, I have never worked with someone whose skillset is so different from mine, yet compliments it so perfectly. We were (and still are) an incredible team. Your contributions to our EEG analysis were invaluable, and I don't know if we would have been able to find someone with such unique abilities as yours. I consider you one of my best friends, and I am so glad we still have the ability to get together (for whoever is currently reading this: sometimes Joey and I put together dinners for our friends and they are basically like

fine dining menus. It's actually quite remarkable!). Judy, I have you to thank the most for my success in this program. When I entered the lab, I had so much to learn. I felt like I was behind, and out of place because I had no previous neuroimaging experience, nor had I ever programmed my own experiment. First, I need to thank you for being so patient and allowing me to develop the necessary skills before tackling the more difficult challenges ahead. You are one of the most empathetic people I have ever met. Every step of building this research program was incredibly difficult, and without feeling like I was safe to learn and make mistakes, I don't think I would have lasted in this program. Second, it is notable how different all of the Ph.D. projects were in your lab (seriously, in what other world would Nicole and I be in the same lab?). I think this clearly shows how encouraging you are as a supervisor and that you truly want every student to follow their own research interests, even if it leads them outside of your own expertise. Thank you for having the strength to trust your students and allowing them to take complete ownership over projects that might have been less than comfortable for you. In my opinion, that is the sign of an incredible leader.

Finally, I believe that without support from outside of academia, very few people would be able to complete a Ph.D. program. Growing up with a supportive family, having a tight-knit group of friends, and attending three universities, I have been so lucky to meet many amazing people. My family and friends have shown unconditional support and patience for me while I have been away pursuing my dreams. I am so thankful to have such wonderful people in my life. Every single member of my family and friends has in some way, made me who I am today and helped me endure this demanding program.

Table of Contents

Lay Abstract iii

Abstract iv

Acknowledgments v

Table of Contents ix

Preface xvi

List of Figures xviii

List of Tables xx

CHAPTER 1: Introduction 1

Defining Self-Motion Perception 4

Reference Frames 4

Egocentric Reference Frames 6

Allocentric Reference Frames 8

Visual Self-Motion Perception 10

Physiology 10

Visually-Induced Vection 13

Body-Based Self-Motion Perception 15

Physiology – The Vestibular System 15

Semicircular Canals 16

Otolith 17

Vestibular Nucleus 17

Proprioceptive System 18

Muscle Spindles 18

Stimulating the Vestibular System 20

Galvanic Vestibular Stimulation 20

Caloric Vestibular Stimulation 21

Sound Induced Vestibular Stimulation 22

Vestibular Stimulation Through Body-Based Motion 24

Rotatory Chairs 24

Motion Platforms 25

Visual-Vestibular Integration 29

Selective Attention 32

Selective Attention in Multisensory Integration 37

Stimulus-Driven Attention 38

Goal-Directed Attention 39

Selective Attention in Pilot Training 41

Neural Imaging Studies of Self-Motion Perception in Humans 43

Issues Related to Recording the Brain During Full-Body Motion 43

Potential Sources of Artifacts 45

Vestibulo-Ocular Reflexes 46

Vestibulo-Spinal Reflexes 47

Avoiding EOG and EMG Artifacts 48

Electrophysiological Oscillations Related to Sensorimotor Processing 49

Theta-Band Oscillations 49

Alpha-Band Oscillations 52

Beta-Band Oscillations 54

Beta Rebound 55

Gamma-Band Oscillations 57

Issues Localizing EEG Signals 58

Independent Components Analysis 60

Measure Projection Analysis 64

Overview of Empirical Chapters 66

CHAPTER 2: Attention Modulates Event-Related Spectral Power in Multisensory Self-Motion Perception 68

Preface 68

Abstract 70

Introduction 71

Materials and Methods 75

Participants 75

Data and code availability 75
Stimuli 75
Visual-motion stimuli 75
Physical-motion stimuli 76
Experimental Design and Behavioural Analyses 79
Procedure 79
EEG Data Acquisition 80
EEG Preprocessing 81
ERSP Measure Projection Analysis 82
Stimulus Validation 83
Results 84
Behavioural Results for Total Sample 84
High-vs. Low-Accuracy Group Comparison 85
Behavioural Results for High-vs. Low-Accuracy Groups 85
Oscillatory Power (ERSP) for High-vs. Low-Accuracy Groups 88
Results for High-Accuracy Group 92
Behavioural Results (High-Accuracy Group) 92
Oscillatory Power (ERSP) for High-Accuracy Group 93
Discussion 98
Beta Oscillations in Physical Motion Processing 98
Alpha Oscillations in Motor Processing 101
Theta Oscillations in Sensorimotor Integration 103

Limitations of the Present Study 106

Conclusion 107

Appendix 109

CHAPTER 3: Beta-Band Power is an Index of Multisensory Weighting During Self-Motion Perception 113

Preface 113

Abstract 115

Introduction 116

Materials and Methods 121

Participants 121

Stimuli 121

Visual-Motion Stimuli 122

Physical-Motion Stimuli 122

Procedure 125

EEG Data Acquisition 125

EEG Preprocessing 125

ERSP Measure Projection Analysis 126

Data and Code Availability 128

Results 129

Behavioural Results 129

Oscillatory Power 129

Power differences between modalities 130

Power differences between headings 131

Discussion 134

Beta Oscillations 135

Theta ERS 138

Alpha ERD 140

Limitations and Future Directions 142

Conclusion 143

Appendix 144

CHAPTER 4: Stimulus Onset Asynchrony Affects Weighting-Related ERSP in Self-Motion Perception 146

Preface 146

Abstract 148

Introduction 150

Materials and Methods 154

Participants 154

Stimuli 154

Visual-Motion Stimuli 154

Physical-Motion Stimuli 155

Procedure 158

EEG Data Acquisition 159

EEG Preprocessing 159

ERSP Measure Projection Analysis 160
Data and Code Availability 162
Results 162
Behavioural Results 162
Accuracy 162
Response Time 163
Oscillatory Power 164
Effects of SOA in Attend-Visual task 164
Effects of SOA in Attend-Physical task 167
Effects of Attention Allocation Across SOA Conditions 169
Discussion 171
The Effects of Timing Onset Within an Attended Modality 171
The Interaction of Stimulus Timing and Attentional Selection 173
Feature-Binding Gamma ERS in Visual-Vestibular Integration 175
Conclusion 176
Appendix 178
CHAPTER 5: General Discussion 180
Visual-Vestibular Weighting 183
Heading Processing and Theta Oscillations 192
Cognitive Demands and Alpha Oscillations 194
Future Direction 196

Conclusion 200

References 203

Preface

This is a "sandwich thesis", meaning that the empirical chapters are all stand-alone publications that are either published or submitted for publication. Chapters 2 and 3 are published in peer-reviewed journals, and Chapter 4 is submitted for publication in a peer-reviewed journal. For each of these empirical chapters, I am the first author. For Chapter 2, my collaborators Joey Legere, Shannon O'Malley, and Martin von Mohrenschildt are second, third and fourth authors, respectively, and my supervisor, Dr. Judith Shedden, is the final author. For Chapters 3 and 4, my collaborators are Joey Legere, Martin von Mohrenschildt and Judith Shedden, respectively. My contributions to each of these manuscripts are outlined below.

The first empirical chapter (Chapter 2) is a reprint of Townsend, B., Legere, J., O'Malley, S., v. Mohrenschildt, M., & Shedden, J. M. (2019). Attention modulates event-related spectral power in multisensory self-motion perception. *NeuroImage, 191*, 68-80. My role in the manuscript included experimental design, data collection from human participants, and data analysis. I was also the primary writer.

The second empirical chapter (Chapter 3) is a reprint of Townsend, B., Legere, J., v. Mohrenschildt, M., & Shedden, J. M. (2022). Beta-band power is an index of multisensory weighting during self-motion perception. *NeuroImage: Reports, 2*, 100102. My role in the manuscript included experimental design, data collection from human participants, and data analysis. I was also the primary writer.

The third empirical chapter (Chapter 4) is the following manuscript: Townsend, B., Legere, J., v. Mohrenschildt, M., & Shedden, J. M. (Submitted). Stimulus onset asynchrony

affects weighting-related ERSP in self-motion perception. *Journal of Cognitive Neuroscience*. Manuscript ID: JOCN-2022-0167. My role in the manuscript included experimental design, data collection from human participants, and data analysis. I was also the primary writer.

Note that, because these manuscripts are intended to be standalone publications, there will be some redundancy within the introductions, methods and discussions of these chapters. Despite this overlap, each chapter contains unique experiments intended to answer different theoretical questions, all of which are related to the common issues presented in this thesis.

List of Figures

CHAPTER 1

Figure 1. Motion simulator 28

Figure 2. Heatmaps of EOG and EMG. 63

CHAPTER 2

Figure 1. Time course of physical- and visual-motion stimuli. 78

Figure 2. MPA (Measure Projection Analysis) domains for low-accuracy and high-accuracy participants. 87

Figure 3. Left motor areas identified by MPA and their respective ERSP analysis for low-accuracy and high-accuracy participants. 91

Figure 4. Left and right motor area identified by MPA and respective ERSP analysis in high-accuracy participants. 95

Figure 5. Left and right occipital area identified by MPA and respective ERSP analysis in high-accuracy participants. 97

Figure A1. Motion simulator 109

Figure A2. EEG analysis pipeline 110

Figure A3. Left and right motor areas identified by MPA and their respective ERSP analysis for low-accuracy participants. 111

Figure A4. Left and right occipital area identified by MPA and respective ERSP analysis in low-accuracy participants. 112

CHAPTER 3

Figure 1. Time course of physical- and visual-motion stimuli. 124

Figure 2. Left motor area and right motor area identified by MPA and respective ERSP analysis. 132

Figure A1. Motion simulator 144

Figure A2. EEG analysis pipeline 145

CHAPTER 4

Figure 1. Time course of physical- and visual-motion stimuli. 157

Figure 2. Attend-Visual Task: Left motor area and right motor area identified by MPA and respective ERSP analysis. 166

Figure 3. Attend-Physical Task: Left motor area and right motor area identified by MPA and respective ERSP analysis. 168

Figure 4. Right motor area identified by MPA and respective ERSP analysis. 170

Figure A1. Motion simulator 178

Figure A2. EEG analysis pipeline 179

List of Tables

CHAPTER 2

Table 1. Behavioural means. 93

CHAPTER 1: Introduction

Motion simulators are valuable tools for training pilots and drivers. Training in a simulator is inherently safe and particularly safer for novices and those training for dangerous situations (e.g., flying in turbulence, driving in heavy traffic). Decades of research has shown that augmenting in-aircraft training with simulator training improves training effectiveness, more so than aircraft-only training (for review see, de Winter, Dodou & Mulder, 2012). Many high-fidelity flight and drive simulators incorporate full-body motion, typically with a motion platform that engages the vestibular, proprioceptive and tactile systems. Although the effectiveness of flight simulators for pilot training is well established, the need for a physical-motion system remains a topic of debate. On one hand, pilots have shown almost a unanimous subjective preference for platform motion (Miletović et al., 2017), and there is a small body of literature that has shown platform motion to improve performance on specific tasks involving disturbance motion (de Winter et al., 2012; O'Malley, Rajagobal, Grundy, Mohrenshildt & Shedden, 2016). On the other hand, there is little scientific evidence to suggest that adding physical motion to pilot training improves overall training effectiveness beyond visual-only simulations (McCauley, 2006). Moreover, estimated costs to construct and maintain a high-fidelity flight simulator with platform motion are approximately $10 million USD over the lifetime of the simulator (Parsons, 2019).

With the advancements in scientific methods and technology, researchers have recently taken a different approach to solving this debate. Many researchers are exploring the underlying cognitive and sensory processes that play a role in how humans perceive sensory cues provided by motion simulators, whether that be with psychophysical tasks (e.g., the vestibular just noticeable difference task), or more applied tasks you might find in pilot training programs (e.g.,

recovering from an unusual attitude). Of all the cognitive and sensory processes relevant to pilot and driver training and performance in motion simulators, self-motion perception is a concept that has been heavily studied (for review see, Greenlee et al., 2016). This is unsurprising because flying an aircraft or driving a ground vehicle involves operator perception of self-motion through the surrounding environment.

Although there is a very large body of literature exploring self-motion perception, there is currently a gap in the literature related to two different branches of research that would benefit from convergence – the neural correlates of self-motion perception and the behavioural correlates of multisensory self-motion perception. The neural correlates of self-motion perception relate to the online processes engaged when an organism perceives itself to be moving through its environment. Extensive research has been conducted in this area involving non-human primates (e.g., Mackrous, Carriot, Cullen & Chacron, 2020), however less is known about the online processes related to human self-motion perception, particularly multisensory processes that engage the vestibular and proprioceptive systems. This lack of research is due to technological and methodological limitations. Most human neuroimaging techniques (e.g., functional magnetic resonance imaging [fMRI], positron emissions tomography [PET] and electroencephalography [EEG]) require the participant to be relatively immobile during testing, and are poorly equipped to record signals from the brain if participants are being physically moved. Researchers using these neuroimaging techniques to study self-motion perception have typically relied on visual displays (optic flow; e.g., Kovács, Raabe & Greenlee, 2008). These studies are invaluable to our understanding of visual self-motion perception, however, in everyday life, self-motion perception is naturally a multisensory phenomenon that usually engages more than just the visual system. Therefore, studies exploring visual self-motion

perception are explaining only part of the story. As we will discuss in the following sections of this introduction chapter, combining visual cues to motion with physical cues that engage the vestibular and proprioceptive systems is critical to fully understanding the neural processes underlying human self-motion perception.

There have been many studies that have explored the multisensory nature of self-motion perception (e.g., Kenney et al., 2020). These studies have covered topics such as visual-vestibular weighting in multisensory integration (Fetsch, Turner, DeAngelis & Angelaki, 2009), multisensory integration in aging (Kenney, Jabbari, von Mohrenschildt & Shedden, 2021), and the effects of multisensory cues on flight task performance (O'Malley et al., 2016). Thus far, multisensory research related to self-motion perception has typically been behavioural, particularly research engaging the vestibular and proprioceptive systems, due to the technological issues discussed above. There has been a recent push to use commercial mobile EEG systems with relatively few electrodes to record cortical oscillations while participants walk or ride stationary bicycles (e.g. Storzer et al., 2016). Fully-mobile EEG systems (e.g., TMSi, Enschede, Netherlands; Muse, Toronto, Canada), however, have only been shown to capture large ERP components such as the P_3 or prominent ERSP such as alpha waves (Storzer et al., 2016). Researchers have also attempted to solve this issue by stimulating the vestibular system with techniques like galvanic vestibular stimulation or caloric vestibular stimulation, in combination with visual-motion stimuli while recording the brain using fMRI or PET (e.g., Fink et al., 2003). This technique works well for simulating simple physical movements like swaying to the left or right. It is difficult, however, to know precisely which angle the participant experienced movement, and if this simulated physical motion synchronized spatially with the

visual stimulus. To date, the only way to precisely control for spatial synchrony between visual and physical cues to motion is to use inertial full-body motion.

The current gap in the literature, as discussed above, reflects the need for full-body motion to precisely stimulate the vestibular and proprioceptive systems and the challenge of simultaneously recording neural responses with required spatial resolution to estimate neural generators. The following subsections of this chapter will review the few attempts at recording brain responses during physical full-body motion. For many of these studies there were challenges in achieving high quality data. The current line of research discussed in this dissertation aims to bridge the gap between neuroimaging studies that typically present visual-only self-motion stimuli and behavioural studies that combine platform motion with visual cues to self-motion. The experiments described in the following data chapters recorded EEG while presenting self-motion cues in a virtual environment mounted on a Stewart motion platform with 6 degrees of freedom motion, with visual and physical full-body cues to motion. Participants were asked to complete heading discrimination tasks which allowed us to observe cortical oscillations related to attention and visual-vestibular integration during self-motion perception. To set the context for these data chapters, this introduction chapter will define self-motion perception, review what is currently known about the neural processes related to self-motion perception, and present a detailed discussion about the appropriate methods to collect and analyze EEG data recorded while participants experience full-body physical motion.

1.1 Defining Self-Motion Perception

1.1.1 Reference Frames

Spatial navigation is a critical function in the everyday lives of all mobile organisms. It is important for goals such as finding food, finding mates, and escaping predators. Self-motion

perception plays a critical role in spatial navigation for organisms that need to understand how their own movements affect their location and orientation within the surrounding environment. Much of what we currently understand about spatial navigation and associated neural correlates was built upon rodent research (O'Keefe, 1979). A large body of research suggests that three distinct types of cells in the hippocampus and surrounding areas encode location information (place and grid cells), and directional information (heading direction cells; for review see O'Keefe, 1979). Research involving human participants points to these processes taking place in similar brain regions to those of rodents (Jacobs et al., 2013; Vass & Epstein, 2013). The aforementioned cells work together, such that if the organism's direction changes, heading direction cells sensitive to the new heading will be more active instead of cells sensitive to the previous heading. This shift in firing from the heading direction cell network modulates the firing of place cells. Individual place cells are sensitive to the organism's location within the environment. In other words, while the organism is located in a specific area, specific place cells sensitive to being in that location will be more active, while place cells sensitive to being in a different location will be less active. These differences in location sensitivity are called place fields, which allow organisms to form a cognitive map of the environment. Heading direction cells modulate place-cell firing such that changes in heading lead to changes in heading direction cell responsivity, which causes place fields to rotate by a corresponding amount. Researchers have described this function of heading direction cells as supporting an internal compass that represents an organism's heading (i.e., the direction it faces), which updates as the organism moves through the environment (Marchette, Vass, Ryan & Epstein, 2014). An internal compass, however, is not useful for self-motion perception and spatial navigation unless the heading coordinates are defined relative to fixed features of the environment (i.e., landmarks). Research

has shown that this assumption is, in fact, the case (Marchette, Vass, Ryan & Epstein, 2014). Heading direction, place, and grid cells combine the organism's perceived orientation relative to visual landmarks, in order to anchor its sense of direction, which can then be maintained dynamically through first-person visual cues to self-motion (Valerio & Taube, 2012). In order for this process to occur, the organism must be able to separate its own sense of heading direction from the relative position of environmental landmarks. For example, it must be possible to distinguish between a change in heading direction and the representation of the location of a landmark, which does not necessarily move in space. This hypothesis has guided research exploring egocentric and allocentric reference frames (Marchette, Vass, Ryan & Epstein, 2014), which will be discussed in the following sub-sections. I acknowledge that there are some conceptual issues around egocentric and allocentric reference frames. Some previous literature has characterized these reference frames as representing distinct processes despite there being evidence of egocentric and allocentric reference frames working in parallel or in a hierarchical relationship (for review see Meilinger & Vosgerau, 2010). The relationships between egocentric and allocentric reference frames typically become more complex as the environment becomes more complex.

1.1.1.1 Egocentric Reference Frames

Actions such as reaching for an object, or estimating the distance between self and the next turn while walking or driving, require egocentric reference frames (for review see, Klatzky, 1998). Egocentric reference frames involve reference to the organism's current body position relative to external objects in the environment. Humans typically employ egocentric reference frames to avoid collisions with objects and navigating their immediate space (Wang & Spelke, 2000). A popular theory proposed by Burgess, Spiers and Paleologou (2004) posits that

information about distances and angles from the self to each object in the environment is coded independently. This information has to be dynamically updated after every movement (e.g., steps, neck movements) by adjusting the displacement vector of each environmental object relative to the organism. This system creates a perception where the environment is constantly changing while the organism remains spatially fixed in the center of the reference system. However, in complex environments that require navigating through very large spaces (Souman, Frissen, Sreenivasa & Ernst, 2009), or that introduce spatial disorientation (Waller & Hodgson, 2006), egocentric reference frames may not be sufficient and other spatial representations such as allocentric reference frames become necessary.

Egocentric reference frames are usually associated with the posterior parietal cortex in both human and non-human studies (Committeri, 2004). Monkey studies have identified neurons in the posterior parietal cortex and in connected regions of the premotor cortex that code spatial position relative to body parts (Cohen & Andersen, 2002; Colby, 1998). Human neuropsychological studies have shown that patients with lesions to the posterior parietal cortex can have difficulty guiding their hands towards external objects during reaching tasks (e.g., Perenin & Vighetto, 1988). Moreover, in unilateral neglect patients, the neglected sector of space is usually defined by an egocentric reference frame (Bisiach, 1997; Vallar, Guariglia, & Rusconi, 1997). Neuroimaging studies have also provided support for the involvement of parietal–frontal cortex in the egocentric coding of space in non-clinical human participants. A posterior parietal–frontal premotor network increases activation when visual stimuli, such as landmarks, are processed with respect to the body's midsagittal plane (Vallar et al., 1999). This parietal-frontal premotor activation occurs for both tactile and visual stimuli (Galati, Committeri, Sanes, &

Pizzamiglio, 2001), and is far more robust than when an allocentric-based judgement is performed on the same stimuli (Galati, Lobel, et al., 2000).

1.1.1.2 Allocentric Reference Frames

The importance of allocentric reference frames for spatial navigation was first demonstrated in rodents during the formation of cognitive maps (Tolman, 1948). An allocentric reference frame is referenced to multiple landmarks within the visual scene, discrete from an organism's current body position. This generally involves a minimum of three landmarks in two-dimensional space due to the need to define a plane in X–Y space (Ekstrom & Isham, 2017). Alternatively, Klatzky (1998) demonstrated that an environmental boundary and landmark can also create a strong allocentric reference frame because a point (landmark) and a line (boundary) can also define a two-dimensional plane. One commonly-used exercise to demonstrate an allocentric reference frame is to draw a cartographic map of an environment. Drawing a map is not possible without accurate representations of the relative distances and directions of fixed landmarks (Zhang, Zherdeva & Ekstrom, 2014). Another common task to test allocentric reference frames is judgments of relative direction (JRD; e.g., Waller & Hodgson, 2006). This task requires participants to imagine themselves standing at one location, facing a second location, and pointing to a third location.

Allocentric reference frames do not necessarily require landmarks. Mou, Zhao and McNamara (2007), demonstrated that visible boundaries of an environment are all that is necessary to produce a powerful cue for organizing an externally referenced cognitive map. More specifically, it was found that while performing the JRD task, participants pointed more accurately when their sagittal plane was parallel with the major axis of the surrounding environmental boundaries, compared to when they were misaligned with the same axes. This

finding has been replicated several times under different environmental conditions (Chan, Baumann, Bellgrove & Mattingley, 2013; Frankenstein, Mohler, Bülthoff & Meilinger, 2012; Richard & Waller, 2013), suggesting that, contrary to previous belief (Klatzky, 1998; O'keefe & Nadel, 1978), the surrounding spatial geometry defined by environment boundaries may play a larger role in developing allocentric reference frames than landmarks.

Cells with allocentric properties have been uncovered in the hippocampal areas of monkeys (Rolls & O'Mara, 1995), humans (for review see, Epstein, Patai, Julian & Spiers, 2017), and freely-moving rats (O'Keefe & Dostrovsky, 1971). Moreover, lesions to the hippocampal area in humans are generally accompanied by difficulties in memory storage and/or recall of spatial location and identity of landmarks in both new and/or learned environments (Aguirre & D'Esposito, 1999). The retrosplenial cortex is also activated when participants complete tasks requiring allocentric reference frames. This result has been demonstrated in rats (Chen, Lin, Green, Barnes, & McNaughton, 1994), and humans (Epstein & Kanwisher, 1998). Human participants with retrosplenial lesions have been shown to be unable to orient themselves to a goal location if heading information is withdrawn during spatial navigation tasks (Aguirre & D'Esposito, 1999). Place cells are typically thought to respond to allocentric information in both humans and non-humans. Ground breaking research by O'Keefe and Dostrovsky (1971) showed that hippocampal place cells are sensitive to particular locations in the cognitive map. Place cells are not sensitive to specific heading directions, the previous location of the organism, or current body movements.

Spatial navigation can be an incredibly complex task that requires a combination of egocentric and allocentric references frames in order to arrive at the goal location. For example, the seemingly simple task of driving to work requires a knowledge of the spatial location of

landmarks along the way, and their relative distance from one another, in order to form a cognitive map of the path (allocentric information). Next, one must continually update self-motion information such as heading direction and velocity (egocentric information) to be able to process where they are within that cognitive map, in order to arrive at the target location (work). Although allocentric reference frames rely primarily on vision (with respect to human spatial navigation), egocentric reference frames can be more multisensory (Marsh & Hillis, 2008; Town, Brimijoin & Bizley, 2017), engaging the auditory (Town et al., 2017), vestibular (Pavlidou, Ferrè & Lopez, 2018), tactile (Marsh & Hillis, 2008; Yang & Kim, 2004), and proprioceptive (Yang & Kim, 2004) systems. The present line of research is primarily interested in multisensory self-motion perception, from an egocentric frame of reference. Given the simple self-motion stimuli used in our series of experiments, we suggest that interpretation of our results can assume that participants are operating within an egocentric reference frame. We administer visual and physical (vestibular, proprioceptive and tactile stimulation) cues to self-motion and ask participants to judge heading directions relative to their body position. Visual, vestibular and proprioceptive self-motion perception within egocentric reference frames is of the greatest interest to us. These sensory systems will be reviewed in the following sub-sections.

1.1.2 Visual Self-Motion Perception

1.1.2.1 Physiology

Several networks in the human cortex are sensitive to visual self-motion. Most of these regions are situated along the dorsal visual pathway, which includes the striate cortex (V1), several extrastriate areas including V3A and MT/V5, and higher areas of the temporal and parietal lobes (Palmisano, Allison, Schira & Barry, 2015). Functional neuroimaging studies (primarily fMRI) have attempted to identify the neural correlates of visual self-motion perception

by examining the brain activity generated by visual optic flow (e.g., Beer, Blakemore, Previc & Liotti, 2002; Wall & Smith, 2008). It is important to note that the studies discussed in this section do not incorporate physical motion that stimulates the vestibular system (studies that use methods such as caloric vestibular stimulation are discussed in Section 1.1.4). The majority of these studies have examined areas sensitive to coherent optic flow versus different types of control stimuli. Unfortunately, the collective results of this body of literature are difficult to interpret due to the diversity of control stimuli. For example, some studies have used random (incoherent) dot motions (e.g., Cardin & Smith, 2010), static dot patterns (e.g., Tokumaru, Kaida, Ashida, Yoneda & Tatsuno, 1999; Deutschländer et al., 2004), or spatially scrambled versions of the original self-motion stimulus (e.g., Barry et al., 2014b).

An alternative approach to identifying brain regions that process visual self-motion information has been to compare neural responses to periods when vection is, versus is not elicited by the same visual displays of self-motion (e.g., Brandt, Bartenstein, Janek & Dieterich, 1998; Kleinschmidt et al., 2002; Kovács et al., 2008). The experience of illusory vection can be illustrated by imagining an optic flow star field. During the illusion of vection, the participant experiences the sense of self-motion through the field, whereas when the illusion of vection is lacking, the participant experiences the stars as objects moving past them. Illusory vection is measured by self-report. This approach has two key advantages compared to the previously discussed experimental designs. First, the experimenter can be more confident that the stimuli actually elicited vection, as opposed to making an assumption. Second, this allows researchers to use identical stimuli between conditions, which controls for any visually-induced differences due to stimulus features unrelated to self-motion perception. This symmetry controls for the potential confound that different visual stimuli may simply be inducing different neural responses earlier

in the visual processing line. This potential confound could mean that the differences found in brain activity may be due to irrelevant dimensions of the stimuli rather than visual self-motion processing (Palmisano et al., 2015).

The previously discussed experimental approaches have identified several cortical areas associated with visual self-motion processing. These brain regions include the medial temporal area (MT/V5), the medial superior temporal (MST) area and its dorsal subdivision (MSTd), the dorsomedial area (V6), the ventral intraparietal area (VIP) and the cingulate sulcus visual area (CSv; Palmisano et al., 2015). There is a strong possibility that the network processing self-motion information is highly distributed, however, there are also reasons to doubt that the network is as complex as some believe. First, the findings within this body of literature have been inconsistent, resulting in considerable disagreement about the involvement of multiple brain regions in visual self-motion processing (e.g., MST/MSTd; Kleinschmidt et al., 2002; Morrone et al., 2000; Wall & Smith, 2008). Second, there are very few studies that have directly compared neural responses to different types of optic flow. For example, during visual self-motion, an organism can be presented with spiral, translational, radial, and circular patterns of optic flow. Most neuroimaging studies only use one pattern of optic flow, and the types of flow examined have varied from study to study (e.g., Brandt et al., 1998; Kleinschmidt et al., 2002; Tokumaru et al., 1999; Wall & Smith, 2008). Given the varying results, it is difficult to understand whether different brain areas are responsive to different types of optic flow stimuli, or if other methodological factors between studies played a role in the inconsistent findings. Third, different neural activity for optic flow versus control displays does not necessarily provide evidence for self-motion processing. It is possible that in some studies, differences in neural activity might have been generated by different irrelevant stimulus features. For example,

Tokumaru et al. (1999) found different cortical activation for optic flow compared to a static control. This may be evidence for cortical self-motion processing but it could simply be showing differences in the processing of moving versus stationary versions of the same stimulus. Finally, many studies that investigated visual self-motion did not check whether their displays induced vection during scanning (e.g., Cardin & Smith, 2010; de Jong, Shipp, Skidmore, Frackowiak & Zeki, 1994). Of the few studies that tested their stimuli for the induction of vection, this was typically done in a separate environment from the fMRI or PET scanners. These environments often used larger displays and/or longer durations of optic flow stimuli (Palmisano et al., 2015). Only a few studies measured the induction of vection within the scanner (e.g., Brandt et al., 1998; Kleinschmidt et al., 2002; Kovács et al., 2008), so it is unclear which of the neuroimaging experiments conducted to date actually induced vection during the experiment.

The visual system is an incredibly complex network that subsumes a large portion of the human brain. Visual self-motion processing is only one complex component of the visual system that interacts with the vestibular system, and presents many challenges for scientists to fully understand it. Although there still remains controversy about exactly which neural structures contribute to this process, and in which ways, it seems that structures within the dorsal visual pathway are predominantly responsible for visual self-motion perception, including networks around the temporal-parietal junction and motor cortex (Palmisano et al., 2015)

1.1.2.2 Visually-Induced Vection

Self-motion can be perceived without the vestibular and/or the proprioceptive systems being stimulated. As long as other sensory systems (most typically the visual system) perceive the changes that would be expected from being rotated or translated through the environment, the organism will likely experience self-motion perception (Burki-Cohen et al., 2007). This

perception of real or illusory full-body motion is known as vection. Wong and Frost (1978) demonstrated vection in a series of experiments. After being presented with rotational optic flow for 30 seconds, without any vestibular stimulation, participants reported the experience of self-motion. Some researchers cite long latencies to detect vection, such as Wong and Frost (1978), as evidence that vection is not necessarily relevant to the participant's behaviour (Palmisano et al., 2015). These long latencies, however, are only demonstrated when multisensory self-motion cues create conflict between the senses. For example, visually-induced vection (both real and illusory) can be induced much faster if presented with congruent multisensory information (Berger, Schulte-Pelkum & Bülthoff, 2010) or when the visual stimulus is of a high fidelity (e.g., a full-scale moving room; Allison, Howard & Zacher, 1999). Several other studies within the field of cognitive psychology have uncovered factors that lead to the production and/or enhancement of vection. Dichgans and Brandt (1978) demonstrated that the subjective experience of vection can be enhanced as objects move faster in visual scenes. Furthermore, the field of view subtended by the moving visual stimuli is also important. Larger stimuli generally enhance vection in all measures, although Andersen and Braunstein (1985) demonstrated that stimuli as small as 7.5° of the visual field can induce vection. Optic flow subtending the full visual field induces the strongest vection, and in some cases has been shown to be indistinguishable from actual egocentric full-body motion (Brandt et al., 1973).

Early studies reported that optic flow is more effective in inducing vection when presented to the peripheral visual field compared to when presented to the central field of vision (Brandt et al., 1973; Johansson, 1977). Later studies, however, demonstrated that optic flow presented in the peripheral and central fields of vision have similar influences on vection when the visual stimuli are perceived at equal depth. Vection strength increased linearly with

increasing stimulus size when perceived depth was held constant, regardless of where the stimulus was presented in the visual field (Andersen & Braunstein, 1985).

With decades of research consistently demonstrating the illusion of egocentric motion using purely visual stimuli, it is quite clear that the visual system plays a critical role in the perception of self-motion (Brandt et al., 1973; Warren & Kurtz, 1992). Several multisensory studies within aviation research have suggested that motion simulators may produce redundant multisensory cues when presented with visual displays of motion. If the perception of egocentric motion is adequately produced through a visual display, adding physical motion may provide minimal benefits to pilot performance (Eriksson, 2009; Kappé, Van Erp & Korteling, 1999). The phenomenon of vection is a primary reason why the need for simulating physical motion when using broad angle high-fidelity visual displays is a subject of debate (Burki-Cohen et al., 2007). With the depth of research demonstrating the optimal methods of producing the illusion of egocentric motion and the visual display technology to incorporate these methods, it is possible that physical cues to motion may not be necessary at all for flight/drive simulators. It is, however impossible to ignore the data that consistently demonstrate the more naturalistic behaviours of pilots during simulation training when physical motion cues are provided (Burki-Cohen et al., 2007; O'Malley et al., 2016). This positive behavioural evidence along with pilots' consistent subjective dislike for flight simulators with no physical motion is what perpetuates the debate over the usefulness of physical motion in simulation-based training. It is now important to further our understanding of exactly how the visual system interacts with the vestibular and proprioceptive systems in relation to self-motion perception.

1.1.3 Body-Based Self-Motion Perception

1.1.3.1 Vestibular System

The vestibular system is the non-auditory portion of the inner ear that plays a primary role in sensing physical accelerations and perceiving spatial orientation of the head. This system is sensitive to the magnitude and angular motion of head movements as an individual rotates or translates through space (Moore, Hirasaki, Raphan & Cohen, 2001). The sensory information is then carried through the central nervous system and to the vestibular nuclei where it is processed. Afterwards this information is projected to areas that integrate it with spatial information collected by other sensory systems (Cohen, Maruta & Raphan, 2001). The vestibular system is composed of two separate but complementary organs that are sensitive to different types of head movements. These organs are the semicircular canals, which are responsive to rotational movements of the head, and the otolith organs, which are responsive to translational movements (i.e. linear accelerations; Camis & Creed, 1930).

1.1.3.2 Semicircular Canals

The inner ear is equipped with three interconnected tubes (known as the semicircular canals) that are each responsible for detecting separate directions of head rotations. These three canals include the horizontal canal, which senses the head rotating left and right, the superior canal, which detects the head nodding up and down, and the posterior canal, which detects tilting of the head (Rabbitt, Damiano & Grant, 2004). Each canal is partially filled with fluid known as endolymph, and equipped with a dome-shaped structure - the ampullary cupula - which houses bundles of hair cells (cilia). When the head rotates in a specific orientation, the endolymph of the corresponding canal will flow through the canal, which displaces the cupula and cilia within it. In contrast, linear accelerations of the head produce equal forces on both sides of the cupula, which does not create a displacement. The movement of the cilia modulates the receptor potential of the hair cell, which transduces the motion signal of the endolymph into electrical

signals that are sent through the vestibular nerve and initially to the vestibular nucleus of the brain stem (for review see Rabbitt et al., 2004).

1.1.3.3 Otolith

The otolith organs are located proximal to the ampullary culpa of the semicircular canals within the inner ear, and are responsive to translational accelerations commonly produced by inertial or gravitational force. The utricle and saccule are the two main otolith organs. These organs consist of gravity crystals, or otoconia, which are embedded in a gelatinous membrane that also encapsulates cilia that are fixed relative to the skull. The otoconia becomes displaced within the gelatinous membrane during translational accelerations, which then bends the cilia. Much like the cilia of the semicircular canals, the bending of the otolith cilia creates electrical impulses, which are then projected to the vestibular nucleus (Rabbitt et al., 2004).

1.1.3.4 Vestibular Nucleus

Once the cilia of the semicircular canals and/or otolith have transduced vestibular information into electrical impulses, the signals move through the vestibular nerve and into the brain stem to an area known as the vestibular nucleus (Wilson & Melvill Jones, 1979). The vestibular nucleus is the primary processor of vestibular input and consists of four major regions - medial, superior, lateral, and inferior. The medial and superior vestibular nuclei receive input from the semicircular canals and send signals to the motor nuclei of the extraocular muscles in order to stabilize the eyes on a visual target while the head is moving (vestibulo-ocular reflex). The medial nucleus also sends input to the cervical spinal cord in order to coordinate movements between the head and neck (vestibulospinal reflex; Khan & Chang, 2013). The lateral vestibular nucleus receives signals from the cerebellum, the semicircular canals, and otolith organs and sends input to the spinal cord. The primary function of this nucleus is to coordinate reflexive

tone in the trunk muscles and limbs in order to maintain balance and posture. Finally, the inferior vestibular nucleus receives information from the otolith organs and then projects to the other vestibular nuclei as well as the cerebellum (Khan & Chang, 2013). Input from the inferior vestibular nucleus is used by the cerebellum to monitor vestibular performance and to readjust reflexive muscles during changes in acceleration. The cerebellum plays a primary role in updating vestibular information in order for the brain to accurately perform the vestibulo-ocular and vestibulospinal reflexes.

1.1.3.5 Proprioceptive System

The proprioceptive system consists of the interconnection of the spinal cord, muscles and joints. It performs functions such as sensing the position of body parts relative to neighbouring parts, or perceiving the magnitude of muscle and joint movements (Proske & Gandevia, 2012). The proprioceptive system is the primary sense that allows organisms to navigate through the space around them and react rapidly to changing environments, which happens through the displacement of its receptors (Proske & Gandevia, 2012). Proprioceptive receptors - or proprioceptors - are found throughout the body, within the skin, joints, and muscles. They commonly interact with one another before their sensory information reaches the brain. For example, the displacement of the knee is commonly accompanied by the displacement of surrounding skin cells and leg muscles, which all contribute information to the corresponding cortical areas (Proske & Gandevia, 2012).

1.1.3.6 Muscle Spindles

Muscle spindles have been accepted by most physiologists as the primary proprioceptor, as opposed to proprioceptors within the joints and skin (Proske & Gandevia, 2012). Muscle spindles are composed of two types of nerves, which are called primary and secondary endings.

Primary endings respond to changes in a muscle's length due to stretching, and the speed at which the change in length occurs (Matthews, 1972). Primary endings are therefore believed to contribute both to the perception of movement velocity and limb position. Secondary endings are found within the same muscle fibers but are not sensitive to the velocity of muscle length change. Secondary endings signal only the length change itself, so contribute only to the sense of position and not muscle movement (Proske & Gandevia, 2009). Once stimulated, these nerve endings transduce the kinesthetic energy from the moving muscle into electrical impulses, which are then projected to the spinal cord through primary and secondary sensory fibers and then to the dorsal column medial lemniscus pathway for processing. Electrical impulses for limb position and movement velocity project through the spinal cord and into the brain (Proske & Gandevia, 2009). Information regarding limb position and movement velocity project to the premotor cortex, which is a site of convergence of tactile, proprioceptive and visual, tactile information; it is also involved in the control of movement of the mouth, neck, and limbs. Within the areas of premotor cortex associated with the limbs, many neurons respond to tactile stimulation of the corresponding limb and also respond to visual stimuli placed near the tactile receptive field (Graziano, 1999).

The systems discussed above all contribute to the ultimate perception of self-motion. We designed our EEG experiments with this in mind to limit EEG artifacts due to muscle and eye movements (discussed in Section 1.2.1.1.3). All three experiments in the current line of research incorporated the same physical-motion stimuli. These stimuli were smooth, forward translations at 35° left versus right, with no rotational movements. This linear forward translational movement involves responses in the otolith organs (as opposed to the semicircular canals), and

limits the input from the proprioceptive system, although small neck movements could not entirely be avoided. We discuss this approach in detail in Section 1.2.1.1.3.

1.1.4 Stimulating the Vestibular System

1.1.4.1 Galvanic Vestibular Stimulation

Galvanic vestibular stimulation (GVS) is a method that uses a direct electrical current applied to the skin. An electrode is typically placed over the mastoid processes to stimulate the vestibular system (both the semicircular canals and otolith organs; Wagner, Akinsola, Chaudhari, Bigelow & Merfeld, 2021). Research on healthy adults shows that GVS can result in a variety of responses such as postural sway toward the anode (the positively charged channel; Welgampola, Ramsay, Gleeson & Day, 2013), an illusion of tilt (Watson et al., 1998) or rotation (Peters, Blouin, Dalton & Inglis, 2016), and an increase in EMG signals from the muscles that would typically be engaged in a postural task (Fitzpatrick & Daym 2004).

GVS is often used in clinical research as a relatively inexpensive and space-efficient means to stimulate the vestibular system without physically moving the participant (Dlugaiczyk, Gensberger & Straka, 2019). Researchers have employed this method to explore many different avenues related to vestibular system function and dysfunction. GVS has contributed significantly to our knowledge of the role of the vestibular system in posture, locomotor control, gaze and spatial perception in human subjects (for review see, St George & Fitzpatrick, 2011).

A meta-analysis was conducted by Lopez, Blanke & Mast (2012), in order to localize the neural activation elicited by GVS, caloric vestibular stimulation (CVS) and sound induced vestibular stimulation (SIVS), along with converging neural activation between the stimulation techniques (CVS and SIVS are discussed below). Several clusters of neural activation related to GVS were revealed by the meta-analysis. The most prominently activated areas included the

temporo-parietal junction (Lobel, Kleine, Bihan, Leroy-Willig & Berthoz, 1998), putamen (Bense, Stephan, Yousry, Brandt & Dieterich, 2001), insula (Bense et al., 2001; Eickhoff, Weiss, Amunts, Fink & Zilles, 2006; Stephan et al., 2005), thalamus (Bense et al., 2001; Stephan et al., 2005), cerebellum (Stephan et al., 2005), hippocampus (Stephan et al., 2005), and premotor regions of the frontal lobe (Lobel et al., 1998). As will be discussed, there are similarities in activated areas across studies, however there are many differences that could be due to method of stimulation or inconsistencies in measurements.

1.1.4.2 Caloric Vestibular Stimulation

Another method of stimulating the vestibular system consists of irrigating the external auditory canals with water (cold or warm) or puffs of air (Maes et al., 2007). This method is known as caloric vestibular stimulation (CVS). The vestibular sensors in the semicircular canals are stimulated when thermal energy from water or air is transmitted through the temporal bone to the inner ear, creating a convective flow of the endolymph (Lopez et al., 2012). CVS predominantly stimulates the horizontal semicircular canals, however Aw, Haslwanter, Fetter and Dichgans, (2000) showed that CVS can stimulate the vertical canals, to a lesser degree. Moreover, CVS has been shown to indirectly affect the processing of otolithic signals, particularly the perception of tilt and translation (Merfeld, Park, Gianna-Poulin, Black & Wood, 2005). Research focussed on CVS-evoked nystagmus showed that these modulations of otolithic processing occur at the oculomotor level (Peterka, Gianna-Poulin, Zupan & Merfeld, 2004). Unfortunately for researchers wanting to adopt CVS as method to study multisensory self-motion perception, CVS commonly evokes a nystagmus in parallel with self-motion perception. Eliciting these processes in combination often leads to vertigo and nausea (Lopez et al., 2012).

CVS has typically been used as a diagnostic technique to assess vestibular function and in some cases brain death, throughout history (Quality Standards Subcommittee of the American Academy of Neurology, 1995). Its origins in medicine can be traced back to the first century A.D. when irrigating the external ear canal with water was used to purge foreign material (Feldmann, 1999). More recently, CVS has been applied beyond neurodiagnostics and used as a tool to observe the role of the vestibular system in a wide range of cognitive and sensory functions in both clinical and non-clinical contexts. Some of these research topics include spatial navigation (Bottini et al., 2001; Fink et al., 2003), visual-vestibular integration (for review see, Dieterich & Brandt, 2000), nystagmus (Bense et al., 2005), spatial neglect (Karnath, 1994; Pizzamiglio, Frasca, Guariglia, Incoccia & Antonucci, 1990), and the therapeutic potential of CVS for clinical disorders of the anterior cingulate cortex (ACC) such as autism (Kana, Keller, Minshew & Just, 2007) and obsessive-compulsive disorder (López-Ibor & López-Ibor, 2003).

The meta-analysis conducted by Lopez et al. (2012), revealed that CVS activates similar regions of the brain as GVS. Converging regions include the hippocampus (Suzuki et al., 2001), putamen (Bottini et al., 1994), temporo-parietal junction (Bottini et al., 1994; Bottini et al., 2001), thalamus (Marcelli et al., 2009; Suzuki et al., 2001), cerebellum (Marcelli et al., 2009), and insula (Bottini et al., 1994; Bottini et al., 2001; Deutschländer et al., 2002; Marcelli et al., 2009; Suzuki et al., 2001). There were, however, some prominent areas activated by CVS that were not active during GVS, including the ACC (Bottini et al., 1994; Suzuki et al., 2001), precentral gyrus (Dieterich et al., 2003), and somatosensory area II (Bottini et al., 2001).

1.1.4.3 Sound-Induced Vestibular Stimulation

Auditory stimuli such as short-tone bursts and clicks can stimulate the vestibular system. Sounds have been thought to activate the neural pathways running from the saccular receptors

within the otolith organs that sense vertical accelerations (Lopez et al., 2012). More recent non-human electrophysiological studies suggest that afferents from the semicircular canals can also be activated by sounds (Zhu et al., 2011). Specifically, Zhu et al. (2011) demonstrated that SIVS activates 81% of otoliths afferents and 43% of semicircular canal afferents, in a study involving mice. The most commonly used stimuli for SIVS in human neuroimaging studies are high-intensity clicks at 120 dB and short-tone bursts at the frequency of 500 Hz (102 dB during 10 ms; Miyamoto, Fukushima, Takada, de Waele & Vidal, 2007, Janzen et al., 2008, Schlindwein et al., 2008).

Less vestibular research has been conducted using SIVS than the other methods discussed in this chapter (for review see, Ertl & Boegle, 2019). Neuroimaging studies and clinical practices incorporating SIVS typically focus on the vestibular evoked myogenic potential (VEMP). In order to record the VEMP, two electrodes are placed on the neck and a third on the forehead. The auditory stimulation of SIVS elicits an EMG from the neck muscles. VEMP elicits characteristic wave-forms and latencies that are recorded using EEG (Colebatch and Rothwell, 2004). Using sound as a stimulus allows for millisecond precision when stimulating the vestibular system, which makes SIVS a powerful method for observing Event Related Potentials, particularly related to auditory-vestibular integration. Consequently, SIVS has been used in various EEG studies. Research topics have included short-latency vestibular evoked potentials (Todd, Rosengren & Colebatch, 2008), cortical potentials of multisensory brain regions (Kammermeier, Singh, Noachtar, Krotofil & Bötzel, 2015), and evaluating VEMPs as an assessment of saccular function (McNerney, Lockwood, Coad, Wack & Burkard, 2011). One issue that complicates the interpretation of VEMPs is that auditory stimulation is unavoidable (Ertl & Boegle, 2019). Researchers incorporating fMRI have attempted to control for the auditory co-stimulation by

adding a white noise condition with the same intensity (Janzen et al., 2008; Schlindwein et al., 2008). It is more challenging to find a control condition for EEG experiments due to the high temporal resolution. In this case, the control stimulus would need to have the same duration but different impulse characteristics, which may be difficult, given the short time interval of a few milliseconds per stimulus.

Lopez, Blanke & Mast (2012), revealed that SIVS also causes similar neural activation as GVS and CVS. These converging brain areas include the premotor cortex (Miyamoto et al., 2007), insula (Janzen et al., 2008; Schlindwein et al., 2008), temporo-parietal junction (Miyamoto et al., 2007), anterior cingulate cortex (Miyamoto et al., 2007). Areas of activation specific to SIVS included prefrontal cortex (Miyamoto et al., 2007), and inferior parietal cortex (Janzen et al., 2008; Schlindwein et al., 2008).

1.1.4.4 Vestibular Stimulation Through Body-Based Motion

It is important to note that the three previously discussed methods differ in which vestibular organs are stimulated (semicircular canals and/or otoliths). This means that the nature of the perceived self-motion may be different depending on which stimulation technique is used. For example, participants will experience rotation if the semicircular canals are stimulated, versus translation if the otoliths are stimulated (or possibly a combination of both). This variability makes comparisons across neuroimaging studies that use different vestibular stimulation methods quite challenging. Full-body motion is currently the best way to control the perceived direction and timing of the motion stimuli. The following subsections review the two primary devices used to provide full-body physical motion.

1.1.4.4.1 Rotatory Chairs

The vast majority of studies exploring the online processes of full-body self-motion perception have used rotatory chairs (Hood, 1983; Schneider, Kolchev, Constantinescu & Claussen, 1996; Probst Ayan, Loose & Skrandies, 1997). This method produces motion on the yaw axis, which stimulates the horizontal semicircular canals. Rotatory chairs allow for precise onsets of the acceleration and direction of movement well above the perceptual threshold. The motion profiles used in these studies to evoke self-motion perception typically involve smooth movements, with peak velocities above 100°/s (e.g., Hood, 1983). Some studies have used even greater velocities — up to 12,500°/s² — with comparatively short durations (less than 100 ms; Elidan et al., 1991).

Rotatory chairs have two disadvantages when it comes to recording the brain during full-body motion. First, motion along the yaw axis elicits electroocular reflexes (EOG) and electromyographic reflexes (EMG), which contaminate the EEG data (these are discussed in detail in Section 1.2.1.1). Second, rotations in one direction have been shown to elicit gradual adaptation effects that have widely varied in onset time between studies (Young & Oman, 1969; Malcolm & Jones, 1970; Glover et al., 2014). This inconsistency makes comparing results between studies a challenge. Within the past decade, researchers have begun using translational movements with motion platforms to address the methodological issues related to recording the brain during full-body motion presented by rotatory chairs (Nolan et al., 2012; Ertl et al., 2017)

1.1.4.4.2 Motion Platforms

Motion platforms consist of a frame with six or more extendable actuators connecting a fixed hexagon-shaped base (attached to the floor) to a moveable platform (typically supporting a virtual environment, such as a cockpit or car; see Figure 1 for an example). These motion systems are commonly used for flight simulators in military pilot training and are required by the

Federal Aviation Administration (FAA) and Transport Canada (Burki-Cohen, Sparko, Jo & Go, 2009). The actuators expand and contract independently in order to move the virtual environment in all possible directions in three-dimensional space, also known as 6 degrees of freedom. These axes of motion include, surge (forward and backward), sway (side to side), heave (up and down), bank (tilting of the horizontal axis side to side), pitch (tilting of the vertical axis forward and backward), and yaw (a movement of the nose from side to side). With 6 degrees of freedom capabilities, researchers and training professionals can accurately engage any of the vestibular organs, as well as the proprioceptive and tactile systems. Compared to rotatory chairs, motion platforms are restricted to relatively short sensory stimulations due to the limited displacements of the actuators. They can typically move at a maximum of 0.5 m in any direction, with a maximum acceleration of less than 1 g (Ertl & Boegle, 2019). Another disadvantage of motion platforms compared to rotatory chairs is the background vibration. This vibration may cause undesired sensory stimulation, which could be problematic, especially during psychophysical experiments, such as vestibular threshold testing. Nonetheless, motion platforms provide the most accurate, consistent and natural vestibular stimulation of any current method, and offer the best opportunity to collect robust neuroimaging data, with relatively minimal artifacts. It should be noted there are other devices that have been used to provide physical-motion stimuli. Examples include dynamic motion seats (Pasma, Grant, Gamble, Kruk & Herdman, 2011), and hoverbeds (Dyde & Harris, 2008). In some cases, these alternative methods have shown promising results in the limited capacity they have been used. For example, empirical findings suggest that pilots' performance and subjective acceptance for dynamic motion seats is similar to that of full-platform motion (Burki- Cohen et al., 2009). Unfortunately, these bodies of literature

are very small and the devices typically have even greater spatial limitations than motion platforms.

The method of using platform motion for vestibular stimulation has contributed little to the current understanding of the cortical areas that process vestibular information in humans. Localizing these brain regions using typical neuroimaging methods such as fMRI or PET is not possible as these methods require the participant to remain stationary (reviewed in Section 1.2.1), and typical EEG analysis provides low spatial acuity (reviewed in Section 1.2.3). However, relatively recent methodological advancements in EEG analysis (Measure Projection Analysis) allow for better spatial acuity of EEG signals (reviewed in Section 1.2.3.2). The following subsections of this introduction section outline the best practices for combining the methodological benefits of platform motion with the localization benefits of advanced EEG analysis techniques in order to explore the online processes of human multisensory self-motion perception and the integration of the visual and vestibular systems during this process. Visual-vestibular integration will be reviewed in the following section.

Figure 1. A motion simulator that provided physical- and visual-motion stimuli for the research conducted for this doctoral thesis. The simulator is composed of an enclosed cabin equipped to provide an immersive virtual environment. The cabin is supported by a MOOG © Stewart platform with capability of six-degrees-of-freedom motion.

1.1.5 Visual-Vestibular Integration

Perception of self-motion typically takes place in dynamic environments where sensory cues to motion continually change. Motion cues from one sensory system may be more reliable at a given time point than information from another sensory system, because it is possible that the reliability of information encoded in one or more systems changes as the environment changes (e.g., onset of turbulence while piloting an aircraft). In order to maintain optimal spatial awareness within dynamic environmental conditions, the nervous system continually changes the amount it relies on motion cues from each relevant sense during multisensory integration. This process is called weighting, and it is a critical function of self-motion perception.

Many of the studies exploring multisensory integration specific to self-motion perception focus on visual-vestibular integration due to its relative importance to the process (for review see, DeAngelis & Angelaki, 2012). Visual-vestibular weighting and reweighting, require complex computations that have been demonstrated in multiple studies of multisensory perception of egocentric motion (Morgan, DeAngelis & Angelaki, 2008; Angelaki, Gu & DeAngelis, 2009). The weighting computation underlying visual-vestibular integration is an adaptive process in which the central nervous system down-weights (or up-weights) sensory information relative to more (or less) reliable sensory stimuli (DeAngelis & Angelaki, 2012). Weighting can be affected by previously learned contextual information, or the strength of neural activation in unimodal cortical areas (Blair, Kiemel, Jeka & Clark, 2012). I review attention processes in the next section.

Of all cortical areas that respond to both visual (optic flow) and vestibular (head movements) inputs, the medial superior temporal cortex (MST) shows the greatest amount of activation to both visual and vestibular information related to egocentric motion (Morgan et al.,

2008). The MST therefore has been assumed to be the primary cortical area for the integration of the visual and vestibular systems. Bimodal cells in the MST do not show the same activation patterns as other (more intensively studied) multisensory areas responsive to visuotactile and audiovisual integration (Angelaki et al., 2009; Morgan et al., 2008). Unlike bimodal cells associated with integrating other sensory information, bimodal cells in the MST predominantly show a subadditive firing pattern. Subadditive means that the given cortical area responds to multisensory stimuli with stronger activation than the greatest unimodal response, but less than the sum of both (or all) unimodal responses (Morgan et al., 2008). This firing pattern suggests that there may be deactivation of unimodal sensory processing after the initial weighting of the multiple inputs. The MST typically weights visual information greater than vestibular information during self-motion perception (for review see, Fetsch, DeAngelis & Angelaki, 2010). However, a non-human primate study by Morgan et al. (2008), found that when the coherence of optic flow stimuli in a starfield was reduced, the MST systematically decreased the visual weights and increased the vestibular weights. In a study involving human participants, Brandt, et al. (1998) induced circularvection using a rotating visual display (this study was visual-motion only). Through the use of Positron Emission Tomography (PET) they found significant activation of the medial parieto-occipital visual area (V6; a cortical region known for motion perception) as well as inhibition of the posterior insula of the vestibular cortex (an area where vestibular and proprioceptive inputs integrate). This study also demonstrated the inverse deactivation pattern in a different condition that incorporated caloric vestibular stimulation, in which the visual centres associated with visual-vestibular integration were inhibited during the vestibular stimulation. Moreover, Seemungal et al. (2013) demonstrated that vestibular activation with Transcranial Magnetic Stimulation (TMS; and no visual cues to motion) was accompanied

by an inhibition in visual area V5 (associated with egocentric motion perception), whereas activation in visual areas insensitive to motion – visual areas V1 and V2 – remained the same. This inhibitory effect on V5 activation seems to be specific to visual-vestibular integration, as Seemungal et al. (2013) did not demonstrate an inhibition of V5 neurons when presenting participants with auditory vection. According to the previously discussed studies, visual-vestibular interaction is not necessarily always dominated by either the visual or vestibular systems but is dependent on the relative reliability of the stimuli.

Seemingly conflicting results were found by Nishiike et al. (2002). This study demonstrated co-activation of visual and vestibular cells in the parieto-insular vestibular cortex during visual displays of egocentric accelerations, despite a no-motion signal from the vestibular system (i.e., no vestibular stimuli). Palmisano, Kim, Allison, and Bonato (2011) proposed that these conflicting results occur due to differences in the stimuli. The Nishiike et al. (2002) study provided visual-motion stimuli that changed in acceleration compared to studies such as Brandt et al. (1998), whose visual-motion stimuli held a constant velocity. It is possible that vestibular suppression only takes place during constant velocity visual displays because the vestibular system is only sensitive to changes in velocity. Therefore, it would not be surprising if vestibular inputs were inhibited in favour of visual inputs, such as in the case of Brandt et al., (1998). The relatively small amount of research involving humans contains inconsistencies in how the visual and vestibular systems interact with one another, and which cortical areas are involved in this integration process. This inconclusiveness is likely due to differences in methodology. The non-human primate literature, however, seems to more consistently show that visual-vestibular integration is a subadditive process (Angelaki et al., 2009; Morgan et al., 2008).

One factor that greatly affects visual-vestibular weighting that has not been discussed in this review is selective attention (Abernethy, 1988; DeAngelis et al., 2012). The current line of research presented in this dissertation explores how selective attention modulates the interaction between these two sensory systems during full-body self-motion perception. The following subsections will discuss selective attention in detail and how it plays a critical role in visual-vestibular integration and in self-motion perception in general.

1.1.6 Selective Attention

Our environment provides a complex array of sensory information that is constantly being collected and processed by our sensory systems. The vast majority of the sensory information we take in is not important to our daily goals, and thus goes unnoticed as we carry out our actions. The sensory inputs that are important to our behaviours and goals are then enhanced by further processing and are made more salient. This process is called selective attention and has been of great interest to cognitive psychologists for decades. Summarizing the definition of selective attention is currently quite challenging, as there has been a multitude of models proposed throughout the decades, with thousands of studies showing complex and sometimes conflicting results. This subsection will briefly touch on some of the pioneering work that has set the foundation of our current understanding of selective attention, without discussing the entire exhaustive timeline. The aim is to provide the reader with enough background to understand the role of selective attention in the present line of research.

Before researchers began using EEG to study mechanisms of attention, it was poorly understood whether selective attention was a process that occurred shortly after sensory inputs (early), or later on the timeline of cognitive processing, during memory and response selection (late). This debate was driven by two competing theoretical models of selective attention that

began by exploring the auditory system. Human perceptual systems are constantly processing sensory information despite the fact that we have a limited capacity to perceive such inputs. Therefore, our representations of the environment might become skewed due to sensory overload. Treisman and Geffen (1967) argued that the role of selective attention is to filter out the unimportant sensory information to a manageable subset. This function stops sensory overload from taking place, and allows for a more manageable representation of the environment to be perceived, and more selective with respect to task relevance. In contrast, Deutsch and Deutsch (1963) argued that human perceptual systems are not as limited as Treisman and Geffen (1967) believed, and are capable of processing much more sensory input in parallel at early stages. The limited capacity resides in humans' post-perceptual cognitive abilities, such as decision-making and response selection. Deutsch and Deutsch (1963) therefore argued that selective attention is a mechanism that modulates cognitive processes after sensory input is perceived. Although both groups demonstrated findings that supported their respective models of selective attention, simple behavioural experiments that relied on response times and accuracy were not sensitive enough to conclusively determine whether selective attention is an early or late process.

Incorporating EEG provided clarity on the function of selective attention because it allowed observation of electrical components, with millisecond temporal resolution, providing insight into the timeline of stages of processes. In an influential study by Hillyard, Hink, Schwent and Picton (1973), participants were presented with four different auditory tones. There were non-target tones presented to the left ear that differed from the tones presented to the right ear. There were also target tones with a unique oddball pitch that differed for right and left ears (10% of tones). Participants were required to count the oddball tones presented to one ear and

ignore the tones presented to the other ear. Hillyard et al. (1973) found that target and non-target tones presented to the attended ear elicited an enhanced N_1 (~75% larger) component of the evoked potential, compared to target and non-target tones in the unattended channel. This was the first experiment that demonstrated an effect of selective attention on an evoked potential at such an early stage in processing (~100 ms post-stimulus). The rapid effect of selective attention on N_1 provided evidence that the underlying attentional process acts as a filter at an early sensory stage (e.g., left ear), as opposed to an active discrimination of stimuli from both ears later in processing. This experiment provided support for the early-selection hypothesis of Treisman and Geffen (1967).

Although early selective attention research was concerned mainly with audition, moving forward, most work focused on vision (for review see, Driver, 2001). Research on visual selective attention has produced similar results as the early vs. late selection debate in audition. Exploring the visual system allowed for a deeper understanding of selective attention. Specifically, feature integration theory (Treisman & Gelade, 1980) proposed that simple features of visual stimuli, such as their colour or orientation, are extracted 'pre-attentively' in parallel. However, identifying a conjunction of features (e.g. a red circle among red and blue circles and squares) requires a serial attentional search through the array of items. The metaphor used was the "spotlight" of attention, because attention to the location of the item was required to integrate or bind multiple features together as an object. Evidence for feature integration theory first came from visual search tasks, through the finding of the "pop-out" effect in which, due to targets being defined by a unique feature that does not occur in any of the distractors (e.g., a single red circle in an array of blue and green circles and squares), performance in a visual search task shows little or no effect of the number of distractors. This finding implies that the feature map

(e.g., colour) is processed in parallel, because identification of the unique feature (e.g., red) does not require a serial search (Driver, 2001). This model of selective attention has since been supported by research focused on several areas of study, including spatial neglect patients (e.g., Freidman-Hill, Robertson & Treisman, 1995), human neuroimaging studies (for review see, Desimone & Duncan, 1995), and animal research (e.g., Chelazzi, Miller, Duncan & Desimone, 1993).

Several models since feature integration theory (Treisman & Gelade, 1980) have been proposed, however advances in the field of neuroscience have led to multiple key conclusions about the nature of selective attention. In an extensive review of the neuroscience literature, Duncan and Desimone (1995) made several observations which suggest that at several points between input and response, objects in the visual field compete for limited processing resources, which allow the attended stimulus to guide behaviour. Bottom-up and top-down mechanisms bias this competition. For example, bottom-up attention selects stimulus objects that are distinct from their background (in both time and space), while top-down mechanisms select for objects that are relevant to the current task. Stimulus components such as object features and/or spatial location can affect how these processes interact.

Top-down and bottom-up attention play a critical role in selective attention. In earlier studies of the visual system, top-down and bottom-up attention were generally considered to be two distinct attention systems that have different behavioural effects and partially unique neural substrates (Chica, Bartolomeo & Lupiáñez, 2013; Mysore & Knudsen, 2013). The relationship between top-down and bottom-up mechanisms has been considered in several models of attention (for review see, Tang, Wu & Shen, 2016). Studies have suggested that although it may be metaphorically useful to think of these mechanisms as constituting two distinct attention

systems, they draw on the same limited cognitive resources (Busse, Katzner & Treue, 2008). Moreover, within this capacity-limited system, top-down and bottom-up attention compete for the control over selective attention (Godijn & Theeuwes, 2002), the winner of which determines where or what is to be attended. Regardless of whether top-down and bottom-up attention are two distinct systems, or are two modes of a single system, the majority of studies in the field have at least shown that the two mechanisms differentially modulate stimulus processing (Tang et al., 2016). This finding suggests that top-down and bottom-up attention may also differentially modulate multisensory integration.

It should be noted that we now understand that information flow is more complex than the metaphor of bottom-up and top-down implies. Information flow is not only feedforward (from early to late stages), and it may not be necessary to consider bottom-up and top-down processing systems as separate. Information flows from higher levels of brain processing to early perceptual processing areas, such that processing of sensory information can be altered by higher level processes like expectations and task demands. This reentry into so-called early processing areas happens at all stages of processing. Numerous studies have confirmed the existence of reciprocal signalling between cortical regions. The body of literature for object recognition alone contains many studies that demonstrate reentrant processes from early visual processing stages such as V2 and throughout the visual processing stream (for review, see Di Lollo, 2018). The following data chapters in this dissertation make a case for theta and beta oscillations being associated with reentrant processes. In Chapter 3 we demonstrated theta event-related synchronization (ERS) to be involved in processing of heading information, regardless of whether the stimulus input was generated by visual or physical motion. In Chapter 2, we showed a robust congruency effect; during trials when visual and physical cues to motion were spatially

incongruent (e.g., one cued a left heading while the other cued a right heading), theta was suppressed (event-related desynchronization; ERD) compared to when the cues were spatially congruent. We also hypothesized that beta ERS is associated with inhibition of down-weighted multisensory stimuli. This hypothesis is supported by the beta rebound literature (for review see, Kilavik, Zaepffel, Brovelli, MacKay & Riehle, 2013). I will discuss the concept of reentry as it relates to the theta and beta bands in further detail in each subsequent chapter of this dissertation.

The concept of selective attention affecting multisensory integration (reviewed in greater detail in the following subsection) is critical to the present line of research. In each experiment we demonstrate robust attentional effects in the theta, alpha and beta bands, thus confirming that selective attention indeed modulates the online processes of multisensory integration.

1.1.6.1 Selective Attention in Multisensory Integration

It is not entirely clear through what mechanisms, and under what circumstances attention and multisensory integration interact. Multiple studies have established that attention has a strong modulatory effect on multisensory integration (Harrar et al., 2014; Alsius, Navarra & Soto-Faraco, 2007), however, attention does not need to be directed towards the integrated stimuli for multisensory integration to take place (Spence and Driver, 2000; Bertelson, Vroomen, De Gelder & Driver, 2000). To date, several models have been proposed to explain these interactions (for review see, Tang, Wu & Shen, 2016; Talsma, Senkowski, Soto-Faraco & Woldorff, 2010; De Meo, Murray, Clarke & Matusz, 2015). These models typically focus on the modulatory roles of top-down versus bottom-up attention, and there is a much larger literature exploring the effects of top-down attention on multisensory integration (Tang et al., 2016). Top-down and bottom-up processes have been shown to be reciprocal (for review, see Awh, Belopolsky & Theeuwes, 2012).

As discussed in the previous section, selective attention is more complex than a simple binary top-down versus bottom-up processing model might imply. However, the concepts are still widely used in the literature. For clarity, we define voluntarily allocated attention (including top-down attention) as goal-directed attention, and involuntary perceptual capture (including bottom-up attention) as stimulus-driven attention in order to avoid binary language throughout the rest of this dissertation. Goal-oriented versus stimulus-driven attention modulate multisensory processing in different ways, as described below.

1.1.6.2 Stimulus-Driven Attention

Before multisensory integration can take place, unisensory inputs with unique stimulus features must be processed. The physical strength of a given stimulus is initially what determines perceptual salience. Stimuli with high intensities recruit more attention and elicit more activation within the unisensory processing centres (Irwin, Colcombe, Kramer & Hahn, 2000). If individual sensory inputs have a large disparity in intensity during multisensory integration, one modality will likely dominate the weighting process, which could greatly reduce integration effects (Miller, Pluta, Stein & Rowland, 2015).

The temporal features of the stimuli also affect multisensory integration. The temporal coherence of stimuli during multisensory perception strengthens binding between modalities, which enhances the responsiveness of multisensory neurons (Meredith, Nemitz & Stein, 1987). As we demonstrated in Chapter 4, temporal mismatches between multisensory stimuli greatly affected how the stimuli were processed. We showed that ERSP patterns associated with attending to dominant visual-motion stimuli were modulated by presenting a temporally offset vestibular stimulus 100 ms prior to the onset of the visual stimulus. Another example of temporal features affecting multisensory integration is the sound-induced flash illusion (Shams, Kamitani

& Shimojo, 2000). When one visual flash is presented simultaneously with multiple auditory beeps, participants perceive an illusion of multiple visual flashes. Auditory stimuli are typically perceived faster than visual stimuli (Recanzone, 2003), which creates a temporal mismatch, and in the case of the sound-induced flash illusion, the auditory stimuli are weighted greater than the visual stimuli, causing the visual illusion. Compared to goal-directed attention, fewer studies have been conducted to understand the role of stimulus-driven attention in multisensory integration. Further research is needed to understand how cortical connectivity between sensory processing centres affects multisensory perception.

1.1.6.3 Goal-Directed Attention

There is a large body of literature demonstrating that goal-directed attention can modulate multisensory integration through spatial or modality selectivity (Tang et al., 2016). Selective spatial attention occurs when a participant directs attention towards a specific location (e.g., the right side of the computer screen), or widens the aspect of attention to include multiple locations (e.g., upper left and lower right corners of the computer screen) before stimulus onset. Many studies have shown that spatial attentional selectivity can facilitate responses to multisensory stimuli in attended compared to unattended spatial locations (for review, see Spence & Santangelo, 2009). Behavioural effects discussed in the previously cited review have been supported by neuroimaging data. For example, Talsma, Doty and Woldorff (2007) demonstrated a larger EEG component P_1 amplitude to attended audiovisual stimuli compared to the same stimuli in unattended locations. Audiovisual integration typically demonstrates a superadditive weighting process (Rowland & Stein, 2014). This means that sensory processing centres produce more activity to multisensory audiovisual stimuli than the combined activity elicited by the same unisensory visual and auditory stimuli presented separately. Several neuroimaging studies have

shown that superadditive responses to audiovisual stimuli are enhanced when the stimuli are spatially congruent and within the attended location (Li, Wu & Touge, 2010; Talsma & Woldorff, 2005; Senkowski, Talsma, Herrmann & Woldorff, 2005).

Attention can also be allocated to a specific modality in multisensory streams through goal-directed processes. This occurs, for example, when pilots are trained to ignore their vestibular and proprioceptive senses and focus on visual instruments during turbulence training. Attending to a specific modality (while ignoring others) can speed up sensory processing of the attended input in low-level cortical areas (Vibell, Klinge, Zampini, Spence & Nobre, 2007). This effect has been demonstrated in behavioural and EEG studies primarily of audiovisual (for review see Tang et al., 2016) and visual-tactile (for review see, Spence, 2002) integration. Researchers have studied this process under modality-specific (attending to one modality and ignoring other modalities) and divided-modality (attending to multiple modalities) selective attention conditions. Unsurprisingly, attending to only one modality or dividing attention among multiple modalities affects multisensory integration in different ways. For example, multisensory integration has typically been shown to enhance performance on behavioural tasks such as speeded response tasks (Kenney et al., 2020), or temporal order judgements (Spence, Baddeley, Zampini, James & Shore, 2003) in which more than one modality is task relevant. EEG studies have shown that multisensory integration occurs earlier under conditions in which there are multiple task-relevant modalities (Giard & Peronnet, 1999; Talsma et al., 2007). However, under conditions of modality-specific selective attention, behavioural performance can actually be significantly reduced (Wu et al., 2012).

Goal-directed attention modulates multisensory integration at multiple processing stages that can be based on spatial location or modality. Multiple studies have shown that selective attention

under divided conditions – spatial or modality – come with a heavier cognitive load than attending to one specific spatial location or modality. Multiple studies have shown that these two types of attentional selectivity (spatial and modality) are not independent, and interact with one another (Santangelo et al., 2010; Vibell et al., 2007). For example, Santangelo et al. (2010) asked participants to either simultaneously monitor auditory and visual stimuli at a single location, or in two distinct hemifields, or attend to a single modality at one or two distinct hemifields (a 2[modality: attend to one modality vs. both] x 2[location: attend to one location vs. both] design). Surprisingly, the behavioural results showed that participants were more successful at simultaneously monitoring auditory and visual inputs if their spatial attention was divided, compared to attending to only one location. This study demonstrates that attentional selectivity to location versus modality do not work independently. The way spatial attention is divided will impact the ability to allocate attention among sensory modalities. Future research exploring this interaction may play an important role in guiding pilot training in virtual environments, as selective attention to both space and modality plays a crucial role in flight training tasks. The following subsection further discusses the importance of selective attention in pilot training, and how advancing our understanding of selective attention in multisensory integration will benefit future pilots and training programs.

1.1.6.4 Selective Attention in Pilot Training

Flying an aircraft or driving a car is a multisensory experience. Self-motion information is typically collected from multiple sensory systems, including the visual, auditory, vestibular, tactile and proprioceptive systems. Selective attention can be critical to safely operating a car or aircraft in such a perceptually-rich environment. Particularly high-risk and perceptually-complex situations such as flying through turbulence, or in white-out conditions can create sensory

illusions such as spatial disorientation (Cheung, 2013), where selective attention is critical for safely operating the vehicle. Novice military pilots who fail training often do so because they cannot appropriately divide attention among concurrent activities or sensory signals, or because they are not fast enough to recognize critical signals arriving in unattended sensory systems (Gopher & Kahneman, 1971).

Of all sensory issues pilots may face during flight, spatial disorientation is particularly problematic. It is a factor in at least 25 – 33% of all aircraft mishaps and causes the highest number of fatalities (Gibb, Ercoline & Scharff, 2011). Spatial disorientation occurs when the pilot incorrectly senses the heading, attitude, or position of the aircraft with respect to the surface of the Earth (Rollin Stott & Benson, 2016). These incidents occur due to visual or vestibular illusions caused by issues with multisensory integration (Gibb et al., 2011). It is unsurprising then, that learning to avoid spatial disorientation is typically included in flight training. For example, the British Army Air Corps have included spatial disorientation demonstrations since 1982, and have expanded and refined this training component since that time (Braithwaite, 1997). Training includes recovering from unusual attitudes, which is a common cause of spatial disorientation. The student is taught to direct attention to the visual instruments as opposed to their perceived body orientation (vestibular input). This strategy lessens the distractions and/or illusions from multisensory integration that could aggravate further disorientation.

The emphasis of this training is on recovery, not the causes or solutions of spatial disorientation. It is clear that there is a complex interaction between selective attention and visual-vestibular integration but there is not enough research to fully understand these cognitive processes. The present line of research attempts to lay the foundation for better understanding the role of selective attention in visual-vestibular integration and its underlying neural processes.

Having a better grasp of this concept will allow us to answer applied questions such as what causes spatial disorientation and how can pilots be better trained to deal with it.

1.2 Neural Imaging Studies of Self-Motion Perception in Humans

1.2.1 Issues Related to Recording the Brain During Full-Body Motion

As mentioned in previous sections, most studies exploring human multisensory self-motion perception are behavioural. The vast majority of what we understand about the online processes related to self-motion perception is either drawn from non-human studies (e.g., Angelaki, Gu & DeAngelis, 2011), or human studies providing only visual-motion stimuli (e.g., Kovács et al., 2008). Some researchers have engaged the vestibular system using GVS or CVS in combination with optic flow, and recorded the brain using fMRI or PET in attempts to bridge this gap (for review see, Brandt et al., 2002). These studies have greatly contributed to our understanding of the neural processes of visual-vestibular integration. However, as outlined in Section 1.1.4, it is difficult to precisely induce the perception of physical motion at a specific angle or at a specific velocity using GVS or CVS. This imprecision combined with the spatially precise nature of optic flow may cause issues with synchronizing the multisensory stimuli. Platform motion produces the most natural and spatially-precise physical-motion stimuli to pair with optic flow. Recording the brain with fMRI or PET during full-body motion would greatly advance our ability to map the online processes underlying self-motion perception, however, there is one methodological hurdle that has not been solved up to this point. Engaging the vestibular system with platform motion inevitably leads to head and neck movements. These movements are problematic because fMRI and PET are sensitive to any movements of the head and the resulting magnetic field changes (Birn, Cox & Bandettini, 2004). Movement artifacts in

fMRI or PET recordings typically show up as false-positive activity or activity that contaminates signals from the neural processes under investigation (Lemmin et al., 2010).

Studies attempting to map the neural processes of speech output show that head movements and the resulting magnetic field deformations are the major contributors to motion artifacts in fMRI (Birn et al., 2004). Brain activation is mapped in 3-dimensional space by a matrix of voxels, which are defined by a coordinate frame fixed to the scanner. Head movements create a discrepancy between the scanner and head coordinates, which causes a shift of voxels relative to the head. Voxels may move into a different region of the brain model if the head displacement is great enough. This unintended contamination of the neighbouring brain region may lead to misinterpretation of the data, especially if the neighbouring region engages in different functions or has different signal intensities (Lemmin et al., 2010). Several methods of movement correction, such as retrospective image realignment, have been proposed to correct for artifacts caused by head and body movements (for review see Zaitsev, Akin, LeVan & Knowles, 2017), however, there are no current approaches that are ideal to correct for artifacts caused by full body motion.

Motor processing such as self-motion perception is especially vulnerable to these artifacts. The centres for motor processing are located on the cortex, which is the closest boundary of the brain to the skull. A review by Birn et al. (2004) reported that fMRI motion artifacts most frequently appear at contrast edges, such as the boundary between the cortex and skull. Moreover, a study by Lemmin et al. (2010) demonstrated that even small adjustments in shoulder position created magnetic field deformation artifacts over the cerebellum and lower occipital lobe. Stationary neuroimaging techniques such as fMRI and PET are so vulnerable to motion artifacts that even experiments requiring relatively slight movements such as speaking

may experience issues with recording clean data (for review see, Munhall, 2001). Full-body motion from a motion platform would likely cause far greater displacements of the head and neck (and potentially other body parts), which could lead to poor quality of fMRI or PET data. Common neuroimaging methods with high spatial resolution (fMRI and PET) are not equipped to record high-quality images of the brain during full-body motion; we therefore need to look to techniques that are mobile enough to move with the participants as they move through space.

EEG has the advantages of having greater temporal resolution and is relatively mobile compared to fMRI and PET, despite not having high spatial resolution. This relative mobility is due to EEG electrodes being mounted on the head of participants, which move as the participant moves. This is in contrast to fMRI and PET magnets being fixed to the device. Multiple studies have demonstrated that EEG P3 and N2b signals can be recorded while participants walk (Debener, Minow, Emkes, Gandras & De Vos, 2012; Storzer et al., 2016) or ride a stationary bicycle (Scanlon, Sieben, Holyk & Mathewson, 2017; Storzer et al., 2016). Simulators mounted on a motion base typically have a seat for the participant to sit in, which helps decrease the amount of EMG noise caused by limb movements compared to walking or cycling. We believe that at this point in time, EEG offers the best opportunity to observe cortical processes related to self-motion perception during platform motion. Despite the relative mobility of EEG, recording neural oscillations during full-body platform motion still presents potential issues with signal quality. The following subsections outline potential problems that may occur while recording EEG during full-body motion, and why we chose the specific methodology we did in order to attain the most clean and robust data as possible.

1.2.1.1 Potential Sources of Artifacts

Behavioural studies have shown that humans can accurately discriminate heading through vestibular signals alone (de Winkel et al. 2010; MacNeilage et al. 2010). To date, only a few studies have investigated electrophysiological responses to physical self-motion perception in humans. These have mainly been event-related potential (ERP) studies that aimed to detail the primary sensory responses of the vestibular and proprioceptive systems to rotational stimuli (Loose et al. 2002; Rodionov et al. 1996). These measures have shown some potential for clinical research applications but are not particularly representative of motion in an everyday context. Moreover, problems such as electrooculogram (EOG) and electromyogram (EMG) artifacts from rotational stimuli are frequently reported due to vestibulo-ocular reflexes and vestibulospinal reflexes respectively (e.g., Rodionov et al. 1996). Thus, the utility of these measures remains somewhat limited for understanding the online processes related to self-motion perception during operations such as walking, spatial navigation, driving, and other movement-related operations.

1.2.1.1.1 Vestibulo-Ocular Reflexes

Gaze shifts during circularvection cause the eyes and head to rapidly orient to a new visual target. In this case, the eyes typically reach the target by a rapid saccadic movement, which is then followed by a head turn towards the target. In order to maintain the eyes on the target position during the turning of the head, the eyes must turn in the opposite direction of the head turn at the same rate. This is known as the vestibulo-ocular reflex. This reflex is generally a product of the interaction of the visual and vestibular systems (Lackner & DiZio, 2005). Ebenholtz and Shebilske (1975) have shown that even in the dark, with no visual cues presented, the vestibulo-ocular reflex produces involuntary eye movements that reposition the eyes when the body is presented with angular accelerations. These involuntary eye movements gradually

stop if the semicircular canal signals decay due to habituation to constant rotation. In contrast to rotation in the dark, visual cues to motion will continue to drive the vestibulo-ocular reflex (Lackner et al., 2005). Reflexive eye movements can also be induced by linear accelerations, and are dependent on the orientation of the presented physical motion. These compensatory eye movements include ocular counter-rolling when the body is tilting (Miller & Graybiel, 1962), and during head pitch (the doll's eye reflex; Ebenholtz & Shebilske, 1975). The vestibulo-ocular reflex can also be affected by the visual aspects of a target. For example, when an individual is translating side to side, the amplitude of lateral eye movements rapidly increases when the visual target becomes closer in distance, as would be required to prevent losing sight of the closer object (Telford, Seidman & Paige, 1997).

Vestibulo-ocular reflexes contaminate the EEG signal with EOG artifacts because the eye forms an electric dipole due to the cornea being positively charged, while the retina is negatively charged. The vestibulo-ocular reflex causes this dipole to rotate, which changes the electric fields around the eye, which in turn affects the electrical fields over the scalp generated by neural potentials (Gratton, 1998).

1.2.1.1.2 Vestibulo-Spinal Reflexes

Vestibular information is used for postural control, particularly in the case of gravitational force (Lackner et al., 2005). Antigravity reflexes are key to standing upright without constant conscious awareness of body position. Reflexes related to standing, balance and body position are usually generated by a complex interaction of the visual, vestibular and proprioceptive systems. For example, when a pilot is presented with physical motion in the yaw axis, they will first experience a vestibulo-ocular reflex of counter rolling of the eyes and then the head, in the opposite direction of the yaw motion. This reflex is then followed by the

corresponding counter-rolling of the shoulders, and other task-appropriate body parts (Wilson et al., 1979). With regards to the EEG artifacts created by the vestibulo-spinal reflex, EMG contamination has been shown to peak in the beta band (Goncharova, McFarland, Vaughan & Wolpaw, 2003). Increases have also been shown in gamma band activity (> 30 Hz) due to muscle movements related to the vestibulo-spinal reflex (Nolan et al., 2012).

1.2.1.1.3 Avoiding EOG and EMG Artifacts

Research by Nolan et al. (2012) has demonstrated that EOG and EMG artifacts are avoidable under specific self-motion conditions. By translating participants forward, in linear motion trajectories, high-quality EEG signals can be recorded without noticeable EOG or EMG artifacts (Nolan, Whelan, Reilly, Bulthoff & Butler, 2009). In a pioneering experiment, Nolan et al. (2012) investigated change detection of physical-motion heading while recording high-density event-related potentials. They adapted the classical two-stimulus oddball paradigm (Polich, 1993) whereby participants were presented a series of frequent standard stimuli (80%; a blocked left or right heading) and occasional target stimuli (20%; the opposite heading as the standard stimuli). Participants were required to respond when they detected a target stimulus. Importantly, the physical-motion stimuli were translations of 45°, either left or right at 0.49 m/s^2. These stimulus dimensions were above human detection thresholds for both direction (de Winkel et al., 2010) and acceleration (Benson, Spencer & Stott, 1986). Nolan et al. (2012) uncovered a waveform with a parieto-central distribution, which is a typical P3 topography elicited by an oddball paradigm (Polich & Heine, 1996). This result indicated that vestibular oddball stimuli are processed in a similar fashion as other sensory modalities.

The findings of Nolan et al. (2012) most relevant to the present line of research are related to EOG and EMG artifacts elicited by the physical-motion stimuli. Time–frequency

analysis of their data revealed that there was very little activity that would indicate EOG or EMG activity (based on the findings of Goncharova et al., 2003). Moreover, the topographic heat maps of the ERPs did not exhibit the typical activity that would suggest EMG activity. EOGs were also minimal, as the parieto-central topographic distribution did not resemble the unipolar frontal topographies obtained from EOG activity. Taken together, Nolan et al. (2012) demonstrated that forward translations of 45°, left or right at 0.49 m/s^2, will not run into the same problems with EOG and EMG artifacts that were present in past studies using full-body rotational motion such as Rodionov et al. (1996) and Loose et al. (2002). For this reason, we decided to use similar physical motion stimuli as Nolan et al. (2012) in order to avoid our EEG signals being corrupted with EOG and EMG artifacts related to vestibulo-ocular and vestibulo-spinal reflexes. We translated participants 35° left or right at 0.98 m/s^2. Although our physical-motion stimuli accelerated at a greater rate than Nolan et al. (2012), we completed rigorous pilot testing in order to determine a smooth enough translation that did not produce jerk (and a subsequent EMG). EOG and EMG artifacts are likely to affect EEG data even if all of the aforementioned precautions are taken. We used a common mathematical approach for detecting artifacts in the raw EEG data – known as Independent Components Analysis (Palmer, Kreutz-Delgado & Makeig, 2012; for review see Section 1.2.3.1) - along with our stimuli that were developed for limiting EOG/EMG artifacts.

1.2.2 Electrophysiological Oscillations Associated with Self-Motion Perception

1.2.2.1 Theta Oscillations

Theta rhythms (4-7 Hz) were first discovered in the rabbit by Jung & Kornmuller (1938). Scientific interest in theta rhythms continued to grow during the following decades, and researchers uncovered theta rhythms in other species as well, including cats, rats, and monkeys

(e.g., Green & Arduini, 1954). Throughout the history of theta research, scientists have generally understood that the medial septum (MS) generates theta rhythms, based on the finding that lesioning or inactivating the MS disrupts the production of theta oscillations (for review see, Vertes & Kocsis 1997). Medial septum pacemaker cells are believed to be GABAergic inhibitory interneurons (Toth, Freund & Miles, 1997). These interneurons fire rhythmically at theta frequencies and are phase-locked to theta rhythms in the hippocampus (Hangya, Borhegyi, Szilágyi, Freund & Varga, 2009). Research by Goutagny, Jackson and Williams (2009), has brought into question the belief that the MS is responsible for generating theta oscillations. They found that theta rhythms spontaneously emerge in vitro in an intact hippocampus lacking any connections with the MS. Although the hippocampus may possess the ability to produce theta intrinsically in vitro, much evidence indicates that the MS plays a role in theta generation in behaving animals (for review see Colgin, 2013). Lesioning or inactivating the MS disrupts theta in structures that receive MS projections, such as the hippocampus and parahippocampal area (Green & Arduini, 1954). The MS produces theta rhythms before theta appears in the hippocampus (Bland, Oddie & Colom, 1999). These cells are phase-locked to hippocampal theta, occurring ~80 ms later (Hangya et al. 2009), supporting the idea that septohippocampal projections initiate theta rhythms.

Most early work exploring the function of hippocampal theta was conducted on rats. For example, O'Keefe and Recce (1993) found that when a rat enters the firing field of a place cell, spiking of hippocampal cells in the theta band occurs at the late phase of a separate hippocampal theta rhythm. As the rat moves through the firing field, spiking shifts to the earlier phase of the theta rhythm. In a following study, O'Keefe and Burgess (1996) also discovered the boundary vector cells, which respond with theta rhythms when the animal reaches specific distances from

barriers in the environment. These studies laid the foundation for investigating spatial navigation via the theta rhythm of the hippocampal and parahippocampal networks.

More recent research in human participants suggests that theta oscillations are typically produced in cortical structures associated with all stages of processes involved in determining heading (Colgin, 2013). Studies have demonstrated that the theta band is sensitive to heading direction changes and spatial orientation (Kahana et al., 1999). This finding has been fairly consistent across studies and has been exhibited using physical-motion cues, visual-motion cues, or a combination of both (Chen, King, Burgess & O'Keefe, 2013; Fattahi, Sharif, Geiller & Royer, 2018; Li, Arleo & Sheynikhovich, 2020). The literature generally associates theta ERS induced within parahippocampal networks to play a critical role in path integration (Burgess, 2008). Decades of research has shown that hippocampal place cells and entorhinal grid cells work within a network to create a cognitive map (O'Keefe & Dostrovsky, 1971). Place cells process allocentric sensory inputs that create a representation of the external environment, while grid and heading direction cells process egocentric self-motion information. Together this network allows for the perception of the organism's dynamic egocentric position relative to external landmarks and boundaries (O'Keefe & Burgess, 2005). Burgess, Barry and O'Keefe (2007), proposed the oscillatory interference model, which states that the dynamic updating of egocentric location within a given environment is modulated by the phase of two separate theta rhythms generated within the parahippocampal area. One theta rhythm is sensitive to the organism's location with respect to allocentric inputs, and this is indexed by place cell activity which changes as the organism moves through place fields. As the organism moves through a given place field, the phase of the theta rhythm becomes earlier. The other theta rhythm remains constant. The organism moving through different place fields causes continuously changing

phase discrepancies between the two theta rhythms, which allows for the perception of changes in velocity and heading direction. The oscillatory interference model is based off of animal research beginning with the previously discussed O'Keefe and Recce (1993).

The current line of research presented in this dissertation makes multiple observations regarding human theta oscillations during egocentric self-motion perception. Our EEG methods do not have the spatial resolution of the previously discussed literature, and are not recording directly from the hippocampus and parahippocampal area. It is clear, however, that the conditional differences in theta recorded in our series of experiments reveal processes associated with heading processing. We believe it is possible that these heading-induced differences in theta are linked to the hippocampal processes discussed above. In each data chapter we show that the induction of theta ERS is earlier in response to visual self-motion perception than physical self-motion perception. Chapters 2 & 3 are of particular interest with regards to theta ERS. Our data showed that changes in the theta band could be induced in the motor cortex by visual or physical cues to motion, and was sensitive to direction. This theta ERS was not sensitive to differences in multisensory weighting. We believe that these findings suggest that processing indexed by the demonstrated theta ERS is occurring later in the unisensory self-motion processing stream and is not affected by multisensory weighting. In Chapter 2 we also showed that spatial incongruity between visual and physical self-motion inputs can induce a theta ERD; to our knowledge there is little known about this interesting cortical response.

1.2.2.2 Alpha Oscillations

Many studies have shown the alpha rhythm (8-12 Hz) to be highly distributed throughout the brain, and evoked by sensory stimulation or cognitive tasks (for review see, Başar, 1980). Facilitation of alpha (ERS) has been associated with inhibition or deactivation of brain areas that

are not relevant to the task at hand, while suppression of alpha (ERD) is induced by high cortical activation of that specific brain region (Klimesch, 2012). For example, Neuper and Pfurtscheller, (2001) demonstrated alpha ERD over respective areas of the homunculus during motor tasks. These induced alpha ERD are accompanied by alpha ERS in surrounding areas of the motor cortex and more distant areas unrelated to the task. This data, along with several other studies (e.g., Avanzini et al., 2012; Del Percio et al., 2011) have led to the development of the neural efficiency hypothesis (for review see, Bazanova & Vernon, 2014). This hypothesis posits that a decrease in focal amplitude in the alpha band is generated by activation of the respective brain region; whereas an increase in alpha amplitude reflects inhibition of the neighbouring areas that are not task-relevant. Effective cognition, according to this theory, is not a function of how hard the brain works but rather its efficiency in doing so (Del Percio et al., 2011; Klimesch, Sauseng & Hanslmayr, 2007). Several studies support this hypothesis, such as Tuladhar et al. (2007), who demonstrated that the amplitude of alpha ERS is associated with inhibition of processing irrelevant visual stimuli during working memory tasks. Moreover, multiple studies have shown that amplitudes of resting alpha ERS are positively correlated with intelligence scores (Basar, 2006; Doppelmayr, Klimesch, Hödlmoser, Sauseng & Gruber, 2005). Taken together, this line of research suggests that those who experience higher amplitudes of alpha ERS may be more able to efficiently inhibit irrelevant processes depending on the needs of the given cognitive or sensory event.

Sensorimotor tasks such as perceptual judgement have been shown to induce alpha ERD. Moreover, conditions requiring more attentional resources have been shown to induce more powerful alpha ERD (Niedermeyer and Lopes da Silva, 2004). Conversely, multiple studies

(Niedermeyer, 2004; Sterman & Egner, 2006) demonstrated a strong increase in alpha ERS over the motor cortex when participants rested their limbs.

Finally, it should be noted that some researchers have argued that alpha ERD simply represents top-down processing due to task demands (Cooper, Croft, Dominey, Burgess & Gruzelier, 2003; von Stein et al., 2000). Similar to the neural efficiency hypothesis, these authors believe that top-down attention is engaged as a mechanism for improving the signal to noise ratio within the specific cortical network in order to inhibit conflicting processes or take up cognitive resources from the attended task. In Chapter 4 of this thesis, we will demonstrate that alpha ERD in sensorimotor tasks does not likely represent top-down attention exclusively. For example, comparing two conditions that require the same top-down attentional resources, significant differences in alpha power can be induced by a small difference in stimulus onset asynchrony.

1.2.2.3 Beta Oscillations

Beta-band oscillations (~13–30 Hz) have been of interest to researchers since the first study by Berger (1929). They are most commonly observed over the sensorimotor cortex (for review see, Kilavik et al., 2013). A large body of literature has indicated that beta power fluctuates more during sensorimotor processes than relaxed states (e.g., Takahashi, Saleh, Penn & Hatsopoulos, 2011); robust ERD are observed during movement periods and ERS during postural stability (e.g., Spinks, Kraskov, Brochier, Umilta & Lemon, 2008). However, physical movements are not always necessary. For example, beta ERD have also been demonstrated during motor imagery (Nakagawa et al., 2011), observing movement of others (Koelewijn, van Schie, Bekkering, Oostenveld & Jensen, 2008), passive movement (Keinrath, Wriessnegger, Müller-Putz & Pfurtscheller, 2006; Qiu et al., 2015), and kinesthetic illusion (Keinrath et al., 2006). In a review, Engel and Fries (2010) hypothesized that the role of beta oscillations is to

maintain currently engaged cognitive or motor states (i.e. "status quo"). This theory is based on a previous hypothesis suggesting the beta rhythm as a marker of an "idling" state of the motor system (Pfurtscheller, Stancak & Neuper, 1996).

Beta power in sensorimotor tasks shows the most robust ERD during movement execution and muscle contraction (Tzagarakis, Ince, Leuthold & Pellizzer, 2010). This ERD is reported for both self-paced and stimulus-triggered movements (Alegre et al., 2003; Gaetz, Macdonald, Cheyne & Snead, 2010) as well as for movement of different parts of the body such as fingers (Gaetz et al., 2010) and feet (Pfurtscheller and Lopes da Silva, 1999). The decrease in beta power lasts as long as the body is in motion (Wheaton, Fridman, Bohlhalter, Vorbach & Hallett, 2009) or during continuous changes in muscle contraction (Omlor, Patino, Mendez-Balbuena, Schulte-Mönting & Kristeva, 2011). Beta power increases (ERS) as soon as the muscle contraction or posture stabilizes (van Elk, Van Schie, Van Den Heuvel & Bekkering, 2010). Interestingly, movement-related beta ERD does not seem to be affected by factors such as the speed of the movements (Stančák & Pfurtscheller, 1995), or the amount of force used to complete the movement (Pistohl, Schulze-Bonhage, Aertsen, Mehring & Ball, 2012).

The movement-related beta ERD is typically observed bilaterally over sensorimotor areas (e.g., Pfurtscheller et al., 1996; Stančák & Pfurtscheller, 1995). The current understanding is there is a somatotopic organization of the movement-related beta ERD (Crone, Miglioretti, Gordon & Lesser, 1998; Stančák, Feige, Lücking & Kristeva-Feige, 2000). For example, the ERD induced by an index finger movement is more distal than the power decrease generated by a foot movement (Kilavik et al., 2013). However, given the relative lack of spatial acuity of EEG, the precise cortical localization is still not clear.

1.2.2.3.1 Beta Rebound

Typically following the movement-related beta ERD is the post-movement beta rebound (beta ERS). This ERS is defined by a short but powerful increase in beta power occurring 300 to 1000 ms after the movement (Kilavik et al., 2013). Interestingly, the beta rebound has also been demonstrated in participants imagining performing a movement (Pfurtscheller and Solis-Escalante, 2009; Solis-Escalante, Müller-Putz, Pfurtscheller & Neuper, 2012).

The beta rebound does not seem to have the same spatial distribution as the preceding beta ERD (Gaetz et al., 2011). Cortical generators for the beta rebound have been localized to multiple areas within the motor cortex, including primary motor cortex and supplementary motor area (Koelewijn et al., 2008; Stančák et al., 2000). Moreover, evidence from electrocorticographical (ECoG; electrodes placed directly on the brain during surgery) studies reflect the idea that the generation of beta rebound occurs in a distributed cortical network, including the sensorimotor and premotor area (Crone et al., 1998; Sochůrková, Rektor, Jurák & Stančák, 2006; Szurhaj et al., 2003). The previously discussed studies involve human participants. Little progress has been made localizing the beta rebound in monkey studies because of methodological issues (Kilavik et al., 2013). The challenge lies in dissociating from processes related to the post-movement reward versus ERSP related to actual movements from the task. In past studies these ERSP responses occur at similar times, which greatly compromises the interpretation of post-movement beta activity in non-human primates.

A commonly-accepted hypothesis regarding the beta rebound is that this post-movement period may be used to recalibrate the motor system to new conditions, in order to prepare for a subsequent movement. Once the beta rebound is complete, the beta oscillation cycle begins again with the preparation for a new movement (Engel & Fries, 2010). This theory is supported by research by Gaetz and Cheyne (2006) who used synthetic aperture magnetometry to localize

neuromagnetic oscillations to tactile stimulation of a finger, lip and toe. They found that the location within the motor cortex, and the peak amplitude of beta rebound (but not beta ERD) are different depending on which area is stimulated. For example, they demonstrated that somatotopically-organized beta ERS from toe stimulation peaked higher in the beta band than beta ERS elicited by finger stimulation. The authors propose that these results point to beta ERS reflecting the dynamic coordination of sensory input and motor output, which is maintained by sensory afferents that inhibit associated areas of the motor cortex.

The present line of research in this dissertation proposes that beta rebound reflects an alternative process, possibly providing insight into the dynamic coordination of sensory inhibition of motor cortex. Given the combined results of the three experiments in this thesis, we believe the beta cycle might be engaged as part of a perceptual weighting mechanism. Similar to the hypothesis proposed by Gaetz and Cheyne (2006), we suggest that beta ERS works to dynamically suppress the processing of some multisensory inputs. We believe, however, that this is related to multisensory weighting. Chapters 2 and 4 show that the same self-motion stimuli can elicit vastly different beta ERS responses due to attention-related manipulations in multisensory weighting. The integration of the visual and vestibular systems is a subadditive process (Angelaki et al., 2009). The robust beta rebound we demonstrate in trials where participants attend to visual-motion stimuli might reflect an inhibitory process during visual-vestibular integration in which the sensory information of the provided visual-motion stimulus is weighted greater than the opposing lesser-weighted vestibular signal.

1.2.2.4 Gamma Oscillations

The temporal correlation hypothesis (Singer & Gray, 1995) posits that synchronization of gamma-band oscillations (>30 Hz, but in the case of multisensory integration, 30 – 50 Hz) is a

key mechanism for integration across distributed cortical networks. Evidence supporting this hypothesis has been demonstrated in multiple studies (e.g., Sakowitz, Quiroga, Schürmann & Başar, 2001; Senkowski, Talsma, Grigutsch, Herrmann & Woldorff, 2007) that typically focus on audiovisual integration. For example, Senkowski et al. (2007) presented human participants with audiovisual stimuli with varying degrees of temporal asynchrony, and required them to attend to one modality-specific stimuli while ignoring the other. They found that gamma ERS was not significantly different between modalities but, for both modalities, significantly more gamma ERS was elicited when temporal asynchrony was 25 ms or less, compared to longer SOAs. In Chapter 4 of the present thesis, we tested the temporal correlation hypothesis, which predicts that the simultaneous conditions (AP(S) and AV(S)) elicit stronger gamma ERS compared to the visual-first and physical-first conditions.

1.2.3 Issues Localizing EEG Signals

Electroencephalography measures the voltage potential of the brain at various locations on the scalp using highly sensitive electrodes. Signal processing techniques are then applied to the data to estimate the current sources of these electrical signals inside the brain that best fit this data. Although EEG signals are commonly localized in clinical practice, such as detecting epilepsy (Koles, 1998), these signals tend to be localized to gross regions of the brain, such as a specific hemisphere or lobe, unless electrodes are placed directly on the brain during surgery (ECoG), in which case more precise localization can be estimated (Buzsáki, Anastassiou & Koch, 2012). EEG has historically been viewed as having low spatial resolution due to multiple factors. First, activity recorded by a given electrode cannot be attributed to neural activation at that specific site. The same electrical activity in one location can be detected at distant electrode sites. One example is observing a visual response across all electrodes. Second, EEG analyses

often attempt to measure electrical events several centimeters below the scalp-mounted electrodes. Consequently, the measured electrical current may need to travel through multiple layers of cortex, meninges, and most problematic of all layers, the skull (Nunez et al., 1994). These various layers – particularly the skull – act as a low-pass filter, which creates a blurring effect at the scalp level (Srinivasan, Nunez, Tucker, Silberstein & Cadusch, 1996). The resulting measurement is a mixture, or weighted sum of the underlying oscillatory processes. Finally, additional spatial smearing is created by the necessity for a reference electrode to measure differences in the recorded potential (Burle et al., 2015).

We used the BioSemi ActiveTwo electrophysiological system (www.biosemi.com) which digitizes raw EEG signals compared to EEG systems that digitize EEG signals at recording time, and for which the reference must be selected prior to recording. Common reference electrode sites are Cz, or the average between two ear electrodes, or the average between two mastoid electrodes. The BioSemi ActiveTwo system allows re-referencing the raw EEG data after recording, providing flexibility and independence from a particular reference site. We chose to use the common average reference (subtraction of the average of all electrodes) to reference our raw EEG data. A study by Qin, Xu and Yao (2010) compared the referencing methods of common average reference, linked mastoids, and left mastoid for accuracy reproducing two dipoles in simulated EEG data. The common average reference method was determined to be significantly more accurate than referencing to linked or left mastoid at reproducing the two simulated dipoles from the original data.

One relatively new approach to improving the spatial resolution of EEG is through the use of Independent Components Analysis (ICA; Delorme and Makeig, 2004), followed by Measure Projection Analysis (MPA; Bigdely-Shamlo, Mullen, Kreutz-Delgado & Makeig,

2013). Combining these computational methods allows the EEG data to be fit into a three-dimensional model of the brain. Both ICA and MPA are described in the following subsections.

1.2.3.1 Independent Components Analysis

Contamination of EEG activity by EOG, EMG, line noise and heart beat are serious problems for EEG analysis and interpretation. Removing segments of the EEG data by artifacts potentially results in a sizeable loss of data, and may be impractical if the experiment cannot compensate with many trials. Several methods have been proposed to remove EOG artifacts from EEG recordings, as these are one of the most frequent EEG artifacts (Jung et al., 1998). Before Independent Components Analysis (ICA) was commonly practiced, researchers would record EEG and EOG simultaneously and then perform regression in the time or frequency domain to characterize EOG artifacts in the raw EEG data. However, EEG data contaminated with EOG artifacts also contains relevant brain signals (Peters, 1967), so regressing out EOG activity inevitably led to losing some of the relevant EEG signal from the data. Unfortunately, regression cannot be used to remove line noise or EMG, since these do not typically have reference channels. ICA began as a mathematical method for removing a wide variety of artifacts from EEG data without losing as much of the relevant brain signals (Bell & Sejnowski, 1995). In general, this method performs blind source separation on linear mixtures of independent source signals with either super-Gaussian or sub-Gaussian distributions. The results of Jung et al. (1998), demonstrate that ICA can effectively detect, separate, and remove activity in EEG recordings from several artifactual sources. These results compare favorably to previous studies using regression-based methods.

ICA can now be used in more advanced analytical methods than simply removing artifacts in the EEG recording. ERP and ERSP signals can be composed of several dynamic

underlying cortical processes (Makeig et al., 1999). Research beginning with Bell and Sejnowski (1995) demonstrated that ICA can be used as a method for blindly deconstructing a set of mixed signals to uncover the relative contribution of constituent processes to many ERSP or ERP scalp components. Examples of EEG components that can be deconstructed by ICA include the N_2 (Hu, Mouraux, Hu, & Iannetti, 2010), the N_1 during a selective spatial attention task (Makeig et al., 1999), isolating response-related brain activity during a visual selective attention experiment (Jung et al., 2001), and the novelty P3 and P3b response (Debener, Makeig, Delorme, & Engel, 2005). Thus, although ICA can be applied to a diverse set of electrocortical processes, distributed widely throughout the brain, the nature of the information gained by ICA shares two similarities. Firstly, independent electrocortical processes can be isolated that are otherwise mixed when assessed at a scalp recording site, or completely lost if regressed out of the EEG data. Secondly, ICA provides an improved signal-to-noise ratio at the level of the single trial, which increases the power of statistical tests relative to previous analysis techniques (Desjardins & Segalowitz, 2013).

In the present line of research, we incorporated ICA into our EEG analysis for two functions. ICA was performed for 1) a data cleaning technique to remove EEG artifacts such as EOG and EMG, and 2) the first step of a two-step process in attempts to localize our EEG signals related to self-motion perception. ICA was used to decompose EEG signals of all participants into their constituent components, which were then fit into a three-dimensional model of the brain and clustered using Measure Projection Analysis (MPA; Bigdely-Shamlo et al., 2013). Clustering was based on source location and relative ERSP activity of between-subjects ICs. It should be noted that these two functions occurred simultaneously – ICs

resembling artifacts (see Figure 2 for an example) were withdrawn from the data, while ICs resembling electrocortical processes were fit into the brain model.

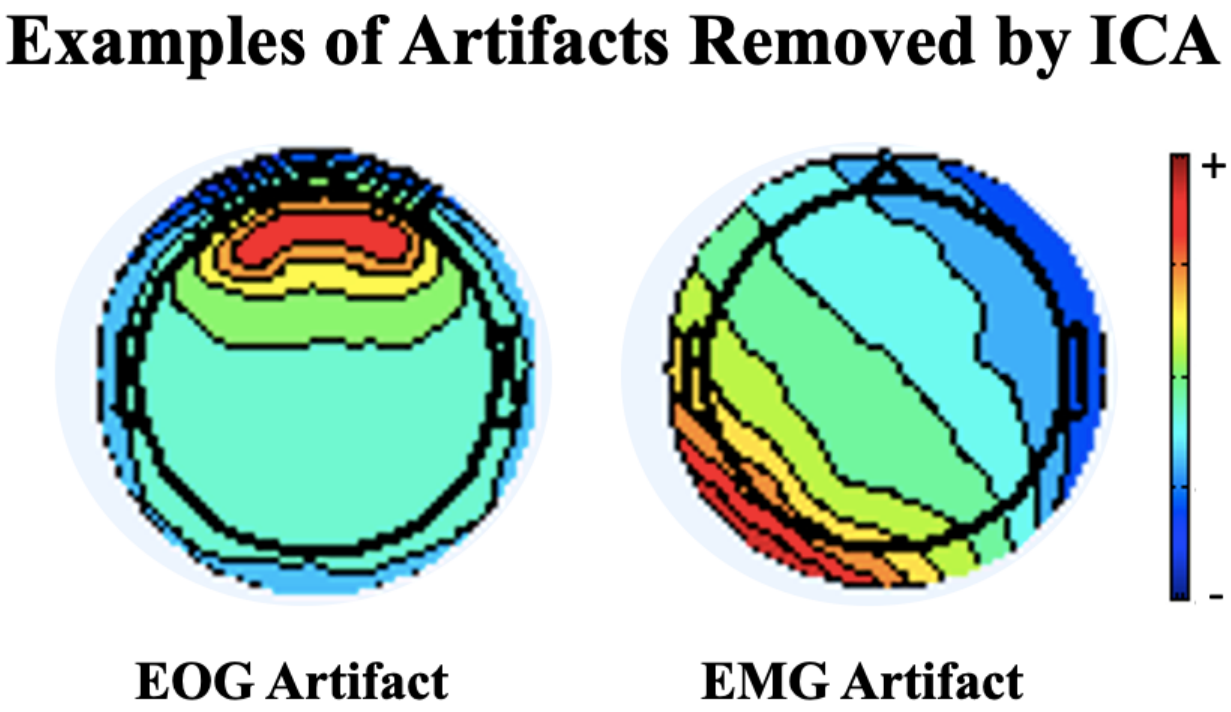

Figure 2. These are two examples of topographical heat maps of typical EOG (eye blink; image on the left) and EMG (muscle movement; image on the right) artifacts that were removed from the data using ICA.

1.2.3.2 Measure Projection Analysis

Measure projection analysis (MPA) is a mathematical method for characterizing the localization and consistency of EEG components across sessions of EEG recordings (Bigdely-Shamlo et al., 2013). It allows the use of EEG as a three-dimensional clustering method for ERP or ERSP, with near-cm scale spatial resolution. MPA defines anatomical regions of interest by clustering independent components (ICs) based on having spatially similar dipole models as well as similar ERP/ERSP activity. The domains (clusters of ICs) are then fit to a three-dimensional model of the brain, which allows for probabilistic mapping of the calculated domains to the atlas of human cortical structures, provided by the Laboratory of NeuroImaging (LONI) project (Shattuck et al., 2008). The MPA brain model is a cubic space grid with 8-mm spacing that is laid out according to Montreal Neurological Institute (MNI) space. Independent components localized to voxels outside the brain model (e.g., EMG, heartbeat artifacts) are excluded from the analysis. Local convergence values are then calculated based on the algorithm explained in detail by Bigdely Shamlo et al. (2013) for the ICs falling within the brain model. The present line of research incorporated a significance threshold for convergence at each brain location based on bootstrap statistics. Following convention in previous literature (e.g., Bigdely-Shamlo et al., 2013, Misra, Wang, Archer, Roy & Coombes, 2017), the raw voxel significance threshold was set to $p<0.001$.

One potential issue with clustering of single-subject components using MPA is that, in extreme cases, some of the resulting domains may not equally represent the entire sample. This occurs because some domains may not be composed of ICs from all participants, or may be severely biased towards ICs from some participants compared to others (Huster, Plis & Calhoun, 2015). This issue affects the ability of the researcher to make statistical inferences at the group

level if there are extreme inequalities between participant representation within a given domain. This issue can be considered a benefit in non-extreme cases. Domains are only composed of ICs with a high probability of reflecting the true representation of the latent sources. Therefore, the output from MPA demonstrates high integrity when representing electrophysiological processes. Information regarding the composition of MPA domains is typically not reported in published EEG studies. This lack of information makes it difficult to evaluate the appropriateness of a given domain, and to develop standards in order to alleviate concerns about poor representation of the given sample. The few studies that do describe the composition of their domains report simple descriptive statistics, such as the proportion of participants whose ICs are included for each domain (Alayrangues, Torrecillos, Jahani & Malfait, 2019), or simply that each domain contains at least one IC from each participant (Ofori, Coombes & Vaillancourt, 2015). Although at this time there are no concrete methods to evaluate the representativeness of a MPA domain, it appears as though domains from the current line of research represent the samples equally or greater than other published work that reported the composition of their domains. On average, each participant contributed 2.45 ICs to each domain within their respective experiment. Furthermore, on average, each domain contained ICs from 88% (*SD* = 1.59) of participants within its respective sample, with the lowest representation being 82% (one domain) and the highest representation being 100% (three domains). These representation scores compare favourably to another published EEG study (Alayrangues, Torrecillos, Jahani & Malfait, 2019), where on average, each domain contained ICs from 64% of participants within its respective sample, with the lowest representation being 42% and the highest representation being 78%. Overall, we believe that our MPA domains represent their respective samples relatively well, and

that our data benefits from the high degree of integrity MPA allows for observing online processes.

1.3 Overview of Empirical Chapters

Flight and drive simulators capable of full-body physical motion, with visual displays subsuming the entire visual field have been used for research and training since the mid twentieth century. There has been a large body of literature accumulating over the past decades focussed on the behavioural correlates of self-motion perception. We have gained invaluable insights from this line of work. This work ranges from basic research, focussed on how our perceptual systems detect inertial motion, to more applied research, exploring concepts such as cognitive ergonomics in simulated flight training. Despite the abundance of behavioural studies, there is a clear lack of research exploring the online processes associated with full-body, multisensory self-motion perception in humans. Much of what is known about the neural correlates of self-motion perception comes from either the animal literature, or from human neuroimaging studies only administering visual self-motion stimuli. This gap in the literature is primarily due to technological and methodological deficiencies of the past several decades. We are just now discovering effective ways to record the brain during full-body motion, and robust ways to analyze the resulting neuroimaging data. Our research team has worked tirelessly to lay the foundation to bridge the gap between understanding the behavioural correlates of full-body self-motion perception, and the underlying neural processes of the human brain. The goal of this thesis is to understand how the predominant electrophysiological oscillations underlying full-body self-motion perception are related to multisensory integration processes such as perceptual weighting and selective attention. Specifically, in Chapter 2 of this thesis, we examine the effects of attention allocation and congruency of visual and physical cues to motion on the event-related

spectral power. We determined that alpha and beta oscillations are sensitive to attention allocation, and theta oscillations likely index heading direction and sensorimotor integration. In Chapter 3 we recorded the electrophysiological responses to visual-only or physical-only motion stimuli. Based on the findings of Chapter 3, we demonstrated that beta oscillations are an index of visual-vestibular weighting, and right-lateralized theta ERS are sensitive to heading direction for both visual and vestibular inputs. Finally, in Chapter 4, we incorporate a stimulus onset asynchrony to examine the effects of stimulus onset timing on the weighting-related self-motion ERSP. This experimental design allowed us to confirm our hypothesis that beta oscillations index visual-vestibular integration. Moreover, based on our observations of beta-band activity, we concluded that the onset timing of the visual- and physical-motion stimuli has a more powerful influence on visual-vestibular weighting than does attention allocation. The results of all three complimentary studies are examined together in the General Discussion chapter in order to propose theorized functions of theta, alpha and beta oscillations associated with cognitive processes underlying self-motion perception.

CHAPTER 2: Attention modulates event-related spectral power in multisensory self-motion perception

Townsend, B., Legere, J.K., O'Malley, S., v. Mohrenschildt, M., & Shedden, J.M. (2019)

NeuroImage, 191, 68-80.

Preface

Chapter 2 was our first experiment in the present line of research, and was exploratory in nature. Given the lack of research on ERSP signatures of full-body motion, we had to rely on literature exploring body movements, such as finger tapping and arm extensions, in order to formulate hypotheses. Based on the previous research, we understood that theta, alpha and beta oscillations would likely be frequencies of interest, however, at that point, we could not anticipate exactly how they would be associated with fully-body motion. The goals of the experiment were to develop our understanding of 1) attention-related ERSP during fully-body motion, and 2) potential ERSP signatures of failed visual-vestibular integration due to spatial incongruence. These two constructs were of interest to us because they can be applied to pilot simulator training against spatial disorientation, which is a strong motivation for our research group. We decided to focus on attention and visual-vestibular integration because these are two key constructs of interest within the pilot training literature, however there is very little research exploring the neural basis of these constructs that can be directly applied to pilot simulator training. This experiment was a 2x2 design, which presented visual- and physical-motion stimuli

simultaneously, and participants completed a heading judgement task (determine left or right heading) that required either attention to the visual-motion stimuli (while ignoring physical-motion stimuli), or attention to the physical-motion stimuli (while ignoring visual-motion stimuli) in separate blocks. Within each block the motion stimuli were either spatially congruent (both left, or both right), or incongruent (one left and one right). The ERSP revealed that attention to the visual-motion stimuli resulted in earlier theta ERS and alpha ERD, and stronger beta ERS, while attention to the physical-motion stimuli resulted in stronger beta ERD. These results laid the foundation for our understanding of attention-related ERSP during self-motion perception. Another result was that the incongruent attend-visual motion condition elicited stronger theta ERD. This may be a biomarker of spatial disorientation that is typically experienced during perceptually-complex flight scenarios, when visual and physical cues to motion do not align.

Abstract

Humans integrate visual and physical (vestibular and proprioceptive) cues to motion during self-motion perception. Theta and alpha-band oscillations have been associated with the processing of visual motion (e.g., optic flow). Alpha and beta-band oscillations have been shown to be associated with sensory-motor processing (e.g., walking). The present study examined modulation of theta, alpha, and beta oscillations while participants made heading direction judgments during a passive self-motion task which required selective attention to one of the simultaneously presented visual or physical motion stimuli. Attention to physical (while ignoring visual) motion produced a different time course of changes in spectral power compared to attention to visual (while ignoring physical) motion. We observed stronger theta event-related desynchronization (ERD), as well as stronger beta and later onset of alpha event-related desynchronization (ERD) in the attend-physical condition compared to the attend-visual condition. We observed individual differences in terms of ability to perform the task. Specifically, some participants were not able to ignore or discount the visual input when visual and physical heading direction was incongruent; this was reflected by similar event-related spectral power for both conditions. The results demonstrated a possible electrophysiological signature of the time course of 1) cue conflict (congruency effects), 2) attention to specific motion cues, and 3) individual differences in perceptual weighting of motion stimuli (high-vs. low-accuracy effects).

1. Introduction

The perception of self-motion draws on the integration of the visual, vestibular and proprioceptive systems. These sensory inputs contribute through a continuous re-weighting process, which has been demonstrated in multisensory studies of self-motion perception (Angelaki et al., 2009; Butler et al., 2010; De Winkel et al., 2017; Morgan et al., 2008). The reweighting process underlying visual and physical (vestibular and proprioceptive systems) motion integration is a subadditive process in which the brain down-weights unreliable sensory stimuli while simultaneously up-weighting more reliable sensory stimuli.

The dorsal medial superior temporal cortex (MSTd) is thought to be the primary cortical area for the integration of visual and vestibular motion inputs and a possible site for the reweighting process (Morgan et al., 2008). Using single-cell recordings in macaques, Morgan et al. (2008) showed that the MSTd produces the greatest amount of activation related to self-motion from both visual (optic flow) and vestibular (forward translations) motion stimuli. There is an advantage for multi- sensory presentations. When trained to discriminate between left and right translations provided by unisensory or multisensory cues, monkeys showed optimal perceptual sensitivity when visual and vestibular motion stimuli were combined as opposed to presented separately (Gu et al., 2008). This effect was not found when combined motion stimuli were spatially incongruent. MSTd contains separate clusters of neurons that respond optimally to either spatially congruent or incongruent pre- sentations of visual and vestibular motion stimuli. Differences in activity of these cell types may play a role in parsing retinal image motion into self-motion versus motion from objects in the environment. If visual and vestibular motion stimuli are incongruent, it is likely that these inputs are being produced by separate events, such

as seeing other objects move independently through the visual field during physical self-motion (Gu et al., 2008).

In humans, unisensory neuroimaging studies using visual self-motion have reported a variable set of cortical areas involved with self-motion processing including MSTd, parieto-insular vestibular cortex, medial temporal area (MT/V5), and ventral intraparietal area (Brandt et al., 1998; Palmisano et al., 2015). Although it is probable that self-motion processing is distributed across multiple brain areas, the findings of these studies are variable with respect to which areas show activation. One problem may be that some studies attempt to induce the vection illusion. The strength of vection in individuals is difficult to measure objectively (for review, see Pitzalis et al., 2013). It is possible that the varying success of vection induction between participants and studies may explain the inconsistencies in replicating localized brain activity (Palmisano et al., 2015). These neuroimaging studies have focused on visual stimuli to elicit vection because analysis of fMRI brain-imaging data is challenging when participants are in physical motion. Further- more, presenting visual-motion stimuli in the absence of vestibular and proprioceptive stimuli can lead to sensory conflict when visual process- ing signals self-motion while proprioceptive and vestibular processing signals no self-motion (Campos and Bülthoff, 2012). Incorporating both physical and visual motion would provide a more realistic and objective means to explore the multisensory nature of self-motion perception in humans.

Recent work has shown that electroencephalography (EEG) can be used successfully to record brain activation in a physically moving environment (Grundy et al., 2013; Nolan et al., 2012; Shedden et al., 2012; Townsend et al., 2015). EEG research has consistently shown that oscillations in the theta- (3–7 Hz), alpha- (8–12 Hz) and beta- (13–30 Hz) bands are associated with a variety of processes related to self-motion perception and motor function. Specifically,

motor output has been associated with theta event-related synchronization (ERS; amplitude enhancement), and alpha and beta event-related desynchronization (ERD; blocking responses) (Pfurtscheller, 1992). Theta oscillations are diagnostic in spatial navigation and sensorimotor tasks for both human (Caplan et al., 2003) and non-human subjects (Koenig et al., 2011), and may be an index for a process that is critical for spatial computations such as forming cognitive maps (Koenig et al., 2011). Unisensory visual studies have shown greater alpha ERD in response to optic flow compared to static or spatially scrambled visual stimuli (Palmisano et al., 2016; Vilhelmsen et al., 2015). Changes in alpha ERD are also associated with other sensory modalities. During sensorimotor tasks, for example, alpha ERD is greater in motor regions compared to task-irrelevant brain areas (Pfurtscheller, 1992; Ofori et al., 2015). However, alpha ERD is more robust when induced by visual optic flow compared to flow from other sensory modalities (Klimesch et al., 2007). Beta ERD is induced by both active (Stancak and Pfurtscheller, 1996), and passive (Alegre et al., 2002), motor movements, suggesting that alpha and beta ERD index visual and motor processing, respectively. Coupled alpha- and beta-band ERD have been associated with multisensory body movements (Allen and MacKinnon, 2010; Cruikshank et al., 2012; Kilavik et al., 2013; McFarland et al., 2000; Ofori et al., 2015; Seeber et al., 2014). This observation further highlights the importance of observing responses to visual and physical motion together. Brain networks process multisensory inputs to self-motion, to the extent that unisensory self-motion cues may actually produce sensory conflict if motion is induced by one sense and not another (Campos and Bülthoff, 2012).

Of interest to this study was whether observation of these oscillatory patterns may be diagnostic of self-motion perception during full-body accelerations through space, as is experienced while driving or flying. This type of experience can be simulated in driving and

flight simulators with motion-based platforms. Over the past 30 years, there have been dramatic increases in both the research and application of motion-based simulator training in aviation and driving (for reviews see De Winter, Dodou & Mulder, 2012; Pinto et al., 2008). Recent research has begun exploring basic cognitive and sensory processes that play an underlying role in how humans perceive sensory cues provided by simulators (Eriksson, 2009). For example, several studies have shown that in multisensory simulated environments, attention to a specific modality can change behaviour of the operator in several ways (Brickman et al., 2000; Prewett et al., 2012).

There is a strong literature looking at integration of the visual, vestibular and proprioceptive systems, including age-related changes in multisensory integration that provide understanding of temporal and spatial windows within which optimal integration occurs (Ramkhalawansingh et al., 2018). Studies such as Butler et al. (2010), De Winkel et al. (2017), and Ohmi (1996), have used angular discrepancies between visual and vestibular cues (e.g., cue conflict) to measure relative cue weighting between the senses. This concept can be applied to flight and driving simulations, as drivers and pilots encounter visual-vestibular conflict when slowly accelerating or turning a vehicle (Ohmi, 1996). To avoid the costs of cue conflict, pilots and other operators of susceptible vehicles are often trained to discount physical cues to motion and attend to their visual instruments (Newman et al., 2012).

The goal of the present study was to examine whether attention to visual versus physical motion information would affect oscillatory power within the alpha, beta and theta ranges. Participants discriminated be- tween left and right directions by attending to either visual or physical motion. Because beta ERD are more prevalent during active body movements, while alpha ERD are most robust during visual motion processing tasks, we hypothesized that

allocating attention to physical motion stimuli would produce greater beta ERD and allocating attention to visual-motion stimuli would produce greater alpha ERD. Critically, our interest was in the modulation of these effects due to selection of one stimulus while ignoring another congruent or incongruent stimulus. We presented simultaneous visual and physical motion stimuli, which were either congruent or incongruent in direction. Incongruent cues to motion were incorporated to simulate visual-vestibular conflict. Using a directed attention task, we compared event-related spectral power (ERSP) during natural (congruent) motion conditions with conflicting (incongruent) conditions to observe whether cue congruency moderated ERSP.

2. Materials and methods

2.1 Participants

Thirty-seven participants (24 female) were recruited from the McMaster University psychology participant pool and the McMaster community. Ages ranged from 18 to 26 years (M 1⁄4 19, SD 1⁄4 2.01). Those recruited from the participant pool were compensated with course credits. All participants self-reported normal or corrected-to-normal vi- sual acuity and reported no major problems with vertigo, motion sickness or claustrophobia. This experiment was approved by the Hamilton Integrated Research Ethics Board and complied with the Canadian tri-council policy on ethics.

2.1.1 Data and code availability

The data and code are available upon direct request of the corresponding author.

2.2 Stimuli

2.2.1 Visual motion stimuli

Visual-motion stimuli were presented on a 43-inch LCD panel 51 inches in front of the participant, subtending a visual angle of 41.23º. The panel had a resolution of 1920 x 1080

(1080p) and refresh rate of 60 Hz. At the beginning of each trial participants were presented with two yellow lines (tracks), demarking driving trajectories extending 35º of visual angle left and 35º right of center (see Figure 1). To simulate a realistic driving environment, a blue sky with white clouds was displayed above the driving tracks. A fixation cross was presented at the center of the display for the entire trial. Visual motion consisted of a first-person view of moving forward along one of the yellow tracks. The timeline was forward left (or right) motion for 700 ms, followed by a 1200 ms pause at the end of the track, which signaled the end of the trial (1900 ms total). At the end of each trial the visual display was reset to the starting point of the two yellow driving tracks.

2.2.2 Physical motion stimuli

A motion simulator provided physical-motion stimuli. The motion simulator pod was supported by a MOOG © platform with six-degrees-of- freedom motion (MOOG series 6DOF2000E; see Inline Supplementary Figure A1). Participants were seated in a bucket-style car seat fixed to the floor of the simulator pod. A button box was used for collecting behavioural responses, which participants held with their thumbs on color- coded buttons to make left/right responses. A camera mounted within the simulator was used to monitor participants throughout the experiment. Participants were provided with earplugs, and white audio noise was played inside the simulator in order to mask the sound of the motors.

Each physical-motion stimulus consisted of a forward linear translation at 35º left or right for 330 ms at 0.1 g (the longest our motion simulator could be moved given the spatial restrictions of the motion platform), followed by a corresponding washout for 1330 ms which returned the pod to the original position (1660 ms total). The acceleration intensity was selected based on preliminary testing to achieve a clear perception of forward motion within the spatial

restrictions of the movement of the platform while avoiding compensating movements of the head, neck or upper body. Physical forward accelerations were well above vestibular thresholds of 0.009 g as discussed by Kingma (2005). The motion force, s(t), was described by:

$$s(t) = \begin{cases} A_1\ 0\ \leq t\ \leq t_p \\ -A_2\ t_p\ \leq t_b \\ A_2\ t_b\ \leq t\ \leq t_e \\ 0\ else \end{cases}$$

where t represents time in seconds, *tp* represents present time, *tb* represents the breakpoint and *te* represents the end time. *A1* describes the initial forward acceleration, -*A2* describes the initial (backwards) acceleration of the washout, and *A2* describes the deceleration of the washout. Acceleration was measured using an Endevco accelerometer (model number 752A13), calibrated to approximately 1 mV/g sensitivity.

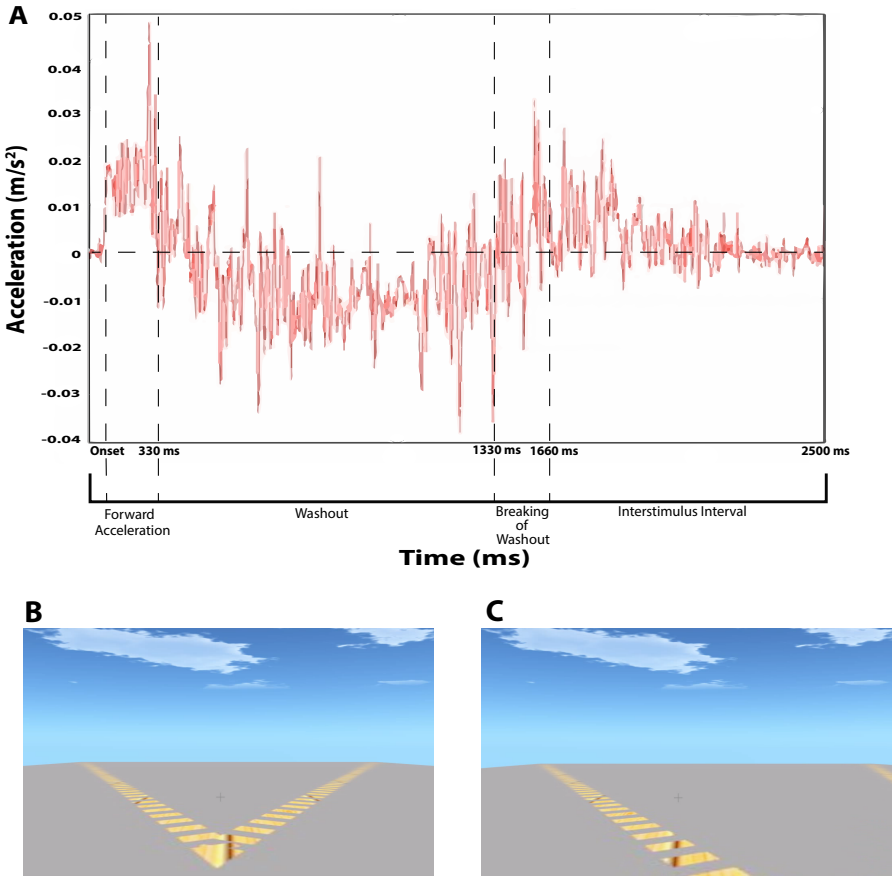

Figure 1. Time course of physical- and visual-motion stimuli. Panel A shows an example of the profile of physical motion measured during a single trial by an accelerometer (red line); the variance shown is due to the high sensitivity of the accelerometer. The x-axis represents time and the y-axis represents acceleration (g 1⁄4 m/s2). The acceleration profile is similar for 35° left and 35° right physical-motion trials. Panel B shows the visual display before motion onset; at this point the participant does not know whether visual motion will indicate travel along the left or right track. Panel C shows a still picture of the dynamic visual motion display at approximately 700 ms for a left visual motion trial.

2.3 Experimental design and behavioural analyses

The present study had a 2 (Modality: Attend visual-motion vs. Attend physical-motion) x 2 (Congruency: Congruent [same direction] vs. Incongruent [opposing directions]) experimental design. To avoid task-switching effects, the attend visual-motion (AV) and attend physical-motion (AP) conditions were separated into blocks. The task required participants to direct attention to either the visual-motion stimulus (attend visual or AV condition) or the physical-motion stimulus (attend physical or AP condition), and respond with a button press to indicate whether the direction of the relevant sensory motion was left or right. There was a practice AP block presented first, followed by 4 experiment blocks. During pilot testing we observed much lower accuracy for the incongruent AP trials in which participants had a difficult time ignoring the incongruent visual stimulus. Therefore, 3 of the 4 experimental blocks were AP compared to 1 AV block. This was done to ensure there would be enough correct trials in the incongruent AP condition for EEG analysis. The order of the 4 blocks was counterbalanced so that an equal number of participants received the AV block first, second, or third.

Within each block, 50% of trials were congruent (i.e., visual- and physical-motion stimuli signaled movement in the same direction, either left or right), and 50% were incongruent (i.e., visual-motion stimuli signaled motion to the left when physical-motion stimuli signaled movement to the right, and vice versa). Trial order was randomized within each block. Behavioural data were analyzed with two 2 x 2 repeated-measures ANOVAs for measures of judgment accuracy and response time.

2.4 Procedure

The entire session was between 1.5 and 2 h in duration. The timeline of the session included collection of demographic information (age, gender, and handedness; 5 min), followed

by completion of one practice block (30 trials; 2 min), application of EEG electrodes (25 min), completion of four experimental blocks (199 trials each; 40 min), and clean up (40 min).

The timeline of each trial was as follows. The trial began with the visual display at the starting position of the two yellow tracks and the motion platform stationary at central position. The onset of visual- and physical-motion was simultaneous on each trial (see Figure 1) signaling forward motion at an angle 35° to the left or right of center. A motion simulator is limited in that it is not possible to accelerate for an extended period of time due to mechanical limitations, but realistic perception of self-motion in a simulator is facilitated by the fact that the brain detects acceleration but not velocity. The physical- and visual-motion stimuli were synchronized as follows. The duration of the visual motion included 330 ms acceleration (to match physical motion acceleration) followed by 370 ms continued motion at the end velocity (700 ms). There was an additional 1200 ms delay at the end of the visual track (1900 ms). This corresponded to the 330 ms physical acceleration, a1000 ms below threshold washout and a 330 ms breaking of the washout (1660 ms). Note that the initial 330 ms acceleration of the physical motion can be thought of as a ramp up to the end velocity; the visual motion was matched so that both are perceived to accelerate for 330 ms followed by a period of continued movement at the end velocity. Overall, each trial lasted 1900 ms, with the visual motion lasting 1900 ms and the physical motion lasting 1660 ms. The inter-trial interval was a random value be- tween 1300 and 1500 ms, during which the motion platform remained at the central position.

To avoid excessive EEG artifacts due to eye movements and blinks, participants fixated on a central fixation cross during the trials and were provided with a blink break every 15 trials.

2.5 EEG data acquisition

EEG data were collected using the BioSemi ActiveTwo electrophysiological system (www.biosemi.com) with 128 sintered Ag/AgCl scalp electrodes. An additional four electrodes recorded eye movements (two placed laterally from the outer canthi and two below the eyes on the upper cheeks). Continuous signals were recorded using an open pass band from direct current to 150 Hz and digitized at 1024 Hz.

2.6 EEG preprocessing

All processing was performed in MATLAB-2014a using functions from EEGLAB (Delorme and Makeig, 2004) on the Shared Hierarchical Academic Research Computing Network (SHARCNET: www.sharcnet.ca). A flowchart illustrating the signal-processing pipeline can be found in the supplementary materials (see Inline Supplementary Figure A2). EEG data were band-pass filtered between 1 and 50 Hz, and epoched from 1000 ms pre-stimulus to 2000ms post-stimulus. Each epoch was baseline corrected using the whole-epoch mean (Groppe et al., 2009). After referencing, channels with a standard deviation exceeding 200μV were interpolated (on average, 0.5 channels interpolated per participant). Bad epochs were rejected if they had voltage spikes exceeding 500 μV, or were rejected by EEGLAB's joint probability functions (Delorme et al., 2007).

Single-subject EEG data were submitted to an extended Adaptive Mixture Independent Component Analysis (AMICA) (Palmer et al., 2012) with an N – (1 þ interpolated channels) Principal Components Analysis reduction. Decomposing an EEG signal into independent components (ICs) allows for analysis of each individual signal produced by the brain that would otherwise be indistinguishable (Desjardins and Segalowitz, 2013). Following AMICA, dipoles were fit to each IC using the fieldtrip plugin for EEGLAB (Oostenveld et al., 2011). ICs for which the dipole fit explained less than 85% of the weight variance, or whose dipoles were

located outside the brain, were excluded from further analysis. On average, 5.2 ICs per subject were excluded from analysis.

2.7 ERSP Measure Projection Analysis

Event-related spectral power (ERSP) was computed for each of the remaining ICs. Fifty log-spaced frequencies between 3 and 50 Hz were computed, with 3 cycles per wavelet at the lowest frequency up to 25 at the highest. Measure Projection Analysis (MPA) was used to cluster ICs across participants using the Measure Projection Toolbox for MATLAB (Bigdely-Shamlo et al., 2013). MPA is a method of categorizing the location and consistency of EEG measures, such as ERSP, across single-subject data into 3D domains. These domains are subsets of ICs that are identified as having spatially similar dipole models, as well as similar ERSP activity (measure-similarity). MPA fits the selected ICs into a 3D brain model comprised of a cubic space grid with 8-mm spacing according to normalized Montreal Neurological Institute (MNI) space. Cortical regions of interest were identified by the MPA toolbox by incorporating the probabilistic atlas of human cortical structures provided by the Laboratory of Neuroimaging Project (Shattuck et al., 2008). Voxels that fell outside of the brain model (muscle artifacts, etc.) were excluded from the analysis.

We then calculated local convergence values, using an algorithm based on Bigdely-Shamlo et al. (2013) to deal with the multiple com- parisons problem. Local convergence calculates the measure-similarity of dipoles within a given domain and compares them with randomized dipoles. In order to compare dipoles, a pairwise IC similarity matrix was created by estimating the signed mutual information between independent component-pair ERSP measure vectors, assuming a Gaussian distribution. As explained in detail by Bigdely-Shamlo et al. (2013), signed mutual information was estimated to improve the spatial smoothness of the

obtained MPA significance value beyond determining similarity of dipoles through correlation. We used bootstrap statistics to obtain a significance threshold for convergence at each location of our 3D brain model. Following past literature, we set the raw voxel significance threshold to $p <$ .001 (Bigdely-Shamlo et al., 2013; Chung et al., 2017).

For each domain calculated by MPA, ERSP was computed for each experimental condition. Within each domain, bootstrap statistics were used to assess differences in ERSP between conditions to uncover main effects of modality and congruency. Differences at each power band were computed by projecting the ERSP for each condition to each voxel in the domain. For each participant, this projection was weighted by dipole density per voxel and then normalized by the total domain voxel density. Analysis of projected source measures were separated into discrete spatial domains by threshold-based Affinity Propagation clustering based on a similarity matrix of pair-wise correlations between ERSP measure values for each position. Following Chung et al. (2017), we used the maximal exemplar-pair similarity, which ranges from 0 to 10 to set a value of 0.8 (Bigdely-Shamlo et al., 2013; Chung et al., 2017; Ofori et al., 2015).

2.8 Stimulus validation

Perception of the onset of vestibular stimuli is a slower process than perception of the onset of visual stimuli (Barnett-Cowan and Harris, 2009, 2013). In our experiment, the onset and acceleration of movement of the physical and visual stimuli were synchronous to simulate a realistic experience. Because our interest was focused on performance based on selective attention when both physical and visual cues were present, it was important to make sure that the cues to motion in the two tasks (attend visual vs. attend physical motion) were equally salient. To

this end, we collected a set of behavioural data prior to the EEG experiment to compare accuracy of responses to our visual- and physical-motion stimuli.

Twenty-one participants (12 female) were tested in two conditions. In the visual-motion condition there was no physical motion; the simulator was parked. In the physical-motion condition there was no visual motion; the yellow tracks were removed from the screen. All other aspects of the experiment were the same as the EEG experiment, including central fixation cross, timing parameters, and task. There was no difference in accuracy between visual- and physical-motion responses (M = 99% in both conditions), which supports the assumption that the salience of the physical-motion stimuli and the visual-motion stimuli were comparable in our experiment. Response time is not as diagnostic because we know that perception of physical motion is slower than visual motion (Barnett-Cowan and Harris, 2009). As expected, participants were slower to respond in the physical-motion condition (M = 1212 ms, SE = 114.41), than the attend-physical than the visual-motion $t(20) = 3.76$, $p < .01$.

3. Results

We first analyzed accuracy and response times for the whole group. Based on the accuracy results, we identified two groups with differing abilities to ignore the prepotent visual motion information (high vs. low accuracy in the incongruent AP condition). We first present the whole group analysis (section 3.1). We then present a statistical comparison of the high and low accuracy groups (section 3.2). The focus of the remainder of the analyses is on the high-accuracy group (section 3.3).

3.1 Behavioural results for total sample

Initial 2 x 2 repeated-measures ANOVAs examined Modality (attend- visual vs. attend-physical) by Congruency (congruent vs. incongruent) for accuracy and response time.

Participants were more accurate at discriminating direction in the attend-visual condition (M = 99%, SE = 0.17) than the attend-physical condition (M = 74%, SE = 2.38), $F(1, 42) = 117.65$, $p < .001$, $\eta^2_p = 0.74$, and more accurate during congruent trials (M = 96%, SE = 0.47) than incongruent trials (M = 77%, SE = 2.38), $F(1, 42) = 61.34$, $p < .001$, $\eta^2_p = 0.59$. There was a significant modality x congruency interaction $F(1, 42) = 62.48$, $p < .001$, $\eta^2_p = 0.60$. Fisher's least significant difference (LSD) revealed that participants were significantly more accurate in the congruent attend-physical condition (M = 93%, SE = 0.94) than the incongruent attend-physical condition (M = 55%, SE = 4.69) ($p < .001$), however there was no significant difference in accuracy between the congruent (M = 99%, SE = 0.12) and incongruent (M = 99%, SE = 0.25) attend-visual conditions (see Table 1).

Participants were faster at discriminating direction in the attend- visual condition (M = 810 ms, SE = 49.67) than the attend-physical condition (M = 1257 ms, SE = 43.08), $F(1, 42) = 111.39$, $p < .001$, $\eta^2_p = 0.73$, and faster during congruent trials (M = 1003 ms, SE = 42.06) than incongruent trials (M = 1065 ms, SE = 41.57), $F(1, 42) = 27.33$, $p < .001$, $\eta^2_p = 0.39$. There was a significant modality x congruency interaction $F(1, 42) = 22.30$, $p < .01$, $\eta^2_p = 0.35$. LSD revealed that response times were significantly shorter in the congruent attend- physical condition (M = 1199 ms, SE = 43.77) than the incongruent attend-physical condition (M = 1316ms, SE = 45.24) ($p<.001$), how- ever there was no significant difference in response time between the congruent (M = 807 ms, SE = 49.19) and incongruent (M = 814 ms, SE = 50.38) attend-visual conditions. Table 1 shows mean accuracy and response times between conditions.

3.2 High-vs. low-accuracy group comparison

3.2.1 Behavioural results for high-vs. low-accuracy groups

Due to the large accuracy difference between the incongruent AP condition and the other conditions, we looked at the data from the incongruent AP condition more closely. Within this condition we observed accuracy differences that ranged between 5% and 93%. Further analysis indicated that some individuals were not successfully ignoring the incongruent visual motion when performing in the AP condition. To test this hypothesis, we compared two groups created by selecting high- (> 70% accuracy, $n = 16$) and low-accuracy (< 30% accuracy, $n = 11$) participants based on accuracy in the incongruent AP condition. The remaining 10 participants were discarded for the high-vs. low-accuracy comparison.

It was not the case that low-accuracy participants were incorrectly attending to the visual motion instead of the physical motion in the incongruent AP condition. If they were, we would expect response times to be similar between the incongruent AV and incongruent AP conditions. However, a 2 (high-vs. low-accuracy groups) x 2 (Modalities: attend-visual vs. attend-physical) x 2 (Congruency: congruent vs. incongruent) mixed ANOVA showed that response times across all trials (correct and incorrect) did not differ between high- and low-accuracy groups. Response times were faster in the attend-visual condition ($M = 764$ ms, $SE = 66.53$) compared to the attend-physical condition ($M = 1125$ ms, $SE = 53.05$), $F(1,23) = 37.38$, $p < .001$, $\eta^2_p = 0.62$ for both high- and low-accuracy participants, suggesting that low-accuracy participants attempted to attend to the direction of the physical motion but failed to ignore the direction of the visual motion. This hypothesis is supported by the comparison of ERSP for high-vs. low-accuracy.

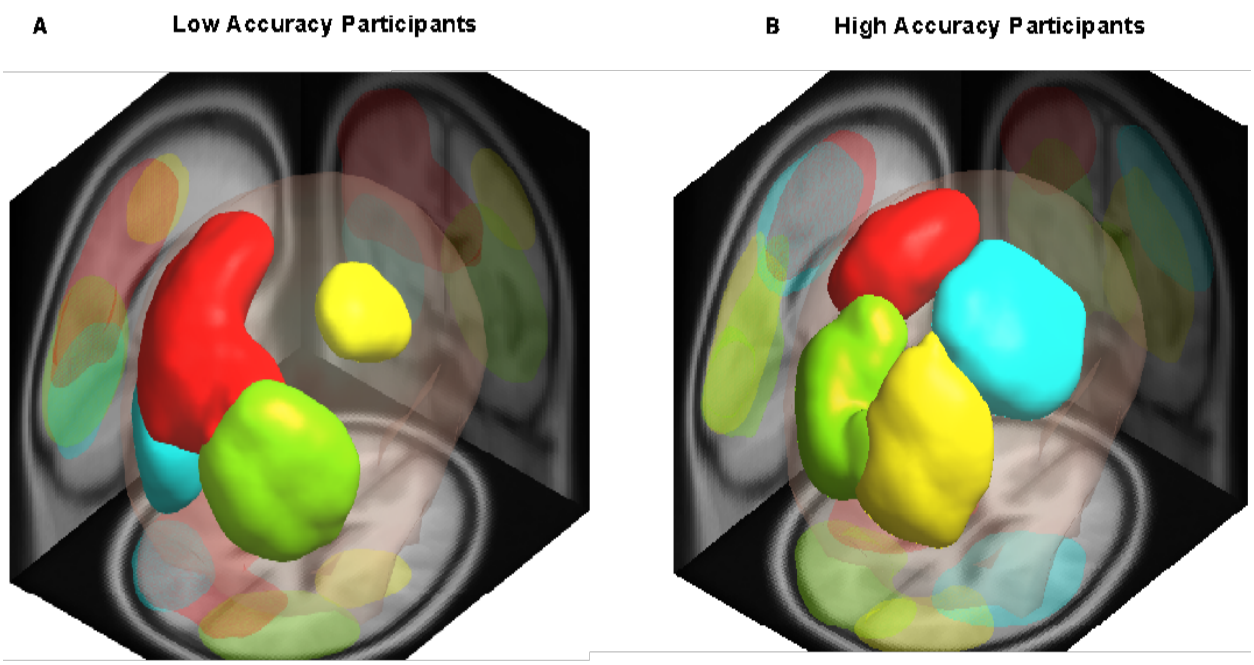

Figure 2. MPA (Measure Projection Analysis) domains for low-accuracy and high-accuracy participants. Note that domains are ranked in terms of dipole density, with red being the densest, followed by green, blue and yellow respectively. Panel A shows a 3D representation of the brain model for low-accuracy participants. The red region represents the MPA domain with the greatest concentration of dipoles consistent with left dorsal posterior cingulate cortex (Brodmann area [BA] 31). The yellow region represents the MPA domain with the greatest concentration of dipoles consistent with right primary motor and primary somatosensory cortices (BA 4 and 3). The blue region represents the MPA domain with the greatest concentration of dipoles consistent with left associative visual and occipitotemporal area (BA 19 and 37). The green region represents the MPA domain with the greatest concentration of dipoles consistent with right secondary visual (V2), and associative visual (V3) areas (BA 18 and 19). Panel B shows a 3D representation of the brain for high-accuracy participants. The red region represents the MPA domain with the greatest concentration of dipoles consistent with left premotor and supplementary motor and primary motor cortex (BA 6 and 4). The blue region represents the MPA domain with the greatest concentration of dipoles consistent with right primary somatosensory and primary motor cortex (BA 3 and 4). The green region represents the MPA domain with the greatest concentration of dipoles consistent with left secondary visual (V2), and associative visual (V3) areas (BA 18 and 19). The yellow region represents the MPA domain with the greatest concentration of dipoles consistent with right secondary visual (V2), and associative visual (V3) areas (BA 18 and 19).

3.2.2 Oscillatory power (ERSP) for high-vs. low-accuracy groups

All domains identified by the Measure Projection Analysis (MPA) in both high- and low-accuracy participants are shown in Figure 2. In Figure 3 we show the left motor areas of the high- and low-accuracy participants to provide a side-by-side comparison of how attending to a specific stimulus affected the ERSP activity in both groups. All ERSP is representative of a difference in oscillatory power compared to baseline (pre-trial) ERSP activity, where an ERS (event-related synchronization) represents more spectral power than baseline and an ERD (event-related desynchronization) represents less spectral power than baseline. We only show the left motor areas for the two groups because 1) the left motor area has the highest dipole density for both groups, and 2) there are no other MPA domains that have significant differences between conditions within the low-accuracy group (see Inline Supplementary Figures A3 and A4 for a complete MPA analysis of the low-accuracy participants). In Figure 3, Panel A shows the left motor area in low-accuracy participants, which has the highest dipole density in dorsal posterior cingulate cortex (Brodmann area [BA] 31), and Panel D shows the left motor area in high-accuracy participants, which has the highest dipole density in somatosensory and primary motor cortex (BA 3 and 4). In Panels B, C (low-accuracy), E and F (high-accuracy) we show the associated ERSP plots for the congruent attend-physical (CAP) versus the congruent attend-visual (CAV), and incongruent attend-physical (IAP) versus the incongruent attend-visual (IAV) conditions. The ERSP plots are followed by boot- strapped comparisons between conditions for low- and high-accuracy participants within the left motor areas of both groups.

Theta-band activity: Comparing attend-visual with attend-physical in the congruent condition (CAV vs. CAP), the CAV condition elicited greater theta ERD ($p < .05$) from ~500 ms to 600 ms post-stimulus compared to CAP in low-accuracy participants (Panel B). There were

different findings in the theta band for high-accuracy participants. Comparing the CAV versus the CAP, the CAV condition elicited greater theta ERS from ~100 ms to 500 ms post-stimulus (Panel E). No differences in theta were found when comparing attend-visual with attend-physical in the incongruent condition (IAV vs. IAP) in low-accuracy (Panel C) or high-accuracy participants (Panel F).

Alpha-band activity: Both low- and high-accuracy groups showed similar differences within the alpha-band when attending to visual vs. physical motion, but to different extents. For low-accuracy participants, the CAV condition elicited greater alpha ERD than CAP from stimulus onset to ~250 ms post-stimulus. This effect was due to an earlier onset of alpha ERD in the CAV condition (Panel B). When comparing IAV vs. IAP, there were no effects in the alpha band for low-accuracy participants (Panel C). High-accuracy participants showed a similar latency difference in alpha ERD but with more robust differences. Comparing the CAP versus the CAV, the CAV condition elicited greater alpha ERD ($p < .05$) from stimulus onset to ~600 ms post stimulus than the CAP condition (Panel E). A similar effect was observed when comparing the IAP and IAV conditions; IAV elicited greater alpha ERD ($p < .05$) from stimulus onset to ~600 ms post stimulus (Panel F).

Beta-band activity: For low-accuracy participants, the CAV condition elicited greater beta ERS than CAP from ~500 ms to ~1100 ms post- stimulus (Panel B), and similarly the IAV condition elicited greater beta ERS than IAP from ~600 ms to 1000 ms post-stimulus (Panel C). High-accuracy participants showed a different activity pattern in the beta band compared to low-accuracy participants. While attending to the physical motion, high-accuracy participants produced a longer lasting beta ERD that created more robust effects. The CAP condition elicited greater beta ERD than CAV from ~500 ms to the end of the trial (Panel E). The same effect was

found when comparing IAV vs. IAP, the IAP condition elicited greater beta ERD from ~500 ms to the end of the trial (Panel F).

The data clearly show that attending to visual versus physical motion stimuli elicited differences in spectral power within the high-accuracy participants. There were robust differences in theta, alpha and beta power between sensory modalities. In comparison, the low-accuracy participants showed minimal differences in spectral power between the same conditions. Moreover, these effects were only found in the left motor area; there were no differences between AP and AV conditions in the right motor area (see Appendix, Figure A3). There were also no congruency-related differences in the occipital regions within low- accuracy participants (see Inline Supplementary Figure A4). Even though low-accuracy participants were slower to respond when making heading judgments in the AP condition, their spectral power for the AP condition resembles the spectral power of the AV condition for both low- and high-accuracy participants. It is possible that these results reveal a bias towards greater weighting of visual-motion stimuli in low-accuracy participants. This bias could have potentially led to difficulties with ignoring the incongruent visual stimulus, and thus low accuracy in the IAP condition.

Only data from the high-accuracy group were included for the remainder of the analyses.

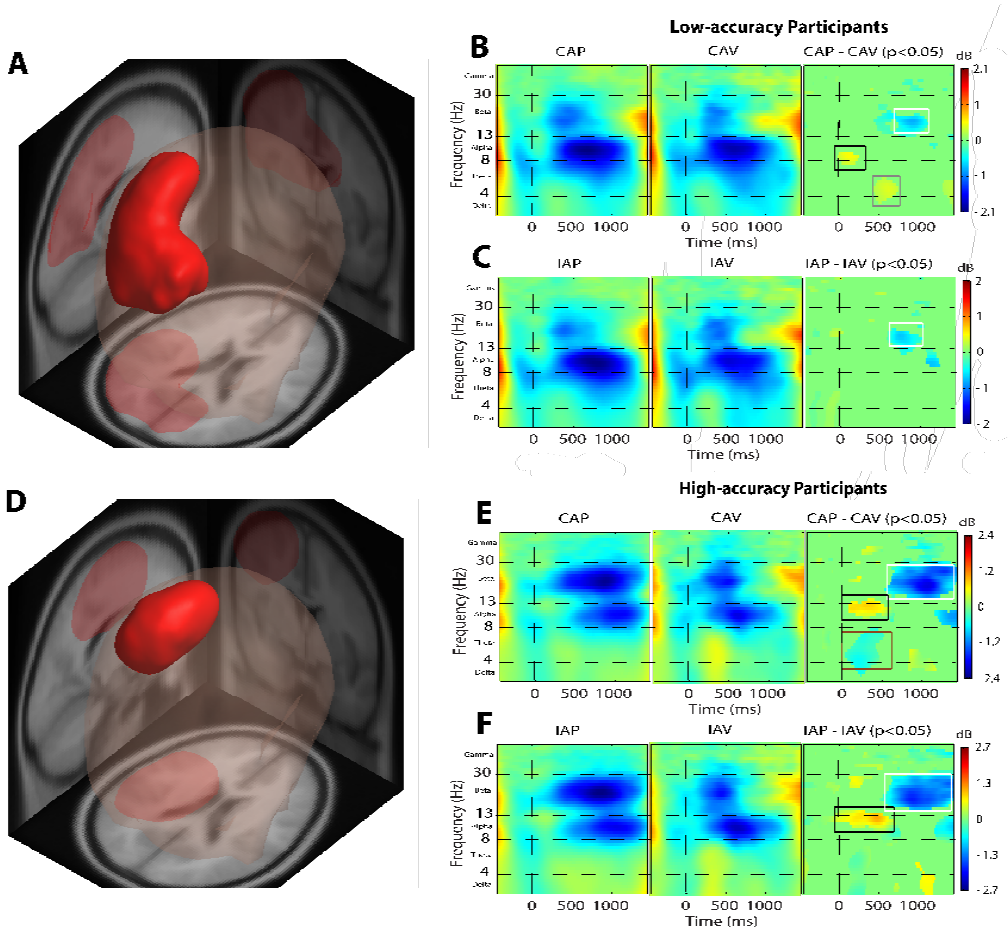

Figure 3. Left motor areas identified by MPA and their respective ERSP analysis for low-accuracy (Panels A, B, and C) and high-accuracy (Panels D, E, and F) participants. The ERSP plots show time (ms) across the x-axis and frequency of the EEG signal along the y-axis. Panels B, C, E, and F show the associated ERSP plots for the congruent and incongruent attend-physical (CAP, IAP) and attend-visual (CAV, IAV) conditions, and the bootstrapped comparisons ($p < 0.05$) between attend-physical and attend-visual conditions (CAP – CAV; IAP – IAV). ERS power is depicted in yellow/red, ERD power is depicted in blue, and green shows no difference in spectral power compared to baseline. Low-accuracy participants: Panel A shows a 3D representation of the brain model with the red region representing the MPA domain with the greatest concentration of dipoles consistent with left dorsal posterior cingulate cortex (BA 31). In Panel B, results of bootstrapped comparisons contrasting CAP with CAV are highlighted in the white square, showing significantly more beta ERD in the CAP condition. The black square highlights significantly more alpha ERD in the CAV condition (note that due to subtraction CAP-CAV, greater ERS power in CAV is represented in blue and greater ERD power in CAV is represented in yellow/red). The grey square highlights significantly more theta ERD in the CAV condition. Panel C: The white square highlights significantly more beta ERD in the IAP condition. High-accuracy participants: Panel D shows a 3D representation of the brain with the red region representing the MPA domain with the greatest concentration of dipoles consistent with left premotor and supplementary motor and primary motor cortex (BA 6 and 4) for high-accuracy participants. Panel E: The white square highlights significantly more beta ERD in the CAP condition. The black square highlights significantly more alpha ERD in the CAV condition. The brown square highlights significantly more theta ERS in the CAV condition. Panel F: The white square highlights significantly more beta ERD in the IAP condition. The black square highlights significantly more alpha ERD in the IAV condition.

3.3 Results for high-accuracy group

High-accuracy participants were analyzed separately to more effectively observe differences between successful responses in the attend- visual and attend-physical conditions.

3.3.1 Behavioural results (high-accuracy group)

Participants were more accurate at discriminating direction in the attend-visual condition (M = 99%, SE = 0.15) than the attend-physical condition (M = 88%, SE = 1.29), $F(1, 15) = 70.61$, $p < .001$, $\eta^2_p = 0.83$, and more accurate during congruent trials (M = 96%, SE = 0.67) than incongruent trials (M = 91%, SE = 0.91), $F(1, 15) = 26.40$, $p < .001$, $\eta^2_p = 0.64$. There was a significant modality x congruency interaction $F(1, 15) = 27.19$, $p < .001$, $\eta^2_p = 0.64$. LSD revealed that participants were significantly more accurate in the congruent attend-physical condition (M = 93.60%, SE = 0.88) than the incongruent attend-physical condition (M = 84.14%, SE = 1.30) ($p < .01$), however there was no significant difference in accuracy between the congruent (M = 99.59%, SE = 0.60) and incongruent (M = 99.73%, SE = 0.69) attend-visual conditions (see Table 1).

Participants were faster at discriminating direction in the attend- visual condition (M = 802 ms, SE = 87.05) than the attend-physical condition (M = 1286 ms, SE = 55.91), $F(1, 15) = 38.89$, $p < .001$, $\eta^2_p = 0.72$, and faster during congruent trials (M = 1012 ms, SE = 60.78) than incongruent trials (M = 1076 ms, SE = 63.78), $F(1, 15) = 30.05$, $p < .001$, $\eta^2_p = 0.67$. There was a significant modality x congruency interaction $F(1, 15) = 15.02$, $p < .01$, $\eta^2_p = 0.50$. LSD revealed that response times were significantly shorter in the congruent attend- physical condition (M = 1256ms, SE = 63.72) than the incongruent attend-physical condition (M = 1341 ms, SE = 64.10) ($p < .01$), however there was no significant difference in response time between the congruent (M = 788 ms, SE = 76.39) and incongruent (M = 815 ms, SE = 83.60) attend-visual conditions.

Table 1 shows mean accuracy and response times between conditions.

Accuracy (percent correct)

	CAV	IAV	CAP	IAP
High	99 (0.60)	99 (0.69)	94 (0.88)	84 (1.30)
Low	99 (0.61)	98 (0.97)	95 (1.16)	12 (1.80)
All	99 (0.12)	99 (0.25)	93 (0.94)	55 (4.69)

Response times (ms)

	CAV	IAV	CAP	IAP
High	788 (76)	815 (84)	1256 (64)	1341 (64)
Low	728 (101)	724 (111)	946 (85)	956 (85)
All	807 (49)	814 (50)	1199 (44)	1316 (45)

Table 1. Behavioural means. Accuracy (percent correct) and response times (ms) are shown for groups (high-accuracy [High], low-accuracy [Low] and all participants [All]), by conditions: congruent attend-visual (CAV), incongruent attend-visual (IAV), congruent attend-physical (CAP), and incongruent attend-physical (IAP). Standard errors are represented in brackets.

3.3.2 Oscillatory power (ERSP) for high-accuracy group

In Figure 4 we show the left and right motor areas of the high-accuracy participants to provide a side-by-side comparison of how attending to a specific stimulus affected the ERSP activity in both MPA domains. These were the only two domains that showed a significant main effect of modality. In Figure 4, Panel A shows the left premotor and supplementary motor and primary motor cortex (BA 6 and 4), and Panel D shows the right motor area, consistent with the somatosensory and primary motor cortex (BA 3 and 4). In Panels B, C (left motor), E and F (right motor) we show the associated ERSP plots for the congruent attend-physical (CAP) versus the congruent attend-visual (CAV), and incongruent attend- physical (IAP) versus the

incongruent attend-visual (IAV) conditions. The ERSP plots are followed by bootstrapped comparisons between conditions for left and right motor areas.

Theta-band activity: Comparing CAV versus CAP, the CAV condition elicited greater theta ERS ($p < .05$) from ~100 ms to 500 ms post-stimulus compared to CAP in the left motor area (Panel B). There were different findings in the theta band for the right motor area. Comparing the CAV versus the CAP, the CAP condition elicited greater theta ERS from ~600 ms to ~1000 ms post-stimulus (Panel E). No differences in theta were found when comparing attend-visual with attend-physical in the incongruent condition (IAV vs. IAP) in the left motor (Panel C), however, in the right motor area, IAP elicited greater theta ERS from ~600 ms to ~1000 ms post-stimulus than IAV (Panel F).

Alpha-band activity: Both left and right motor areas showed similar differences within the alpha-band when attending to visual vs. physical motion. For the left motor area, the CAV condition elicited greater alpha ERD ($p < .05$) from stimulus onset to ~600 ms post stimulus than the CAP condition (Panel B). Comparing the CAP versus the CAV in the right motor area, the CAV condition elicited greater alpha ERD ($p < .05$) from stimulus onset to ~200 ms post stimulus than the CAP condition (Panel E). When comparing IAV vs. IAP, both the left and right motor areas showed greater alpha ERD from stimulus onset to ~600 ms post stimulus (Panels C and F).

Beta-band activity: Differences in beta-band activity were the same for each comparison. When comparing CAV versus CAP (Panels B and E), and IAV versus IAP (Panels C and F), the AP conditions elicited greater beta ERD ($p < .05$) from ~600 ms to 1500 ms post-stimulus in both the left and right motor areas.

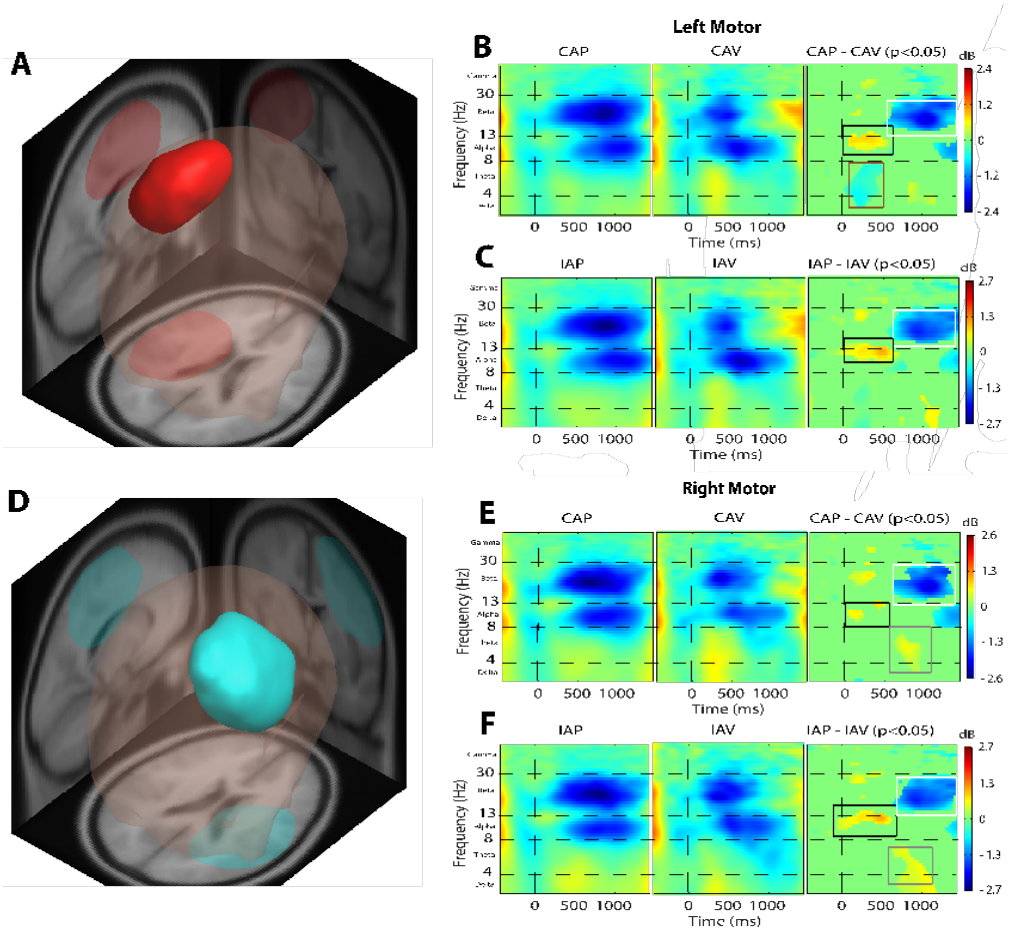

Figure 4. Left (Panels A, B, and C) and right (Panels D, E, and F) motor area identified by MPA and respective ERSP analysis in high-accuracy participants. The ERSP plots show time (ms) across the x-axis and frequency of the EEG signal along the y-axis. Panels B, C, E, and F show the associated ERSP plots for the congruent and incongruent attend-physical (CAP, IAP) and attend-visual (CAV, IAV) conditions, and the bootstrapped comparisons ($p < 0.05$) between attend-physical and attend-visual conditions (CAP – CAV; IAP – IAV). **Left motor area:** Panel A shows a 3D representation of the brain with the red region representing the MPA domain with the greatest concentration of dipoles consistent with left premotor and supplementary motor and primary motor cortex (BA 6 and 4). Panel B: Results of bootstrapped comparisons contrasting CAP with CAV are highlighted in the white square, showing significantly more beta ERD in the CAP condition. The black square highlights significantly more alpha ERD in the CAV condition (note that due to subtraction CAP-CAV, greater ERS power in CAV is represented in blue and greater ERD power in CAV is represented in yellow/red). The brown square highlights significantly more theta ERS in the CAV condition. Panel C: The white square highlights significantly more beta ERD in the IAP condition. The black square highlights significantly more alpha ERD in the IAV condition. **Right motor area:** Panel D shows a 3D representation of the brain with the blue region representing the MPA domain with the greatest concentration of dipoles consistent with right primary somatosensory and primary motor cortex (BA 3 and 4). Panel E: The white square highlights significantly more beta ERD in the CAP condition. The black square highlights significantly more alpha ERD in the CAV condition. The grey square highlights significantly more theta ERR in the CAP condition. Panel F: The white square highlights significantly more beta ERD in the IAP condition. The black square highlights significantly more alpha ERD in the IAV condition. The grey square highlights significantly more theta ERS in the CAP condition.

In Figure 5 we show the left and right occipital areas of the high- accuracy participants to provide a side-by-side comparison of how stimulus congruency affected the ERSP activity in both MPA domains. These were the only two domains that showed a significant main effect of congruency. In Figure 5, Panel A shows the left occipital area that is consistent with the secondary visual (V2), and associative visual (V3) areas (BA 18 and 19), and Panel D shows the right occipital area, also consistent with the secondary visual (V2), and associative visual (V3) areas (BA 18 and 19). In Panels B, C (left occipital), E and F (right occipital) we show the associated ERSP plots for the incongruent attend- physical (IAP) versus the congruent attend-physical (CAP), and incongruent attend-visual (IAV) versus the congruent attend-visual (CAV) conditions. The ERSP plots are followed by bootstrapped comparisons between conditions for left and right occipital areas.

Theta-band activity: Comparing IAP versus CAP, the IAP condition elicited greater theta ERD ($p < .05$) from ~100 ms to 500 ms post-stimulus compared to CAP in the left occipital area (Panel B). Congruency did not elicit any ERSP differences in any other MPA domain (Panels C, E and F).

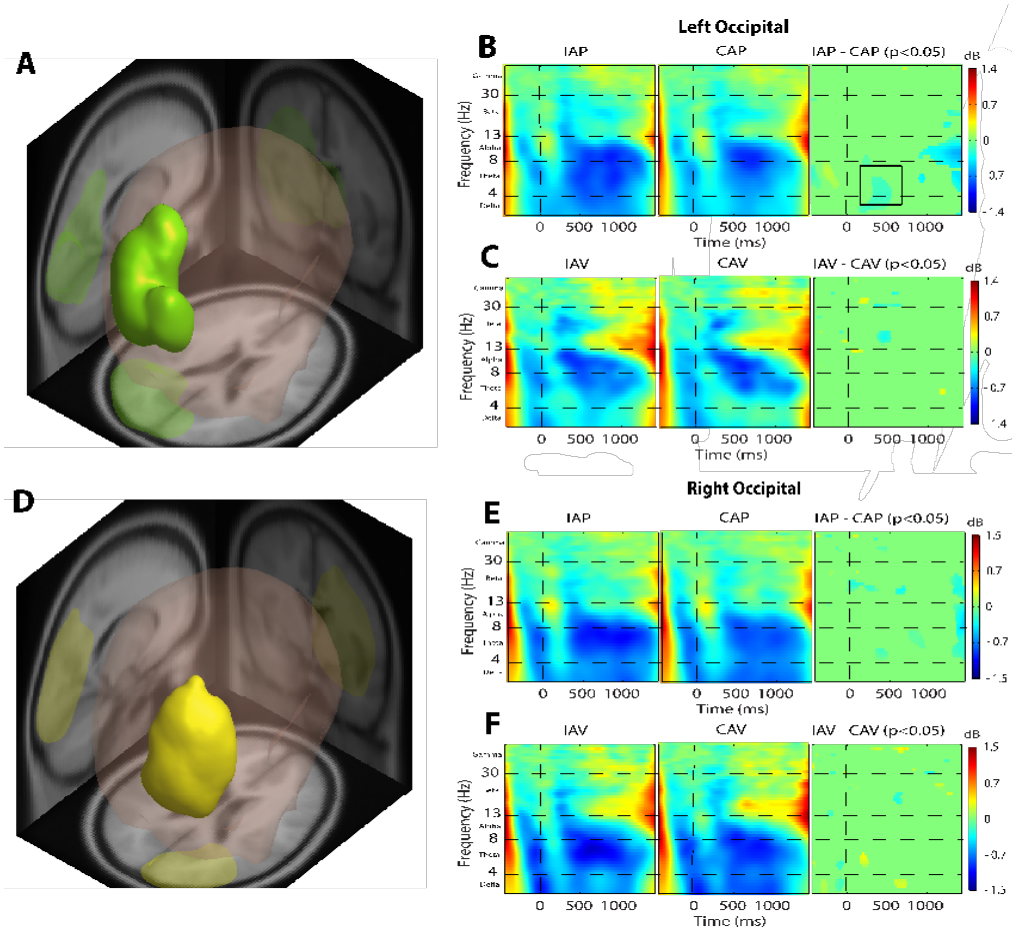

Figure 5. Left (Panels A, B, and C) and right (Panels D, E, and F) occipital area identified by MPA and respective ERSP analysis in high-accuracy participants. The ERSP plots show time (ms) across the x-axis and frequency of the EEG signal along the y-axis. Panels B, C, E, and F show the associated ERSP plots for the incongruent and congruent attend-physical (IAP, CAP) and attend-visual (IAV, CAV) conditions, and the bootstrapped comparisons ($p < 0.05$) between incongruent and congruent conditions (IAP – CAP; IAV – CAV). ERS power is depicted in yellow/red, ERD power is depicted in blue, and green shows no difference in spectral power compared to baseline. **Left occipital area:** Panel A shows a 3D representation of the brain with the green region representing the MPA domain with the greatest concentration of dipoles consistent with left secondary visual (V2), and associative visual (V3) areas (BA 18 and 19). Panel B: Results of bootstrapped comparisons comparing IAP with CAP are highlighted in the black square, showing significantly more theta ERD in the IAP condition. Panel C: There are no significant effects of congruency. **Right occipital area:** Panel D shows a 3D representation of the brain with the yellow region representing the MPA domain with the greatest concentration of dipoles consistent with right secondary visual (V2), and associative visual (V3) areas (BA 18 and 19). Panel E and F: There are no significant effects of congruency.

4. Discussion

We present the first high-density electrophysiological study to explore the effects of attention and congruency on the perception of multisensory self-motion. We combined visual- and physical-motion stimuli in a direction discrimination task in which attention was directed either to visual- or physical-motion cues. The direction of self- motion in the attended modality was either congruent or incongruent with the direction of self-motion in the ignored modality.

We were able to compare ERSP in the conditions with conflicting motion cues to ERSP in the congruent self-motion conditions and observe oscillatory differences elicited by attending to one motion cue and ignoring the other.

4.1 Beta oscillations in physical motion processing

The time-course of beta oscillations during motor output has drawn attention over the past several decades (for review see Kilavik et al., 2013). During static hold (holding a single posture), beta oscillations show an increase in power about 300 ms after stabilization following the beta ERD elicited by the movement that produced the form of the given posture. The time period leading up to a movement that terminates the static hold (planning the movement) is characterized by a gradual decrease in beta power, reaching a peak ERD at movement onset. This pre-movement beta ERD may be modulated by uncertainty about the direction of the forthcoming movement (Tzagarakis et al., 2010). For example, using an instructed-delay reaching task with one or multiple possible target directions, Tzagarakis et al. (2010) demonstrated that the pre-movement beta ERD was greater if the participant was uncertain of the required direction of movement during the pre-movement phase of the task.

Consistent with these time-course studies, beta ERD is strongest during movement execution and during changes in isometric muscle contraction (Alegre et al., 2002; Ofori et al.,

2015; Tzagarakis et al., 2010). It lasts until the movement is complete, and is typically observed bilaterally over sensorimotor areas (Salmelin and Hari, 1994; Stancak and Pfurtscheller, 1996). Beta power rapidly increases if movement is not performed, for example after presentation of a No-Go signal (Alegre et al., 2004), or as soon as the muscle contraction or posture stabilizes (Baker et al., 1999). This increase in beta power following the offset of movement is known as beta rebound, and it typically occurs 300–1000 ms post-movement (for review see Kilavik et al., 2013). The power of the beta rebound seems to parallel the speed of the preceding movement (Parkes et al., 2006), although some investigators have reported no difference between varying speeds of movements (Stancak and Pfurtscheller, 1996). Similar to the motor imagery beta ERD described by Nakagawa et al. (2011), the beta rebound has also been demonstrated in motor imagery tasks (Solis-Escalante et al., 2012). A hypothesis proposed by Gaetz and Cheyne (2006), is that the function of beta rebound may be to recalibrate or reset the motor system to new conditions, in order to prepare for a subsequent movement. After the onset of beta rebound, the beta oscillation cycle begins again with the preparation for a new movement.

The present study observed this bilateral beta ERD after stimulus onset regardless of the attentional requirements of the condition or high versus low accuracy group. This finding is not surprising, as each condition delivered identical physical motion stimuli. In high-accuracy participants, there were no significant differences in beta ERD between the attend-physical and attend-visual conditions until 600ms post- stimulus. Beginning at about 600 ms post-stimulus, a higher amplitude beta ERD was found in the motor areas when participants attended to physical- vs. visual-motion stimuli. The only difference between the attend-physical and attend-visual conditions was an instruction difference in which participants were informed which sensory modality to attend (i.e. the motion stimuli were identical), so the difference in beta ERD is

unlikely to be due to sensory stimuli alone. We believe this finding reflects increased and longer lasting motor processing because attending to the physical-motion information is more difficult than attending to the visual-motion information. Moreover, in high-accuracy participants, there was a significant difference in beta power at an even later stage (>1000 ms post-stimulus). This can be described as follows. As described above, a large beta ERD was observed beginning about 600 ms in both the attend-physical condition and the attend-visual condition. When participants attended the physical motion, the beta ERD maintained until the end of the trial. In contrast, when participants attended the visual motion, there was a noticeable beta ERS (beta rebound) beginning around 1000 ms (see Figure 4). There may be two possible explanations for this difference in beta power between the attend-physical and attend- visual conditions. If observation of beta rebound reflects termination of motion output (Kilavik et al., 2013), it may be that sustained attention to the physical motion suppressed the beta rebound. This hypothesis would support motor imagery studies that show beta ERD can be elicited by a top-down activation of the motor area entirely through attention, in the absence of physical motion (Nakagawa et al., 2011; Koelewijn et al., 2008). In our experiment the motion simulator was completing the washout phase during the beta rebound, which may still be consistent with the hypothesis mentioned above, in which the function of beta rebound recalibrates the motor system to new conditions (Gaetz and Cheyne, 2006). However, in that case we would expect to observe beta rebound in both attention conditions. Alternatively, the observation of beta rebound in the attend-visual condition, when attention was directed to the visual motion, might be part of a mechanism to suppress the ignored physical motion processing. Considering that the integration of the visual and vestibular systems is a subadditive process (Angelaki et al., 2009; Morgan et

al., 2008), this robust beta ERS (beta rebound) might reflect an inhibitory process during visual-vestibular integration in which visual motion is weighted greater than vestibular motion.

Low-accuracy participants did not show the same differences in beta oscillatory power between modalities. Although they showed slight modality differences in beta oscillations in the left motor cortex, the differences were minimal and were not found in any other MPA domain. It is possible that the difference between high- and low-accuracy participants is that the low-accuracy participants attended to the visual motion stimuli, regardless of whether the condition required visual or vestibular attention. We propose, however, that since low-accuracy participants responded significantly slower during the attend-physical condition, that they were at least attempting to attend to the physical motion. We suggest that low-accuracy participants had difficulties inhibiting the processing of the visual motion during the attend-physical condition, which led to poor performance in the incongruent attend- physical condition. We observed beta ERD for about 700 ms followed by a beta ERS in every condition with the low-accuracy participants. If we are correct and low-accuracy participants have difficulty inhibiting visual processing, our finding supports the hypothesis that the beta rebound might be part of a mechanism to inhibit physical-motion processing during visual-vestibular integration.

4.2 Alpha oscillations in motor processing

Alpha ERD has been associated with high focal cortical activation, while alpha ERS has been associated with deactivation or inhibition, particularly within task-irrelevant brain areas (Klimesch, 2012). For example, Foxe et al. (1998) presented participants with audio-visual stimuli in a multisensory selective attention paradigm. They showed alpha ERD over parieto-occipital sites (associated with visual attention) during an attend-visual condition, while the uninvolved brain regions showed alpha ERS. Conversely, they found alpha ERS in the parieto-

occipital area induced by the same stimuli during an attend-auditory condition. This oscillatory alpha pattern has also been shown in the motor cortex when Pfurtscheller (1992) observed alpha ERD during execution of hand motor tasks. In the same experiment, during visual tasks, Pfurtscheller (1992) observed alpha ERD at posterior-parietal areas (non-motor) and alpha ERS over hand motor regions. However, it should be noted that alpha ERD in task-relevant brain areas tends to have the greatest power in visual tasks compared to other sensory modalities (Klimesch et al., 2007).

Alpha ERD can also be evoked by the onset of visual motion stimuli (Vilhelmsen et al., 2015). This association was demonstrated by Vilhelmsen et al. (2015) when participants passively viewed an optic flow pattern consisting of a virtual road with poles at both sides to enhance the subjective experience of visual forward motion. Three conditions consisted of different driving speeds (25, 50, and 75 km/h) followed by a static control condition. Vilhelmsen et al. (2015) found alpha ERD in the visual-motion conditions compared to alpha ERS in the static control within the midline parietal region. No differences in alpha power were found between motion speeds.

The present study found robust alpha ERD in every condition within the left and right motor and occipital regions. The alpha ERD within occipital regions was not modulated by the attended modality, or stim- ulus congruency, so the discussion of alpha power is restricted to motor regions. We found significantly greater alpha ERD (between 0 and 600 ms) in both motor cortices (there were no lateralized effects) when participants attended to visual motion compared to physical motion. This is likely due to the fact that in the attend-visual condition, alpha ERD began at stimulus onset, whereas in the attend-physical condition the induced alpha ERD had a later onset (~450 ms post-stimulus). This latency difference between conditions produces the

alpha ERD differences shown in the subtraction boxes of Fig. 4. Others have demonstrated that the motor regions produce alpha ERD during processing of both visual and physical motor output when presented separately (Vilhelmsen et al., 2015; Pfurtscheller, 1992; Ofori et al., 2015). The alpha ERD latency difference in the attend-visual versus attend-physical conditions in our experiment likely represents an attentional effect on cortical activation associated with different processes (i.e., visual and physical motion pro- cessing). This latency hypothesis is consistent with Barnett-Cowan and Harris (2009) who demonstrated that perception of visual versus vestibular information has different time-courses.

It is also possible that the latency of alpha ERD is diagnostic of individual differences in the way that the visual- and physical-motion cues are being processed when participants are asked to distinguish between them during simultaneous presentation. Low-accuracy participants produced alpha ERD at visual stimulus onset regardless of whether they were attending to visual or physical motion, and these participants performed poorly in the attend-physical condition when attempting to ignore incongruent visual motion cues. We believe this is further evidence to support our hypothesis that latency of alpha ERD is diagnostic of which modality is being processed. In other words, the low-accuracy participants found great difficulty in ignoring the visual motion information and this was reflected in the latency of alpha ERD.

4.3 Theta oscillations in sensorimotor integration

Theta oscillations have long been studied in relation to spatial navigation in the hippocampus of the rat (Grastyan et al., 1966; O'keefe and Conway, 1978). They have been shown to be correlated with complex spatial behaviours such as exploring (Grastyan et al., 1966), and forming cognitive maps (O'keefe and Conway, 1978). More recently, Bland (2009) proposed an alternate model where theta oscillations facilitate integration between the sensory

and motor systems. The model states that the hippocampus and associated areas use theta oscillations to provide sensory and motor systems with a feedback loop to update one another on their performance relative to dynamic changes in the sensory environment. The model was developed to explain sensorimotor integration in rats but has since been applied to human behaviour (Caplan et al., 2003; Cruikshank et al., 2012). In an instructed delayed reaching paradigm, Cruikshank et al. (2012) asked participants to press and hold a button to begin each trial, which was then followed by the presentation of a black dot on a touch screen in front of them. Shortly after the presentation of the dot, an auditory tone sounded and, under two conditions, participants were required to release the button and touch the area of the screen where the dot was presented. In condition 1, the dot disappeared as soon as the button was released (movement onset), and in condition 2 the dot disappeared simultaneously with the tone (before movement onset). This paradigm required that participants integrate visuo-spatial information about the dot in order to coordinate a goal-directed movement. Cruikshank et al. (2012) found greater theta ERS during movement initiation and execution than during periods of stillness. They also found greater theta ERS over temporal sites during response initiation in condition 2 than in condition 1. Note that condition 2 requires greater integration and planning compared to condition 1. They propose that this is evidence of sensorimotor integration based on converging evidence that perceptual brain mechanisms in the ventral stream of the visual system are engaged when planning perceptually driven hand movements. For example, increased theta power has been shown during the planning phases of a catching task (Tombini et al., 2009), during the planning and execution phases of a choice-reaction task (Perfetti et al., 2010), and during motor imagery for sensorimotor planning (Hinterberger et al., 2008). Cruikshank et al.

(2012) did not find differences in theta ERS between conditions at any other electrode sites, suggesting that this temporal theta ERS was task-specific to the preparation of the reaching.

The present study prompted simpler spatial behaviours than Cruikshank et al. (2012) yet still required sensorimotor integration, and still found robust differences in theta power. Differences in theta power were elicited by manipulations in both the attended modalities and congruency of the visual and physical self-motion cues. We found different patterns of theta power when comparing the attend-physical vs. the attend-visual conditions. In the attend-visual condition we found a powerful but brief theta ERS between stimulus onset and 500ms post-stimulus, followed by a return to baseline. Whereas in the attend-physical condition we found less powerful but longer-lasting theta ERS beginning from around 200 ms post-stimulus and lasting until the end of the trial. The subtraction boxes in Fig. 4 show that theta ERS is significantly greater between stimulus onset and 500 ms post-stimulus during attend-visual trials (specifically in the left motor area). During attend-physical trials, theta ERS is significantly greater from around 500 ms post-stimulus to 1000 ms post-stimulus (specifically in the right motor area) compared to attend-visual trials. Differences in theta may reflect the different processing demands required when attending to the different sensorimotor stimuli. The brief but powerful theta burst in the attend-visual condition may reflect fast processing at stimulus onset and a cessation of processing of the visual-motion cue after the appropriate response had been determined. The long-lasting theta ERS during the attend-physical condition may reflect more extended processing of the physical-motion stimulus, which we know has a slower perceptual response (Barnett-Cowan and Harris, 2009).

We also found that incongruent attend-physical trials elicited greater theta ERD than congruent attend-physical trials. This main effect was found around 100 ms and lasted to 500 ms

post-stimulus in the left occipital area. This effect was only found while participants attended to physical motion stimuli, and not in the attend-visual condition, and was only shown in the left occipital area. It is likely that we did not find this effect in the incongruent attend-visual condition because the physical- motion stimuli in this experiment were less salient and thus less challenging for the participant to ignore than the visual-motion stimuli. Participants likely dealt with more interference from incongruent visual stimuli in the attend-physical condition.

We believe that this decrease in theta power may be due to the breaking of sensorimotor integration when self-motion cues are incongruent. We did not find any effect of congruency within our low-accuracy participants in any MPA domain, which is likely due to the fact that they had great difficulty ignoring the visual stimuli, and thus may not have noticed the spatial mismatch. This pattern of theta ERD in response to incongruent self-motion stimuli may be the neural response to visual- vestibular conflict.

4.4 Limitations of the present study

There are two limitations of the present study that are important to discuss. Both attend-visual and attend-physical conditions required participants to fixate on a central fixation cross. This is an important part of the design of the EEG experiment to reduce the contribution of eye-movement artifacts. However, one might argue that this set up an un- equal comparison between the two conditions because the visual fixation was the same modality as the target motion in the attend-visual condition but was a different modality as the target motion in the attend-physical condition. We acknowledge that it is possible that processing was affected by the requirement to fixate. However, we know that it is possible to disassociate eye movements and attention (e.g., Posner, 1980; Ramkhalawansingh et al., 2018), especially when the information at fixation is not task relevant, which may help to reduce concerns about the impact of the fixation requirement.

The second limitation relates to the relatively poor spatial resolution of EEG data compared to other brain-imaging methods such as fMRI and PET. It is wise to be cautious about attributing brain activity to specific brain regions using EEG. The IC dipoles clustered via MPA have an associated probability of membership to a brain domain (Acar & Makeig, 2013).

5. Conclusion

The present study is the first to use EEG to explore the effects of attention and cue congruency while participants are presented with simultaneous visual and physical self-motion stimuli. There were three main findings. 1) There was a difference in theta power between congruent and incongruent trials in the left occipital area when participants completed the attend-physical condition. Incongruent trials elicited a more robust theta ERD than congruent trials. Theta power is commonly associated with sensorimotor integration and this robust congruency difference may be due to a breaking of integration. It may be that this theta power difference only occurs while attending to physical motion because in this experiment, the visual motion stimuli were more salient, thus more disruptive during integration when it was incongruent with the physical-motion cue. We believe the difference in theta due to congruency may reflect a neural response to visual-vestibular conflict. 2) Alpha, beta and theta power in the motor areas were shown to change when participants attended to a specified stimulus while simultaneously ignoring the other. There were more powerful alpha and beta ERD and less powerful and later onset of theta ERS while participants attended to the physical motion. Previous research has demonstrated all three frequencies in the motor areas during unisensory visual- and physical-movement tasks. We have demonstrated that these power/latency differences are reflective of attentional allocation considering the stimuli in both attentional conditions were identical. 3) Participants who per- formed at thirty percent accuracy or less on the incongruent attend-

physical condition showed a minimal difference in alpha, beta and theta oscillations between the attend-visual and attend-physical conditions but only in the left motor cortex. Significant differences in oscillatory power were not found in any other MPA domain for the low- accuracy participants despite response times being significantly slower in the attend-physical than the attend-visual conditions. The ERSP of low- accuracy participants in both sensory modalities closely resembled the ERSP of high-accuracy participants during the attend-visual condition. These null results may reflect a greater visual bias for the low-accuracy participants, which would explain the relatively low accuracy (12%) during the incongruent attend-physical condition but high accuracy (95%) for the congruent attend-physical condition. To our knowledge, this is the first study to explore neural oscillations associated with visual- vestibular conflict. Further research is required to understand the nature of this theta ERD and exactly how it relates to the sensorimotor integration loop proposed by Bland (2009).

Appendix

Supplementary Materials

Figure A1. The motion simulator pod was supported by a MOOG © platform with six-degrees-of-freedom motion (MOOG series 6DOF2000E).

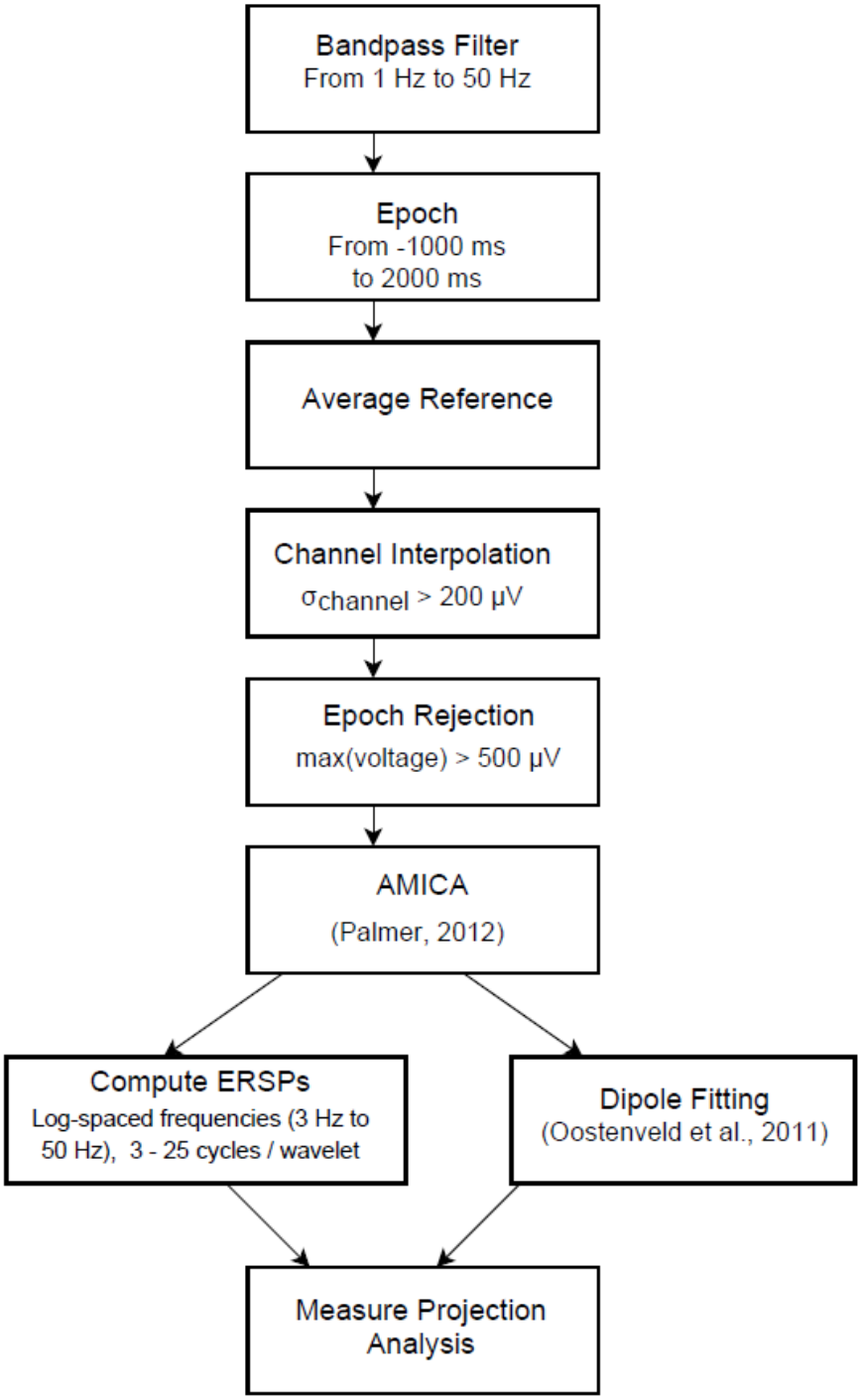

Figure A2. This flowchart illustrates the signal processing pipeline. The Measure Projection Analysis (MPA) pipeline is described in section 2.9 (ERSP Measure Projection Analysis), and a flowchart can be found in Bigdely-Shamlo, Mullen, Kreutz-Delgado & Makeig, 2013.

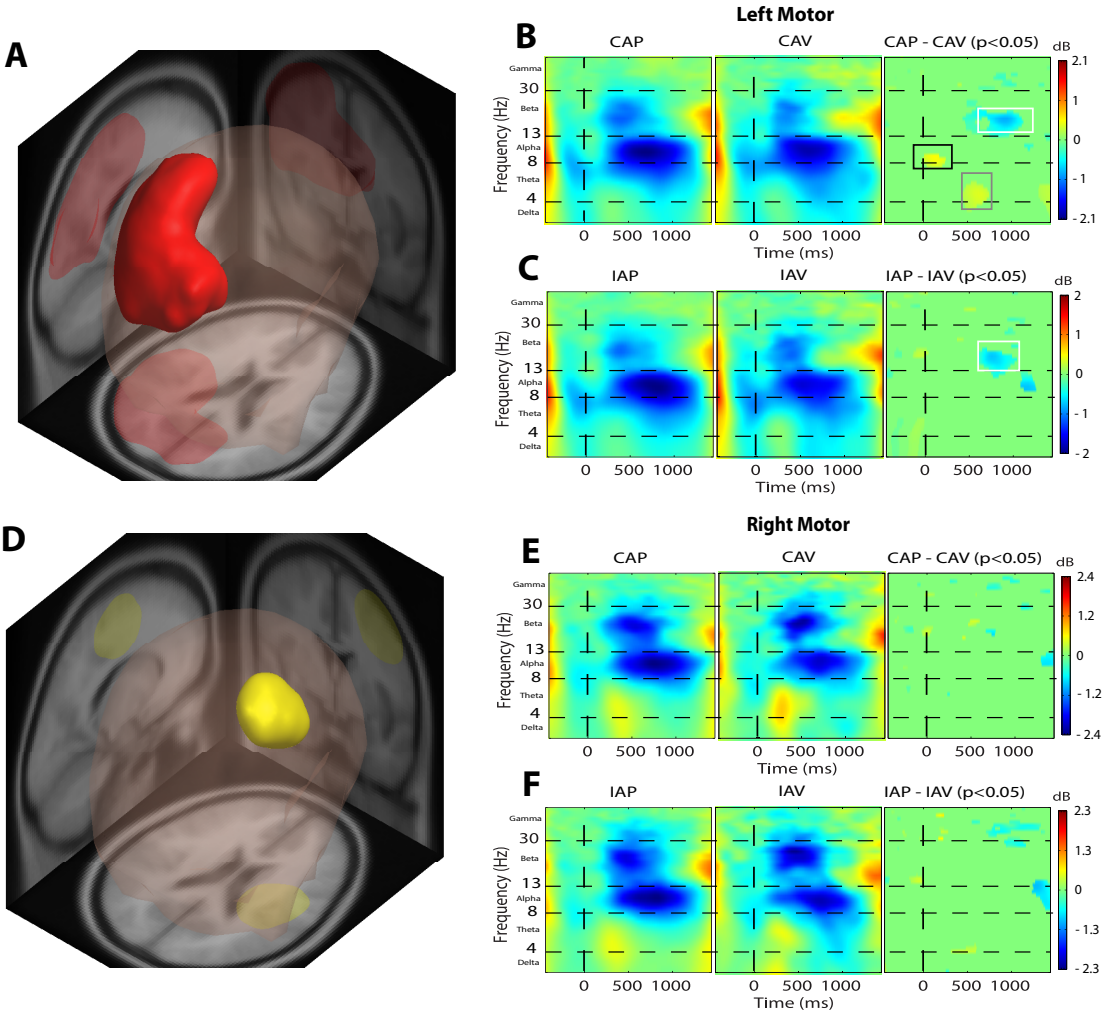

Figure A3. Left (Panels A, B, and C) and right (Panels D, E, and F) motor areas identified by MPA and respective ERSP analysis in low-accuracy participants. The ERSP plots show time (ms) and frequency of the EEG signal. Panels B, C, E, and F show the associated ERSP plots for the congruent and incongruent attend-physical (CAP, IAP) and attend-visual (CAV, IAV) conditions, and the bootstrapped comparisons ($p < 0.05$) between attend-physical and attend-visual conditions (CAP – CAV; IAP – IAV). ERS power is depicted in yellow/red, ERD power is depicted in blue, and green shows no difference in spectral power compared to baseline. **Left motor area:** The red region in Panel A represents the MPA domain with the greatest concentration of dipoles consistent with left dorsal posterior cingulate cortex (BA 31). Panel B contrasts CAP with CAV. The white square highlights greater beta ERD in the CAP condition based on bootstrapped comparisons. The black square highlights greater alpha ERD in the CAV condition (note that due to subtraction CAP-CAV, greater ERS power in CAV is represented in blue and greater ERD power in CAV is represented in yellow/red). The grey square highlights greater theta ERD in the CAV condition. Panel C: The white square highlights greater beta ERD in the IAP condition. **Right motor area:** The yellow region in Panel D represents the MPA domain with the greatest concentration of dipoles consistent with right primary somatosensory and primary motor cortex (BA 3 and 4). Panels E and F show no meaningful differences in ERSP activity between CAP vs. CAV, and IAP vs. IAV.

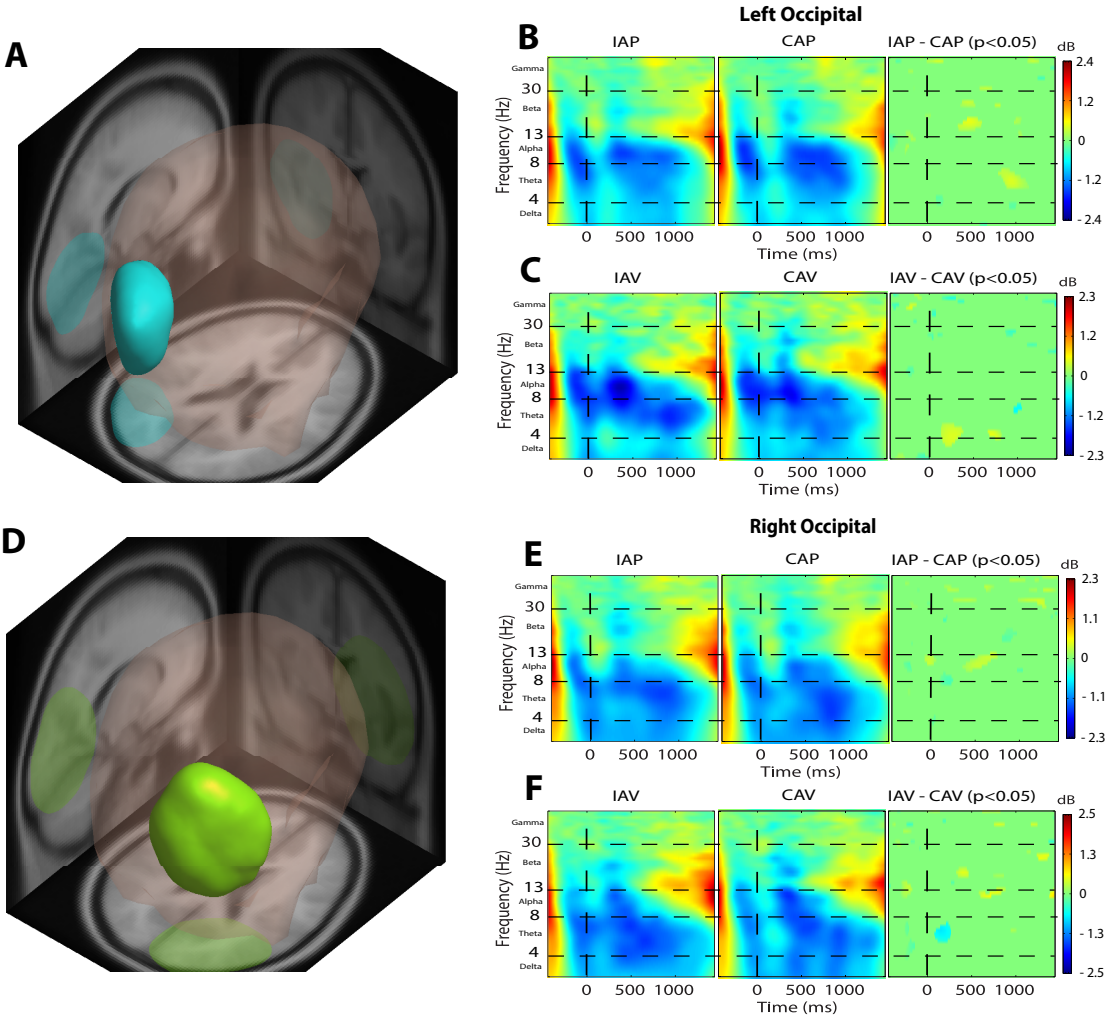

Figure A4. Left (Panels A, B, and C) and right (Panels D, E, and F) occipital area identified by MPA and respective ERSP analysis in low-accuracy participants. The ERSP plots show time (ms) across the x-axis and frequency of the EEG signal along the y-axis. Panels B, C, E, and F show the associated ERSP plots for the incongruent and congruent attend-physical (IAP, CAP) and attend-visual (IAV, CAV) conditions, and the bootstrapped comparisons ($p < 0.05$) between incongruent and congruent conditions (IAP – CAP; IAV – CAV). ERS power is depicted in yellow/red, ERD power is depicted in blue, and green shows no difference in spectral power compared to baseline. **Left occipital area:** Panel A shows a 3D representation of the brain with the blue region representing the MPA domain with the greatest concentration of dipoles consistent with left associative visual (V3) area (BA 19). Panels B and C show no meaningful differences in ERSP activity between IAP vs. CAP, and IAV vs. CAV. **Right occipital area:** Panel D shows a 3D representation of the brain with the green region representing the MPA domain with the greatest concentration of dipoles consistent with right secondary visual (V2) area (BA 18). Panel E and F: There are no meaningful effects of congruency.

CHAPTER 3: Beta-band power is an index of multisensory weighting during self-motion perception

Townsend, B., Legere, J.K., v. Mohrenschildt, M., & Shedden, J.M. (2022)

NeuroImage: Reports, 2, 100102.

Preface

The key findings of Chapter 2 were that theta band oscillations were associated with direction processing, beta ERD power was associated with attention to physical-motion cues, and beta ERS power was associated with attention to visual-motion cues. Chapter 2 was critical for establishing that theta, alpha and beta oscillations are associated with processes underlying self-motion perception, however, we were unable to determine whether the observed power changes were due to processes such as visual-vestibular weighting, unisensory processing, or attention-related functions, because visual- and physical-motion cues were presented simultaneously. Chapter 3 was the next logical step to identify the cognitive processes that were indexed by individual electrophysiological frequencies. Chapter 3 presents the results of a study that contrasted the ERSP elicited by visual-only versus physical-only presentations of self-motion. This experiment required participants to complete the same heading judgement task, and presented the same visual- and physical-motion stimuli as Chapter 2, however, each experimental block displayed only the visual- or physical-motion stimuli independently. We introduced far more weighting bias towards one stimulus in Chapter 3, because only one was

presented at a time. We hypothesized that if an oscillatory frequency is associated with multisensory weighting, we would find much different power changes between conditions in Chapter 3 versus Chapter 2 due to the different weighting demands between studies. This was the case with the beta band, as beta ERS was significantly stronger in the visual-only condition. This led us to believe that the beta band indexed visual-vestibular weighting. Presenting the motion stimuli independently also allowed us to explore whether any frequencies were sensitive to right versus left heading direction. We found that theta ERS was sensitive to heading direction for both visual- and physical-only conditions. This suggests that direction processing, regardless of sensory input, is likely indexed by theta oscillations.

ABSTRACT

Human self-motion perception largely relies on the integration of the visual, vestibular and proprioceptive systems. Much behavioural research has been conducted in order to understand this integration process; however, little is known about the online processes in humans during self-motion perception. Of the few studies to physically move human participants with full-body motion while recording the brain, most have used EEG due to its relative mobility. Past research provides evidence that multisensory self-motion perception elicits theta, alpha, and beta oscillations. It is important, however, to understand the individual contribution of each sense to fully understand how these oscillatory frequencies contribute to self-motion perception. To our knowledge, there has yet to be a study that directly compares the EEG correlates of visual self-motion with a no-motion physical input, versus physical-self motion with a no-motion visual input. We recorded event-related spectral power within a motion simulator controlled by a MOOG Stewart platform. Participants were given a visual or physical stimulus and made heading direction judgments. Compared to physical-only trials, visual-only trials produced earlier theta ERS and alpha ERD early in the trial, and more robust beta ERS late in the trial. We suggest beta-band power is likely associated with the process of visual-vestibular weighting. Moreover, within the right motor area, we found differences in theta power associated with left versus right headings. Theta ERS in the right motor area appears to be associated with heading processing for both the visual and vestibular systems but is minimally affected by multisensory weighting.

1. Introduction

The perception of self-motion has been of interest to scientists from a broad range of disciplines for the past several decades. These varying areas of study include (but are not limited to) spatial navigation (Moffat, 2009), fall prevention (Lupo & Barnett-Cowan, 2018; St. George & Fitzpatrick, 2011) and driver and pilot training (De Winter, Dodou & Mulder, 2012). It has been well established that self-motion perception is a multisensory phenomenon. The senses involved in this phenomenon include the visual, vestibular, proprioceptive, tactile and auditory systems (Gu, Angelaki & DeAngelis, 2008). The vestibular system detects linear and rotational movements of the head (for review see, Angelaki & Cullen, 2008), while the proprioceptive system detects body movements through the displacement of receptors in muscles (for review see, Proske & Gandevia, 2012). Together the vestibular and proprioceptive systems allow humans and other organisms to experience physical self-motion, or inertial motion, which then integrates with the available self-motion information from the visual and/or auditory systems (Gu et al., 2008).

Researchers in the aviation and driver training industries have paid particularly close attention to the integration processes of visual and physical self-motion. This research emphasis is likely due to Transport Canada (TC) and the Federal Aviation Administration's (FAA) requirements for the highest fidelity physical-motion systems for military pilot training, despite decades of mixed results regarding their training effectiveness (Burki-Cohen & Go, 2005). Moreover, high-fidelity motion-based platforms for pilot training are extremely expensive and labor intensive to maintain. This lack of conclusive evidence in favor of physical motion for pilot training may be, in part, because the benefit of physical motion during training is limited to specific flight tasks. For example, compared to visual-motion cues only, some studies

demonstrated a training benefit of incorporating physical-motion cues that simulated disturbance motion (external forces such as wind gusts, engine failure, etc.), but not for physical-motion cues that simulated correlated motion (movements of the vehicle controlled by the operator) (De Winter, Dodou & Mulder, 2012; O'Malley, Rajagobal, Grundy, v. Mohrenshildt & Shedden, 2016). High-fidelity motion systems continue to be required in TC and FAA policy primarily due to expert pilots' subjective preference for high-fidelity motion systems (Jones, 2016; Miletović et al., 2017). Given the perceived benefits and the high cost of motion simulators, it is important to improve understanding of the specificity of the contribution of physical-motion cues to effective training.

There exists substantial behavioural research focusing on how humans perceive (Harris & Barnes, 1987), integrate (Butler, Campos & Bülthoff, 2015) and learn (Hays, Jacobs, Prince & Salas, 1992) from cues to self-motion in simulated environments. Neuroimaging research exploring the online processes related to perceiving and interpreting cues to physical self-motion is sparser. This lack of research is likely due to the technological difficulties of recording from the brain while participants are physically moving. Neuroimaging techniques like functional magnetic resonance imaging (fMRI), positron emission topography (PET), and electroencephalography (EEG) generally require participants to stay as stationary as possible (Lopez, Blanke, Mast, 2012). Of these methods, EEG provides the most promise for reliable brain measures during physical movement because the equipment can move with the participant (unlike fMRI or PET).

Early studies exploring the online processes of self-motion perception primarily used rotatory chairs to present motion stimuli, while recording EEG. This method produces motion on the yaw axis, which stimulates the horizontal semicircular canals. Cortical activity was typically

analyzed in the time domain, which demonstrated a number of perturbation-evoked potentials (PEPs; Hood, 1983; Probst Ayan, Loose & Skrandies, 1997; Schneider, Kolchev, Constantinescu & Claussen, 1996). A relatively recent review of PEPs (Varghese, McIlroy & Barnett-Cowan, 2017) concluded that PEPs are distributed over fronto-centro-parietal areas. According to Varghese et al. (2017), the time course of a PEP is composed of a small positive potential (P1) that peaks around 30–90 ms after perturbation onset, this is followed by large negative potential (N1) peaking around 90–160 ms, and finally, positive (P2) and negative (N2) potentials between 200 and 400 ms. A study by Varghese et al. (2014) examined cortical responses to vestibular perturbations in the frequency domain. They determined that the PEP N1 response is composed of activity in the delta (1-4 Hz), theta (4-7 Hz), alpha (8-12 Hz), and beta (13-30 Hz) bands.

Townsend, Leger, O'Malley, v. Mohrenschildt and Shedden (2019) used linear translation cues to examine event-related spectral power (ERSP) signatures of multisensory visual and vestibular/proprioceptive (physical) self-motion perception. They observed theta, alpha, and beta oscillations in response to simultaneous visual- and physical-motion stimuli. Participants attended to either the visual-motion and ignored physical-motion cues, or attended to the physical-motion and ignored visual-motion cues. The task was to make heading judgements (left or right) based on the direction of perceived self-motion indicated by the stimulus in the attended modality. This design allowed an examination of ERSP differences elicited by attention allocation. Attending to the visual-motion stimulus (while ignoring the physical-motion stimulus) evoked earlier theta event-related synchronization (ERS) and alpha event-related desynchronization (ERD), whereas attention to the physical-motion stimulus (while ignoring the visual-motion stimulus) evoked longer-lasting and more powerful beta ERD, all in the motor area. Townsend et al. (2019) were also able to demonstrate a congruency effect in the theta band.

Incongruent motion stimuli elicited significantly stronger theta ERD power in the occipital area. Past research supports the idea that these three oscillatory frequencies are commonly recorded in the motor area during sensorimotor processing and output. Functionally, theta ERS is associated with heading processing (Burgess, 2008), alpha ERD is commonly linked to selective attention (Klimesch, 2012), and beta ERD reflects processes involved in preparing and executing motor output (Gaetz, Macdonald, Cheyne & Snead, 2010; Ofori, Coombes & Vaillancourt, 2015; Tzagarakis, Ince, Leuthold & Pellizzer, 2010).

Importantly, the Townsend et al. (2019) study showed individual differences in visual-vestibular weighting. Some participants found it more difficult to attend to the physical-motion cues and ignore the visual-motion cues, evidenced by poor accuracy identifying physical-motion heading direction on the incongruent trials. Participants who performed with high accuracy in that condition exhibited greater beta ERD power than those with poor accuracy. We believe that these differences in accuracy may be due to individual differences in visual-vestibular weighting, with low-accuracy participants having greater bias towards visual information. The beta band observations may point to a network that plays a key role in the weighting process. To further clarify the relationship between beta ERD power and a multisensory weighting process, it would be helpful to compare the Townsend et al. (2019) results with a design that does not present visual and physical cues simultaneously. Thus, the present study examined visual-only and physical-only conditions to compare the neural signatures revealed by theta, alpha and beta oscillations for each sensory system. One limitation of Townsend et al. (2019) is that there was no way of isolating potential reflexive cortical activity from any of the conditions because there was physical motion in all conditions. By isolating the visual from vestibular modalities and then directly comparing the induced cortical activity, the present experimental design allowed us to

distinguish oscillatory frequencies caused by potentially reflexive movements (cortical activity that occurs only in the physical-only condition) versus those that index more general processes related to self-motion perception (cortical activity that occurs in both conditions) such as direction processing, attention, and multisensory weighting.

The goals of the present study were threefold. First, we wanted to determine whether the previously discussed oscillatory frequencies were affected by multisensory weighting. In the Townsend et al. (2019) experiment, two strong self-motion stimuli were presented simultaneously, therefore it was not possible to determine whether the observed power changes were due to weighting, or other factors such as unisensory processing, or attention-related functions. The present study used the same task and stimuli as Townsend et al (2019) but differed in how the stimuli were (theoretically) perceptually weighted. We introduced far more weighting bias towards each stimulus in the present study, because only one stimulus was presented at a time. Based on our previous findings, we predicted that the beta band may be most affected by multisensory weighting. We hypothesized that if the beta band is in fact associated with multisensory weighting, we would find much different beta power changes between conditions (more so than theta and alpha) in the present study versus Townsend et al. (2019) due to the different weighting demands between studies.

Second, we used the heading discrimination task to explore whether any frequencies were sensitive to right versus left heading direction. We hypothesized that theta ERS was most likely to be direction sensitive, based on the sensitivity of theta to spatial incongruency in the Townsend et al. (2019) study. This congruency effect is only possible if theta oscillations are sensitive to heading in both the visual and vestibular modalities.

Third, most of the previous studies that recorded cortical activity during physical motion (e.g., Ditz, Schwarz & Müller-Putz, 2020; Townsend et al., 2019; Varghese et al., 2014) either provided simulated visual cues to motion on a display screen, or provided egocentric visual cues as participants moved through an environment with stable objects. These experimental designs provided simultaneous physical and visual cues to motion, and therefore did not isolate cortical activity based on sensory input. In the present study, participants were fully enclosed inside the cabin, thus all of the objects within the visual field moved with them during physical motion, minimizing any visual cues to motion in the physical-only condition. This design allowed us to isolate cortical responses to physical versus visual motion. This element of the design is particularly important for gaining insights into cortical activity induced by compensatory reflexes in response to physical motion. If our physical-motion stimuli are inducing strong reflexive responses, there will be powerful, and consistent differences in the motor cortices, between the physical-only and visual-only conditions directly following stimulus onset (Peterson & Ferris, 2018).

2. Materials and methods

2.1 Participants

Eleven participants (8 female) were recruited from the McMaster University psychology participant pool and the McMaster community. Ages ranged from 18 to 28 years (M = 19, SD = 3.07). Those recruited from the participant pool were compensated with course credits. All participants reported normal or corrected-to-normal vision, and no known problems with vertigo, motion sickness or claustrophobia. This experiment was approved by the Hamilton Integrated Research Ethics Board and complied with the Canadian tri-council policy on ethics.

2.2 Stimuli

2.2.1 Visual-motion stimuli

Visual stimuli were presented on a 43-inch LCD panel at a resolution of 1920 x 1080 (1080p) and refresh rate of 60 Hz; with 51 inches between the screen and the participant. The screen subtended a horizontal visual angle of 41°. The visual-motion stimuli were presented in the same cabin as the physical-motion stimuli.

The visual display consisted of a fixation cross in the centre of the display and two tracks on a grey surface along which the perception of self-motion would occur. Each track consisted of a series of yellow dashes perpendicular to the length of the track, drawn in perspective to a vanishing point so that the track appeared to extend into the distance. Each track demarked a trajectory beginning at the lower center of the display; one track veered left by 35° and one track veered right by 35°. Both tracks together subtended a horizontal visual angle of 33.69°. The scene was demarcated by the grey surface below (upon which the tracks laid) the horizon and a blue sky with white clouds above, accentuating the perception of traveling along a track into the distance. The perception of self-motion was achieved via a first-person viewpoint animation that simulated moving forward along one of the tracks (two temporal snapshots are illustrated in Panels B and C of Figure 1). The timing of each visual-motion trial was a forward motion along the left or right track for 700 ms followed by a pause at the end of the track for 1200 ms. The visual display was then reset to the starting position, ready for the next trial.

In the physical-motion task, participants saw the fixation cross, grey surface, and blue sky/clouds only; the yellow tracks were not present and there were no visual cues to self-motion.

2.2.2 Physical-motion stimuli

A motion simulator provided physical motion stimuli. An enclosed cabin equipped to provide an immersive virtual environment was supported by a MOOG © Stewart platform with

capability of six-degrees-of-freedom motion (Moog series 6DOF2000E; see Inline Supplementary Figure A1). Participants were seated in a bucket-style car seat fixed to the floor of the cabin.

Each physical-motion stimulus consisted of a linear translation of the cabin, moving forward at an angle of 35° left or 35° right. The duration of the movement was 330 ms at 0.1 g (the longest our motion simulator could be moved given the spatial restrictions of the motion platform). This surge was followed by a corresponding washout for 1330 ms which returned the cabin to the original position (see Panel A in Figure 1). The acceleration intensity was selected based on preliminary testing to achieve a clear perception of forward motion within the spatial restrictions of the movement of the platform while minimizing compensating movements of the head, neck or upper body (Townsend et al., 2019). Physical forward accelerations were well above vestibular thresholds of .009 g., as discussed by Kingma (2005). The motion force, s(t), was described by:

$$s(t) = \begin{cases} A_1 \; 0 \; \leq t \; \leq t_p \\ -A_2 \; t_p \; \leq t_b \\ A_2 \; t_b \; \leq t \; \leq t_e \\ 0 \; else \end{cases}$$

where t represents time in seconds, tp represents present time, tb represents the breakpoint and te represents the end time. A1 describes the initial forward acceleration, -A2 describes the initial (backwards) acceleration of the washout, and A2 describes the deceleration of the washout. Acceleration was measured using an Endevco accelerometer (model number 752A13), calibrated to approximately 1 mV/g sensitivity.

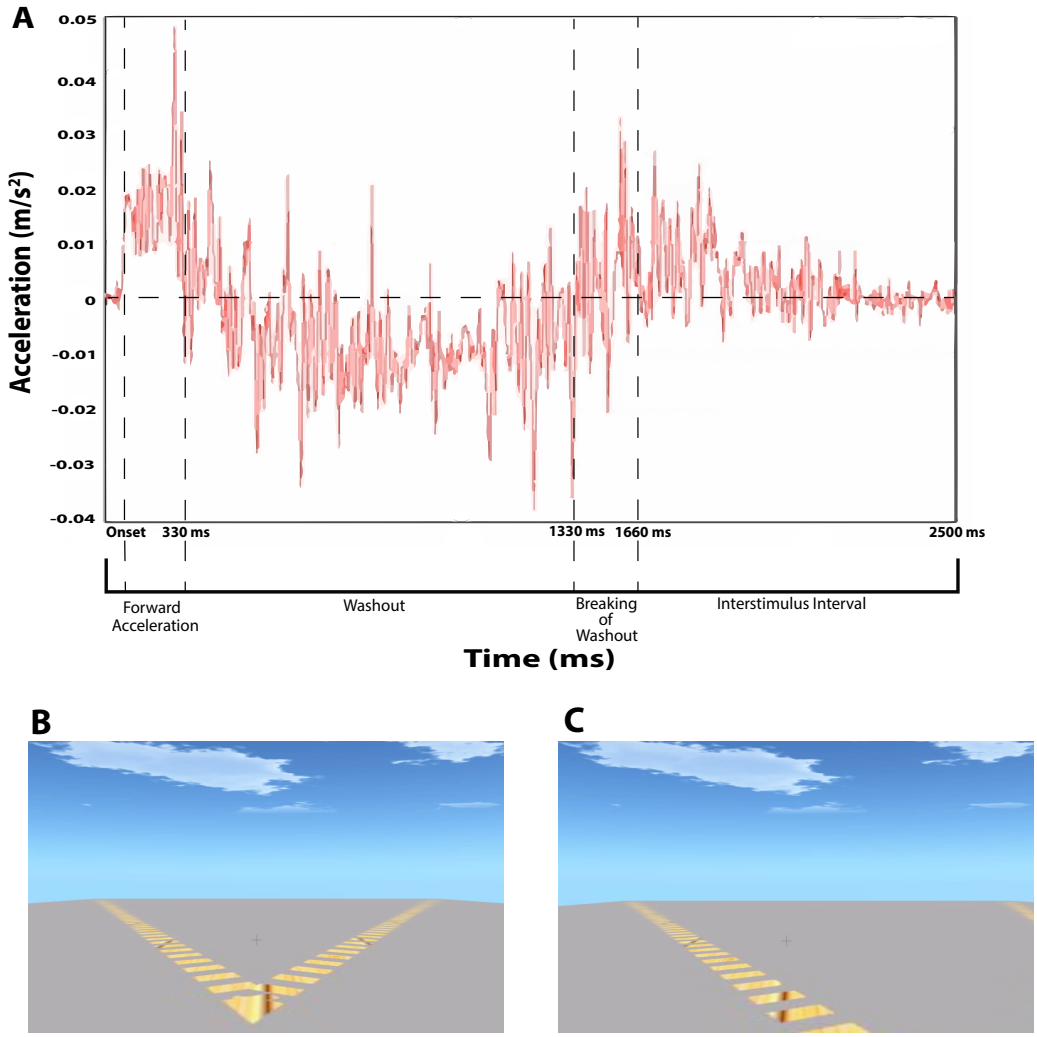

Figure 1. Time course of physical- and visual-motion stimuli. Panel A shows an example of the profile of physical motion measured during a single trial by an accelerometer (red line); the variance shown is due to the high sensitivity of the accelerometer. The x-axis represents time and the y-axis represents acceleration (g = m/s2). The acceleration profile is similar for 35° left and 35° right physical-motion trials. Panel B shows the visual display before the onset of visual motion; at this point the participant does not know whether visual motion will indicate travel along the left or right track. Panel C shows a still picture of the dynamic visual-motion display at approximately 1s after visual onset of a left visual motion trial.

2.3 Procedure

The entire session was between 1.5 and 2 hours in duration. The timeline of the session included collection of demographic information (age, gender, and handedness), followed by completion of 30 practice trials (2 minutes), application of EEG electrodes (25 minutes), completion of two experimental blocks (40-50 minutes), and participant cleanup and debriefing (15 minutes).

Visual-motion trials and physical-motion trials were blocked (199 trials per block); block order was counterbalanced. Participants were provided with earplugs and white audio noise was played inside the simulator to mask the sound of the motors during the physical-motion trials. Although the motion simulator was parked during the visual-motion trials (i.e., the cabin remained stationary), earplugs and white noise were applied in both visual- and physical-motion conditions for consistency. The interior of the cabin was monitored via a video camera.

Participants held a button box in their lap so that left and right thumbs rested on two response buttons. Their task was to respond with a button press to indicate the direction of perceived self-motion (left or right). Participants maintained fixation on the fixation cross throughout each trial and were provided with a "blink" break every 15 trials.

2.4 EEG data acquisition

EEG data were collected using the BioSemi ActiveTwo electrophysiological system (www.biosemi.com) with 128 sintered Ag/AgCl scalp electrodes. An additional four electrodes recorded eye movements (two placed laterally from the outer canthi and two below the eyes on the upper cheeks). Continuous signals were recorded using an open pass band from direct current to 150 Hz and digitized at 1024 Hz.

2.5 EEG preprocessing

All processing was performed in Matlab 2014a using functions from EEGLAB (Delorme & Maekig, 2004) on the Shared Hierarchical Academic Research Computing Network (SHARCNET: www.sharcnet.ca). A flowchart illustrating the signal-processing pipeline can be found in the supplementary materials (see Inline Supplementary Figure A2). EEG data were band-pass filtered between 1 and 50 Hz, and epoched from 1000 ms pre-stimulus to 2000 ms post-stimulus. Each epoch was baseline corrected using the whole-epoch mean (Groppe, Makeig & Kutas, 2009). After referencing, channels with a standard deviation exceeding 200 μV were interpolated (overall, only one channel was interpolated). Bad epochs were rejected if they had voltage spikes exceeding 500μV, or were rejected by EEGLAB's joint probability functions (Delorme, Sejnowski & Makeig, 2007).

Single-subject EEG data were submitted to an extended Adaptive mixture independent component analysis (AMICA) with an N – (1 + interpolated channels) Principal Components Analysis reduction (Makeig, Bell, Jung & Sejnowski, 1996). Decomposing an EEG signal into independent components (ICs) allows for analysis of each individual signal produced by the brain that would otherwise be indistinguishable. Following AMICA, dipoles were fit to each IC using the fieldtrip plugin for EEGLAB (Oostenveld, Fries, Maris & Schoffelen, 2011). ICs for which the dipole fit explained less than 85% of the weight variance, or whose dipoles were located outside the brain, were excluded from further analysis. On average, 22.64 ICs per subject were excluded from analysis.

2.6 ERSP measure projection analysis

Event-related spectral power (ERSP) was computed for each of the remaining ICs. Fifty log-spaced frequencies between 3 and 50 Hz were computed, with 3 cycles per wavelet at the lowest frequency up to 25 at the highest. Measure projection analysis (MPA) was used to cluster

ICs across participants using the Measure Projection Toolbox for MATLAB (Bigdely-Shamlo, Mullen, Kreutz-Delgado & Makeig, 2013). MPA is a method of categorizing the location and consistency of EEG measures, such as ERSP, across single-subject data into 3D domains. These domains are subsets of ICs that are identified as having spatially similar dipole models, as well as similar cortical activity (measure-similarity). MPA fits the selected ICs into a 3D brain model comprised of a cubic space grid with 8-mm spacing according to normalized Montreal Neurological Institute (MNI) space. Cortical regions of interest were identified by the MPA toolbox by incorporating the probabilistic atlas of human cortical structures provided by the Laboratory of Neuroimaging project (Shattuck et al., 2008). Voxels that fell outside of the brain model (muscle artifacts, etc.) were excluded from the analysis. Note that the spatial resolution of EEG data compared to other brain-imaging methods such as fMRI and PET is relatively poor. It is important to practice caution when attributing brain activity to specific brain regions using EEG. The IC dipoles clustered via MPA have an associated probability of membership to a brain domain (Acar & Makeig, 2013).

We then calculated local convergence values, using an algorithm based on Bigdely-Shamlo et al. (2013) to deal with the multiple comparisons problem. Local convergence calculates the measure-similarity of dipoles within a given domain and compares them with randomized dipoles. In order to compare dipoles, a pairwise IC similarity matrix was created by estimating the signed mutual information between independent component-pair ERSP measure vectors, assuming a Gaussian distribution. As explained in detail by Bigdely-Shamlo et al. (2013), signed mutual information was estimated to improve the spatial smoothness of the obtained MPA significance value beyond determining similarity of dipoles through correlation. We used bootstrap statistics to obtain a significance threshold for convergence at each location of

our 3D brain model. Following past literature, we set the raw voxel significance threshold to $p < .001$ (Bigdely-Shamlo et al., 2013; Chung, Ofori, Misra, Hess & Vaillancourt, 2017).

Two relevant domains were analyzed: the right motor area, with the greatest concentration of dipoles consistent with right premotor and supplementary motor area (BA 6), and the left motor area, with the greatest concentration of dipoles consistent with left premotor and supplementary motor area (BA 6). For the right motor area, each participant contributed on average 2.27 (±1.27) ICs, with each participant contributing at least one IC, with a range from 1 – 5 ICs. For the left motor area, each participant contributed on average 2.18 (±1.17) ICs, with each participant contributing at least one IC, with a range of 1 – 4 ICs.

For each domain calculated by MPA, ERSPs were computed for each experimental condition. Within each domain, bootstrap statistics were used to assess differences in ERSP between conditions to uncover main effects of task and congruency. Differences at each power band were computed by projecting the ERSP for each condition to each voxel in the domain. For each subject, this projection was weighted by dipole density per voxel and then normalized by the total domain voxel density. Analysis of projected source measures were separated into discrete spatial domains by threshold-based Affinity Propagation clustering based on a similarity matrix of pair-wise correlations between ERSP measure values for each position. Following Chung et al. (2017), we used the maximal exemplar-pair similarity, which ranges from 0-10 to set a value of 0.8 (Bigdely-Shamlo et al., 2013; Chung et al., 2017; Ofori et al., 2015).

2.7. Data and code availability

The data and code for all analyses are available online at https://github.com/bentownsend11/Beta-band-power-is-an-index-of-multisensory-weighting-during-self-motion-perception.

3. Results

3.1 Behavioural results

We ran two 2 (input: visual-motion vs physical-motion) x 2 (direction: left heading vs right heading) ANOVAs to analyze participants' accuracy and response time. Outliers were defined as trials with response times greater than three standard deviations above or below the mean in each condition, and were eliminated from all further analyses. Accuracy was high overall and there were no significant differences in accuracy between the physical-motion (M = 98.71, SE = .72) and visual-motion conditions (M = 99.88, SE = .08), $F(1,9) = 2.56$, $p = .14$, nor were there differences between right (M = 99.24, SE = .30) versus left heading directions (M = 99.40, SE = .44), $F(1,9) = .19$, $p = .68$.

The present study did uncover a significant difference in response times between the blocked physical-motion (M = 931 ms, SE = 91.20) and visual-motion conditions (M = 571 ms, SE = 43.68), $F(1,9) = 23.42$, $p < .001$, $\eta p2 = .72$. This difference was expected due to faster perceptual processing of visual inputs versus vestibular inputs (Barnett-Cowan & Harris, 2013). There were no significant differences in response time between right (M = 747 ms, SE = 62.16) versus left (M = 754 ms, SE = 60.61) headings, $F(1,9) = .28$, $p = .61$, and no input x direction interaction. These results are consistent with previous work reported in the literature but may be interpreted with caution due to the small sample size.

3.2 Oscillatory power

In Figure 2 we show the left and right motor areas to provide side-by-side comparisons of how modality and direction of motion cues affected cortical activity. All ERSP is representative of a difference in oscillatory power compared to baseline (pre-trial) cortical activity, where an ERS (event-related synchronization) represents more spectral power than baseline and an ERD

(event-related desynchronization) represents less spectral power than baseline. In Figure 2, Panel A shows the left motor area, which has the highest dipole density in left premotor and supplementary motor areas (Brodmann area [BA] 6), and Panel D shows the right motor area, which has the highest dipole density in right premotor and supplementary motor areas (BA 6). In Panels B and E, we show the associated ERSP plots for each condition. Panels C and F show the bootstrapped comparisons between conditions within their respective motor areas.

3.2.1 Power differences between modalities

Theta-band activity: Comparing physical vs visual rightward conditions, PR elicited greater theta ERS than VR ($p < .05$) from ~400 ms to 550 ms post-stimulus in the left motor area (Panel C).

Alpha-band activity: Both left and right motor areas showed differences within the alpha-band in the visual- versus physical-motion conditions. In the left motor area, the VL condition, due to an earlier latency, elicited greater alpha ERD than PL ($p < .05$) from stimulus onset to ~400 ms post stimulus. Whereas within a later time window, the PL condition elicited greater alpha ERD than VL ($p < .05$) from ~600 ms to 1000 ms post-stimulus (Panel C). Comparing rightward conditions, PR elicited greater alpha ERD than VR ($p < .05$) from ~600 ms to 900 ms post-stimulus onset (Panel C).

In the right motor area, the PL condition elicited greater alpha ERD than VL ($p < .05$) from ~550ms to ~1000 ms post stimulus (Panel F), whereas no alpha band differences were observed between PR and VR in the right motor area (Panel F).

Beta-band activity: Each comparison resulted in significant differences in beta-band activity. In the left motor area, comparing leftward conditions, the VL condition elicited greater beta ERS than PL ($p < .05$) from ~700 ms post stimulus onset to end of trial (Panel C). Comparing

rightward conditions, VR elicited greater beta ERS than PR ($p < .05$) across a slightly longer but overlapping time window, from ~500 ms to end of trial (Panel C). The VR condition elicited greater beta ERD compared to PR ($p < .05$) over an earlier time window from stimulus onset to ~250 ms post stimulus onset.

In the right motor area, comparing leftward conditions, the VL condition elicited greater beta ERD than PL ($p < .05$) from stimulus onset to ~250 ms post stimulus, and greater beta ERS than PL from ~450 ms to end of trial (Panel F). Comparing rightward conditions, VR elicited greater beta ERD than PR ($p < .05$) from stimulus onset to ~200 ms post stimulus, and greater beta ERS than PR from ~550 ms to end of trial (Panel F).

3.2.2 Power differences between headings

Theta-band activity: We found robust directional differences in the theta band only. The theta-band differences were observed in the right motor area, but not the left. In the right motor area the PR condition elicited more powerful theta ERS compared to PL (from ~250 ms to 600 ms post-stimulus; Panel F). Similarly, VR elicited more powerful theta ERS compared to VL (from ~100 ms to 750 ms post-stimulus; Panel F).

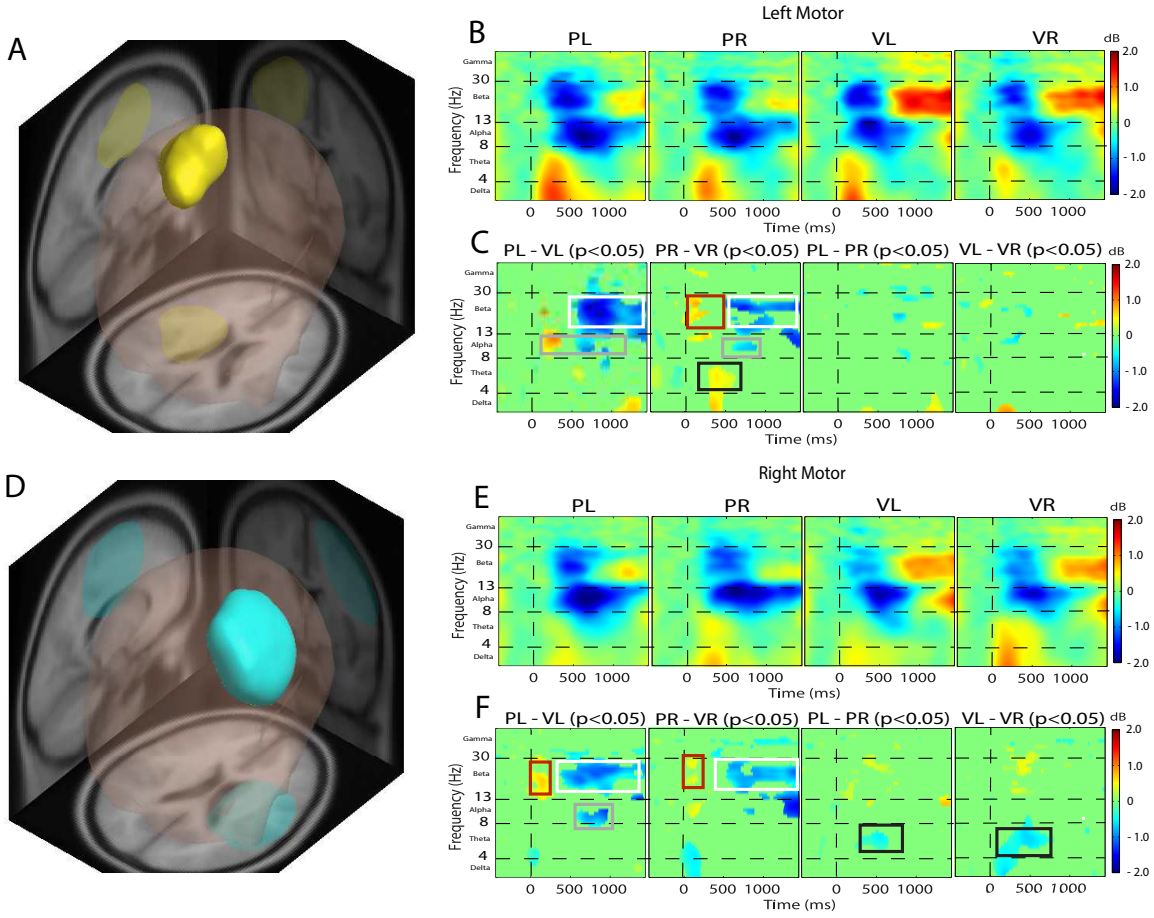

Figure 2. (EEG Results). Left motor area (Panels A, B, and C) and right motor area (Panels D, E, and F) identified by MPA and respective ERSP analysis. The ERSP plots show time (ms) across the x-axis and frequency of the EEG signal along the y-axis. Panels B (left motor) and E (right motor) show the associated ERSP plots for each condition. Panels C (left motor) and F (right motor) show the bootstrapped comparisons ($p < 0.05$) between each pair of conditions that are relevant to our hypotheses. ERS power is depicted in yellow/red, ERD power is depicted in blue, and green shows no difference in spectral power compared to baseline. Left motor area: Panel A shows a 3D representation of the brain with the yellow region representing the MPA domain with the greatest concentration of dipoles consistent with left premotor and supplementary motor area (BA 6). Panel B: ERSP plots for each condition. Panel C: Results of bootstrapped comparisons. PL-VL: the white square, showing significantly more beta ERS in the VL condition (note that due to subtraction PL-VL: Greater ERS power in VL is represented in blue). The grey square highlights a significant latency difference in alpha ERD between the PL and VL conditions. PR-VR: The red square highlights significantly more beta ERD early in the trial due to an earlier latency in the VR condition. The white square highlights more powerful beta ERS later in the trial for VR versus the PR condition. The grey square highlights significantly more alpha ERD in the PR condition. The black square highlights significantly more theta ERS in the PR condition. Contrasting PL-PR, and VL-VR show no robust differences in power. Right motor area: Panel D shows a 3D representation of the brain with the blue region representing the MPA domain with the greatest concentration of dipoles consistent with right premotor and supplementary motor area (BA 6). Panel E: ERSP plots for each condition. Panel F: Results of bootstrapped comparisons PL-VL: The red square highlights significantly more beta ERD early in the trial due to an earlier latency in the VL condition. The

white square highlights more powerful beta ERS later in the trial for VL versus the PR condition. The grey square highlights significantly more alpha ERD in the PL condition. PR-VR: The red square highlights significantly more beta ERD early in the trial due to an earlier latency in the VR condition. The white square highlights more powerful beta ERS later in the trial for VR versus the PR condition. PL-PR: The black square highlights significantly more theta ERS for PR versus the PL condition. VL-VR: The black square highlights significantly more theta ERS for VR versus the VL condition.

4. Discussion

As we move through the world, self-motion perception is a function of multisensory integration of visual, vestibular, proprioceptive, and auditory cues to self-motion. Observation of localized neural oscillations contributes to understanding of how ERSPs reflect the integration process. Multisensory integration works through a weighting process whereby more salient or reliable cues drive the perception of self-motion (Angelaki, Gu & DeAngelis, 2009). These processes are most often studied by presenting simultaneous multisensory motion cues. For example, previous studies explored theta, alpha, and beta oscillations elicited in during a heading discrimination task in which participants attended to one or the other of simultaneous visual and physical motions cues (Townsend et al., 2019). Visual and physical cues were incongruent on half the trials, producing strong sensory conflict on the incongruent trials which increased the demand for multisensory weighting processes. A more powerful beta ERD was observed when attention was directed to the physical motion, whereas a more powerful beta ERS, and earlier induction of theta ERS and alpha ERD were observed when attention was directed to the visual motion. A limitation of the Townsend et al. (2019) study was that it did not include a condition in which visual (or physical) motion was presented alone, therefore it is not certain that the results observed in the attention conditions reflect a multisensory weighting process.

The present study aimed to address this gap in the literature by contrasting theta, alpha, and beta oscillations elicited in response to single modality visual-only versus physical-only motion cues. Thus, the multisensory weighting process was more heavily biased towards either visual or physical signals compared to the Townsend et al. (2019) study. An important motivation for the present study was to generate hypotheses about whether the theta, alpha and

beta oscillations reflect a multisensory integration process or a more general process engaged during self-motion perception.

We observed modality differences in the theta and alpha bands localized to left and right motor areas. We suggest that theta ERS and alpha ERD may be associated with processes other than multisensory weighting because theta and alpha band power in the present study replicated Townsend et al. (2019) despite a large difference in demand for multisensory weighting between the two studies. In contrast, strong beta ERD and ERS responses support the hypothesis of Townsend et al. (2019) that beta oscillations are an index of processes that play a key role in multisensory weighting during visual-vestibular integration. We discuss beta oscillations, theta ERS, and alpha ERD in detail below.

4.1 Beta oscillations

The most notable modality-induced ERSP power and latency differences within the present study and Townsend et al. (2019) were in the beta band. The present study uncovered a significantly longer lasting and more powerful beta ERS (~700 ms – end of trial), in the visual-motion condition compared to the physical-motion condition (~850 ms – end of trial). The modality differences in the beta band observed by Townsend et al. (2019) were driven by a more powerful and longer-lasting beta ERD in the attend physical-motion conditions compared to attend visual-motion conditions. The ERSP power and time course differences in the beta band between the two studies could be due to the difference in multisensory weighting processes. Considering beta-band oscillations are so strongly linked with sensorimotor processing, it is intuitive that this difference in stimulus presentation and attention requirements (regardless of both experiments using the same stimuli) caused different ERSP power and time courses within the beta band.

Much research has shown that beta ERD is associated with motor output (Ofori et al., 2015; Woolrich et al., 2019), motor planning (Tzagarakis et al., 2010) and motor imagery (Pfurtscheller, Neuper, Brunner & Da Silva, 2005). Moreover, beta ERD amplitude, duration and onset time have been shown to be modulated by task parameters such as certainty of movement, or number of movement options (Tzagarakis, et al., 2010). Beta ERD lasts until the movement or imagery is complete, and is typically observed bilaterally over sensorimotor areas (Salmelin and Hari, 1994; Stancak and Pfurtscheller, 1996). Beta ERS power rapidly increases if movement is not performed, for example after presentation of a No-Go signal (Alegre et al., 2004), or as soon as the motor output ceases (Baker et al., 1999). This increase in beta ERS power following the offset of movement is known as beta rebound, and it typically occurs 300–1000 ms post-movement (for review see Kilavik, Zaepffel, Brovelli, MacKay & Riehle, 2013). Similar to the motor imagery beta ERD described by Pfurtscheller et al. (2005), the beta rebound has also been demonstrated in motor imagery tasks (Solis-Escalante, Müller-Putz, Pfurtscheller, Neuper, 2012). One hypothesis is that the function of beta rebound is to recalibrate or reset the motor system to new conditions, in order to prepare for a subsequent movement (Gaetz & Cheyne, 2006). Once the beta rebound has expired, the beta oscillation cycle begins again with the preparation for a new movement. If the beta rebound were simply reflecting the recalibration of the motor system, we would not expect such a robust power difference between visual versus physical cues to motion, as we demonstrated in the present study. Alternatively, Townsend et al. (2019), suggested that the beta cycle might be engaged as part of a mechanism to suppress the processing of stimuli that are unattended or no longer require processing. For example, in the present experiment, the “no-motion" signal of the unstimulated sensory modality (i.e. the vestibular/proprioceptive systems during the visual-motion condition, or vice versa). The

integration of the visual and vestibular systems is a subadditive process (Angelaki, Gu & DeAngelis, 2009; Morgan, DeAngelis & Angelaki, 2008). This robust beta rebound might reflect an inhibitory process during visual-vestibular integration in which the sensory information of the provided motion stimulus is weighted greater than the opposing no-motion signal. We believe the difference in beta rebound power between the two modalities may reflect visual bias in the visual-vestibular integration that has been reported by previous studies (e.g., Angelaki, Gu & DeAngelis, 2009), considering the beta rebound was much stronger in the visual-only condition of the present study and the attend-visual condition of Townsend et al. (2019).

Finally, it should be noted that we did not find the longer lasting beta ERD in the physical condition compared to the visual condition that was found in Townsend et al. (2019). The 2019 study demonstrated a more powerful and longer-lasting beta ERD, starting at ~600 ms and maintaining to the end of the trial in the attend-physical condition. We believe this different result could be due to the different attentional requirements of the task in Townsend et al. (2019) compared to the present study. The past study presented both visual- and physical-motion stimuli simultaneously and in conflict with one another on half of the trials, which required a greater need for sustained attention to the physical-motion stimulus during the attend-physical task. If attending to physical-motion stimuli elicits a beta ERD, then we would expect a longer-lasting beta ERD during sustained attention to the physical-motion stimulus, and that is exactly what was demonstrated in Townsend et al. (2019). In contrast, the present study only provided one sensory stimulus at a time. With minimal conflict between the visual and vestibular information, fewer attentional resources were required to complete the task, and intuitively we found shorter beta ERD at the beginning of the trials (~150 – 700 ms). Combining our observations of beta ERS (rebound) and ERD, we believe that beta oscillations are critical to the weighting process

during multisensory integration. The power of early onset beta ERD may reflect the attentional demands of unisensory or multisensory stimuli, while the power of the beta rebound may correlate with the magnitude of inhibition directed towards the lesser-weighted sensory modality during subadditive integration.

4.2 Theta ERS

Human (Kahana et al., 1999) and non-human (Shin, 2010; Welday, Shlifer, Bloom, Zhang & Blair, 2011) studies have shown that processes indexed by theta ERS are sensitive to spatial orientation and heading direction changes. These studies generally link theta ERS produced by grid cells and place cells distributed throughout the hippocampus and parahippocampal areas to the function of path integration (Burgess, 2008). A highly accepted hypothesis is that the entorhinal grid cells and hippocampal place cells work together to create an internal representation of the organism's location within its environment (Krupic, Bauza, Burton & O'Keefe, 2018). Place cells process external perceptual information to create an allocentric representation of the external environment, while grid cells process self-motion information, leading to a perception of one's dynamic egocentric position in relation to the external objects (O'Keefe & Burgess, 2005). According to the oscillatory interference model (Burgess, Barry & O'keefe, 2007), grid cell firing, and its modulation by self-motion, may result from two oscillations within the theta band which are distinguished by phase-change differences in response to the velocity of the moving organism. The phase of one theta oscillation becomes increasingly earlier as the animal moves through a given place field, while the other theta oscillation remains constant. Changes in the discrepancies of these theta oscillations' phase allows for the perception of changes in velocity and heading direction.

The current study found theta ERS to be sensitive to heading direction during both visual and physical self-motion perception. This effect, however, was only found in the right motor area. This lateralized effect is supported by past research, which has shown a right-lateralized brain network involved in spatial attention in humans (for review see Dieterich & Brandt, 2018). Studies focussed on spatial attention (for review see Bonato, 2012) and navigation (Buxbaum et al., 2008; Turton et al., 2009) in neglect patients shed light on the lateralized nature of spatial processing. Neglect patients typically fail to orient or respond to stimuli in the hemifield opposite of the acquired brain lesion (i.e., the contralesional side of space within a reference frame centered on the observer; Bonato, 2012). A study by Beis et al., (2004), found that 35-42% of stroke patients with a lesion to the right hemisphere suffered from neglect versus only 8-13% in patients with damage to the left hemisphere.

The present study also revealed a latency difference in theta ERS when comparing the time course of ERSP power between modalities, in which theta ERS was elicited later (100 – 550 ms) in the physical-only condition versus the visual-only condition (stimulus onset – 450 ms). This effect was similar to the effect found in Townsend et al. (2019). In both studies, theta ERS induction was earlier when visual motion information was the target stimulus (visual-motion only in the present study or attend-visual in the previous study). Considering the results of both of these experiments, it seems that this early theta ERS is not primarily driven by multisensory weighting processes, and is not specific to one sensory input (visual or vestibular). This finding also suggests that early theta ERS is likely not elicited by reflexive movements caused by physical motion. Based on previous literature (e.g., Peterson & Ferris, 2018), we would expect significant theta ERS power differences in the motor cortices if this were the case. Theta ERS seems to be engaged by sensory processing related to self-motion perception. In fact, this claim

is supported by decades of research demonstrating that theta is an index of the initial stages of heading processing (for reviews see Başar, Başar-Eroglu, Karakaş & Schürmann, 2001 and Colgin, 2013).

Importantly, modality affected the time course of theta ERS similarly in both the present study and the Townsend et al. (2019) study, despite very different demands for multisensory weighting between the two studies. One conclusion is that the process indexed by theta ERS is occurring before visual-vestibular weighting takes place. Moreover, in the present study there was an interaction involving the right-lateralized heading differences observed for both the visual-only and physical-only modalities. The fact that both modality conditions showed similar right-lateralized theta-band changes points to this process being farther along the spatial processing timeline than merely sensing the stimulus. Taken together, this suggests that the early burst of theta ERS reflects a process that occurs after the sensation of the motion stimuli but is not affected by multisensory weighting. Although the limitations of spatial resolution with EEG recordings must be taken into account, the theta ERS oscillatory pattern could represent a contribution from activation of a network associated with place and grid cells from the parahippocampal area that are known to facilitate theta rhythms. Several studies have demonstrated that subsets of these cells are sensitive to visual-motion cues, physical-motion cues or a combination of both (Chen, King, Burgess & O'Keefe, 2013; Fattahi, Sharif, Geiller & Royer, 2018; Li, Arleo & Sheynikhovich, 2020).

4.3 Alpha ERD

The visual- and physical-motion conditions elicited alpha ERD with different latencies. Alpha ERD is currently understood to be associated with high focal cortical activation, while alpha ERS is associated with deactivation or inhibition, particularly within task-irrelevant brain

areas (Klimesch, 2012). It has been demonstrated that engaging in perceptual judgment or increased attentiveness leads to an increase in alpha ERD power (Adrian & Matthews, 1934; Niedermeyer & Lopes da Silva, 2005). This association has been shown across a variety of cognitive tasks (and their respective brain areas), such as reading (Angelakis & Lubar, 2002), auditory oddball tasks (Yordanova, Kolev & Polich, 2001), and observing the motor output of others (Avanzini et al., 2012). It is unsurprising then that alpha ERD is also found within the motor area during full-body self-motion perception in experiments such as the present study and Townsend et al. (2019). In a series of four large-scale EEG experiments, Fink, Grabner, Neuper and Neubauer (2005), showed that alpha ERD power may simply reflect the attentional demands of the current task; the more demanding the task, the stronger the alpha ERD (i.e., stronger cortical activation). We found an earlier alpha ERD during the visual-motion task versus the physical-motion task. Research has shown that the perception of visual information is faster than vestibular and proprioceptive information (Barnett-Cowan & Harris, 2013). The differences in the timeline of alpha ERD power in the present study corresponds with the findings of Fink et al. (2005), and Barnett-Cowan and Harris (2013). If the visual-motion stimulus is perceived faster than the physical-motion stimulus, intuitively the attentional demands should be greater earlier in the trial during the visual-motion task compared to the physical-motion task, thus creating a latency difference in alpha ERD. In the present study, we believe this latency difference reflects the timing differences of when attentional resources are engaged during visual versus physical self-motion perception. Considering this alpha ERD is recorded from the motor area, it is possible that this process indexed by alpha ERD might be part of multisensory integration. However, based on the data from the present study and Townsend et al. (2019), it is clearly not affected by the difference in multisensory weighting demands across the two studies.

4.4 Limitations and future directions

We did not record electromyographic (EMG) signals to directly remove movement-related artifacts from any reflexive compensatory adjustments in response to the physical motion. It is likely that our EEG data were only minimally affected because in the time range in which these movements would occur our visual-only condition elicited similar cortical activity as the physical-motion condition, however we cannot exclude the possibility of movement artifacts. PEPs related to compensatory movements commonly show up in the first 100 ms after stimulus onset (Varghese et al., 2017). In that time window our spectral data showed only latency differences, with oscillations in the theta, alpha and beta band occurring earlier in the visual-only condition. Future studies should account for compensatory adjustments by recording EMG of the neck muscles. This is especially important if participants are moved along axes known to elicit strong compensatory adjustments (e.g., roll).

A second potential limitation involves the timing of the visual- and physical-motion stimuli. The duration of the visual motion stimulus was 700 ms whereas the duration of the acceleration phase of the physical motion stimulus was 330 ms followed by a 1330 ms washout. This is typical in a motion simulator environment due to technological and spatial limitations of the motion platform (Pinto, Cavallo & Ohlmann, 2008). Typically, visual and physical motion are presented together; it works well because vestibular processes detect acceleration but not velocity. The acceleration of the washout is close to zero and does not contribute to the perception of acceleration in the heading or opposite direction (Figure 1). Thus, the perception is acceleration in the heading direction followed by constant velocity associated with the optic flow. The present experiment decoupled the visual and physical stimuli, and there is a possibility that the washout may be more detectable perceptually, and thus contribute to the ERSP

measures, than in a typical experiment that presents visual and physical simultaneously. Future experiments should address this systematically by comparing a set of acceleration-washout durations, within the range of technological and spatial limitations of the motion platform.

Finally, our heading discrimination task required participants to push a button in order to make a heading judgement. It is possible that the preparation and execution of thumb movements contributed to the cortical activity in the motor cortices. Response time differences in timing of motor output may be reflected in the observed oscillations. The heading judgement task satisfied important objectives to 1) ensure that participants attended to the motion cues to elicit the cortical activity, and 2) provide behavioural measures. Future designs might include a passive condition to examine whether motor responses affect the cortical activity between the visual and physical motion perception conditions.

5. Conclusion

The present study examined cortical activity elicited in response to single modality visual-only versus physical-only motion cues. An important motivation was to generate hypotheses about whether the theta, alpha and beta oscillations reflect a multisensory integration process or a more general process engaged during self-motion perception. Beta ERD and ERS responses support the hypothesis that beta oscillations index processes in multisensory weighting during visual-vestibular integration. Theta ERS and alpha ERD may be associated with processes other than multisensory weighting and are likely related to a more general cognitive process in self-motion perception.

Appendix

Supplementary Materials

Figure A1. The motion simulator pod was supported by a MOOG © platform with six-degrees-of-freedom motion (MOOG series 6DOF2000E).

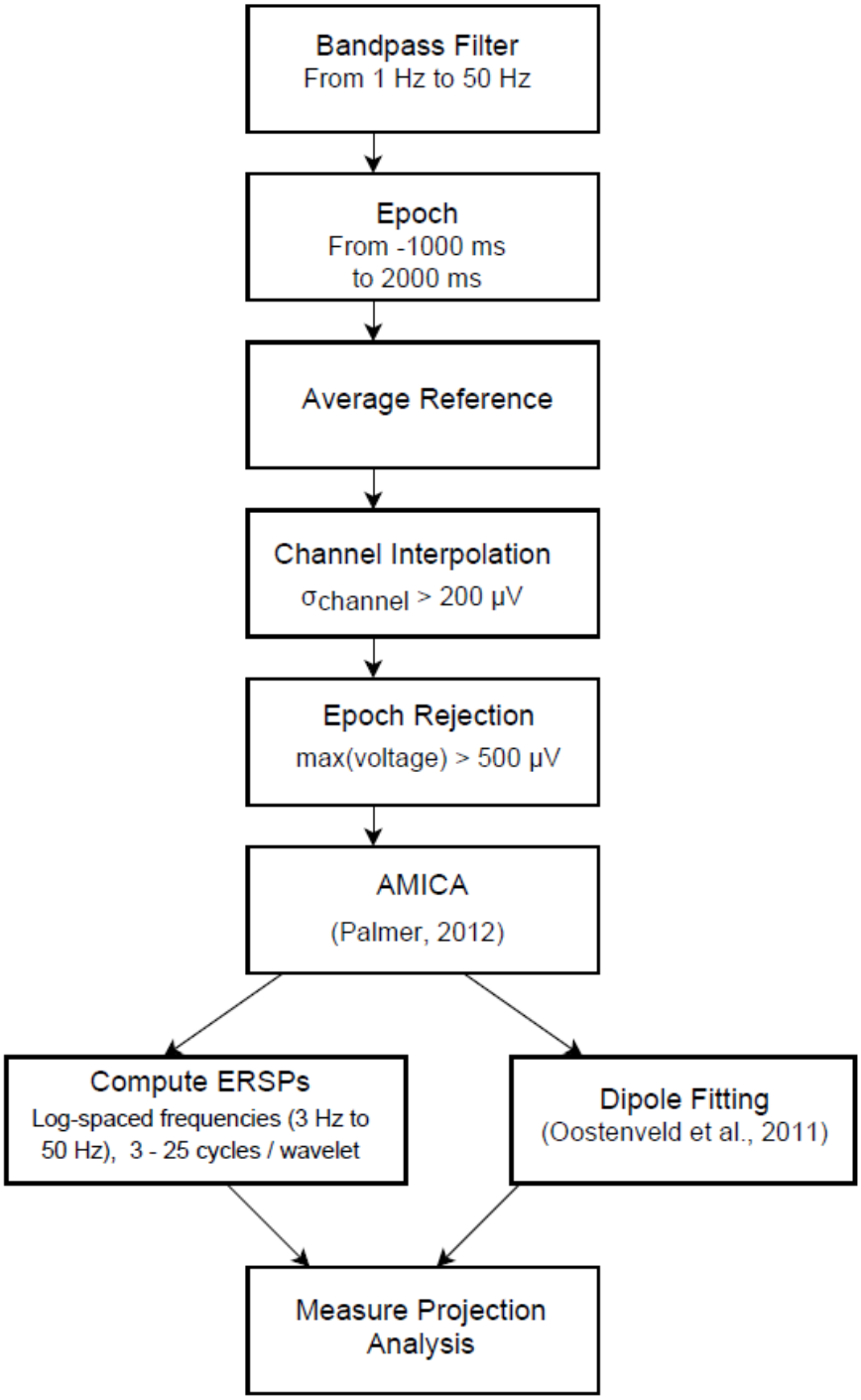

Figure A2. This flowchart illustrates the signal processing pipeline. The Measure Projection Analysis (MPA) pipeline is described in section 2.9 (ERSP Measure Projection Analysis), and a flowchart can be found in Bigdely-Shamlo, Mullen, Kreutz-Delgado & Makeig, 2013.

CHAPTER 4: Stimulus onset asynchrony affects weighting-related ERSP in self-motion perception

Townsend, B., Legere, J.K., v. Mohrenschildt, M., & Shedden, J.M. (Submitted)

Journal of Cognitive Neuroscience.

Manuscript ID: JOCN-2022-0167

Preface

Chapter 4 presents the results of an experiment in which visual- and physical- motion cues were presented in every trial, and the onset timing of the cues was manipulated. Chapters 2 and 3 established that the beta band indexes visual-vestibular weighting, and that these weighting-related beta oscillations can be modulated by attention allocation. In Chapter 4 we wanted to 1) further test our hypothesis that beta ERS power indexes visual weighting bias, and beta ERD power indexes vestibular weighting bias, and 2) determine whether attention allocation or stimulus onset timing had a greater effect on weighting bias. This experiment was a 2x3 design, which presented the same motion stimuli as previous chapters, either simultaneously, with the visual cue preceding the physical cue by 100 ms, or with the physical cue preceding the visual cue by 100 ms. Participants completed the same heading judgement task from previous chapters, which required either attention to the visual-motion stimuli (while ignoring physical-motion stimuli), or attention to the physical-motion stimuli (while ignoring visual-motion stimuli) in separate blocks. Stimulus onset asynchrony created a weighting advantage for the motion cue that was presented first, regardless of which motion cue was being attended to. Our results further supported our hypothesis that beta ERS power indexes visual weighting bias, and

beta ERD power indexes vestibular weighting bias. Based on the effects of the SOA conditions on beta power, we also found that stimulus onset timing has a greater effect on weighting-related ERSP than attention allocation.

ABSTRACT

Self-motion perception primarily relies on the integration of the visual, vestibular and proprioceptive systems. One complicating factor in this integration process is that each of these cues to motion are perceived on different timelines. For example, perception of visual motion onset occurs faster than perception of vestibular motion onset (e.g., ~220 ms for vision and ~440 ms for vestibular). There is a gap in understanding how a temporal lag between visual and physical motion cues affects visual-vestibular weighting during self-motion perception. The beta band is an index of visual-vestibular weighting, in that robust beta ERS is associated with visual weighting bias, and robust beta ERD is associated with vestibular weighting bias. The present study examined modulation of ERSP during a heading judgment task in which participants attended to either visual or physical motion cues. The temporal lag between the onset of visual and physical motion cues was manipulated to produce three lag conditions: simultaneous onset, visual before physical motion onset, and physical before visual motion onset. There were two main findings. First, the temporal lag elicited changes in the beta band, within both conditions of attention allocation. Importantly, we demonstrated that when the attended motion cue was presented before an ignored cue, the power of beta associated with the attended modality was greater than when visual-vestibular cues were presented simultaneously, or when the ignored cue was presented first. This was the case for beta ERS when the visual-motion cue was attended to, and beta ERD when the physical-motion cue was attended to. Second, we tested whether the power of feature-binding gamma ERS, demonstrated in audiovisual and visual-tactile integration studies (Senkowski, Schneider, Foxe & Engel, 2008), increased when the visual-vestibular cues were presented simultaneously versus with temporal asynchrony. We did not observe an increase in gamma ERS when cues were presented simultaneously, suggesting that electrophysiological

markers of visual-vestibular binding differ from markers of audiovisual and visual-tactile integration.

1. Introduction

Over the past 30 years, there have been dramatic increases in both the research and application of simulator training in aviation (for reviews see De Winter, Dodou & Mulder, 2012; Pinto, Cavallo & Ohlmann, 2008). Simulators are used as training devices in aviation because they provide a relatively risk-free means to practice complex, and in some cases, dangerous procedures (e.g., recovery from an unusual orientation; Lee & Myung, 2013). Increases in safety awareness within the aviation industry have amplified the demand for simulator training in advanced simulators that can replicate all in-flight scenarios. As a consequence of the growing safety awareness, technological developments in simulation technology continue to improve and the number of commercially-available simulators continues to grow.

A fundamental question is what degree of precision does a flight simulator need to provide the most effective training and research? The fidelity or degree of precision with which a flight simulator replicates actual flight has been a topic of debate within the aviation industry for decades (Hosman & Advani, 2016). Although many aviation researchers and pilots believe that highly precise simulators are needed for adequate flight training, there is little objective evidence to support this belief. Pilots' subjective assessments remain the most common method to assess the effectiveness of the fidelity of a flight simulator (Miletović et al., 2017; Jones, 2016).

The degree of fidelity in training simulators is a major focus for transfer of training research and for setting policies by flight training administration, and regulated and monitored by aviation authorities (e.g., Federal Aviation Administration (FAA) in USA and Transport Canada (TC) in Canada). Currently the FAA and TC require 6-axis platform motion for the highest level of pilot training and evaluation (Robinson, Mania & Perey, 2004). Moreover, FAA and TC require that 1) the onset of physical and visual motion cues be offset so that the physical motion

begins prior to the onset of the simulated visual motion, and that (2) a focus of training involves the skill to ignore cues to physical motion while attending to visual instruments in order to avoid spatial disorientation during perceptually complex scenarios (e.g., unusual changes in attitude). These two practices in combination lead to an important question around the effect of attention when motion cue onset timing and attention allocation are both manipulated. Addressing this question drives the first objective of the present paper.

Researchers in the area of multisensory integration have long grappled with the role of attention in multisensory processing (Macaluso, Noppeney, Talsma, Vercillo, Hartcher-O'Brien & Adam, 2016). Attention can be voluntarily allocated toward a stimulus, a sensory modality, or a specific region of space in order to achieve task goals (Li, Piëch & Gilbert, 2004). However, processing can also be involuntarily captured by sensory events, even when the attention capturing signals are unrelated to the current goal-directed activity (Öhman, Flykt & Esteves, 2001). Electroencephalography (EEG) is a useful tool to explore the online processes related to the interaction between attention and multisensory integration. The high temporal resolution of EEG has been effective in testing hypotheses related to synchronization of neural oscillations as a mechanism for the integration of information across sensory modalities (Senkowski, Schneider, Foxe & Engel, 2008). One hypothesis is that distinct spectral timelines index different local cortical networks involved in sensory processing, attention allocation, and multisensory integration (Siegel, Donner & Engel, 2012). Most studies that support the spectral timelines hypothesis are based on audiovisual or visuotactile integration (for review see Keil & Senkowski, 2018). For example, Senkowski, Talsma, Grigutsch, Herrmann and Woldorff (2007), showed that the closer in time the audiovisual stimuli were presented together, the more feature binding-related gamma event-related synchronization (ERS; > 30 Hz) was elicited early after

stimulus onset. This finding also supports Singer and Gray's (1995) temporal correlation hypothesis, which suggests that oscillations within the gamma band facilitate integration across sensory modalities. As far as we know there is a lack of published studies exploring how the onset timing of multisensory stimuli affect EEG correlates of visual-vestibular integration. This information is important when it comes to understanding how the timing of the onset of visual and physical cues to motion will affect pilots' attentional resources within virtual training environments (i.e., motion simulators). Does the stimulus onset asynchrony (SOA) required by TC and FAA policy affect attention-related processes needed to focus on visual information while simultaneously ignoring physical-motion information?

Townsend, Legere, O'Malley, v. Mohrenschildt and Shedden (2019) used a high-fidelity motion simulator and a high-density EEG array to observe event-related spectral power (ERSP) in response to simultaneous-onset visual- and physical-motion stimuli. To examine the effect of selective attention to visual versus physical motion, in a blocked design participants made heading judgments to visual (or physical) cues only, while ignoring the other modality. The heading of the simultaneous-onset motion cues was either spatially congruent or incongruent (e.g., both visual and physical headings left or right versus one left and the other right). Note again that the visual and physical motion cues were onset simultaneously.

Townsend et al. (2019) demonstrated that when visual and physical cues to self-motion are presented simultaneously, theta- (4-7 Hz), alpha- (8-12 Hz), and beta- (13-30 Hz) band oscillations are the predominant brain oscillations associated with self-motion perception. Moreover, when attention was focused on the visual-motion stimulus (while ignoring physical-motion cues) they found earlier theta ERS and alpha event-related desynchronization (ERD) at the beginning of the trial, and stronger beta ERS later in the trial, compared to attending to the

physical-motion stimulus. Moreover, when attention was focused on the physical-motion stimulus (while ignoring visual-motion cues), they found a more powerful beta ERD later in the trial, compared to focusing on the visual-motion stimulus (Townsend et al., 2019). Thus, previous research suggests that theta ERS is an index of heading processing (Townsend, Legere, v. Mohrenschildt and Shedden, 2022; for review see, Buzsáki & Moser, 2013), alpha ERD/ERS is associated with focal attention and cognitive load (for review see, Klimesch, 2012), and beta ERD/ERS indexes visual-vestibular weighting (Townsend et al., 2019, 2022).

Previous research has demonstrated that the beta band is an index of visual-vestibular weighting, and that attention allocation plays a key role in how weighting is distributed among multisensory inputs (Townsend et al., 2019; 2022). Those studies, however, did not investigate the impact stimulus onset timing has on the process of visual-vestibular weighting within self-motion perception. Previous research has shown that discrepancies in the onset timing of audiovisual stimuli can affect multisensory weighting (Fister, Stevenson, Nidiffer, Barnett & Wallace, 2016; Sheppard, Raposo & Churchland, 2013). The goals of the present study were twofold. The first goal was to examine the effect of temporal asynchrony of visual and physical motion cue onset on induced ERSP, specifically the power and time course of beta oscillations due to its association with visual-vestibular weighting. The second goal was to examine induced gamma oscillations (30 – 50 Hz.). Previous multisensory research (e.g., Senkowski et al., 2007) demonstrated more powerful feature-binding gamma ERS when audio-visual multisensory cue onsets were presented closer in time. We are not aware of any studies that have examined visual-vestibular stimulus onset asynchrony on gamma oscillations. The present study may provide evidence that gamma ERS is an index of general processes related to multisensory binding and integration across multiple sensory systems.

Participants attended to either physical (ignoring visual) or visual (ignoring physical) motion cues and discriminated between left and right self-motion headings. There were three stimulus onset asynchrony conditions: (1) visual motion onset 100 ms before physical motion onset, (2) physical motion onset 100 ms before visual motion onset, and (3) visual and physical motion onset simultaneous.

2. Materials and methods

2.1 Participants

Thirty-six participants (20 female) were recruited from the McMaster University psychology participant pool and the McMaster community. Ages ranged from 17 to 23 years (M = 18, SD = 1.30). Those recruited from the participant pool were compensated with course credits. All participants self-reported normal or corrected-to-normal visual acuity and reported no major problems with vertigo, motion sickness or claustrophobia. This experiment was approved by the Hamilton Integrated Research Ethics Board and complied with the Canadian tri-council policy on ethics.

2.2 Stimuli

2.2.1 Visual motion stimuli

Visual motion stimuli were presented on a 43-inch LCD panel, 51 inches in front of the participant, subtending a visual angle of 41°. The panel had a refresh rate of 60 Hz and a resolution of 1920 x 1080 (1080p).

The visual display, which created the perception of self-motion, was composed of a fixation cross in the center of the display and two tracks on a grey surface. Each track consisted of a series of yellow dashes perpendicular to the length of the track, drawn in perspective to a vanishing point so that the track appeared to extend into the distance. One track veered right,

while the other veered left, both at 35°, starting at the lower center of the display. Both tracks together subtended a horizontal visual angle of 33.69°. A horizon line was created by a grey surface upon which the tracks laid, and a blue sky with white clouds above, accentuating the perception of traveling along a track into the distance. The perception of self-motion was created via a first-person viewpoint animation that simulated a forward trajectory along one of the two tracks (see Figure 1, Panels B and C for two temporal snapshots). The duration of the visual-motion stimulus on each trial was 700 ms, followed by a 1200 ms pause in the final position at the end of the track. At the completion of the trial the stimulus was reset to the starting position.

2.2.2 Physical motion stimuli

A motion simulator provided physical-motion stimuli. The motion simulator cabin was supported by a MOOG © Stewart platform with six-degrees-of-freedom motion (Moog series 6DOF2000E; see Online Supplementary Figure A1). Participants were seated in a bucket-style car seat fixed to the cabin floor.

Each physical-motion stimulus consisted of the cabin moving in a forward linear translation, 35° left or right for 330 ms at 0.1 g. This surge was followed by a corresponding washout for 1330 ms which returned the cabin to the original position (1660 ms total; see Panel A in Figure 1). The acceleration intensity was selected based on preliminary testing to achieve a clear perception of forward motion within the spatial restrictions of the movement of the platform while minimizing compensating movements of the head, neck or upper body (Townsend et al., 2019). Physical forward accelerations were well above vestibular thresholds of .009 g, as discussed by Kingma (2005). The motion force, $s(t)$, was described by:

$$s(t) = \begin{cases} A_1 \; 0 \; \leq t \; \leq t_p \\ -A_2 \; t_p \; \leq t_b \\ A_2 \; t_b \; \leq t \; \leq t_e \\ 0 \; else \end{cases}$$

where t represents time in seconds, t_p represents present time, t_b represents the breakpoint and t_e represents the end time. A_1 describes the initial forward acceleration, $-A_2$ describes the initial (backwards) acceleration of the washout, and A_2 describes the deceleration of the washout. Acceleration was measured using an Endevco accelerometer (model number 752A13), calibrated to approximately 1 mV/g sensitivity.

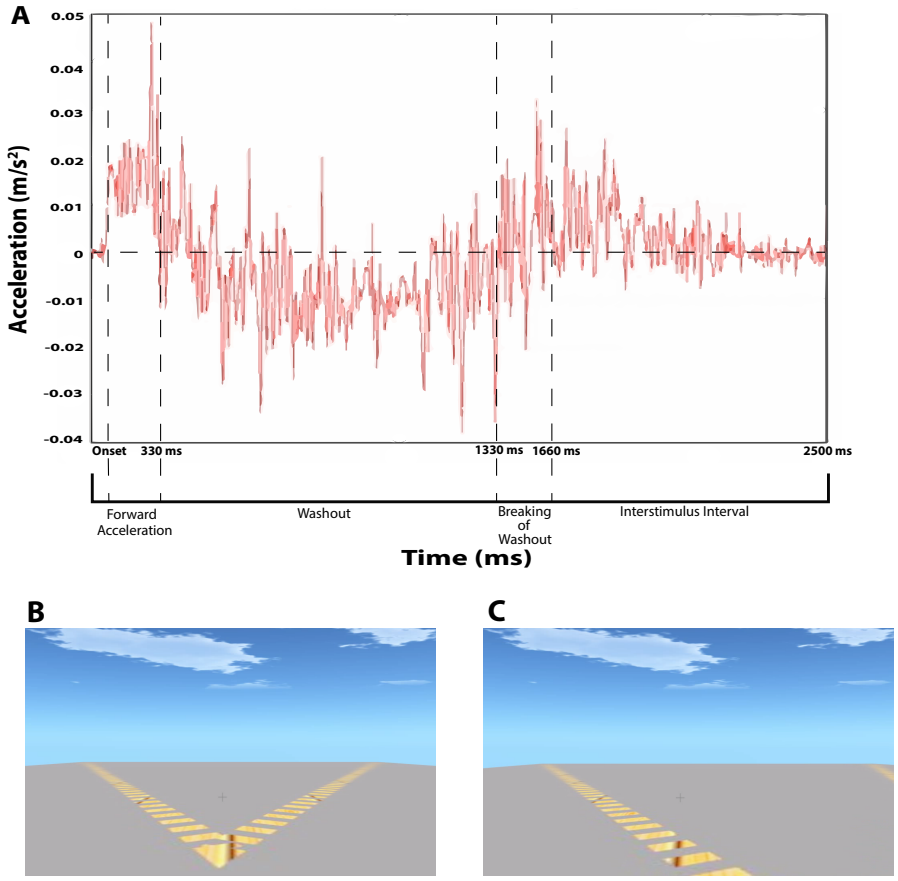

Figure 1. Time course of physical- and visual-motion stimuli. Panel A shows an example of the profile of physical motion measured during a single trial by an accelerometer (red line); the variance shown is due to the high sensitivity of the accelerometer. The x-axis represents time and the y-axis represents acceleration ($g = m/s^2$). The acceleration profile is similar for 35° left and 35° right physical-motion trials. Panel B shows the visual display before the onset of motion; at this point the participant does not know whether visual motion will indicate travel along the left or right track. Panel C shows a still screen capture of the dynamic visual motion display at approximately 1s after visual onset of a left visual motion trial.

2.3 Procedure

The entire session was between 1.5 and 2 hours in duration. The timeline of the session included collection of demographic information, followed by completion of one practice block (30 trials; ~2 minutes), application of EEG electrodes (25 minutes), completion of four experimental blocks (60 minutes), and participant clean up and debriefing (15 minutes).

There were 796 experimental trials divided into 4 blocks of 199 trials each. Participants fixated on the fixation cross for the duration of each trial; a blink break was provided every 15 trials. The AV and AP tasks were blocked to avoid task switching effects. The task required participants to direct attention to the visual-motion stimulus and ignore the physical-motion cues (AV task) or to direct attention to the physical-motion stimulus and ignore the visual-motion cues (AP task). They responded with a button press to indicate whether the direction of the attended-modality motion was left or right heading.

Given the importance of collecting enough clean data with correct responses in each attention condition for EEG analyses, and given that participants have a more difficult time ignoring the visual while attending the physical stimulus (Townsend et al., 2019), we collected three AP blocks compared to one AV block. Presentation order was controlled so that the AV block was presented as the first, second, or third of the four blocks. Moreover, to ensure that participants maintained attention to the intended modality (especially during AP blocks), each block contained 8 catch trials in which the ignored modality heading was incongruent with the attended modality heading.

Stimulus Onset Asynchrony (SOA) was manipulated to produce simultaneous (S), visual-first (V1st), and physical-first (P1st) conditions. In the simultaneous condition, visual and physical motion cues were onset at the same time. In the visual-first condition, the visual motion

stimulus was onset 100 ms before the physical motion, and in the physical-first condition, the physical motion stimulus began 100 ms before the visual motion. There was an equal number of left and right heading trials in each block, randomly presented.

2.4 EEG data acquisition

EEG data were collected using the BioSemi ActiveTwo electrophysiological system (www.biosemi.com) with 128 sintered Ag/AgCl scalp electrodes. Four additional electrodes recorded eye movements (two placed laterally from the outer canthi and two below the eyes on the upper cheeks). Continuous signals were recorded using an open pass band from direct current to 150 Hz and digitized at 1024 Hz.

2.5 EEG preprocessing

All processing was performed in Matlab 2014a using functions from EEGLAB (Delorme & Maekig, 2004) on the Shared Hierarchical Academic Research Computing Network (SHARCNET: www.sharcnet.ca). A flowchart illustrating the signal-processing pipeline can be found in the supplementary materials (see Online Supplementary Figure A2). EEG data were band-pass filtered between 1 and 50 Hz, and epoched from 1000 ms pre-stimulus to 2000 ms post-stimulus. Each epoch was baseline corrected using the whole-epoch mean (Groppe, Makeig & Kutas, 2009). Channels with a standard deviation exceeding 200 μV were interpolated after referencing (on average, 0.97 channels interpolated per subject, with a total of 35 channels interpolated). Bad epochs were rejected if they had voltage spikes exceeding 500μV or violated EEGLAB's joint probability functions (Delorme, Sejnowski & Makeig, 2007).

Single-subject EEG data were submitted to an extended Adaptive mixture independent component analysis (AMICA) with an N – (1 + interpolated channels) Principal Components Analysis reduction (Makeig, Bell, Jung & Sejnowski, 1996). Decomposing an EEG signal into

independent components (ICs) allows for analysis of each individual signal produced by the brain that would otherwise be indistinguishable. Dipoles were then fit to each IC using the fieldtrip plugin for EEGLAB following AMICA (Oostenveld, Fries, Maris & Schoffelen, 2011). ICs for which dipoles were located outside the brain, or explained less than 85% of the weight variance, were excluded from further analysis. On average, 20.47 ICs per subject were excluded from analysis.

2.6 ERSP measure projection analysis

Event-related spectral power (ERSP) was computed for each of the remaining ICs. Fifty log-spaced frequencies between 3 and 50 Hz were computed, with 3 cycles per wavelet at the lowest frequency up to 25 at the highest. Measure projection analysis (MPA) was used to cluster ICs across participants using the Measure Projection Toolbox for MATLAB (Bigdely-Shamlo, Mullen, Kreutz-Delgado & Makeig, 2013). MPA is a method of categorizing the location and consistency of EEG measures, such as ERSP, across single-subject data into 3D domains. Each domain is a subset of ICs that are identified as having spatially similar dipole models, as well as similar cortical activity (measure-similarity). MPA fits the selected ICs into a 3D model of the brain, comprised of a cubic space grid with 8-mm spacing according to normalized Montreal Neurological Institute (MNI) space. The MPA toolbox identified cortical regions of interest by incorporating the probabilistic atlas of human cortical structures provided by the Laboratory of Neuroimaging project (Shattuck et al., 2008). Voxels that fell outside of the brain model (muscle artifacts, etc.) were excluded from the analysis.

We then calculated local convergence values, using an algorithm based on Bigdely-Shamlo et al. (2013) which deals with the multiple comparisons problem. Local convergence calculates the measure-similarity of dipoles within a given domain and compares them with

randomized dipoles. A pairwise IC similarity matrix was created by estimating the signed mutual information between independent component-pair ERSP measure vectors, assuming a Gaussian distribution, in order to compare dipoles. As explained in detail by Bigdely-Shamlo et al. (2013), signed mutual information was estimated to improve the spatial smoothness of the obtained MPA significance value beyond determining similarity of dipoles through correlation. Bootstrap statistics were used to obtain a significance threshold for convergence at each location of our 3D brain model. Following past literature, we set the raw voxel significance threshold to $p < .001$ (Bigdely-Shamlo et al., 2013; Chung, Ofori, Misra, Hess & Vaillancourt, 2017).

Our analyses focused on two relevant domains: the right motor area, with the greatest concentration of dipoles consistent with right premotor and supplementary motor area (BA 6), and the left motor area, with the greatest concentration of dipoles consistent with left premotor and supplementary motor area (BA 6). For the right motor area, each participant contributed on average 2.33 (±1.53) ICs, with each participant contributing at least one IC, with a range from 1 – 7 ICs. For the left motor area, each participant contributed on average 2.19 (±1.51) ICs. There were five participants who did not contribute to this domain. The range of contributed ICs was 0 – 6.

ERSPs were computed for each experimental condition within each domain calculated by MPA. Bootstrap statistics were used to assess differences in ERSP between conditions to uncover main effects of task and stimulus onset asynchrony (SOA). Differences at each power band were computed by projecting the ERSP for each condition to each voxel in the domain. This projection was weighted by dipole density per voxel and then normalized by the total domain voxel density for each participant. Analysis of projected source measures were separated into discrete spatial domains by threshold-based Affinity Propagation clustering based on a

similarity matrix of pair-wise correlations between ERSP measure values for each position. Following Chung et al. (2017), we used the maximal exemplar-pair similarity, which ranges from 0-10 to set a value of 0.8 (Bigdely-Shamlo et al., 2013; Chung et al., 2017; Ofori et al., 2015).

2.7. Data and code availability

The data and code for all analyses are available online at https://github.com/bentownsend11/Stimulus-onset-asynchrony-affects-attention-related-ERSP-in-self-motion-perception

3. Results

3.1 Behavioural results

Behavioural data were analyzed with two 2x3 repeated-measures ANOVAs for measures of judgment accuracy and response time. Outliers were defined as trials with response times greater than three standard deviations above or below the mean in each condition and were eliminated from all further analyses. The Greehouse-Geisser correction was applied to all effects that violated Mauchley's test of sphericity.

3.1.1 Accuracy

Participants were more accurate at discriminating direction in the Attend-Visual task (M= 99%, SE = .003) than the Attend-Physical task (M = 95%, SE = .01), $F(1, 35) = 10.50$, $p < .05$, $\eta_p^2 = .23$. The main effect of SOA on accuracy (Greenhouse-Geisser corrected), $F(1.69, 59.02) = 5.77$, $p < .01$, $\eta_p^2 = .14$, was influenced by a task x SOA interaction $F(2, 70) = 5.00$, $p < .01$, $\eta_p^2 = .13$. Bonferroni corrected pairwise comparisons supported the observation that the SOA effects were apparent during the Attend-Physical task only; there were no significant differences in accuracy between any of the SOA conditions during the Attend-Visual task. More specifically,

participants were more accurate in the Attend-Physical Physical-First (AP(P_{1st})) condition (M = 95.9%, SE = .01) than the Attend-Physical Visual-First (AP(V_{1st})) condition (M = 94.10%, SE = 0.02) (p <.01).

3.1.2 Response Time

Participants were faster at discriminating direction in the Attend-Visual task (M = 1018 ms, SE = 90.20) than the Attend-Physical task (M = 1409 ms, SE = 78.72), $F(1, 35) = 39.43$, $p <$ .001, $\eta_p^2 = .53$, and there was a main effect of SOA, $F(2, 70) = 519.35$, $p < .001$, $\eta_p^2 = .94$. The task x SOA interaction on response times (Greenhouse-Geisser corrected), $F(1.52, 53.22) = 3.48$, $p = .05$, $\eta_p^2 = .9$, differed from the accuracy results such that Bonferroni corrected pairwise comparisons revealed response time differences across conditions in both Attend-Physical and Attend-Visual tasks. During the Attend-Visual task, responses were faster for the Visual-First (AV(V_{1st})) trials (M = 899 ms, SE = 92.99) compared to Simultaneous (AV(S)) trials (M = 1020 ms, SE = 90.19), (p <.01), which were in turn faster than Physical-First (AV(P_{1st})) trials (M = 1135 ms, SE = 88.36), (p <.01). Likewise, during the Attend-Physical task, responses were faster for the AP(V_{1st}) trials (M = 1269 ms, SE = 77.69) compared to Simultaneous (AP(S)) trials (M = 1406 ms, SE = 79.04), (p <.01), which were in turn faster than AP(P_{1st}) trials (M = 1552 ms, SE = 80.12), (p <.01). We interpret this result to suggest that participants benefited more from the visual-motion cue versus the physical-motion cue being presented first due to visual information being perceived faster than vestibular information. This hypothesis is supported by previous literature, such as Barnett-Cowan and Harris (2013). The preceding visual-motion cue was likely a stronger prime. The interaction was driven by the Attend-Physical task being more affected by SOA than the Attend-Visual task. Thus, two important observations are that 1) participants are faster overall when attending to visual motion, but importantly, 2) both Attend-Visual and

Attend-Physical conditions are highly sensitive to which stimulus was presented first. Exploring the ERSP results provides insights into how the temporal order of stimuli may be affecting multisensory integration, and thus leading to differences in accuracy and response times.

3.2 Oscillatory power

3.21 Effects of SOA in Attend-Visual task

Figure 2 presents a comparison of the left and right motor areas to illustrate the effect of the timing of the stimulus onset on the cortical activity during the Attend-Visual conditions in both MPA (measure projection analysis) domains. All ERSP represents a difference in oscillatory power compared to baseline (pre-trial) cortical activity, where an ERS (event-related synchronization) represents more spectral power than baseline and an ERD (event-related desynchronization) represents less spectral power than baseline. In Figure 2, Panel A shows the left motor area, with the highest dipole density in the premotor and supplementary motor area (Brodmann area (BA) 6), and Panel D shows the right motor area, with the highest dipole density in the premotor and supplementary motor area (BA 6). In Panels B (left motor) and E (right motor) we show the associated ERSP plots for the AV(V_{1st}), AV(S) and AV(P_{1st}) conditions. The ERSP plots are followed by bootstrapped comparisons ($\alpha = 0.05$) between each possible pair of conditions for left (Panel C) and right (Panel F) motor areas. The following sections will describe observations of the activity changes associated with experimental conditions across frequency bands theta, alpha, beta, and gamma. All of the comparisons outlined in the following sections were significant at $p < .05$.

Theta-band latency differences:

The AV(P_{1st}) condition elicited theta ERS significantly later than the AV(S) and AV(V_{1st}) conditions. Specifically, in both the left and right motor areas (Panels C and F, respectively),

AV(S) elicited greater theta ERS from ~100 ms to 200 ms post stimulus and AV(P_{1st}) elicited greater theta ERS later in the trial, from ~500 ms to 950 ms post stimulus. Likewise, AV(V_{1st}) elicited greater theta ERS from stimulus onset to 300 ms post stimulus and AV(P_{1st}) elicited greater theta ERS from ~500 ms to 1000 ms post stimulus.

Alpha-band power differences:

In the left and right motor areas (Panels C and F, respectively) AV(P_{1st}) elicited the strongest alpha ERD, compared to AV(S) (~750 – 1500 ms post-stimulus) and AV(V_{1st}) (~600 – 1500 ms post-stimulus), and AV(S) elicited stronger alpha ERD than AV(V_{1st}) (~550 – 1500 ms post-stimulus). Thus, in general, alpha ERD AV(P_{1st}) > AV(S) > AV(V_{1st}).

Beta-band power differences:

Much like the results in the alpha band, we found that the earlier physical motion was presented, the stronger the elicited beta-band ERD power. In the left and right motor areas (Panels C and F, respectively) AV(P_{1st}) elicited the strongest beta ERD, compared to AV(S) (~500 – 1500 ms post-stimulus) and AV(V_{1st}) (~400 – 1500 ms post-stimulus), and AV(S) elicited stronger alpha ERD than AV(V_{1st}) (~300 – 1000 ms post-stimulus). Thus, in general, beta ERD AV(P_{1st}) > AV(S) > AV(V_{1st}).

Gamma-band power differences:

AV(V_{1st}) elicited a more powerful gamma ERS than AV(P_{1st}) from ~600 – 1200 ms post-stimulus in the right motor area (Panel F).

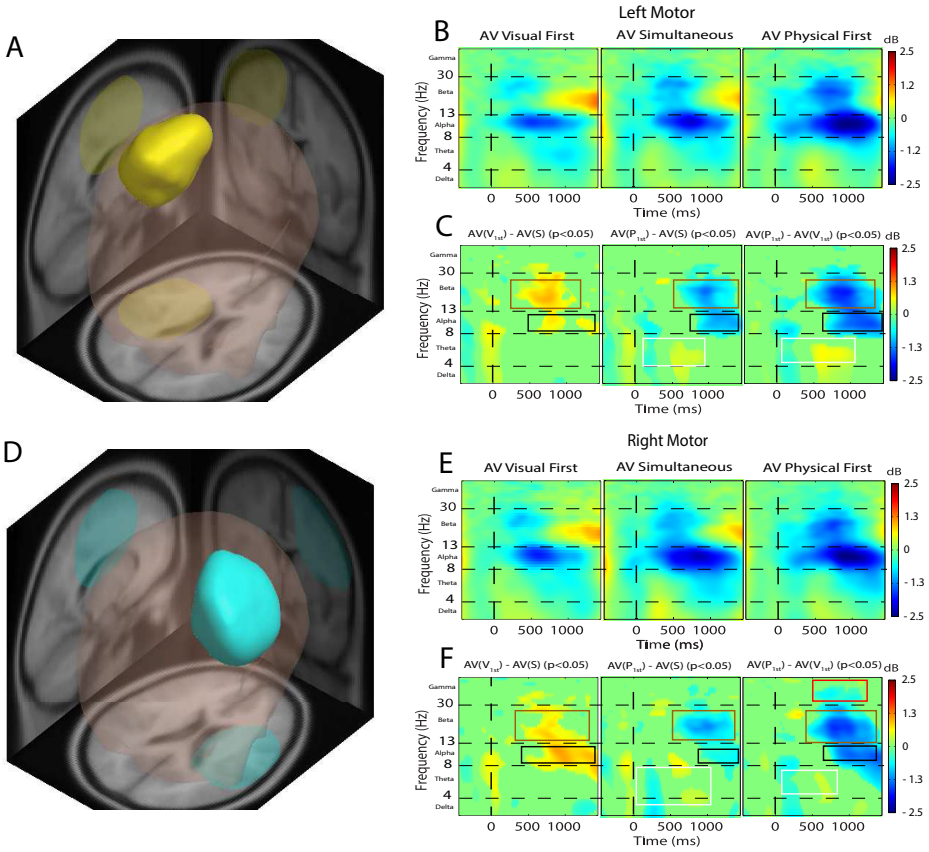

Figure 2 (Attend-Visual Task). Left motor area (Panels A, B, and C) and right motor area (Panels D, E, and F) identified by MPA and respective ERSP analysis. The ERSP plots show time (ms) across the x-axis and frequency of the EEG signal along the y-axis. Panels B (left) and E (right) show the associated ERSP plots for the attend-visual visual first ($AV(V_{1st})$), attend-visual simultaneous (AVS) and attend-visual physical first ($AV(P_{1st})$) conditions. Panels C (left motor area) and F (right motor area) show the bootstrapped comparisons ($p < .05$) between each possible pair of conditions. ERS power is depicted in yellow/red, ERD power is depicted in blue, and green shows no difference in spectral power compared to baseline. **MPA motor areas: Panels A and D** show 3D representations of the brain with the yellow region representing the left motor area and the blue region representing the right motor area. The greatest concentration of dipoles in left and right regions were consistent with premotor and supplementary motor areas (BA 6). **Panels B and E:** ERSP plots for each condition. **Panels C and F:** Bootstrapped comparisons examine each possible pair of conditions; frequency and time of significant comparisons are shown by the coloured boxes. Both left and right motor areas show similar conditional differences. *Theta*: $AV(V_{1st})$ and AV(S) elicits theta ERS significantly earlier than $AV(P_{1st})$ (white boxes). *Alpha*: $AV(P_{1st})$ elicits stronger alpha ERD than AV(S) and $AV(V_{1st})$, and AV(S) elicits strong alpha ERD than $AV(V_{1st})$ (black boxes). *Beta*: $AV(P_{1st})$ elicits stronger beta ERD than AV(S) and $AV(V_{1st})$, and AV(S) elicits stronger beta ERD than $AV(V_{1st})$ (brown boxes). *Gamma*: Differences in gamma existed only in the right motor area: the $AV(V_{1st})$ condition elicited significantly stronger gamma ERS than $AV(P_{1st})$ (red boxes).

3.22 Effects of SOA in Attend-Physical task

Figure 3 presents a comparison of the same left and right motor areas as Figure 2 to illustrate the effect of stimulus onset timing on the cortical activity during the Attend-Physical conditions in both MPA domains. All of the comparisons outlined in the following sections were significant at $p < .05$.

Theta-band latency differences:

The AP(P_{1st}) condition elicited theta ERS significantly later than the AP(S) and AP(V_{1st}) conditions. Specifically, in both the left and right motor areas (Panels C and F, respectively), AP(S) elicited greater theta ERS from stimulus onset to ~300 ms post stimulus and AP(P_{1st}) elicited greater theta ERS later in the trial, from ~500 ms to 600 ms post stimulus. Likewise, AP(V_{1st}) elicited greater theta ERS from stimulus onset to ~400 ms post stimulus and AP(P_{1st}) elicited greater theta ERS from ~500 ms to 600 ms post stimulus.

Alpha-band power differences:

In the left and right motor areas (Panels C and F, respectively) AP(P_{1st}) elicited the strongest alpha ERD, compared to AP(S) (~700 – 1500 ms post-stimulus) and AP(V_{1st}) (~600 – 1500 ms post-stimulus), and AP(S) elicited stronger alpha ERD than AP(V_{1st}) (~600 – 1500 ms post-stimulus). Thus, in general, alpha ERD AP(P_{1st}) > AP(S) > AP(V_{1st}).

Beta-band power differences:

In the left and right motor areas (Panels C and F, respectively) AP(P_{1st}) elicited the strongest beta ERD, compared to AP(S) (~550 – 1500 ms post-stimulus) and AP(V_{1st}) (~500 – 1500 ms post-stimulus), and AP(S) elicited stronger alpha ERD than AP(V_{1st}) (~800 – 1200 ms post-stimulus). Thus, in general, beta ERD AP(P_{1st}) > AP(S) > AP(V_{1st}).

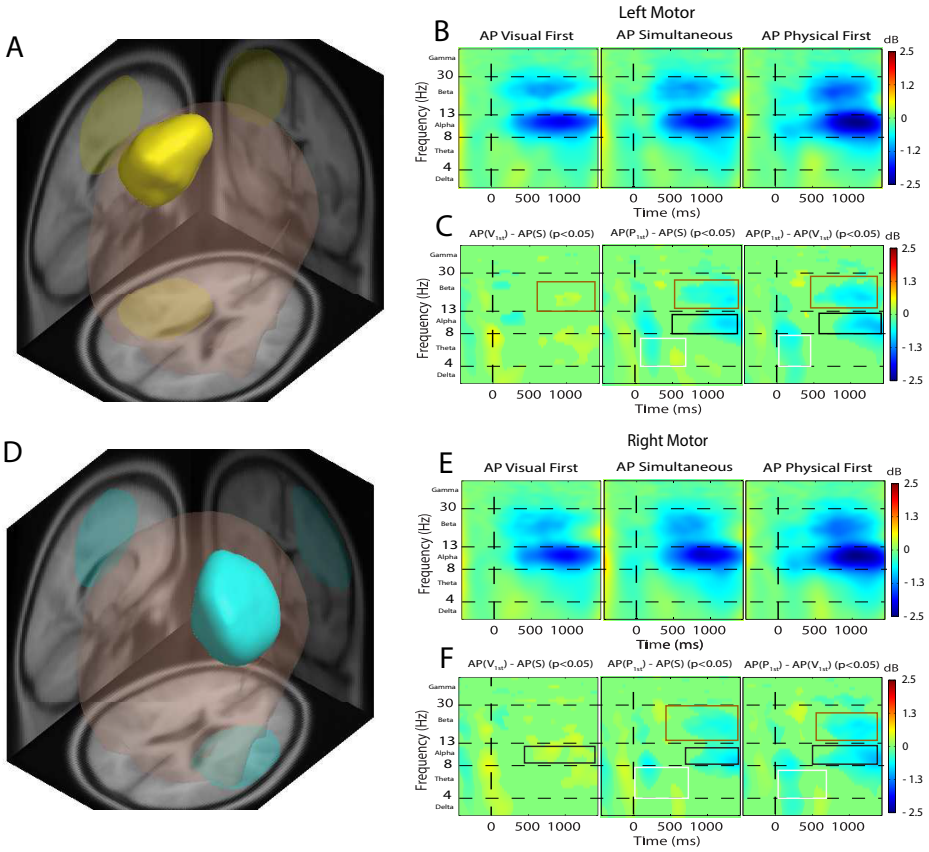

Figure 3 (Attend-Physical Task). Left motor area (Panels A, B, and C) and right motor area (Panels D, E, and F) identified by MPA and respective ERSP analysis. The ERSP plots show time (ms) across the x-axis and frequency of the EEG signal along the y-axis. Panels B (left) and E (right) show the associated ERSP plots for the attend-physical visual first (AP(V_{1st})), attend-physical simultaneous (APS) and attend-physical physical first (AP(P_{1st})) conditions. Panels C (left motor area) and F (right motor area) show the bootstrapped comparisons (p <.05) between each possible pair of conditions. ERS power is depicted in yellow/red, ERD power is depicted in blue, and green shows no difference in spectral power compared to baseline. **MPA motor areas:** Panels A and D show 3D representations of the brain with the yellow region representing the left motor area and the blue region representing the right motor area. The greatest concentration of dipoles in left and right regions were consistent with premotor and supplementary motor areas (BA 6). **Panels B and E:** ERSP plots for each condition. **Panels C and F:** Bootstrapped comparisons examine each possible pair of conditions; frequency and time of significant comparisons are shown by the coloured boxes. Both left and right motor areas show similar conditional differences. *Theta*: AP(V_{1st}) and AV(S) elicits theta ERS significantly earlier than AP(P_{1st}) (white boxes). *Alpha*: AP(P_{1st}) elicits stronger alpha ERD than AP(S) and AP(V_{1st}), and AP(S) elicits strong alpha ERD than AP(V_{1st}) (black boxes). *Beta*: AP(P_{1st}) elicits stronger beta ERD than AP(S) and AP(V_{1st}), and AP(S) elicits stronger beta ERD than AP(V_{1st}) (brown boxes).

3.23 Effects of attention allocation across SOA conditions

Figure 4 presents the same right motor area as Figure 2 and 3 to illustrate the interaction of stimulus onset timing and attention allocation. We compared cortical activity between conditions of attention allocation at each level of the SOA condition (i.e., AV(S) vs AP(S), AV(V_{1st}) vs AP(V_{1st}), and AV(P_{1st}) vs AP(P_{1st})). Similar results were found in the left motor area. All of the comparisons outlined in the following sections were significant at $p < .05$.

Theta-band power differences:

AV(S) elicited a more powerful theta ERS than AP(S) from ~250 ms – 400 ms post stimulus (Panel C).

Alpha-band power differences:

In the right motor area (Panel A) AV(S) elicited a stronger alpha ERD, compared to AP(S) (~50 – 550 ms post-stimulus) (Panel C). AP(V_{1st}) elicited greater alpha ERD than AV(V_{1st}) from ~800 ms – end of trial (Panel D).

Beta-band power differences:

In the right motor area (Panels A), AP(P_{1st}) elicited a stronger beta ERD than AV(P_{1st}) from ~550 – 1500 ms post-stimulus (Panel B), AV(S) elicited a stronger beta ERS than AP(S) from ~800 ms – end of trial (Panel C), and AV(V_{1st}) elicited more powerful beta ERS than AP(V_{1st}) from ~700 ms – end of trial (Panel D).

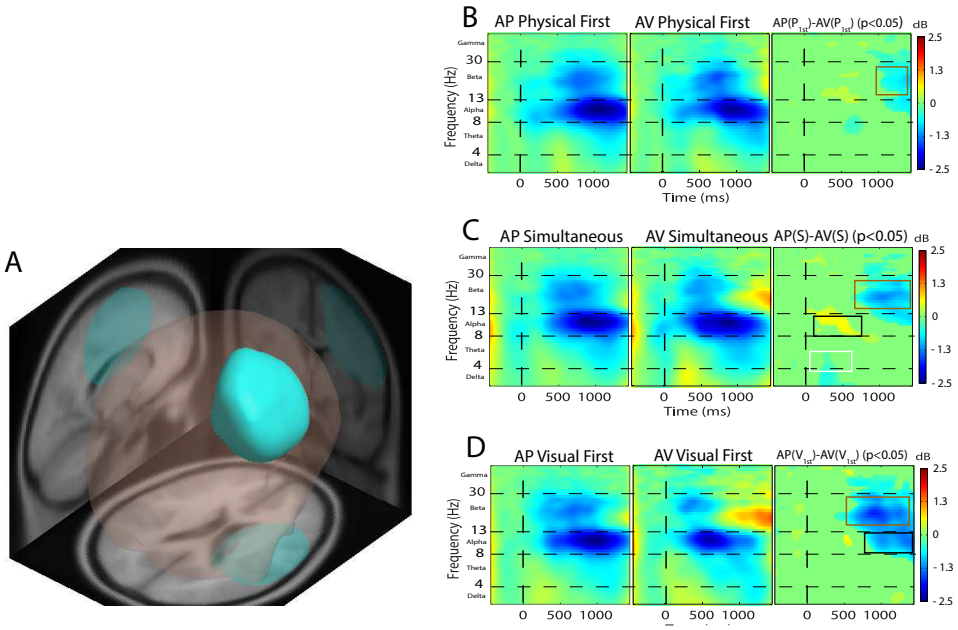

Figure 4 Right motor area identified by MPA and respective ERSP analysis. The ERSP plots show time (ms) across the x-axis and frequency of the EEG signal along the y-axis. Panels B, C and D show the associated ERSP plots for the attend-physical and attend-visual conditions at each level of the SOA condition, and the bootstrapped comparisons (p <.05) between each pair of conditions. ERS power is depicted in yellow/red, ERD power is depicted in blue, and green shows no difference in spectral power compared to baseline. **MPA right motor area:** Panel A shows 3D representations of the brain with the blue region representing the right motor area. The greatest concentration of dipoles in right region were consistent with premotor and supplementary motor areas (BA 6). **Panels B, C and D:** Bootstrapped comparisons examine each possible pair of conditions; frequency and time of significant comparisons are shown by the coloured boxes. *Theta*: AV(S) elicits stronger theta ERS than AP(S) (Panel C; white box). *Alpha*: AV(S) elicits stronger alpha ERD than AP(S) (Panel C), and AP(V_{1st}) elicits stronger alpha ERD than AV(V_{1st}) (Panel D; black boxes). *Beta*: AP(P_{1st}) elicits stronger beta ERD than AV(P_{1st}) (Panel B), AV(S) elicits stronger beta ERS than AP(S) (Panel C), and AV(V_{1st}) elicits stronger beta ERS than AP(V_{1st}) (Panel D; brown boxes).

4. Discussion

The current policies of TC and FAA require physical cues to motion to precede visual cues to motion during pilot simulator training. Pilots are trained to attend to visual instruments and ignore vestibular inputs caused by forces such as turbulence, in order to avoid spatial disorientation (Braithwaite, 1997). One question that arises from this practice is how the temporal asynchrony of the motion cues affect pilots' multisensory processing. Behavioural research has demonstrated a temporal binding window for visual-vestibular integration, in which multisensory integration affects heading perception, temporal order judgements and attention allocation (Rodriguez & Crane, 2021; Shayman et al., 2018). Research exploring the cortical processes underlying this temporal window is currently scarce. In order to better understand the online processes related to multisensory temporal binding, we must look to literature focused on the integration of other senses, such as audiovisual, or visuotactile integration. Studies such as Senkowski et al., (2007), have demonstrated that the closer audiovisual stimuli are presented temporally, the more powerful the elicited feature-binding gamma ERS response. Past multisensory research has demonstrated a Gaussian integration window, in which integration breaks at a temporal asynchrony specific to the senses being integrated (e.g., Rodriguez & Crane, 2021). The present study explored how EEG oscillations related to attention in self-motion perception (theta, alpha and beta; Townsend et al., 2019), and multisensory feature binding (gamma; Senkowski et al., 2007) were affected by varying conditions of stimulus onset asynchrony.

4.1 The effects of timing onset within an attended modality

Recent research by Townsend et al. (2019; 2022) showed that theta, alpha and beta oscillations reveal brain networks involved in the perception of self-motion. Moreover, the

power of these individual oscillations changed dynamically depending on which sensory inputs were attended to. Taken together, our two previous studies demonstrated that the beta band is most sensitive to changes in visual-vestibular weighting. Specifically, these studies showed that a strong beta ERS is an electrophysiological signature of heavy visual weighting, and a strong beta ERD is a signature of vestibular weighting.

The current study revealed changes in the same spectral bands as the previously mentioned studies and contributed additional key insights to the understanding of self-motion perception. One robust result that we observed was when presenting an attended motion cue before an ignored cue, the power of the beta oscillation associated with weighting bias towards the attended modality (ERS for visual and ERD for vestibular) was greater than during simultaneous presentation of the attended and ignored cues. This result suggests that the power of weighting-related beta oscillations during self-motion perception is also sensitive to the timing of the onset, and not just attention allocation. Regardless of which modality is being attended to, the earlier the attended motion cue is presented in relation to the ignored cue, the more powerful the weighting-related ERSP. The inverse was true when the ignored cues were presented before the attended cues. Beta ERS was less powerful in the AV(P_{1st}) condition versus AV(S), and beta ERD was less powerful in the AP(V_{1st}) condition versus AP(S).

The beta cycle has long been thought to reflect an initiation and termination of motor output (for review see Kilavik, Zaepffel, Brovelli, MacKay & Riehle, 2013). Contrary to this hypothesis, Townsend et al. (2019; 2022) demonstrated a beta rebound during passive full-body motion that was induced by attention and suggested that beta oscillations during motor processing may actually reflect perceptual weighting of the visual, vestibular and proprioceptive systems. The beta rebound may reflect the inhibition of processing the physical-motion stimuli,

considering visual-vestibular integration is a subadditive process. Subadditive inhibition typically occurs during integration when there is a discrepancy in the reliability of multiple sensory inputs (Angelaki, Gu, DeAngelis, 2009). The Townsend et al. (2022) study showed that participants performed the heading discrimination task at 99% accuracy in both visual- and physical-motion only conditions (the same motion stimuli as the current study). Considering there were likely no significant differences in reliability between the two sensory inputs, we believe that the temporal advantage caused by the SOA led to strong inhibitory responses during integration. Our results fall in line with Townsend et al. (2019; 2022). We believe the oscillatory differences in the beta band between the stimulus onset timing conditions may be a product of the perceptual weights being changed due to the SOA. For example, the processing of the visual stimulus during the AV(V_{1st}) condition began 100 ms before the processing of the physical-motion stimulus. This perceptual head start could have increased the weighting in favor of the visual stimulus, more so than in the AV(S) condition. A similar weighting bias may have taken place during the attend-physical conditions, as we found similar results (but in beta ERD). These power differences in ERSP did not result in differences in accuracy, however (attend-visual 99% accuracy, attend-physical 95% accuracy). We believe that the tasks may not have been sensitive enough to capture correlations between behavioural differences and oscillatory power. The present study clearly demonstrates that the timing of stimulus onset is a critical component of the visual-vestibular weighting process, and is indexed by dynamic changes in the beta band.

4.2 The interaction of stimulus timing and attentional selection

Not only did we find that the timing of stimulus onsets affected ERSP, we also found an interaction between the timing of onsets and attention allocation. We compared the visual- versus the physical-motion conditions at each SOA condition. Our comparison of AP(S) versus AV(S)

was a replication of a condition in Townsend et al. (2019), and we found similar results in the present study, the most important observation being stronger beta ERS in attend-visual conditions and stronger beta ERD in attend-physical conditions. This comparison acted as a baseline, while the other two comparisons presented novel findings.

The comparisons AP(P_{1st}) versus AV(P_{1st}) (contrasting attention conditions when the physical stimulus onset first), and AP(V_{1st}) versus AV(V_{1st}) (contrasting attention conditions when the visual stimulus onset first) demonstrated an interaction of attention allocation and stimulus onset asynchrony in the beta band. When the physical-motion cue was presented 100 ms before the visual cue, there were fewer ERSP differences between AP(P_{1st}) versus AV(P_{1st}), compared to the baseline comparison. Most notably, the typical beta rebound elicited by attention to the visual-motion cue was not present in the AV(P_{1st}) condition. Based on the findings of Townsend et al. (2019; 2022), the lack of a beta rebound in the AV(P_{1st}) condition suggests that presenting the physical-motion cue before the visual-motion cue resulted in greater weighting of vestibular signals than if the motion cues were presented simultaneously. This finding is relevant to simulator training for pilots. If the vestibular cue to motion is presented before the visual cue, it may disrupt the operator's ability to down-weight potentially disorienting vestibular cues that pilots are trained to ignore.

The lack of a beta rebound in the AV(P_{1st}) condition resulted in relatively little difference in ERSP between AP(P_{1st}) versus AV(P_{1st}). However, when the visual-motion cue was presented 100ms before the physical-motion cue, there was a robust beta ERS in the AV(V_{1st}) condition versus a beta ERD in the AP(V_{1st}) condition. This analysis revealed that visual-vestibular weighting is more sensitive to changes in the onset timing of the visual cues to motion than the vestibular cues. This finding is supported by Barnett-Cowan and Harris (2013), who

demonstrated that perception of visual stimuli is faster than perception of vestibular stimuli. Considering the visual cue naturally has a temporal advantage (during simultaneous presentation), it is likely that the vestibular cue would need to be presented more than 100 ms before the visual cue in order to create the robust ERSP differences that were demonstrated between the conditions of attention allocation when the visual cue was presented first.

4.3 Feature-binding gamma ERS in visual-vestibular integration

We examined gamma ERS under varying conditions of stimulus onset asynchrony in order to test the temporal correlation hypothesis (Engel et al., 2001; Singer & Gray, 1995) in the context of visual-vestibular integration. This hypothesis posits that synchronization of gamma-band oscillations is a key mechanism for integration across distributed cortical networks. Evidence supporting this hypothesis has been demonstrated in multiple studies (e.g., Sakowitz, Quiroga, Schürmann & Başar, 2001; Senkowski et al., 2007) that typically focus on audiovisual integration. For example, Senkowski et al. (2007) presented human participants with audiovisual stimuli with varying degrees of temporal asynchrony, and required them to attend to one modality-specific stimuli while ignoring the other. They found that gamma ERS was not significantly different between modalities but, for both modalities, significantly more gamma ERS was elicited when temporal asynchrony was 25 ms or less, compared to longer SOAs. In the present study, the temporal correlation hypothesis predicts that the simultaneous conditions (AP(S) and AV(S)) elicit stronger gamma ERS compared to the visual-first and physical-first conditions. Our results do not support this hypothesis. The present study only found differences in the gamma band when comparing the AV(V_{1st}) and AV(P_{1st}) conditions, such that AV(V_{1st}) elicited stronger gamma ERS than AV(P_{1st}). We are currently unaware of any literature directly explaining this finding. We offer two possible conclusions for our results. First, visual-vestibular

integration does not rely on gamma ERS to synchronize modality-specific information across cortical networks. This facilitation of gamma ERS could be specific to superadditive integration processes (e.g., audiovisual integration; Dias, McClaskey & Harris, 2021) as opposed to subadditive integration processes (e.g., visual-vestibular integration; Angelaki et al., 2009). Or second, visual-vestibular integration has a broader temporal window than 100 ms for gamma facilitation (compared to the Senkowski et al., 2007, temporal window of 25 ms), and therefore our experimental design was not sensitive enough to detect differences in gamma ERS due to stimulus onset asynchrony. A broader temporal window for visual-vestibular integration would be consistent with behavioural research (Rodriguez & Crane, 2021), and research demonstrating that perception for vestibular inputs being relatively slower than other senses (Barnett-Cowan & Harris, 2013). More research needs to be conducted in order to better understand the role of stimulus timing in visual-vestibular feature binding.

5. Conclusion

The present study examined cortical activity elicited in response to self-motion cues that varied in attention allocation and stimulus onset synchrony. There were two main findings. First, stimulus onset asynchrony produced robust differences in cortical activity during attention to both visual and physical motion. The electrophysiological signatures of visual (strong beta ERS) versus vestibular (strong beta ERD) weighting bias were enhanced when the attended motion cue was presented 100 ms before the ignored cue. When comparing across conditions of attention allocation, presenting the visual-motion cue first created more robust conditional differences than when physical-motion cues were presented first. These results demonstrate that the timing of visual-vestibular stimuli plays a critical role in multisensory weighting during self-motion perception, and that this weighting process is more sensitive to temporal changes in visual stimuli

compared to vestibular stimuli. Second, contrary to the findings of several audiovisual and visuotactile studies, the temporal synchrony of visual- and physical-motion cues did not elicit gamma ERS beyond baseline. It is possible that the 100ms SOA was not long enough to elicit these hypothesized differences. It could also be the case that visual-vestibular integration does not elicit processes indexed by gamma ERS.

Appendix

Supplementary Materials

Figure A1. The motion simulator pod was supported by a MOOG © platform with six-degrees-of-freedom motion (MOOG series 6DOF2000E).

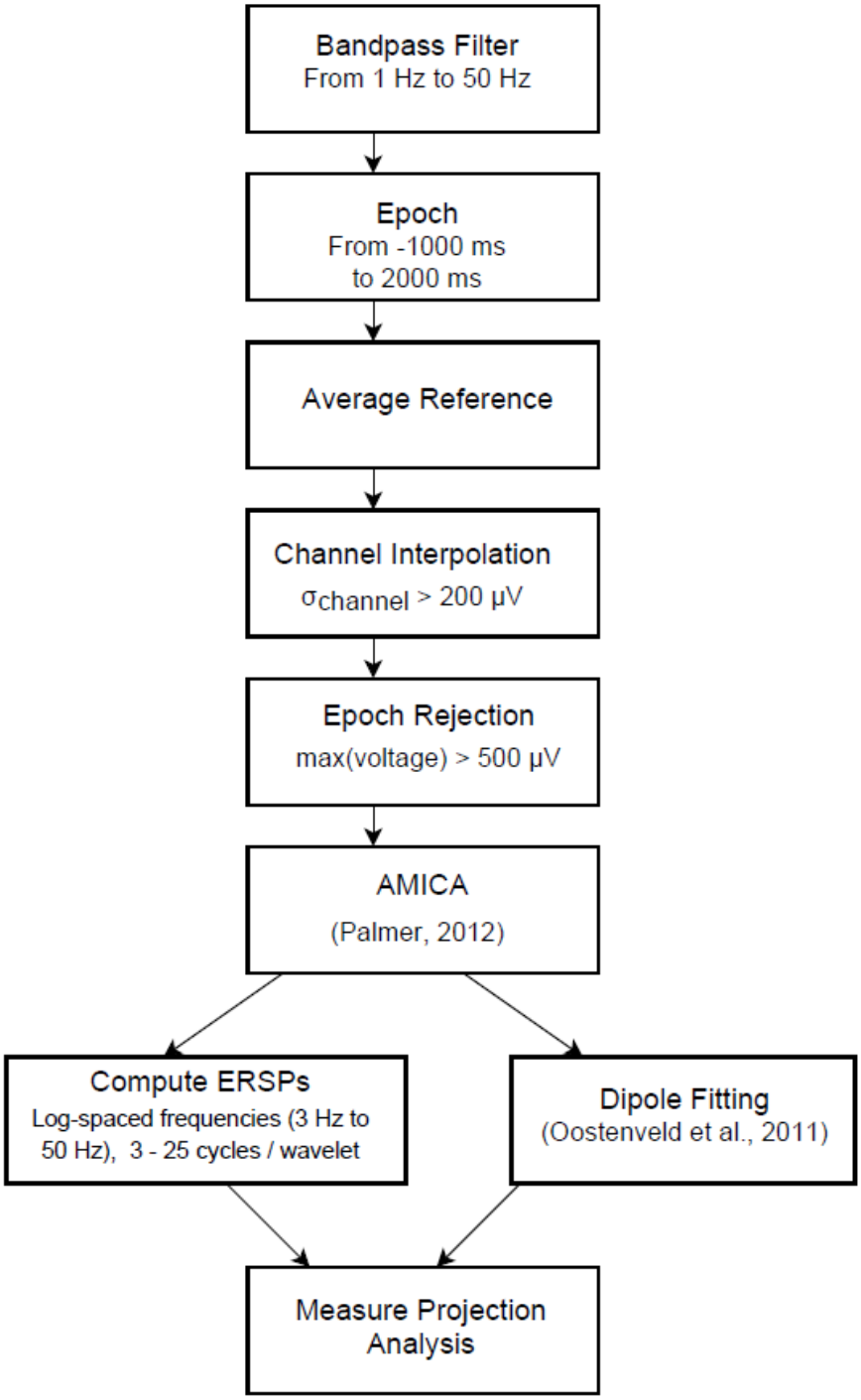

Figure A2. This flowchart illustrates the signal processing pipeline. The Measure Projection Analysis (MPA) pipeline is described in section 2.9 (ERSP Measure Projection Analysis), and a flowchart can be found in Bigdely-Shamlo, Mullen, Kreutz-Delgado & Makeig, 2013.

CHAPTER 5: GENERAL DISCUSSION

There are currently two branches of research focussed on self-motion perception in humans. The first aims to describe the neural correlates of self-motion perception. This line of brain-imaging research aims to reveal the online processes engaged during an organism's perception of moving through the surrounding environment. The literature in this area of study is rich with non-human studies (e.g., Mackrous, Carriot, Cullen & Chacron, 2020), however research with human participants is typically limited to visual self-motion perception due to technological limitations of most brain-imaging techniques regarding sensitivity to physical motion. However, self-motion perception is multisensory, engaging the visual, vestibular, proprioceptive, tactile and auditory systems. Physically moving participants is the most precise way to engage the vestibular, proprioceptive and tactile systems. This thesis combined the physical cues of a motion platform with visual imagery of self-motion to provide an immersive experience of moving through a surrounding environment. Although technology to create these stimuli exists in the form of motion simulators, recording the brain while participants are being physically displaced is challenging with the current neuroimaging technology. The most common techniques to record the human brain (i.e., fMRI, PET and EEG) require the participant to be relatively stationary due to sensitivity to motion artifacts in the brain signal recording. It is because of this limitation that most self-motion perception research on humans has relied on visual-only displays. Therefore, the studies comprising this branch of the self-motion perception literature do not inform us about the multisensory nature of self-motion perception.

The second branch of research in human self-motion perception addresses behavioural correlates of multisensory self-motion perception. This line of research measures accuracy and response times in tasks such as temporal or heading judgements, discrimination, detection to

determine thresholds, etcetera. Behavioural data allow researchers explore the association of neural processes with behavioural output. Another advantage of relying on behavioural measures for self-motion perception studies is that they are not sensitive to movement artifacts like neuroimaging methods. Researchers can physically move participants in any direction to engage the vestibular and proprioceptive systems without compromising the quality of data. This allows researchers to study a wide variety of complex processes related to self-motion perception, such as visual-vestibular weighting in multisensory integration (Fetsch, Turner, DeAngelis & Angelaki, 2009), multisensory integration in aging (Kenney, Jabbari, von Mohrenschildt & Shedden, 2021), and the effects of multisensory cues on flight task performance (O'Malley et al., 2016). Although this behavioural branch of research has led to ground-breaking discoveries related to self-motion perception, and has shaped our understanding of the construct, there remains a gap with regard to understanding the underlying online neural processes contributing to multisensory self-motion perception.

The goal of the present thesis was to bridge the gap between unisensory neuroimaging studies which focus on the visual system, and multisensory behavioural studies which view the brain as a black box. Combining these two branches allowed us to develop a deeper understanding of how electrophysiological oscillations index behavioural output related to self-motion perception. We designed a series of experiments to record ERSP from a high-density EEG array while participants were presented with visual and/or vestibular cues to self-motion. Participants were seated in a virtual environment mounted on a Stewart motion platform with 6 degrees of freedom motion. All three experiments required participants to complete a heading discrimination task. Each experiment presented the same visual and vestibular stimuli but

manipulated the onset of these stimuli in key ways to uncover unique insights related to visual-vestibular integration and the role of attention in this process.

Chapter 2 laid the foundation for the thesis. To our knowledge, this study was the first to explore how attention affects the electrophysiological processes related to multisensory integration in self-motion perception. Participants made heading judgements of simultaneously presented visual-motion versus physical-motion cues that were spatially congruent versus incongruent. The results demonstrated that theta, alpha and beta oscillations are indexes of processes underlying self-motion perception. Specifically, these oscillatory frequencies are the electrophysiological signature of the time course of 1) re-entry processes of visual-vestibular integration, 2) attention to specific motion cues, and 3) individual differences in perceptual weighting of motion stimuli.

The design of the Chapter 2 study did not allow us to determine if the recorded ERSP frequencies were specific to visual or vestibular self-motion perception, or if they were an index of multisensory weighting. Chapter 3 used the same stimuli and task but presented the sensory stimuli separately (visual-only and physical-only) instead of simultaneously as was done in Chapter 2. This design allowed us to confirm that the frequencies from the previous study were not specific to one or the other modality but revealed processes more general to self-motion perception. The design of the Chapter 3 study also introduced far more multisensory weighting bias towards the attended stimulus, because only one modality was presented at a time. This work informed us that beta band frequencies likely index subadditive inhibition during visual-vestibular weighting. We also provided evidence that theta ERS is strongly associated with heading perception for both visual and physical cues to motion, and alpha is likely an index of task-related attentional resources.

Finally, Chapter 4 presented the same stimuli and task as the previous chapters but manipulated the stimulus onset timing in order to explore how the timing of visual and vestibular cues to motion affect ERSP associated with self-motion perception. In this experiment the visual and vestibular stimuli were spatially congruent (excluding catch trials) but were presented as one of three onset timing conditions: visual first by 100ms, physical first by 100 ms, or simultaneous. This experiment demonstrated that the onset timing of the self-motion stimuli is just as important to visual-vestibular weighting as attention, which was indexed by changes in beta power. Interestingly, we also found that feature binding in visual-vestibular integration is not indexed by gamma power increases, as is the case in the integration of other senses such as audiovisual and visuo-tactile integration.

5.1 Visual-Vestibular Weighting

One of the primary contributions of the present line of research was to develop our understanding of the EEG correlates of visual-vestibular weighting. Weighting is necessary during visual-vestibular integration because cue reliability (signal-to-noise ratio) can change dynamically, as a result of changes in the environment or body position (Knill & Pouget, 2004). Moreover, task demands may increase the salience or importance of one cue over the other (Stanford & Stein, 2007). Most of the previous studies that aimed to define multisensory weighting described it as a process that combines sensory cues by taking a weighted average of each input, in which the weights are proportional to the reliability associated with each cue (e.g., Alais & Burr, 2004; Ernst & Banks, 2002). Visual-vestibular weighting has been explored behaviourally in humans (Alberts, de Brouwer, Selen & Medendorp, 2016; Butler, Smith, Campos & Bülthoff, 2010; Ramkhalawansingh, Butler & Campos, 2018), and neurophysiologically in animals (Fetsch et al., 2009; Gu, Angelaki & DeAngelis, 2008),

however, the literature describing the online neural processes of visual-vestibular weighting in humans is currently scarce. We can gain insights into the electrophysiological processes underlying visual-vestibular weighting from research focussed on the integration of other sensory systems.

There is evidence from audiovisual research that sheds some light on the temporal stages of integration and multisensory weighting. Audiovisual research conducted by Rohe, Ehlis, and Noppeney (2019), has demonstrated that the brain initially processes information from each sensory input independently, which leads to reliability estimates used for weighting during audiovisual integration. They found that prestimulus alpha ERD and gamma ERS power was predictive of the two sensory stimuli being subsequently integrated and perceived as one event. Moreover, audiovisual EEG research in the time domain has demonstrated that unisensory reliability estimates (measured by discriminant analysis of ERP data; Kayser, McNair & Kayser, 2016) occur as early as 84 ms after stimulus onset, while neural correlates of perceptual weighting emerged after 120 ms (Boyle, Kayser & Kayser, 2017). There are similarities between the temporal stages of audiovisual and visual-vestibular integration, however the literature around visual-vestibular integration is in comparative infancy.

Other illuminating research comes from visual-tactile integration. Beta power in the motor cortices has been shown to be associated with multisensory weighting. Bauer, Kennett and Driver (2012), conducted a visual-tactile study that investigated how attention to space (left or right) and attention to modality (vision or touch) modulate oscillatory activity in the motor cortex. This study is interesting to us because the design aligns with our attention manipulations. In different blocks, touch or vision was task-relevant, and participants were required to make spatial location judgements in response to stimuli presented either to the left or right. Similar to

Chapter 2 of the present thesis, Bauer et al. (2012) varied sensory weighting between conditions by manipulating attention allocation. They demonstrated that beta ERD localized to the motor cortex was significantly stronger in conditions that required attention to touch compared to vision.

Beta-band oscillations have also been shown to be critical to processes underlying motor processing and output (e.g., Nakamura, Suzuki, Milosevic & Nomura, 2021; Walker et al., 2020). One theory is that the strength of beta rebound (ERS) reflects the active inhibition or reduced excitability of the primary sensorimotor cortex (Pfurtscheller, 1992; Salmelin, Hämäläinen, Kajola & Hari, 1995). Another theory proposed that the beta cycle in the motor cortex is an index of preparation and execution of motor processing and output (beta ERD), followed by recalibration of the motor system (beta ERS; Gaetz & Cheyne, 2006). The findings of the present line of research align closer to the former theory. We demonstrate that the beta cycle is likely an index of visual-vestibular weighting through a series of three experiments.

The results of Chapter 2 laid the foundation for our hypothesis that the beta cycle indexes visual-vestibular weighting. In this experiment, the visual- and physical-motion stimuli were presented simultaneously, and the objective was to make heading judgements while attending to one motion cue, while ignoring the other motion cue. These two conditions presented identical stimuli, and only differed in attention allocation. We found the time-course of the beta band to be significantly different between these two conditions of attention allocation. When attention was allocated to the physical-motion stimulus, beta ERD was elicited ~250 ms post-stimulus and lasted for almost the entirety of the remainder of the trial. This response was vastly different than when attention was allocated to the visual-motion stimulus. During the attend-visual condition, the beta ERD was elicited ~250 ms post-stimulus, but only lasted until ~750 ms post-stimulus,

and was followed by a beta ERS that lasted until the end of the trial. We believe that the longer-lasting beta ERD in the attend-physical condition reflects the sustained processing of vestibular information, due to a larger multisensory weighting bias towards vestibular information via attention allocation. The incongruent attend-physical condition (IAP; attend to the vestibular cue while the visual cue moves in the opposite direction) was critical for this observation. IAP was the most challenging condition to make heading judgments, as participants had to ignore an incongruent visual cue to motion that was much more salient than the vestibular cue, due to the dominance of the visual system during visual-vestibular integration. Heading judgement accuracy varied in this condition far more than in other conditions, to the extent that there were two distinct groups within our sample; those who were able to ignore the visual cue (high-accuracy group; accuracy >70% in IAP, n = 16), versus those who could not (low-accuracy group; accuracy <30% in IAP, n=11). Contrasting these two groups, we found that the time course and power differences in the beta band between the two conditions of attention allocation were entirely driven by high-accuracy participants. Interestingly, the attend-physical and attend-visual conditions elicited minimal differences in beta power and time course within low-accuracy participants. The only difference was a slightly more powerful beta ERS in the attend-visual condition. In low-accuracy participants, the attend-visual and attend-physical conditions elicited similar cortical activity in the beta band; importantly, this activity was almost identical to the cortical activity elicited by the attend-visual condition in high-accuracy participants. We initially believed that this result indicated that low-accuracy participants were simply not following directions, and only responding to the visual-motion cues in all conditions. This hypothesis, however, was not supported by the response time data. Low-accuracy participants responded significantly slower in the attend-physical conditions versus the attend-visual conditions,

matching the response time results found in the high-accuracy group. We believe that these findings point to a weighting difference between the two groups, with the low-accuracy participants demonstrating a stronger visual dominance than the high-accuracy group. The beta ERS that was elicited during the attend-physical condition in low-accuracy participants (but not in high-accuracy participants) could have been the inhibition of down-weighted vestibular inputs, which made the IAP condition extremely challenging for low-accuracy participants, compared to high-accuracy participants.

Comparing the EEG results of Chapters 2 and 3 leads to further support of our hypothesis that beta oscillations index visual-vestibular weighting. The findings of Chapter 2 supported our hypothesis through the analysis of high- versus low-accuracy groups, however, it was impossible to rule out the possibility that these power differences might be due to other cognitive processes (e.g., unisensory processing, attention, etc.) because the two self-motion stimuli were presented simultaneously. Chapter 3 was the next logical step to further clarify the relationship between beta oscillations and visual-vestibular weighting. Chapter 3 replicated the design of Chapter 2 with respect to the visual- and physical-motion stimuli and the heading judgement task, but differed from Chapter 2 by presenting the motion stimuli separately in a blocked design so that there were visual-only and physical-only conditions. This experimental design created extreme perceptual weighting towards the target modality, because there was no competition from the other modality except (arguably) that the lack of motion in the other modality might generate a no-motion perception. Chapter 3 results showed theta, alpha and beta oscillations were induced in both visual- and physical-only conditions. Very similar ERSP differences were observed (compared to Chapter 2) in the theta and alpha bands between conditions, despite differences in weighting between the experiments. This result led us to believe that these differences were not

due to visual-vestibular weighting. However, the only notable modality-induced ERSP power and latency differences between Chapters 2 and 3 were in the beta band. The two studies demonstrated differences in the beta band between their respective conditions of attention allocation. Chapter 2 elicited a more powerful and longer-lasting beta ERD in the attend physical-motion conditions compared to attend visual-motion conditions. Moreover, only the attend visual-motion conditions elicited beta ERS. Conversely, Chapter 3 demonstrated a longer lasting and more powerful beta ERS (~700 ms – end of trial), in the visual-motion condition compared to the physical-motion condition (~850 ms – end of trial).

We believe that the conditional differences in the beta band between studies is evidence of weighting differences. Taken together, the beta band differences and the lack of differences in the theta and alpha bands between Chapters 2 and 3 indicate that the beta band is the most informative index of visual-vestibular weighting.

Previous research has shown that the onset timing of each unisensory stimulus can affect weighting during multisensory integration (Fister, Stevenson, Nidiffer, Barnett & Wallace, 2016; Sheppard, Raposo & Churchland, 2013). In Chapter 4 we manipulated the weighting of the visual-vestibular inputs via stimulus onset asynchrony (SOA). This experimental design allowed us to further test our hypothesis that beta oscillations index visual-vestibular weighting. We used the same stimuli and task as Chapter 2 with the following exceptions: (1) the visual- and physical-motion stimuli were all spatially congruent, and (2) the temporal onset of the visual versus physical cues was asynchronous in some conditions. Chapter 4 demonstrated changes in theta, alpha and beta oscillations across temporal asynchronies, and between conditions of attention allocation. Similar to the previous data chapters, changes in visual-vestibular weighting (via SOA in Chapter 4) led to robust changes in the beta band. This experiment had two main

observations associated with beta activity as supported by the 2 x 3 interaction. Insights about what is driving the interaction can be revealed by first examining attention across the three SOA conditions, and then examining SOA across the two attention conditions.

The first observation compared beta power across SOA conditions within each level of attention allocation (e.g., the effect of SOA on ERSP within the attend-visual condition and separately within the attend-physical condition). Focus for a moment on the visual-attention condition and the beta ERS. Chapters 2 and 3 demonstrated that a strong beta ERS is an electrophysiological signature of heavy visual weighting. In Chapter 4, when participants attended to the visual-motion cue, the strongest beta ERS was elicited when the attended visual cue was presented first, compared to the other two SOA conditions. Moreover, simultaneous presentation elicited a stronger beta ERS than when the ignored physical cue was presented first. Now consider the physical-attention condition and the beta ERD. In Chapter 2 we demonstrated that attention to the physical stimulus elicited a powerful and long-lasting beta ERD. In Chapter 4, attention to the physical stimulus elicited the strongest beta ERD when the physical cue was presented first, compared to the other two SOA conditions, and simultaneous presentation elicited a stronger beta ERD than when the ignored visual cue was presented first. Note the similarity in the pattern of effects for visual attention as reflected by the ERS compared to physical attention as reflected by the ERD; the implications will be discussed below.

The second observation compared beta power between conditions of attention allocation at each level of SOA (e.g., the effect of attention to visual versus physical modalities within each of the SOA conditions). This analysis revealed an interaction between SOA and attention allocation. To facilitate the discussion, recall that our conditions included attend physical (AP) versus attend visual (AV), and three SOA conditions indicated in brackets as visual first (V_{1st}),

physical first (P_{1st}), and simultaneous (S). The comparison between AP(S) versus AV(S) replicated Chapter 2, and acted as a baseline comparison for Chapter 4. Two critical novel comparisons of the attention manipulation were AP(V_{1st}) versus AV(V_{1st}), and AP(P_{1st}) versus AV(P_{1st}). In other words, what is the effect of modality on attention when the visual cue is presented before the physical cue (and visa versa). These novel comparisons revealed ERSP differences compared to the baseline comparison in which onset was simultaneous.

The most notable beta band difference was the comparison of attention conditions when the visual motion cue was presented first (AP(V_{1st}) versus AV(V_{1st})). Attending to the visual modality when the visual cue onset first (the AV(V_{1st}) condition) elicited a powerful beta ERS compared to a relatively weak beta ERS in the AP(V_{1st}) condition. The beta ERS in the AP(V_{1st}) condition is notable because this was the only case in which attention to the physical motion cue, while ignoring the visual motion cue, elicited a beta ERS. In the present line of research, the beta ERS has been an ERSP signature of visual weighting bias. It is notable that the AP condition affected most by the visual-motion cue was the AP(V1st) condition, when the visual cue was given a 100 ms temporal advantage.

An interesting but different kind of advantage was observed for vestibular processing in the AV(P_{1st}) condition in which the physical cue was presented first. Comparing AP(P_{1st}) versus AV(P_{1st}) resulted in fewer observed ERSP differences compared to visual first onset or simultaneous onset (baseline). More specifically, presenting the physical-motion cue first did not elicit a beta ERS in the attend-visual condition. In fact, the only difference between the two attention conditions when the physical cue was presented first was that beta ERD lasted longer in the attend-physical condition. This result is notable because it is the only attend-visual condition in the entire thesis that did not elicit a beta ERS. We believe that the temporal advantage of the

physical-motion cue up-weighted the ignored vestibular signals, which resulted in prolonged beta ERD and a lack of the beta ERS, despite attention being allocated to the visual signal. Attention was not drawn away from the visual cue enough to disrupt performance (participants performed with 99% accuracy) but the ERSP that indexes weighting showed that this process was affected by the SOA. It is possible that accuracy would be disrupted by the ignored cue being presented first if the heading discrimination task was more challenging.

Taken together, each data chapter clearly demonstrated that as visual-motion inputs received greater multisensory weights, the elicited ERS (beta rebound) became more powerful and occurred earlier. The most powerful beta rebound was elicited in the visual-only condition of Chapter 3, when visual motion cues were presented alone (physical motion was absent). The second strongest beta ERS was elicited by the AV(V1st) condition of Chapter 4, when visual inputs had both a temporal and attentional advantage over competing vestibular inputs. Beta ERD was similarly modulated by visual-vestibular weighting. The most powerful and longest-lasting beta ERD was elicited by conditions that most strongly favoured vestibular inputs. For example, the most powerful beta ERD in the present thesis was elicited in the AP(P1st) condition of Chapter 4, when vestibular inputs had both a temporal and attentional advantage over competing visual inputs. Together, these observations indicate that ERS is a biomarker of multisensory weighting biased towards visual self-motion perception and ERD is a biomarker of multisensory weighting biased towards physical self-motion perception.

Interestingly, the physical-only condition of Chapter 3 elicited a beta ERS, and only a brief beta ERD. One might think that this finding violated our expectations based on all other conditions for which vestibular inputs had a weighting advantage (e.g., AP(P1st)). We admit we did expect the physical-only condition of Chapter 3 to elicit the strongest and longest lasting beta

ERD and no beta ERS, because the vestibular motion cues were the only cues presented and thus would not have competition for multisensory weighting. That observation may be insightful for interpreting beta ERD, in that the observation of beta ERD is somehow related to competition with visual motion information. The powerful and long-lasting beta ERD demonstrated in the attend-physical conditions of Chapters 2 and 4 may have occurred due to sustained processing of the vestibular inputs that was required to make physical heading judgements while simultaneously ignoring the visual cues to motion.

5.2 Heading Processing and Theta Oscillations

Spatial navigation represents one of the most fundamental cognitive processes that many organisms rely on for survival. One critical component of spatial navigation is the processing of heading direction, or in other words, the organism's ability to understand the direction in which it is moving. Research on the neurobiological processes underlying heading processing began with Ranck (1984), and the discovery of cells that are sensitive to a rat's head direction in the horizontal plane (unaffected by environmental landmarks). Further non-human primate studies established methodologies to systematically map the organization of cells that process heading (Albright, Desimone & Gross, 1984; Chen, Gu, Takahashi, Angelaki & DeAngelis, 2008). Although empirical data demonstrating the mapping of human cells that process heading is exceedingly difficult to obtain, more recent research has demonstrated that theta oscillations are sensitive to changes in heading (Do, Lin & Gramann, 2020; Lin, Chiu & Gramann, 2015). Many of these studies demonstrated theta sensitivity to visual heading changes in virtual environments (Do et al., 2020; Lin et al., 2015). Chapters 2 and 3 of the current thesis contribute to this literature by demonstrating that theta oscillations are sensitive to both visual and vestibular inputs, and can be modulated by reentrant processes.

Chapter 3 was critical for establishing theta ERS as an index of heading processing for visual and vestibular networks. The visual- and physical-only conditions both elicited differences in theta ERS in the right motor area, between our 35° right versus left headings. This right-lateralized effect is supported by previous work showing that networks associated with spatial attention are typically lateralized to the right hemisphere (for review see Dieterich & Brandt, 2018). Moreover, non-human primate studies have demonstrated that dorsal medial superior temporal cortex (MSTd), and parahippocampal structures contain cells that are sensitive to visual-only, vestibular-only, or visual-vestibular self-motion stimuli (Gu et al., 2008). Considering the relatively low spatial resolution of EEG, our line of research was not able to localize theta oscillations to either of these regions, however, the MSTd was a component of the motor regions revealed by our MPA analyses. It is possible that the theta oscillations localized to motor areas index the network associated with MSTd or the parahippocampal structures responsible for unisensory and multisensory heading processing, based on the similarities between the present data and earlier non-human primate literature. If this is the case, the present line of research demonstrates that theta oscillations index activation of networks, potentially including these areas of interest, for both visual and vestibular heading processing in humans. Our research bridges the gap in the literature between neurobiological studies of non-humans, and electrophysiological studies of humans focussed on visual-only displays of self-motion.

The second contribution of the present thesis associated with theta oscillations was presented in Chapter 2. In that experiment we found increased power of theta ERD in the occipital area when motion heading cues were presented spatially incongruent versus when they were presented congruently. We believe that this oscillatory pattern indexes a reentrant multisensory function, because both cues to motion needed to be processed in order for this

congruency effect to occur. This finding supports the model proposed by Bland (2009) which hypothesizes that theta oscillations facilitate integration between the sensory and motor systems. The model states that the parahippocampal area and other structures associated with spatial processing use theta oscillations to provide sensory and motor systems with a feedback loop to update one another on their performance relative to dynamic changes in the environment. Similar reentrant signalling has been demonstrated in several studies examining multisensory integration. For example, multiple studies have shown that reentrant processes are critical for visual feature binding (Koivisto & Silvanto, 2011) and the associated oculomotor output (Hamker, 2003).

5.3 Cognitive Demands and Alpha Oscillations

The alpha band was another oscillatory frequency modulated in all three chapters of the current thesis. Changes in alpha are commonly elicited by cognitive or sensory tasks. Facilitation of alpha (ERS) has been associated with inhibition or deactivation of brain areas that are not relevant to the task at hand, while suppression of alpha (ERD) is induced by high cortical activation of that specific brain region (Klimesch, 2012). One theory describing the alpha band's association with cognitive and sensory processes is the neural efficiency hypothesis (Bazanova & Vernon, 2014). This hypothesis posits that a decrease in alpha amplitude (ERD) is generated by activation of the respective brain region; whereas an increase in alpha amplitude reflects inhibition of areas that are task-irrelevant. Effective cognition, according to this theory, is not a function of how hard the brain works but rather its efficiency in doing so (Klimesch, Sauseng & Hanslmayr, 2007). Sensorimotor tasks such as perceptual judgement have been shown to induce alpha ERD. Moreover, conditions requiring more attentional resources have been shown to induce more powerful alpha ERD (Niedermeyer and Lopes da Silva, 2004).

The current thesis presents findings that support the neural efficiency hypothesis. Each chapter demonstrated a similar latency difference in alpha ERD within the motor cortices in response to visual- versus vestibular-motion cues. Across all data chapters, if the visual-motion cue was the target stimulus (i.e., attended to or presented by itself) the alpha ERD elicited at the beginning of the trial occurred earlier compared to the conditions in which the physical-motion cue was the target. Research reviewed by Barnett-Cowan and Harris (2013) shows that the perception of visual information is faster than the perception of vestibular and proprioceptive information. If the visual-motion stimulus is perceived faster than the physical-motion stimulus, intuitively the cortical activation indexing cognitive demands should be engaged earlier in the trial during the visual-motion task compared to the physical-motion task. We believe this latency difference reflects the timing differences of when cognitive resources are engaged during visual versus physical self-motion perception.

Taken together, Chapters 2 and 3 ruled out alpha ERD as an index of a multisensory integration process. Both experiments presented the same visual- and physical-motion cues and required participants to complete the same heading discrimination task. The difference between these two experiments was that in Chapter 2, visual- and physical-motion cues were presented simultaneously, whereas in Chapter 3, visual- and physical-motion cues were presented independently (i.e., in separate blocks). This difference in stimulus presentation created differences between the two studies in multisensory weighting bias. Presenting the motion cues independently in Chapter 3 created an extreme weighting bias towards the attended modality, whereas presenting the motion cues simultaneously in Chapter 2 created more competition between the modalities and less weighting bias. In both experiments, we uncovered the aforementioned latency difference in alpha ERD between conditions of visual attention versus

conditions of physical attention. If alpha ERD was sensitive to changes in visual-vestibular weighting, Chapters 2 and 3 would have elicited different conditional differences in the alpha band between the two studies. This hypothesis was only supported by changes in beta-band activity (section 5.1). Therefore, these experiments demonstrated that alpha ERD is not sensitive to changes in visual-vestibular weighting. Given the results demonstrated in Chapters 2 and 3, we believe our data support the neural efficiency hypothesis. We believe that the elicited alpha ERD demonstrated in each chapter of this thesis indexes cortical activation related to the cognitive demands of the heading judgment task.

5.4 Future Direction

Our understanding of the electrophysiological correlates of human self-motion perception is currently in its infancy. Only recently have advancements in technology and methodology allowed for robust recordings of the brain during full-body motion. The relative youth of this area of research created both advantages and disadvantages for my doctoral research. The main disadvantage was that we had very little literature to guide our understanding of this topic before we began. Much of our a priori knowledge was adopted from articles related to recording EEG during sensory-motor tasks such as reaching or finger tapping. Chapter 2 was very much exploratory, and our understanding of the EEG correlates of self-motion perception was built upon that initial experiment. The main advantage was that we could rely on a series of very simple experimental designs. All of our simple experiments elicited robust effects that were highly impactful (and publishable!). Each experiment in this thesis produced unique insights into human self-motion perception while also opening the door for further testable questions.

Chapter 2 presented simultaneous visual- and physical-motion cues that were either spatially congruent or incongruent. One interesting finding was that incongruent cues to motion

elicited more powerful theta ERD in the occipital area. We hypothesized that this theta ERD indexes a reentrant multisensory function, and it supports Bland's (2009) model of sensorimotor integration. Sensorimotor integration has long been linked to the theta band, however, this specific occipital theta ERD in response to incongruent visual-vestibular motion cues has not been previously demonstrated. This lack of literature describing theta ERD associated with spatial incongruence is not surprising however, as technological and methodological limitations in the past made it challenging to observe this phenomenon. More research needs to be conducted to interpret this oscillatory pattern's relationship with visual-vestibular incongruence. A follow-up experiment could observe how the magnitude of incongruence modulates the induced theta ERD by running a similar experimental design but varying the degrees in which the visual- and physical-motion cues are spatially incongruent. If there are theta ERD power differences between, for example, 70º of incongruence (as were the incongruent conditions in Chapter 2) and 50º of incongruence, it might be that theta ERD acts as a complex reentrant signal that detects multisensory discrepancies and affects the weighting process. Moreover, this design would allow us to test if there is a window of spatial incongruence outside of which visual-vestibular integration breaks down.

Research exploring individual differences associated with visual-vestibular weighting would also impact our understanding of this topic. The incongruent attend-physical condition of Chapter 2 demonstrated the existence of individual differences in visual-vestibular weighting during self-motion perception. Some participants in this study could not ignore the incongruent visual-motion cue while they were attending to the physical-motion cue. This difficulty in inhibiting the visual-motion cue led to poor performance on the heading discrimination task (< 30% accuracy, and in some instances < 10% accuracy). Moreover, performance of these low-

accuracy participants was not negatively affected by the incongruent physical-motion cue while attending to visual-motion. One argument is that low-accuracy participants were not doing the task, and simply responding to the visual motion stimulus. However, the response time differences between attend-physical and attend-visual matched the high-accuracy participants, strongly suggesting that low-accuracy participants were attempting to respond to the physical-motion cues in the incongruent attend-physical condition, but could not inhibit the visual-motion cue and thus ended up responding to visual motion in most cases. Importantly, the ERSP results support the idea that low-accuracy participants are not processing the attend-physical conditions in the same way as the high-accuracy participants, and in fact these ERSP results look similar to the ERSP of the attend-visual conditions. We claim that differences in heading judgement accuracy is a result of individual differences in visual-vestibular weighting. Previous behavioural studies have demonstrated visual-vestibular weighting differences based on sex (Barnett-Cowan, Dyde, Thompson & Harris, 2010; Harris et al., 2018; Tremblay, Elliott & Starkes, 2004), age (Baloh, Jacobson & Socotch, 1993; Deshpande & Patla, 2007; Paige, 1994) and clinical factors (Al-Sharif, Roehm, Lindemann, Dumenci & Keshner, 2021; Shim, Song & Park, 2018). Our methodology creates the opportunity to examine individual differences in weighting from the lens of neuroimaging. For example, we can leverage our newly-found understanding of the electrophysiological signatures of visual-vestibular weighting and apply that to the clinical space. A recent study has shown that, compared to healthy, age-matched controls, Parkinson's disease patients perform worse on heading judgement tasks due to overweighting impaired visual-motion cues (Yakubovich et al., 2020). If we can establish biomarkers of the impairments, we will develop a better understanding of the integration and motor impairments that are common in pathologies, such as Parkinson's. Identification of these biomarkers in the pre-diagnostic phase

of the disease could lead to a greater time window for possible preventative measures and earlier treatments (Noyce, Lees & Schrag, 2016).

Chapter 3 presented visual- and physical-motion cues independently. One goal of this experiment was to create a strong weighting bias through the unisensory presentation of motion cues, and then compare the modality differences to those found in Chapter 2. This design allowed us to determine that the beta band is associated with visual-vestibular weighting, as beta ERS and beta ERD were sensitive to weighting differences between studies. The present thesis provides compelling evidence that weighting biased towards visual-motion elicits more powerful beta ERS, and weighting biased towards physical-motion elicits more powerful beta ERD (when visual cues to motion are present). However, in order to develop a more in-depth understanding of how beta ERS and beta ERD are associated with visual-vestibular weighting, future research needs to systematically manipulate the weighting of these inputs and contrast the induced beta activity. For example, the coherence of visual objects in a star field can be changed systematically to manipulated weighting of the visual-motion stimuli. Moreover, physical cues to motion can be manipulated through platform noise or detection thresholds. This is particularly important for understanding beta ERD, as this activity only seems to be sensitive to conditions of competition between the visual and vestibular systems. Understanding the correlation between beta ERS/ERD power and visual-vestibular weighting will provide insights into how beta ERD power indexes the competition between the visual and vestibular systems.

Chapter 4 presented spatially congruent visual- and physical-motion cues in every trial and manipulated the onset timing of the stimuli. Previous literature exploring the integration of other sensory modalities (e.g., audovisual and visual-tactile) showed that multisensory stimuli presented closer in time elicited stronger gamma ERS than stimuli presented with longer

stimulus onset asynchrony (Senkowski, Talsma, Grigutsch, Herrmann & Woldorff, 2007). The temporal correlation hypothesis (Singer & Gray, 1995) posits that the increased gamma ERS is an index of feature binding of the multisensory event; the closer in time the two sensory events occur, the stronger of a feature-binding response will be elicited. We predicted that simultaneously presented visual and vestibular cues to motion would induce more powerful gamma ERS than motion cues presented 100 ms apart. There is a lack of research exploring whether gamma ERS is associated with the binding of visual and vestibular events during self-motion perception. Our research did not find stronger gamma ERS in the simultaneous conditions compared to conditions with a 100 ms stimulus onset asynchrony, therefore our results did not support the temporal correlation hypothesis. In Chapter 4 we discussed the possibility that our experimental design might not have been sensitive enough to detect differences in gamma power between conditions of temporal asynchrony. It is possible that visual-vestibular integration has a broader temporal window than 100 ms for gamma facilitation compared to the Senkowski et al. (2007), temporal window of 25 ms for audiovisual integration. Future studies can incorporate conditions with a greater range of stimulus onset asynchrony compared to Chapter 4 to further investigate whether the temporal correlation hypothesis is a good model of feature binding for visual-vestibular integration. If simultaneous presentation of visual and vestibular events does not elicit stronger gamma ERS than conditions with longer stimulus onset asynchronies (e.g., > 200 ms), it is likely that gamma ERS is not an index of feature binding in visual-vestibular integration.

5.5 Conclusion

In summary, this thesis describes the electrophysiological correlates of self-motion perception. We used a high-fidelity motion simulator to manipulate the interaction of the visual

and vestibular systems to gain insights into cognitive processes related to self-motion perception. Our research developed ground-breaking methodologies for measuring the brain during fully-body motion within virtual environments. Using this methodology, we established biomarkers for human direction processing, and visual-vestibular integration, which had not previously been described in the literature. In Chapter 2 we determined that theta, alpha and beta oscillations are critical biomarkers of these processes. Our experimental design allowed us to compare spatially congruent versus incongruent visual-vestibular stimuli and determine that the theta band is associated with direction processing. This experiment also demonstrated that beta and alpha oscillations are sensitive to which sensory input is being attended to. When participants attended to the visual-motion cues, clusters of brain cells fired synchronously within the beta band (ERS), and while attending to the physical-motion cues, synchronized firing in the beta band was inhibited (ERD). In Chapter 3 we presented visual and physical cues to motion in independent blocks and demonstrated that theta ERS is elicited by both visual and physical cues to motion independently, and is sensitive to direction, thus supporting our hypothesis in Chapter 2 that the theta band indexes direction processing. The independent presentation of motion cues in Chapter 3 created weighting bias towards the independently presented stimulus, compared to Chapter 2, which presented the motion cues simultaneously and thus in competition with one another. The beta band was the only oscillatory frequency that was sensitive to weighting biases between the studies, while theta and alpha oscillations were not. Based on this result, we concluded that beta-band oscillations are an index of visual-vestibular weighting, while theta and alpha oscillations likely index more general processes of self-motion perception such as heading processing and allocation of cognitive resources. Finally, in Chapter 4 we presented the visual- and physical-motion cues in each trial, and manipulated their onset timing. The experimental design allowed us

to investigate the interaction between stimulus onset timing and attention allocation. Conditional differences in the beta band further supported our hypothesis that beta oscillations index visual-vestibular weighting in self-motion perception. Moreover, Chapter 4 demonstrated that the onset timing of the motion stimuli interacts with attention allocation during the process of visual-vestibular weighting. For example, during conditions of physical attention, if the ignored visual cue was presented 100 ms before the physical cue, the power of beta ERD typical of physical attention was greatly reduced. Similarly, during conditions of visual attention, if the ignored physical cue was presented 100 ms before the visual cue, the power of beta ERS typical of visual attention was eliminated. This result further develops our insights into how visual-vestibular weighting works. We have demonstrated that attention and stimulus onset timing play critical roles in determining the dynamic weighting of visual and vestibular cues to motion during integration. Chapter 4 demonstrates that a temporal advantage is more powerful than an attentional advantage when it comes to visual-vestibular weighting. By identifying biomarkers of critical processes involved in self-motion perception, we have opened the door for future lines of research to further develop our relatively limited understanding of the neurophysiological processes of human self-motion perception.

References

Abernethy, B. (1988). Visual search in sport and ergonomics: Its relationship to selective attention and performer expertise. *Human Performance, 1*(4), 205-235.

Acar, Z.A., Makeig, S. (2013). Effects of forward model errors on EEG source localization. *Brain Topography 26*(3), 378–396.

Adams, J. (1961). Some considerations in the design and use of dynamic flight simulators. Selected Papers on Human Factors in the Design and Use of Control Systems (Ed. H. W. Sinaiko), pp. 88-114. Dover Publications, Inc., N.Y.

Adrian, E. D., & Matthews, B. H. (1934). The interpretation of potential waves in the cortex. *The Journal of Physiology, 81*(4), 440-471.

Aguirre, G. K., & D'Esposito, M. (1999). Topographical disorientation: a synthesis and taxonomy. *Brain, 122*(9), 1613-1628.

Al-Sharif, D. S., Roehm, P., Lindemann, T. L., Dumenci, L., & Keshner, E. A. (2021). Visual-vestibular mismatch correlates with headache. *Journal of Vestibular Research, 31*(3), 173-180.

Alais, D., & Burr, D. (2004). The ventriloquist effect results from near-optimal bimodal integration. *Current Biology, 14*(3), 257-262.

Alayrangues, J., Torrecillos, F., Jahani, A., & Malfait, N. (2019). Error-related modulations of the sensorimotor post-movement and foreperiod beta-band activities arise from distinct neural substrates and do not reflect efferent signal processing. *Neuroimage, 184*, 10-24.

Alberts, B. B., de Brouwer, A. J., Selen, L. P., & Medendorp, W. P. (2016). A Bayesian account of visual–vestibular interactions in the rod-and-frame task. *eNeuro, 3*(5).

Albright, T. D., Desimone, R., & Gross, C. G. (1984). Columnar organization of directionally selective cells in visual area MT of the macaque. *Journal of Neurophysiology*, *51*(1), 16-31.

Alegre, M., Gurtubay, I. G., Labarga, A., Iriarte, J., Malanda, A., & Artieda, J. (2003). Alpha and beta oscillatory changes during stimulus-induced movement paradigms: effect of stimulus predictability. *Neuroreport, 14*(3), 381-385.

Alegre, M., Gurtubay, I. G., Labarga, A., Iriarte, J., Valencia, M., & Artieda, J. (2004). Frontal and central oscillatory changes related to different aspects of the motor process: a study in go/no-go paradigms. Experimental Brain Research, 159(1), 14-22.

Alegre, M., Labarga, A., Gurtubay, I.G., Iriarte, J., Malanda, A., & Artieda, J. (2002). Beta electroencephalographic changes during passive movements: Sensory afferences contribute to beta event-related desynchronization in humans. Neuroscience Letters, 331, 29-32.

Allen, D.P., MacKinnon, C.D. (2010). Time–frequency analysis of movement-related spectral power in EEG during repetitive movements: A comparison of methods. Journal of Neuroscience Methods, 186, 107-115.

Allison, R. S., Howard, I. P., & Zacher, J. E. (1999). Effect of field size, head motion, and rotational velocity on roll vection and illusory self-tilt in a tumbling room. *Perception, 28*(3), 299-306.

Alsius, A., Navarra, J., & Soto-Faraco, S. (2007). Attention to touch weakens audiovisual speech integration. *Experimental Brain Research, 183*(3), 399-404.

Andersen, G. J. & Braunstein, M. L. (1985). Induced self-motion in central vision. *Journal of Experimental Psychology: Human Perception and Performance, 11*, 122-132.

Angelaki, D.E., Cullen, K.E. (2008). Vestibular system: The many facets of a multimodal sense. *Annual Review of Neuroscience, 31*, 125–150.

Angelaki, D., Gu, Y., & DeAngelis, G. (2009). Multisensory integration: Psychophysics, neurophysiology, and computation. *Current Opinion in Neurobiology, 19*, 452- 458.

Angelaki, D. E., Gu, Y., & DeAngelis, G. C. (2011). Visual and vestibular cue integration for heading perception in extrastriate visual cortex. *The Journal of Physiology, 589*(4), 825-833.

Angelakis, E., & Lubar, J. F. (2002). Quantitative electroencephalographic amplitude measures in young adults during reading tasks and rest. *Journal of Neurotherapy, 6*(2), 5-19.

Avanzini, P., Fabbri-Destro, M., Dalla Volta, R., Daprati, E., Rizzolatti, G., & Cantalupo, G. (2012). The dynamics of sensorimotor cortical oscillations during the observation of hand movements: an EEG study. *PLoS One, 7*(5), e37534.

Aw, S. T., Haslwanter, T., Fetter, M., & Dichgans, J. (2000). Three-dimensional spatial characteristics of caloric nystagmus. *Experimental Brain Research, 134*(3), 289-294.

Awh, E., Belopolsky, A. V., & Theeuwes, J. (2012). Top-down versus bottom-up attentional control: A failed theoretical dichotomy. *Trends in cognitive sciences, 16*(8), 437-443.

Baker, S. N., Kilner, J. M., Pinches, E. M., & Lemon, R. N. (1999). The role of synchrony and oscillations in the motor output. *Experimental Brain Research, 128*(1-2), 109-117.

Baloh, R. W., Jacobson, K. M., & Socotch, T. M. (1993). The effect of aging on visual-vestibuloocular responses. *Experimental Brain Research, 95*(3), 509-516.

Barnett-Cowan, M., Dyde, R. T., Thompson, C., & Harris, L. R. (2010). Multisensory determinants of orientation perception: task-specific sex differences. *European Journal of Neuroscience*, *31*(10), 1899-1907.

Barnett-Cowan, M., & Harris, L.R. (2009) Perceived timing of vestibular stimulation relative to touch, light and sound. *Experimental Brain Research, 198,* 221-231.

Barnett-Cowan, M., & Harris, L.R. (2013). Vestibular perception is slow: A review. *Multisensory Research, 26,* 387-403.

Barry, R. J., Palmisano, S., Schira, M. M., De Blasio, F. M., Karamacoska, D., & MacDonald, B. (2014). *EEG markers of visually experienced self-motion (vection)*. In Frontiers of Human Neuroscience Conference Abstract: Australasian Society for Psychophysiology, Inc (Vol. 10).

Barutchu, A., Freestone, D. R., Innes-Brown, H., Crewther, D. P., & Crewther, S. G. (2013). Evidence for enhanced multisensory facilitation with stimulus relevance: an electrophysiological investigation. *PLoS One, 8*(1), e52978.

Başar, E. (1980). EEG-brain dynamics: Relation between EEG and brain evoked potentials. Elsevier-North-Holland Biomedical Press.

Başar, E. (2006). The theory of the whole-brain-work. *International Journal of Psychophysiology, 60*(2), 133-138.

Başar, E., Başar-Eroglu, C., Karakaş, S., & Schürmann, M. (2001). Gamma, alpha, delta, and theta oscillations govern cognitive processes. *International Journal of Psychophysiology, 39*(2-3), 241-248.

Bastos, A. M., Vezoli, J., Bosman, C. A., Schoffelen, J. M., Oostenveld, R., Dowdall, J. R., ... & Fries, P. (2015). Visual areas exert feedforward and feedback influences through distinct frequency channels. *Neuron, 85*(2), 390-401.

Bauer, M., Kennett, S., & Driver, J. (2012). Attentional selection of location and modality in vision and touch modulates low-frequency activity in associated sensory cortices. *Journal of neurophysiology, 107*(9), 2342-2351.

Bazanova, O. M., & Vernon, D. (2014). Interpreting EEG alpha activity. *Neuroscience & Biobehavioral Reviews, 44*, 94-110.

Beer, J., Blakemore, C., Previc, F. H., & Liotti, M. (2002). Areas of the human brain activated by ambient visual motion, indicating three kinds of self-movement. *Experimental Brain Research, 143*(1), 78-88.

Beis, J. M., Keller, C., Morin, N., Bartolomeo, P., Bernati, T., Chokron, S., ... & Perennou, D. (2004). Right spatial neglect after left hemisphere stroke: qualitative and quantitative study. *Neurology, 63*(9), 1600-1605.

Bell, A. J., & Sejnowski, T. J. (1995). An information-maximization approach to blind separation and blind deconvolution. *Neural Computation, 7*(6), 1129-1159.

Bense, S., Stephan, T., Bartenstein, P., Schwaiger, M., Brandt, T., & Dieterich, M. (2005). Fixation suppression of optokinetic nystagmus modulates cortical visual–vestibular interaction. *Neuroreport, 16*(9), 887-890.

Bense, S., Stephan, T., Yousry, T. A., Brandt, T., & Dieterich, M. (2001). Multisensory cortical signal increases and decreases during vestibular galvanic stimulation (fMRI). *Journal of Neurophysiology, 85*(2), 886-899.

Benson, A. J., Spencer, M. B., & Stott, J. R. (1986). Thresholds for the detection of the direction of whole-body, linear movement in the horizontal plane. *Aviation, Space, and Environmental Medicine, 57*(11), 1088-1096.

Berger, H. (1929). About the human electroencephalogram. *Archives for Psychiatry and Nervous Diseases, 87*(1), 527-570.

Berger, D. R., Schulte-Pelkum, J., & Bülthoff, H. H. (2010). Simulating believable forward accelerations on a stewart motion platform. *ACM Transactions on Applied Perception (TAP), 7*(1), 1-27.

Bertelson, P., Vroomen, J., De Gelder, B., & Driver, J. (2000). The ventriloquist effect does not depend on the direction of deliberate visual attention. *Perception & Psychophysics, 62*(2), 321-332.

Bigdely-Shamlo, N., Mullen, T., Kreutz-Delgado, K., & Makeig, S. (2013). Measure projection analysis: a probabilistic approach to EEG source comparison and multi-subject inference. *Neuroimage, 72*, 287-303.

Bird, D. (1963). Flight control studies in the small stick deflection area. Presented to AIAA Simulation for Aerospace Flight Conference, Aug. 26-28.

Birn, R. M., Cox, R. W., & Bandettini, P. A. (2004). Experimental designs and processing strategies for fMRI studies involving overt verbal responses. *Neuroimage, 23*(3), 1046-1058.

Bisiach, E. (1997). The spatial features of unilateral neglect. *Experimental Brain Research Series, 25*, 465-496.

Blair, W., Kiemel, T., Jeka, J. J., & Clark, J. E. (2012). Development of multisensory reweighting is impaired for quiet stance control in children with developmental coordination disorder (DCD). *PLoS ONE, 7*, 1-18.

Bland, B. H. (2009). Anatomical, physiological, and pharmacological properties underlying hippocampal sensorimotor integration. *Information processing by neuronal populations*, 283-325.

Bland, B. H., Oddie, S. D., & Colom, L. V. (1999). Mechanisms of neural synchrony in the septohippocampal pathways underlying hippocampal theta generation. *Journal of Neuroscience, 19*(8), 3223-3237.

Bonato, M. (2012). Neglect and extinction depend greatly on task demands: A review. *Frontiers in human neuroscience, 6*, 195.

Bottini, G., Karnath, H. O., Vallar, G., Sterzi, R., Frith, C. D., Frackowiak, R. S., & Paulesu, E. (2001). Cerebral representations for egocentric space: functional–anatomical evidence from caloric vestibular stimulation and neck vibration. *Brain, 124*(6), 1182-1196.

Bottini, G., Sterzi, R., Paulesu, E., Vallar, G., Cappa, S. F., Erminio, F., ... & Frackowiak, R. S. (1994). Identification of the central vestibular projections in man: a positron emission tomography activation study. *Experimental Brain Research, 99*(1), 164-169.

Boyle, S. C., Kayser, S. J., & Kayser, C. (2017). Neural correlates of multisensory reliability and perceptual weights emerge at early latencies during audio-visual integration. *European Journal of Neuroscience, 46*(10), 2565-2577.

Braithwaite, M. G. (1997). The British Army Air Corps in-flight spatial disorientation demonstration sortie. *Aviation, Space, and Environmental Medicine, 68*(4), 342-345.

Brandt, T., Bartenstein, P., Janek, A., & Dieterich, M. (1998). Reciprocal inhibitory visual-vestibular interaction. Visual motion stimulation deactivates the parieto-insular vestibular cortex. *Brain: A Journal of Neurology, 121*(9), 1749-1758.

Brandt, T., Dichgans, J., & Koenig, E. (1973). Differential effects of the central versus peripheral vision on egocentric and exocentric motion perception. *Experimental Brain Research, 16*, 476-491.

Brandt, T., Glasauer, S., Stephan, T., Bense, S., Yousry, T. A., Deutschländer, A., & Dieterich, M. (2002). Visual-vestibular and visuovisual cortical interaction: new insights from fMRI and PET. *Annals of the New York Academy of Sciences, 956*(1), 230-241.

Brickman, B. J., Hettinger, L. J., & Haas, M. W. (2000). Multisensory interface design for complex task domains: Replacing information overload with meaning in tactical crew stations. *The International Journal of Aviation Psychology, 10*(3), 273-290.

Burgess, N. (2008). Grid cells and theta as oscillatory interference: Theory and predictions. *Hippocampus, 18*(12), 1157-1174.

Burgess, N., Barry, C., & O'keefe, J. (2007). An oscillatory interference model of grid cell firing. *Hippocampus, 17*(9), 801-812.

Burgess, N., Spiers, H. J., & Paleologou, E. (2004). Orientational manoeuvres in the dark: dissociating allocentric and egocentric influences on spatial memory. *Cognition, 94*(2), 149-166.

Burki-Cohen, J., Sparko, A. L., & Go, T. H. (2007). *Training value of a fixed-base flight simulator with a dynamic seat*. AIAA Modeling and Simulation Technologies Conference, 20-23 August 2007, AIAA-2007-6564

Burki-Cohen, J., Sparko, A. L., Jo, Y. J., & Go, T. H. (2009). Effects of visual, seat, and platform motion during flight simulator air transport pilot training and evaluation. *Proceeding of the 15th International Symposium on Aviation Psychology, 27-30 April.*

Burle, B., Spieser, L., Roger, C., Casini, L., Hasbroucq, T., & Vidal, F. (2015). Spatial and temporal resolutions of EEG: Is it really black and white? A scalp current density view. International *Journal of Psychophysiology, 97*(3), 210-220.

Buschman, T. J., & Miller, E. K. (2007). Top-down versus bottom-up control of attention in the prefrontal and posterior parietal cortices. *Science, 315*(5820), 1860-1862.

Busse, L., Katzner, S., & Treue, S. (2008). Temporal dynamics of neuronal modulation during exogenous and endogenous shifts of visual attention in macaque area MT. *Proceedings of the National Academy of Sciences, 105*(42), 16380-16385.

Butler, J. S., Campos, J. L., & Bülthoff, H. H. (2015). Optimal visual–vestibular integration under conditions of conflicting intersensory motion profiles. *Experimental Brain Research, 233*(2), 587-597.

Butler, J. S., Smith, S. T., Campos, J. L., & Bülthoff, H. H. (2010). Bayesian integration of visual and vestibular signals for heading. *Journal of Vision*, *10*(11), 23-23.

Buxbaum, L. J., Palermo, M. A., Mastrogiovanni, D., Read, M. S., Rosenberg-Pitonyak, E., Rizzo, A. A., & Coslett, H. B. (2008). Assessment of spatial attention and neglect with a virtual wheelchair navigation task. *Journal of Clinical and Experimental Neuropsychology, 30*(6), 650-660.

Buzsáki, G., Anastassiou, C. A., & Koch, C. (2012). The origin of extracellular fields and currents—EEG, ECoG, LFP and spikes. *Nature Reviews Neuroscience, 13*(6), 407-420.

Buzsáki, G., & Moser, E. I. (2013). Memory, navigation and theta rhythm in the hippocampal-entorhinal system. *Nature neuroscience, 16*(2), 130-138.

Camis, M., & Creed, R.S. (1930). The physiology of the vestibular apparatus. *American Journal of the Medical Sciences, 180*, 849.

Campos, J. L., & Bülthoff H.,H. (2012). Multimodal Integration during Self-Motion in Virtual Reality. In Murray, M.M., & Wallace, M.T. (Eds.), *The Neural Bases of Multisensory Processes* (pp. 603-628). Boca Raton (FL): CRC Press/Taylor & Francis.

Caplan, J. B., Madsen, J. R., Schulze-Bonhage., Aschenbrenner-Scheibe, R., Newman, E. L., & Kahana, M. J. (2003). Human θ oscillations related to sensorimotor integration and spatial learning. *The Journal of Neuroscience, 23*(11), 4726-4736.3

Cardin, V., & Smith, A. T. (2010). Sensitivity of human visual and vestibular cortical regions to egomotion-compatible visual stimulation. *Cerebral Cortex, 20*(8), 1964-1973.

Chan, E., Baumann, O., Bellgrove, M. A., & Mattingley, J. B. (2013). Reference frames in allocentric representations are invariant across static and active encoding. *Frontiers in Psychology, 4*, 565.

Chelazzi, L., Miller, E. K., Duncan, J., & Desimone, R. (1993). A neural basis for visual search in inferior temporal cortex. Nature, 363(6427), 345-347.

Chen, X., Bin, G., Daly, I., & Gao, X. (2013). Event-related desynchronization (ERD) in the alpha band during a hand mental rotation task. *Neuroscience letters, 541*, 238-242.

Chen, A., Gu, Y., Takahashi, K., Angelaki, D. E., & DeAngelis, G. C. (2008). Clustering of self-motion selectivity and visual response properties in macaque area MSTd. *Journal of Neurophysiology*, *100*(5), 2669-2683.

Chen, G., King, J. A., Burgess, N., & O'Keefe, J. (2013). How vision and movement combine in the hippocampal place code. *Proceedings of the National Academy of Sciences, 110*(1), 378-383.

Chen, L. L., Lin, L. H., Green, E. J., Barnes, C. A., & McNaughton, B. L. (1994). Head-direction cells in the rat posterior cortex. *Experimental Brain Research, 101*(1), 8-23.

Cheung, B. (2013). Spatial disorientation: more than just illusion. *Aviation, Space, and Environmental Medicine, 84*(11), 1211-1214.

Chica, A. B., Bartolomeo, P., & Lupiáñez, J. (2013). Two cognitive and neural systems for endogenous and exogenous spatial attention. *Behavioural Brain Research, 237*, 107-123.

Chung, J. W., Ofori, E., Misra, G., Hess, C. W., & Vaillancourt, D. E. (2017). Beta-band activity and connectivity in sensorimotor and parietal cortex are important for accurate motor performance. *NeuroImage, 144*, 164-173.

Cohen, Y. E., & Andersen, R. A. (2002). A common reference frame for movement plans in the posterior parietal cortex. *Nature Reviews Neuroscience, 3*(7), 553-562.

Cohen, B., Maruta, J., & Raphan, T. (2001). Orientation of the eyes to gravitoinertial acceleration. *Annals of the New York Academy of Sciences, 942*, 241-258.

Colby, C. L. (1998). Action-oriented spatial reference frames in cortex. *Neuron, 20*(1), 15-24.

Colebatch, J. G., & Rothwell, J. C. (2004). Motor unit excitability changes mediating vestibulocollic reflexes in the sternocleidomastoid muscle. *Clinical Neurophysiology, 115*(11), 2567-2573.

Colgin, L. L. (2013). Mechanisms and functions of theta rhythms. *Annual Review of Neuroscience*, 36, 295-312.

Committeri, G., Galati, G., Paradis, A. L., Pizzamiglio, L., Berthoz, A., & LeBihan, D. (2004). Reference frames for spatial cognition: different brain areas are involved in viewer-, object-, and landmark-centered judgments about object location. *Journal of Cognitive Neuroscience, 16*(9), 1517-1535.

Cooper, G. (1963). *The use of piloted flight simulators in take-off and landing research.* North Atlantic Treaty Organization, Advisory group for Aeronautical Research and Development, Report 430.

Cooper, N. R., Croft, R. J., Dominey, S. J., Burgess, A. P., & Gruzelier, J. H. (2003). Paradox lost? Exploring the role of alpha oscillations during externally vs. internally directed attention and the implications for idling and inhibition hypotheses. *International Journal of Psychophysiology, 47*(1), 65-74.

Cooray, G., Nilsson, E., Wahlin, Å., Laukka, E. J., Brismar, K., & Brismar, T. (2011). Effects of intensified metabolic control on CNS function in type 2 diabetes. *Psychoneuroendocrinology, 36*(1), 77-86.

Crone, N. E., Miglioretti, D. L., Gordon, B., & Lesser, R. P. (1998). Functional mapping of human sensorimotor cortex with electrocorticographic spectral analysis. II. Event-related synchronization in the gamma band. *Brain: A Journal of Neurology, 121*(12), 2301-2315.

Cruikshank, L.C., Singhal, A., Hueppelsheuser, M., Caplan, J.B. (2012). Theta oscillations reflect a putative neural mechanism for human sensorimotor integration. *Journal of Neurophysiology 107,* 65–77.

De Meo, R., Murray, M. M., Clarke, S., & Matusz, P. J. (2015). Top-down control and early multisensory processes: chicken vs. egg. *Frontiers in Integrative Neuroscience, 9,* 17.

de Winkel, K. N., Katliar, M., & Bülthoff, H. H. (2017). Causal inference in multisensory heading estimation. *PloS one*, *12*(1), e0169676.

de Winkel, K. N., Weesie, J., Werkhoven, P. J., & Groen, E. L. (2010). Integration of visual and inertial cues in perceived heading of self-motion. *Journal of Vision, 10*(12), 1.

de Winter, J. C., Dodou, D., & Mulder, M. (2012). Training effectiveness of whole-body flight simulator motion: A comprehensive meta-analysis. *The International Journal of Aviation Psychology, 22*(2), 164-183.

DeAngelis, G. C., & Angelaki, D. E. (2012). Visual–vestibular integration for self-motion perception. In: The Neural Bases of Multisensory Processes. CRC Press/Taylor & Francis, Boca Raton (FL); 2012.

Debener, S., Makeig, S., Delorme, A., & Engel, A. K. (2005). What is novel in the novelty oddball paradigm? Functional significance of the novelty P3 event-related potential as revealed by independent component analysis. *Cognitive Brain Research, 22*(3), 309-321.

Debener, S., Minow, F., Emkes, R., Gandras, K., & De Vos, M. (2012). How about taking a low-cost, small, and wireless EEG for a walk?. *Psychophysiology, 49*(11), 1617-1621.

Degerman, A., Rinne, T., Pekkola, J., Autti, T., Jääskeläinen, I. P., Sams, M., & Alho, K. (2007). Human brain activity associated with audiovisual perception and attention. *Neuroimage, 34*(4), 1683-1691.

Del Percio, C., Infarinato, F., Marzano, N., Iacoboni, M., Aschieri, P., Lizio, R., ... & Babiloni, C. (2011). Reactivity of alpha rhythms to eyes opening is lower in athletes than non-athletes: a high-resolution EEG study. *International Journal of Psychophysiology, 82*(3), 240-247.

Delorme, A., & Makeig, S. (2004). EEGLAB: an open-source toolbox for analysis of single-trial EEG dynamics including independent component analysis. *Journal of Neuroscience Methods, 134*(1), 9-21.

Delorme, A., Sejnowski, T., & Makeig, S. (2007). Enhanced detection of artifacts in EEG data using higher-order statistics and independent component analysis. *Neuroimage, 34*(4), 1443-1449.

Deshpande, N., & Patla, A. E. (2007). Visual–vestibular interaction during goal directed locomotion: effects of aging and blurring vision. *Experimental Brain Research*, *176*(1), 43-53.

Desimone, R., & Duncan, J. (1995). Neural mechanisms of selective visual attention. *Annual Review of Neuroscience, 18*(1), 193-222.

Desjardins, J. A., & Segalowitz, S. J. (2013). Deconstructing the early visual electrocortical responses to face and house stimuli. *Journal of Vision, 13*(5), 22-22.

Deutsch, J. A., & Deutsch, D. (1963). Attention: Some theoretical considerations. *Psychological Review, 70*(1), 80.

Deutschländer, A., Bense, S., Stephan, T., Schwaiger, M., Dieterich, M., & Brandt, T. (2004). Rollvection versus linearvection: comparison of brain activations in PET. *Human Brain Mapping, 21*(3), 143-153.

Deutschländer, A., Bense, S., Stephan, T., Schwaiger, M., Brandt, T., & Dieterich, M. (2002). Sensory system interactions during simultaneous vestibular and visual stimulation in PET. *Human Brain Mapping, 16*(2), 92-103.

Di Lollo, V. (2018). Attention is a sterile concept; iterative reentry is a fertile substitute. *Consciousness and Cognition, 64*, 45-49.

Dias, J. W., McClaskey, C. M., & Harris, K. C. (2021). Audiovisual speech is more than the sum of its parts: Auditory-visual superadditivity compensates for age-related declines in audible and lipread speech intelligibility. *Psychology and Aging*, *36*(4), 520.

Dieterich, M., Bense, S., Lutz, S., Drzezga, A., Stephan, T., Bartenstein, P., & Brandt, T. (2003). Dominance for vestibular cortical function in the non-dominant hemisphere. *Cerebral Cortex, 13*(9), 994-1007.

Dieterich, M., & Brandt, T. (2000). Brain activation studies on visual-vestibular and ocular motor interaction. *Current Opinion in Neurology, 13*(1), 13-18.

Dieterich, M., & Brandt, T. (2018). Global orientation in space and the lateralization of brain functions. *Current opinion in neurology, 31*(1), 96-104.

Dichgans, J., Brandt, T. (1978). *Visual-vestibular interaction: Effects on self-motion perception and postural control*. Handbook of sensory physiology (Eds. R. Held, H.W. Leibowitz, H.L. Teuber), pp. 756-804. Springer, Berlin.

Ditz, J. C., Schwarz, A., & Müller-Putz, G. R. (2020). Perturbation-evoked potentials can be classified from single-trial EEG. *Journal of Neural Engineering*, *17*(3), 036008.

Dlugaiczyk, J., Gensberger, K. D., & Straka, H. (2019). Galvanic vestibular stimulation: from basic concepts to clinical applications. *Journal of Neurophysiology, 121*(6), 2237-2255.

Do, T. T. N., Lin, C. T., & Gramann, K. (2020). Human retrosplenial theta and alpha modulation in active spatial navigation. *BioRxiv*.

Doppelmayr, M., Klimesch, W., Hödlmoser, K., Sauseng, P., & Gruber, W. (2005). Intelligence related upper alpha desynchronization in a semantic memory task. *Brain Research Bulletin, 66*(2), 171-177.

Driver, J. (2001). A selective review of selective attention research from the past century. *British Journal of Psychology, 92*(1), 53-78.

Dyde, R. T., & Harris, L. R. (2008). The influence of retinal and extra-retinal motion cues on perceived object motion during self-motion. *Journal of Vision, 8*(14), 5-5.

Ebenholtz, S. M., Shebilske, W. (1975). The doll reflex: Ocular counter-rolling with head- body tilt in the median plane. *Vision Research, 15*, 713-17.

Eickhoff, S. B., Weiss, P. H., Amunts, K., Fink, G. R., & Zilles, K. (2006). Identifying human parieto-insular vestibular cortex using fMRI and cytoarchitectonic mapping. *Human Brain Mapping, 27*(7), 611-621.

Ekstrom, A. D., Arnold, A. E., & Iaria, G. (2014). A critical review of the allocentric spatial representation and its neural underpinnings: toward a network-based perspective. *Frontiers in Human Neuroscience, 8,* 803.

Ekstrom, A. D., Caplan, J. B., Ho, E., Shattuck, K., Fried, I., & Kahana, M. J. (2005). Human hippocampal theta activity during virtual navigation. *Hippocampus, 15*(7), 881-889.

Elidan, J., Leibner, E., Freeman, S., Sela, M., Nitzan, M., & Sohmer, H. (1991). Short and middle latency vestibular evoked responses to acceleration in man. *Electroencephalography and Clinical Neurophysiology/Evoked Potentials Section, 80*(2), 140-145.

Engel, A. K., & Fries, P. (2010). Beta-band oscillations—signalling the status quo?. *Current Opinion in Neurobiology, 20*(2), 156-165.

Epstein, R., & Kanwisher, N. (1998). A cortical representation of the local visual environment. *Nature, 392*(6676), 598-601.

Epstein, R. A., Patai, E. Z., Julian, J. B., & Spiers, H. J. (2017). The cognitive map in humans: spatial navigation and beyond. *Nature Neuroscience, 20*(11), 1504.

Eriksson, L. (2009). Toward a visual flow integrated display format to combat pilot spatial disorientation. *The International Journal of Aviation Psychology, 20*, 1- 24.

Ernst, O.M., & Banks, M.S. (2002). Humans integrate visual and haptic information in a statistically optimal fashion. *Nature*, *415,* 429-433.

Ertl, M., & Boegle, R. (2019). Investigating the vestibular system using modern imaging techniques—a review on the available stimulation and imaging methods. *Journal of Neuroscience Methods, 326*, 108363.

Ertl, M., Moser, M., Boegle, R., Conrad, J., zu Eulenburg, P., & Dieterich, M. (2017). The cortical spatiotemporal correlate of otolith stimulation: Vestibular evoked potentials by body translations. *Neuroimage, 155*, 50-59.

Farmer, E., van Rooij, J., Riemersma, J., Joma, P., & Morall, J. (1999). Handbook of Simulator Based Training. Aldershot, Hampshire, UK: Ashgate.

Fattahi, M., Sharif, F., Geiller, T., & Royer, S. (2018). Differential representation of landmark and self-motion information along the CA1 radial axis: self-motion generated place fields shift toward landmarks during septal inactivation. *Journal of Neuroscience, 38*(30), 6766-6778.

Feldmann, H. (1999). Die zweitausendjährige geschichte der ohrenspritze und ihre verflechtung mit dem klistier. *Laryngo-Rhino-Otologie, 78*(08), 462-467.

Fetsch, C. R., DeAngelis, G. C., & Angelaki, D. E. (2010). Visual–vestibular cue integration for heading perception: applications of optimal cue integration theory. *European Journal of Neuroscience, 31*(10), 1721-1729.

Fetsch, C. R., Turner, A. H., DeAngelis, G. C., & Angelaki, D. E. (2009). Dynamic reweighting of visual and vestibular cues during self-motion perception. *Journal of Neuroscience, 29*(49), 15601-15612.

Fink, A., Grabner, R. H., Neuper, C., & Neubauer, A. C. (2005). EEG alpha band dissociation with increasing task demands. *Cognitive Brain Research, 24*(2), 252-259.

Fink, G. R., Marshall, J. C., Weiss, P. H., Stephan, T., Grefkes, C., Shah, N. J., ... & Dieterich, M. (2003). Performing allocentric visuospatial judgments with induced distortion of the egocentric reference frame: an fMRI study with clinical implications. *Neuroimage, 20*(3), 1505-1517.

Fister, J. K., Stevenson, R. A., Nidiffer, A. R., Barnett, Z. P., & Wallace, M. T. (2016). Stimulus intensity modulates multisensory temporal processing. *Neuropsychologia*, *88*, 92-100.

Fitzpatrick, R. C., & Day, B. L. (2004). Probing the human vestibular system with galvanic stimulation. *Journal of Applied Physiology, 96*(6), 2301-2316.

Fontolan, L., Morillon, B., Liegeois-Chauvel, C., & Giraud, A. L. (2014). The contribution of frequency-specific activity to hierarchical information processing in the human auditory cortex. *Nature Communications, 5*, 4694.

Frankenstein, J., Mohler, B. J., Bülthoff, H. H., & Meilinger, T. (2012). Is the map in our head oriented north?. *Psychological Science, 23*(2), 120-125.

Frassinetti, F., Bolognini, N., & Làdavas, E. (2002). Enhancement of visual perception by crossmodal visuo-auditory interaction. *Experimental Brain Research, 147*(3), 332-343.

Freidman-Hill, S.R., Robertson, L. C., & Treisman, A. (1995). Parietal contributions to visual feature binding: evidence from a patient with bilateral lesions. *Science, 269*(5225), 853-855.

Fuster, J. M. (1973). Unit activity in prefrontal cortex during delayed-response performance: neuronal correlates of transient memory. *Journal of Neurophysiology, 36*(1), 61-78.

Gaetz, W., & Cheyne, D. (2006). Localization of sensorimotor cortical rhythms induced by tactile stimulation using spatially filtered MEG. *Neuroimage, 30*(3), 899-908.

Gaetz, W., Macdonald, M., Cheyne, D., & Snead, O. C. (2010). Neuromagnetic imaging of movement-related cortical oscillations in children and adults: age predicts post-movement beta rebound. *Neuroimage, 51*(2), 792-807.

Galati, G., Committeri, G., Sanes, J. N., & Pizzamiglio, L. (2001). Spatial coding of visual and somatic sensory information in body-centred coordinates. *European Journal of Neuroscience, 14*(4), 737-746.

Galati, G., Lobel, E., Vallar, G., Berthoz, A., Pizzamiglio, L., & Le Bihan, D. (2000). The neural basis of egocentric and allocentric coding of space in humans: a functional magnetic resonance study. *Experimental Brain Research, 133*(2), 156-164.

Giard, M. H., & Peronnet, F. (1999). Auditory-visual integration during multimodal object recognition in humans: a behavioral and electrophysiological study. *Journal of Cognitive Neuroscience, 11*(5), 473-490.

Gibb, R., Ercoline, B., & Scharff, L. (2011). Spatial disorientation: decades of pilot fatalities. *Aviation, Space, and Environmental Medicine, 82*(7), 717-724.

Godijn, R., & Theeuwes, J. (2002). Programming of endogenous and exogenous saccades: evidence for a competitive integration model. *Journal of Experimental Psychology: Human Perception and Performance, 28*(5), 1039.

Goncharova, I. I., McFarland, D. J., Vaughan, T. M., & Wolpaw, J. R. (2003). EMG contamination of EEG: spectral and topographical characteristics. *Clinical Neurophysiology, 114*(9), 1580-1593.

Gopher, D., & Kahneman, D. (1971). Individual differences in attention and the prediction of flight criteria. *Perceptual and Motor Skills, 33*(3_suppl), 1335-1342.

Goutagny, R., Jackson, J., & Williams, S. (2009). Self-generated theta oscillations in the hippocampus. *Nature Neuroscience, 12*(12), 1491-1493.

Grastyan, E., Karmos, G., Vereczkey, L., & Kellenyi, L. (1966). The hippocampal electrical correlates of the homeostatic regulation of motivation. *Electroencephalography and Clinical Neurophysiology 21*(1), 34–53.

Gratton, G. (1998). Dealing with artifacts: The EOG contamination of the event-related brain potential. *Behavior Research Methods, Instruments, & Computers, 30*(1), 44-53.

Graziano, M. S. (1999). Where is my arm? The relative role of vision and proprioception in the neuronal representation of limb position. *Proceedings of the National Academy of Sciences of the United States of America, 96*, 10418-10421.

Green, J. D., & Arduini, A. A. (1954). Hippocampal electrical activity in arousal. *Journal of Neurophysiology, 17*(6), 533-557.

Greenlee, M. W., Frank, S. M., Kaliuzhna, M., Blanke, O., Bremmer, F., Churan, J., ... & Smith, A. T. (2016). Multisensory integration in self motion perception. *Multisensory Research, 29*(6-7), 525-556.

Groppe, D.M., Makeig, S., & Kutas, M. (2009). Identifying reliable independent components via split-half comparisons. *NeuroImage*, *45*, 1199-1211.

Grundy, J.G., Mohrenschildt, M.v., Nazar, S.A., & Shedden, J.M. (April 2013). Multisensory integration of visual and vestibular cues in a motion simulator: An analysis of the P3 event-related potential component. 20th Annual Meeting of the Cognitive-Neuroscience-Society, San Francisco, CA

Gu, Y., Angelaki, D.E., & DeAngelis, G.C. (2008). Neural correlates of multisensory cue integration in macaque MSTd. *Nature: Neuroscience, 11*, 1201–1210.

Hamker, F. H. (2003). The reentry hypothesis: linking eye movements to visual perception. *Journal of Vision, 3*(11), 14-14.

Hangya, B., Borhegyi, Z., Szilágyi, N., Freund, T. F., & Varga, V. (2009). GABAergic neurons of the medial septum lead the hippocampal network during theta activity. *Journal of Neuroscience, 29*(25), 8094-8102.

Harrar, V., Tammam, J., Pérez-Bellido, A., Pitt, A., Stein, J., & Spence, C. (2014). Multisensory integration and attention in developmental dyslexia. *Current Biology, 24*(5), 531-535.

Harris, L. R., & Barnes, G. R. (1987). Orientation of vestibular nystagmus is modified by head tilt. *The vestibular system: Neurophysiologic and Clinical Research*, 539-548.

Harris, L. R., Felsner, S., Jenkin, M., Herpers, R., Noppe, A., Frett, T., & Scherfgen, D. (2018). Sex bias in the influence of gravity on perception. [Poster Presentation].

Hays, R. T., Jacobs, J. W., Prince, C., & Salas, E. (1992). Flight simulator training effectiveness: A meta-analysis. *Military Psychology, 4*(2), 63-74.

Hillyard, S. A., Hink, R. F., Schwent, V. L., & Picton, T. W. (1973). Electrical signs of selective attention in the human brain. *Science, 182*(4108), 177-180.

Hinterberger, T., Widman, G., Lal, T. N., Hill, J., Tangermann, M., Rosenstiel, W., ... & Birbaumer, N. (2008). Voluntary brain regulation and communication with electrocorticogram signals. *Epilepsy & Behavior, 13*(2), 300-306.

Hood, J. D. (1983). Vestibular and optokinetic evoked potentials. *Acta oto-laryngologica, 95*(5-6), 589-593.

Hosman, R. J. A. W., & Advani, S. (2016). Design and evaluation of the objective motion cueing test and criterion. *The Aeronautical Journal, 120*(1227), 873-891.

Hu, L., Mouraux, A., Hu, Y., & Iannetti, G. D. (2010). A novel approach for enhancing the signal-to-noise ratio and detecting automatically event-related potentials (ERPs) in single trials. *Neuroimage, 50*(1), 99-111.

Huster, R., Plis, S. M., & Calhoun, V. D. (2015). Group-level component analyses of EEG: validation and evaluation. *Frontiers in Neuroscience, 9*, 254.

Irwin, D. E., Colcombe, A. M., Kramer, A. F., & Hahn, S. (2000). Attentional and oculomotor capture by onset, luminance and color singletons. *Vision Research, 40*(10-12), 1443-1458.

Jacobs, J., Weidemann, C. T., Miller, J. F., Solway, A., Burke, J. F., Wei, X. X., ... & Kahana, M. J. (2013). Direct recordings of grid-like neuronal activity in human spatial navigation. *Nature Neuroscience, 16*(9), 1188-1190.

Janzen, J., Schlindwein, P., Bense, S., Bauermann, T., Vucurevic, G., Stoeter, P., & Dieterich, M. (2008). Neural correlates of hemispheric dominance and ipsilaterality within the vestibular system. *Neuroimage, 42*(4), 1508-1518.

Johansson, G. (1977). Studies on visual-perception of locomotion. *Perception, 6*, 365- 376.

Jones, M. (2016). Optimizing the Fitness of Motion Cueing for Rotorcraft Flight Simulation. *72nd American Helicopter Society Annual Forum, 9-11. May 2016, West Palm Beach, United States*.

Jong, B. D., Shipp, S., Skidmore, B., Frackowiak, R. S. J., & Zeki, S. (1994). The cerebral activity related to the visual perception of forward motion in depth. *Brain, 117*(5), 1039-1054.

Joundi, R.A., Jenkinson, N., Brittain, J.-S., Aziz, T.Z., & Brown, P. (2012). Driving oscillatory activity in the human cortex enhances motor performance. *Current Biology, 22*, 403–407.

Jung, T. P., Humphries, C., Lee, T. W., Makeig, S., McKeown, M. J., Iragui, V., & Sejnowski, T. J. (1998). Extended ICA removes artifacts from electroencephalographic recordings. *Advances in Neural Information Processing Systems*, 894-900.

Jung, R., & Kornmüller, AE (1938). A method of deriving localized potential fluctuations from subcortical brain areas. *Archives for Psychiatry and Nervous Diseases,109*(1), 1-30.

Jung, T. P., Makeig, S., Westerfield, M., Townsend, J., Courchesne, E., & Sejnowski, T. J. (2001). Analysis and visualization of single-trial event-related potentials. *Human Brain Mapping, 14*(3), 166-185.

Kahana, M. J., Sekuler, R., Caplan, J. B., Kirschen, M., & Madsen, J. R. (1999). Human theta oscillations exhibit task dependence during virtual maze navigation. *Nature, 399*(6738), 781-784.

Kammermeier, S., Singh, A., Noachtar, S., Krotofil, I., & Bötzel, K. (2015). Intermediate latency evoked potentials of cortical multimodal vestibular areas: acoustic stimulation. *Clinical Neurophysiology, 126*(3), 614-625.

Kana, R. K., Keller, T. A., Minshew, N. J., & Just, M. A. (2007). Inhibitory control in high-functioning autism: decreased activation and underconnectivity in inhibition networks. *Biological Psychiatry, 62*(3), 198-206.

Kappé, B., Van Erp, J., & Korteling, J. E. (1999). Effects of headslaved and peripheral displays on lane-keeping performance and spatial orientation. *Human Factors, 41*, 453-466.

Karakaş, S. (2020). A review of theta oscillation and its functional correlates. International *Journal of Psychophysiology, 157*, 82-99.

Karakaş, S., Başar-Eroğlu, C., Özesmi, C., Kafadar, H., & Erzengin, Ö. Ü. (2001). Gamma response of the brain: a multifunctional oscillation that represents bottom-up with top-down processing. *International Journal of Psychophysiology, 39*(2-3), 137-150.

Karnath, H. O. (1994). Subjective body orientation in neglect and the interactive contribution of neck muscle proprioception and vestibular stimulation. *Brain, 117*(5), 1001-1012.

Kayser, S. J., McNair, S. W., & Kayser, C. (2016). Prestimulus influences on auditory perception from sensory representations and decision processes. *Proceedings of the National Academy of Sciences, 113*(17), 4842-4847.

Keil, J., & Senkowski, D. (2018). Neural oscillations orchestrate multisensory processing. *The Neuroscientist, 24*(6), 609-626.

Keinrath, C., Wriessnegger, S., Müller-Putz, G. R., & Pfurtscheller, G. (2006). Post-movement beta synchronization after kinesthetic illusion, active and passive movements. *International Journal of Psychophysiology, 62*(2), 321-327.

Kenney, D. M., Jabbari, Y., von Mohrenschildt, M., & Shedden, J. M. (2021). Visual-vestibular integration is preserved with healthy aging in a simple acceleration detection task. *Neurobiology of Aging, 104,* 71-81.

Kenney, D. M., O'Malley, S., Song, H. M., Townsend, B., von Mohrenschildt, M., & Shedden, J. M. (2020). Velocity influences the relative contributions of visual and vestibular cues to self-acceleration. *Experimental Brain Research, 238*(6), 1423-1432.

Khan, S., & Chang, R. (2013). Anatomy of the vestibular system: A review. *Neurorehabilitation, 32*, 437-443.

Kilavik, B. E., Zaepffel, M., Brovelli, A., MacKay, W. A., & Riehle, A. (2013). The ups and downs of beta oscillations in sensorimotor cortex. *Experimental Neurology, 245*, 15-26.

Kingma, H. (2005). Thresholds for perception of direction of linear acceleration as a possible evaluation of the otolith function. *BMC Ear, Nose and Throat Disorders*, *5*(1), 5.

Klatzky, R. L. (1998). *Allocentric and egocentric spatial representations: Definitions, distinctions, and interconnections*. In Spatial cognition (pp. 1-17). Springer, Berlin, Heidelberg.

Kleinschmidt, A., Thilo, K. V., Büchel, C., Gresty, M. A., Bronstein, A. M., & Frackowiak, R. S. (2002). Neural correlates of visual-motion perception as object-or self-motion. *Neuroimage, 16*(4), 873-882.

Klimesch, W. (2012). Alpha-band oscillations, attention, and controlled access to stored information. *Trends in Cognitive Sciences, 16*(12), 606-617.

Klimesch, W., Sauseng, P., & Hanslmayr, S. (2007). EEG alpha oscillations: the inhibition–timing hypothesis. *Brain Research Reviews, 53*(1), 63-88.

Knill, D. C., & Pouget, A. (2004). The Bayesian brain: the role of uncertainty in neural coding and computation. *TRENDS in Neurosciences*, *27*(12), 712-719.

Koelewijn, T., van Schie, H. T., Bekkering, H., Oostenveld, R., & Jensen, O. (2008). Motor-cortical beta oscillations are modulated by correctness of observed action. *Neuroimage, 40*(2), 767-775.

Koenig, J., Linder, A.N., Leutgeb, J.K., & Leutgeb, S. (2011). The spatial periodicity of grid cells is not sustained during reduced theta oscillations. *Science, 332*, 592-595.

Koivisto, M., & Silvanto, J. (2011). Relationship between visual binding, reentry and awareness. *Consciousness and Cognition*, *20*(4), 1293-1303.

Kolchev, C. (1995). Vestibular late evoked potentials (VbEP) processed by means of brain electrical activity mapping (BEAM). *Acta Oto-laryngolica, 115*,130–133.

Koles, Z. J. (1998). Trends in EEG source localization. *Electroencephalography and Clinical Neurophysiology, 106*(2), 127-137.

Kovács, G., Raabe, M., & Greenlee, M. W. (2008). Neural correlates of visually induced self-motion illusion in depth. *Cerebral Cortex, 18*(8), 1779-1787.

Krupic, J., Bauza, M., Burton, S., & O'Keefe, J. (2018). Local transformations of the hippocampal cognitive map. *Science, 359*(6380), 1143-1146.

Lackner, J., & DiZio, P. (2005). Vestibular, proprioceptive, and haptic contributions to spatial orientation. *Annual Review of Psychology, 56*, 115-147.

Lee, B., & Myung, R. (2013). Attitude indicator design and reference frame effects on unusual attitude recoveries. *The International Journal of Aviation Psychology, 23*, 63-90.

Lemmin, T., Ganesh, G., Gassert, R., Burdet, E., Kawato, M., & Haruno, M. (2010). Model-based attenuation of movement artifacts in fMRI. *Journal of Neuroscience Methods, 192*(1), 58-69.

Leocani, L., & Comi, G. (2006). Movement-related desynchronization in neuropsychiatric disorders. *Progress in Brain Reserch, 159*, 351–366.

Li, T., Arleo, A., & Sheynikhovich, D. (2020). Modeling place cells and grid cells in multi-compartment environments: Entorhinal–hippocampal loop as a multisensory integration circuit. *Neural Networks, 121*, 37-51.

Li, W., Piëch, V., & Gilbert, C. D. (2004). Perceptual learning and top-down influences in primary visual cortex. *Nature neuroscience, 7*(6), 651.

Li, Q., Wu, J., & Touge, T. (2010). Audiovisual interaction enhances auditory detection in late stage: an event-related potential study. *Neuroreport, 21*(3), 173-178.

Li, Q., Yang, H., Sun, F., & Wu, J. (2015). Spatiotemporal relationships among audiovisual stimuli modulate auditory facilitation of visual target discrimination. *Perception, 44*(3), 232-242.

Lin, C. T., Chiu, T. C., & Gramann, K. (2015). EEG correlates of spatial orientation in the human retrosplenial complex. *NeuroImage*, *120*, 123-132.

Lobel, E., Kleine, J. F., Bihan, D. L., Leroy-Willig, A., & Berthoz, A. (1998). Functional MRI of galvanic vestibular stimulation. *Journal of Neurophysiology, 80*(5), 2699-2709.

Loose, R., Probst, T., Tucha, O., Bablok, E., Aschenbrenner, S., & Lange, K. W. (2002). Vestibular evoked potentials from the vertical semicircular canals in humans evoked by roll-axis rotation in microgravity and under 1-G. *Behavioural Brain Research, 134*(1-2), 131-137.

Lopez, C., Blanke, O., & Mast, F. W. (2012). The human vestibular cortex revealed by coordinate-based activation likelihood estimation meta-analysis. *Neuroscience, 212*, 159-179.

López-Ibor, J. J., & López-Ibor, M. I. (2003). Research on obsessive-compulsive disorder. *Current Opinion in Psychiatry, 16*, S85-S91.

Lupo, J., & Barnett-Cowan, M. (2018). Impaired perceived timing of falls in the elderly. *Gait & Posture, 59*, 40-45.

Macaluso, E., Noppeney, U., Talsma, D., Vercillo, T., Hartcher-O'Brien, J., & Adam, R. (2016). The curious incident of attention in multisensory integration: bottom-up vs. top-down. *Multisensory Research, 29*(6-7), 557-583.

Mackrous, I., Carriot, J., Cullen, K. E., & Chacron, M. J. (2020). Neural variability determines coding strategies for natural self-motion in macaque monkeys. *Elife, 9*, e57484.

MacNeilage, P. R., Banks, M. S., DeAngelis, G. C., & Angelaki, D. E. (2010). Vestibular heading discrimination and sensitivity to linear acceleration in head and world coordinates. *Journal of Neuroscience, 30*(27), 9084-9094.

Maes, L., Dhooge, I., De Vel, E., D'haenens, W., Bockstael, A., & Vinck, B. M. (2007). Water irrigation versus air insufflation: A comparison of two caloric test protocols: Irrigación con agua versus insuflación con aire: comparación de dos protocolos de pruebas calóricas. *International Journal of Audiology, 46*(5), 263-269.

Makeig, S., Bell, A.J., Jung, T.P., & Sejnowski, T.J. (1996). Independent component analysis of electroencephalographic data. *Advances in Neural Information Processing Systems, 8*, 145.

Makeig S. Westerfield M. Townsend J. Jung T. P. Courchesne E. Sejnowski T. J. (1999). Functionally independent components of early event-related potentials in a visual spatial attention task. *Philosophical Transactions of the Royal Society B: Biological Sciences, 354*(1387), 1135–1144.

Malcolm, R. & Jones, G., M. (1970). A quantitative study of vestibular adaptation in humans. *Acta Otolaryngolica, 70*, 126–35.

Marcelli, V., Esposito, F., Aragri, A., Furia, T., Riccardi, P., Tosetti, M., ... & Di Salle, F. (2009). Spatio-temporal pattern of vestibular information processing after brief caloric stimulation. *European Journal of Radiology, 70*(2), 312-316.

Marchette, S. A., Vass, L. K., Ryan, J., & Epstein, R. A. (2014). Anchoring the neural compass: coding of local spatial reference frames in human medial parietal lobe. *Nature Neuroscience, 17*(11), 1598.

Mardirossian, V., Karmali, F., Merfeld, D. (2014). Thresholds for human perception of roll tilt motion: Patterns of variability based on visual, vestibular, and mixed cues. *Otology and Neurotology, 35*(5), 857-860.

Marsh, E. B., & Hillis, A. E. (2008). Dissociation between egocentric and allocentric visuospatial and tactile neglect in acute stroke. *Cortex, 44*(9), 1215-1220.

Matthews, P. B. C. (1972). *The mammalian muscle receptors and their central actions*. London, England: Edward Arnold.

McCauley, M. E. (2006). *Do army helicopter training simulators need motion bases?.* (No. 1176). Arlington, Virginia: U.S. Army Research Institute for the Behavioral Sciences.

McFarland, D.J., Miner, L.A., Vaughan, T.M., & Wolpaw, J.R. (2000). Mu and beta rhythm topographies during motor imagery and actual movements. *Brain Topography, 12,* 177-186.

McNerney, K. M., Lockwood, A. H., Coad, M. L., Wack, D. S., & Burkard, R. F. (2011). Use of 64-channel electroencephalography to study neural otolith-evoked responses. *Journal of the American Academy of Audiology, 22*(3), 143-155.

Meilinger, T., & Vosgerau, G. (2010, August). *Putting egocentric and allocentric into perspective*. In International Conference on Spatial Cognition (pp. 207-221). Springer, Berlin, Heidelberg.

Meredith, M. A., Nemitz, J. W., & Stein, B. E. (1987). Determinants of multisensory integration in superior colliculus neurons. I. Temporal factors. *Journal of Neuroscience, 7*(10), 3215-3229.

Merfeld, D. M., Park, S., Gianna-Poulin, C., Black, F. O., & Wood, S. (2005). Vestibular perception and action employ qualitatively different mechanisms. II. VOR and perceptual responses during combined tilt & translation. *Journal of Neurophysiology, 94*(1), 199-205.

Michalareas, G., Vezoli, J., Van Pelt, S., Schoffelen, J. M., Kennedy, H., & Fries, P. (2016). Alpha-beta and gamma rhythms subserve feedback and feedforward influences among human visual cortical areas. *Neuron, 89*(2), 384-397.

Miletović, I., Pool, D. M., Stroosma, O., Pavel, M. D., Wentink, M., & Mulder, M. (2017). *The use of pilot ratings in rotorcraft flight simulation fidelity assessment.* In 73rd Annual AHS International Forum and Technology Display: The Future of Vertical Flight 2017 (AHS Forum 73). (pp. 1918-1931).

Miller, R. (1953) Psychological considerations in the design of training equipment. Report no. WADC-TR-54-563, AD 71202. Wright Patterson Air Force Base, OH; Wright Air Development Center.

Miller, E. F., Graybiel, A. (1962). Counterrolling of the human eyes produced by head tilt with respect to gravity. *Acta Oto-laryngologica, 54*, 479-501.

Miller, R. L., Pluta, S. R., Stein, B. E., & Rowland, B. A. (2015). Relative unisensory strength and timing predict their multisensory product. *Journal of Neuroscience, 35*(13), 5213-5220.

Misra, G., Wang, W. E., Archer, D. B., Roy, A., & Coombes, S. A. (2017). Automated classification of pain perception using high-density electroencephalography data. *Journal of Neurophysiology, 117*(2), 786-795.

Mittelstaedt, M. L., & Mittelstaedt, H. (1980). Homing by path integration in a mammal. *Die Naturwissenschaften*, 67(11), 566-567.

Miyamoto, T., Fukushima, K., Takada, T., de Waele, C., & Vidal, P. P. (2007). Saccular stimulation of the human cortex: a functional magnetic resonance imaging study. *Neuroscience letters, 423*(1), 68-72.

Moffat, S. D. (2009). Aging and spatial navigation: What do we know and where do we go? *Neuropsychology Review, 19*(4), 478.

Moore, S. T., Hirasaki, E., Raphan, T., & Cohen, B. (2001). The human vestibulo-ocular reflex during linear locomotion. *Annals of the New York Academy of Sciences, 942*, 139-147.

Morgan, M., DeAngelis, G., & Angelaki, D. (2008). Multisensory integration in macaque visual cortex depends on cue reliability. *Neuron, 59*, 662-673.

Morrone, M. C., Tosetti, M., Montanaro, D., Fiorentini, A., Cioni, G., & Burr, D. C. (2000). A cortical area that responds specifically to optic flow, revealed by fMRI. *Nature Neuroscience, 3*(12), 1322-1328.

Mou, W., Zhao, M., & McNamara, T. P. (2007). Layout geometry in the selection of intrinsic frames of reference from multiple viewpoints. *Journal of Experimental Psychology: Learning, Memory, and Cognition, 33*(1), 145.

Müller, M. M., Gruber, T., & Keil, A. (2000). Modulation of induced gamma band activity in the human EEG by attention and visual information processing. *International Journal of Psychophysiology, 38*(3), 283-299.

Munhall, K. G. (2001). Functional imaging during speech production. *Acta Psychologica, 107*(1-3), 95-117.

Mysore, S. P., & Knudsen, E. I. (2013). A shared inhibitory circuit for both exogenous and endogenous control of stimulus selection. *Nature Neuroscience, 16*(4), 473-478.

Nakagawa, K., Aokage, Y., Fukuri, T., Kawahara, Y., Hashizume, A., Kurisu, K., & Yuge, L. (2011). Neuromagnetic beta oscillation changes during motor imagery and motor execution of skilled movements. *Neuroreport, 22*(5), 217-222.

Nakamura, A., Suzuki, Y., Milosevic, M., & Nomura, T. (2021). Long-lasting event-related beta synchronizations of electroencephalographic activity in response to support-surface perturbations during upright stance: a pilot study associating beta rebound and active monitoring in the intermittent postural control. *Frontiers in systems neuroscience*, *15*.

Neuper, C., & Pfurtscheller, G. (2001). Event-related dynamics of cortical rhythms: frequency-specific features and functional correlates. *International Journal of Psychophysiology, 43*(1), 41-58.

Neuper, C., Wörtz, M., & Pfurtscheller, G. (2006). ERD/ERS patterns reflecting sensorimotor activation and deactivation. *Progress in Brain Research, 159*, 211-222.

Newman, M.C., Lawson, B.D., Rupert, A.H., & McGrath, B.J. (2012). The role of perceptual modeling in the understanding of spatial disorientation during flight and ground-based simulator training. Proceedings of the American Institute of Aeronautics and Astronautics, 15 Aug., Minneapolis, MN.

Niedermeyer, E. (1997). Alpha rhythms as physiological and abnormal phenomena. International *Journal of Psychophysiology, 26*(1-3), 31-49.

Niedermeyer, E., & da Silva, F. L. (Eds.). (2005). *Electroencephalography: basic principles, clinical applications, and related fields*. Lippincott Williams & Wilkins.

Niedermeyer, E., Lopes da Silva, F. (2004). Electroencephalography: Basic Principles, Clinical Applications, and Related Fields, 5th ed. Williams & Wilkins, Baltimore.

Nishiike, S., Nakagawa, S., Nakagawa, A., Uno, A., Tonoike, M., Takeda, N., & Kubo, T. (2002). Magnetic cortical responses evoked by visual linear forward acceleration. *Neuroreport, 13*(14), 1805-1808.

Nolan, H., Butler, J. S., Whelan, R., Foxe, J. J., Bülthoff, H. H., & Reilly, R. B. (2012). Neural correlates of oddball detection in self-motion heading: a high-density event-related potential study of vestibular integration. *Experimental Brain Research, 219*(1), 1-11.

Nolan, H., Butler, J. S., Whelan, R., Foxe, J. J., Bülthoff, H. H., & Reilly, R. B. (2011, April). Electrophysiological source analysis of passive self-motion. In 2011 5th International IEEE/EMBS Conference on Neural Engineering (pp. 53-56). IEEE.

Nolan, H., Whelan, R., Reilly, R. B., Bulthoff, H. H., & Butler, J. S. (2009, April). Acquisition of human EEG data during linear self-motion on a Stewart platform. In *2009 4th International IEEE/EMBS Conference on Neural Engineering* (pp. 585-588). IEEE.

Noyce, A. J., Lees, A. J., & Schrag, A. E. (2016). The prediagnostic phase of Parkinson's disease. *Journal of Neurology, Neurosurgery & Psychiatry, 87*(8), 871-878.

Nunez, P. L., Silberstein, R. B., Cadusch, P. J., Wijesinghe, R. S., Westdorp, A. F., & Srinivasan, R. (1994). A theoretical and experimental study of high-resolution EEG based on surface Laplacians and cortical imaging. *Electroencephalography and Clinical Neurophysiology, 90*(1), 40-57.

O'Keefe, J. (1979). A review of the hippocampal place cells. *Progress in Neurobiology, 13*(4), 419-439.

O'Keefe, J., & Burgess, N. (2005). Dual phase and rate coding in hippocampal place cells: Theoretical significance and relationship to entorhinal grid cells. *Hippocampus, 15*(7), 853-866.

O'Keefe, J., & Dostrovsky, J. (1971). The hippocampus as a spatial map: Preliminary evidence from unit activity in the freely-moving rat. *Brain Research, 34*, 171-175.

O'Keefe, J., & Nadel, L. (1978). *The hippocampus as a cognitive map*. Oxford: Clarendon Press.

O'Keefe, J., & Recce, M. L. (1993). Phase relationship between hippocampal place units and the EEG theta rhythm. *Hippocampus, 3*(3), 317-330.

O'Malley, S., Rajagobal, A., Grundy, J. G., Mohrenshildt, M. V., & Shedden, J. M. (2016). Exposure to Disturbance Motion During Practice in an Analog of a Flight Task Influences Flight Control of Naive Participants. *The International Journal of Aviation Psychology, 26*(3-4), 63-74.

Oddie, S. D., & Bland, B. H. (1998). Hippocampal formation theta activity and movement selection. *Neuroscience & Biobehavioral Reviews, 22*(2), 221-231.

Ofori, E., Coombes, S. A., & Vaillancourt, D. E. (2015). 3D Cortical electrophysiology of ballistic upper limb movement in humans. *Neuroimage, 115*, 30-41.

Öhman, A., Flykt, A. and Esteves, F. (2001). Emotion drives attention: Detecting the snake in the grass. *Journal of Experimental Psychology: General, 130*, 466–478.

Omlor, W., Patino, L., Mendez-Balbuena, I., Schulte-Mönting, J., & Kristeva, R. (2011). Corticospinal beta-range coherence is highly dependent on the pre-stationary motor state. *Journal of Neuroscience, 31*(22), 8037-8045.

Oostenveld, R., Fries, P., Maris, E., & Schoffelen, J.M. (2011). FieldTrip: Open Source Software for Advanced Analysis of MEG, EEG, and Invasive Electrophysiological Data. *Computational Intelligence and Neuroscience, 2011.*

Orgs, G., Dombrowski, J. H., Heil, M., & Jansen-Osmann, P. (2008). Expertise in dance modulates alpha/beta event-related desynchronization during action observation. *European Journal of Neuroscience, 27*(12), 3380-3384.

Paige, G. D. (1994). Senescence of human visual-vestibular interactions: smooth pursuit, optokinetic, and vestibular control of eye movements with aging. *Experimental Brain Research*, *98*(2), 355-372.

Palmer, J.A., Kreutz-Delgado, K., Makeig, S.(2012). AMICA: an Adaptive Mixture of Independent Component Analyzers with Shared Components. Swartz Center for Computatonal Neursoscience, University of California San Diego. Tech. Rep).

Palmisano, S., Allison, R. S., Schira, M. M., & Barry, R. J. (2015). Future challenges for vection research: definitions, functional significance, measures, and neural bases. *Frontiers in Psychology, 6*, 193.

Palmisano, S., Barry, R.J., De Blasio, F.M., & Fogarty, J.S. (2016). Identifying objective EEG based markers of linear vection. *Frontiers in Psychology, 7,* 1205.

Palmisano, S., Kim, J., Allison, R., & Bonato, F. (2011). Simulated viewpoint jitter shakes sensory conflict accounts of vection. *Seeing and Perceiving, 24*(2), 173-200.

Parsons, D. (2019, August 1). Full Flight Simulators Incorporate VR for Next Generation of Pilots. Aviation Today. https://www.aviationtoday.com/2019/08/01/training-brain-mind/.

Pasma, D. L., Grant, S. C., Gamble, M., Kruk, R. V., & Herdman, C. M. (2011, September). Utility of Motion and Motion-Cueing to Support Simulated In-Flight Rotary-Wing Emergency Training. Paper presented at Proceedings of the Human Factors and Ergonomics Society Annual Meeting, Las Vegas, NV.

Parkes, L. M., Bastiaansen, M. C., & Norris, D. G. (2006). Combining EEG and fMRI to investigate the post-movement beta rebound. *Neuroimage, 29*(3), 685-696.

Pavlidou, A., Ferrè, E. R., & Lopez, C. (2018). Vestibular stimulation makes people more egocentric. *Cortex, 101*, 302-305.

Perenin, M. T. (1997). Optic ataxia and unilateral neglect: clinical evidence for dissociable spatial functions in posterior parietal cortex. *Experimental Brain Research Series, 25*, 289-308.

Perfetti, B., Moisello, C., Landsness, E. C., Kvint, S., Pruski, A., Onofrj, M., & Ghilardi, M. F. (2010). Temporal evolution of oscillatory activity predicts performance in a choice-reaction time reaching task. *Journal of Neurophysiology, 105*(1), 18-27.

Peterka, R. J., Gianna-Poulin, C. C., Zupan, L. H., & Merfeld, D. M. (2004). Origin of orientation-dependent asymmetries in vestibulo-ocular reflexes evoked by caloric stimulation. *Journal of Neurophysiology, 92*(4), 2333-2345.

Peters, J. F. (1967). Surface electrical fields generated by eye movements. *American Journal of EEG Technology, 7*(2), 27-40.

Peters, R. M., Blouin, J. S., Dalton, B. H., & Inglis, J. T. (2016). Older adults demonstrate superior vestibular perception for virtual rotations. *Experimental Gerontology, 82*, 50-57.

Peterson, S. M., & Ferris, D. P. (2018). Differentiation in theta and beta electrocortical activity between visual and physical perturbations to walking and standing balance. *eNeuro*, *5*(4).

Pfurtscheller, G. (1992). Event-related synchronization (ERS): An electrophysiological correlate of cortical areas at rest. *Clinical Neurophysiology, 83*(1), 62-69.

Pfurtscheller, G., & Lopes da Silva, F. (1999). Event-related EEG/MEG synchronization and desynchronization: basic principles. *Clinical Neurophysiology, 110*(11), 1842-1857.

Pfurtscheller, G., Neuper, C., Brunner, C., & Da Silva, F. L. (2005). Beta rebound after different types of motor imagery in man. *Neuroscience letters, 378*(3), 156-159.

Pfurtscheller, G., & Solis-Escalante, T. (2009). Could the beta rebound in the EEG be suitable to realize a "brain switch"?. *Clinical Neurophysiology, 120*(1), 24-29.

Pfurtscheller, G., Stancak Jr, A., & Neuper, C. (1996). Post-movement beta synchronization. A correlate of an idling motor area?. *Electroencephalography and Clinical Neurophysiology, 98*(4), 281-293.

Pinto, M., Cavallo, V., & Ohlmann, T. (2008). The development of driving simulators: Toward a multisensory solution. *Le travail humain, 71*(1), 62-95.

Pistohl, T., Schulze-Bonhage, A., Aertsen, A., Mehring, C., & Ball, T. (2012). Decoding natural grasp types from human ECoG. *Neuroimage, 59*(1), 248-260.

Pitzalis, S., Sdoia, S., Bultrini, A., Committeri, G., Di Russo, F., Fattori, P., et al. (2013). Selectivity to translational egomotion in human brain motion areas. *PLoS ONE, 8,* e60241.

Pizzamiglio, I., Frasca, R., Guariglia, C., Incoccia, C., & Antonucci, G. (1990). *Cortex, 26*, 535-540.

Polich, J. (1993). Cognitive brain potentials. *Current Directions in Psychological Science, 2*(6), 175-179.

Polich, J., & Heine, M. R. (1996). P300 topography and modality effects from a single-stimulus paradigm. *Psychophysiology, 33*(6), 747-752.

Pomper, U., Keil, J., Foxe, J. J., & Senkowski, D. (2015). Intersensory selective attention and temporal orienting operate in parallel and are instantiated in spatially distinct sensory and motor cortices. *Human Brain Mapping, 36*(8), 3246-3259.

Prewett, M. S., Elliott, L. R., Walvoord, A. G., & Coovert, M. D. (2012). A meta-analysis of vibrotactile and visual information displays for improving task performance. *IEEE Transactions on Systems, Man, and Cybernetics, Part C (Applications and Reviews), 42*(1), 123-132.

Probst, T., Ayan, T., Loose, R., & Skrandies, W. (1997). Electrophysiological evidence for direction-specific rotary evoked potentials in human subjects–a topographical study. *Neuroscience letters, 239*(2-3), 97-100.

Proske, U., & Gandevia, S. (2012). The proprioceptive senses: their roles in signaling body shape, body position and movement, and muscle force. *Physiological Reviews, 92*, 1651-1697.

Qin, Y., Xu, P., & Yao, D. (2010). A comparative study of different references for EEG default mode network: the use of the infinity reference. *Clinical Neurophysiology, 121*(12), 1981-1991.

Qiu, S., Yi, W., Xu, J., Qi, H., Du, J., Wang, C., ... & Ming, D. (2015). Event-related beta EEG changes during active, passive movement and functional electrical stimulation of the lower limb. *IEEE Transactions on Neural Systems and Rehabilitation Engineering, 24*(2), 283-290.

Quality Standards Subcommittee of the American Academy of Neurology. (1995). Practice parameters for determining brain death in adults (summary statement). *Neurology, 45*, 1012-1014.

Rabbitt, R. D., Damiano, E., R., & Grant, J. W. (2004) Biomechanics of the Semicircular Canals and Otolith Organs. *Springer Handbook of Auditory Research, 19*, 153- 201.

Ramkhalawansingh, R., Butler, J. S., & Campos, J. L. (2018). Visual–vestibular integration during self-motion perception in younger and older adults. *Psychology and aging*, *33*(5), 798.

Ranck Jr, J. B. (1984). Head direction cells in the deep layer of dorsal presubiculum in freely moving rats. In *Society of Neuroscience Abstract* (Vol. 10, p. 599).

Recanzone, G. H. (2003). Auditory influences on visual temporal rate perception. *Journal of Neurophysiology, 89*(2), 1078-1093.

Richard, L., & Waller, D. (2013). Toward a definition of intrinsic axes: The effect of orthogonality and symmetry on the preferred direction of spatial memory. *Journal of Experimental Psychology: Learning, Memory, and Cognition, 39*(6), 1914.

Richmond, B. J., Wurtz, R. H., & Sato, T. (1983). Visual responses of inferior temporal neurons in awake rhesus monkey. *Journal of Neurophysiology, 50*(6), 1415-1432.

Robinson, A., Mania, K., & Perey, P. *Flight simulation: Research challenges and user assessments of fidelity*. London: CAE UK and University of Essex.

Rodionov, V., Elidan, J., & Sohmer, H. (1996). Analysis of the middle latency evoked potentials to angular acceleration impulses in man. *Electroencephalography and Clinical Neurophysiology/Evoked Potentials Section, 100*(4), 354-361.

Rodriguez, R., & Crane, B. T. (2021). Effect of timing delay between visual and vestibular stimuli on heading perception. *Journal of Neurophysiology*, *126*(1), 304-312.

Rohe, T., Ehlis, A. C., & Noppeney, U. (2019). The neural dynamics of hierarchical Bayesian causal inference in multisensory perception. *Nature Communications*, *10*(1), 1-17.

Rollin Stott, J. R., & Benson, A. J. (2016). Spatial orientation and disorientation in flight. In D. P. Gradwell & D. J. Rainford (Eds.), Ernsting's Aviation and Space Medicine (pp. 281–319). Boca Raton, FL: CRC Press.

Rolls, E. T., & O'Mara, S. M. (1995). View-responsive neurons in the primate hippocampal complex. *Hippocampus, 5*(5), 409-424.

Rowland, B. A., & Stein, B. E. (2014). A model of the temporal dynamics of multisensory enhancement. *Neuroscience & Biobehavioral Reviews, 41*, 78-84.

Ryun, S., Kim, J. S., Lee, H., & Chung, C. K. (2017). Tactile frequency-specific high-gamma activities in human primary and secondary somatosensory cortices. *Scientific Reports, 7*(1), 15442.

Sadowski, W., & Stanney, K. (2002). Measuring and managing presence in virtual environments. In K. Stanney (Ed.), Handbook of virtual environments: Design, implementation, and applications. Lawrence Erlbaum Associates.

Sakowitz, O. W., Quiroga, R. Q., Schürmann, M., & Başar, E. (2001). Bisensory stimulation increases gamma-responses over multiple cortical regions. Cognitive Brain Research, 11(2), 267-279.

Salmelin, R., Hämäläinen, M., Kajola, M., and Hari, R. (1995). Functional segregation of movement-related rhythmic activity in the human brain. *NeuroImage* 2, 237–243.

Salmelin, R., & Hari, R. (1994). Spatiotemporal characteristics of sensorimotor neuromagnetic rhythms related to thumb movement. *Neuroscience, 60*(2), 537-550.

Santangelo, V., Fagioli, S., & Macaluso, E. (2010). The costs of monitoring simultaneously two sensory modalities decrease when dividing attention in space. *Neuroimage, 49*(3), 2717-2727.

Scanlon, J. E., Sieben, A. J., Holyk, K. R., & Mathewson, K. E. (2017). Your brain on bikes: P3, MMN/N2b, and baseline noise while pedaling a stationary bike. *Psychophysiology, 54*(6), 927-937.

Schlindwein, P., Mueller, M., Bauermann, T., Brandt, T., Stoeter, P., & Dieterich, M. (2008). Cortical representation of saccular vestibular stimulation: VEMPs in fMRI. *Neuroimage, 39*(1), 19-31.

Schneider, D., Kolchev, C., Constantinescu, L. U. C. I. A., & Claussen, C. (1996). Vestibular Evoked Potentials (VestEP) and Brain Electrical Activity Mapping-A Test of Vestibular Function-A Review (1990-1996). *The International Tinnitus Journal, 2*, 27-43.

Seeber, N., Scherer, R., Wagner, J., Solis-Escalante, T., & Müller-Putz. (2014). EEG beta suppression and low gamma modulation are different elements of human upright walking. *Frontiers in Human Neuroscience.*

Seemungal, B. M., Guzman-Lopez, J., Arshad, Q., Schultz, S. R., Walsh, V., & Yousif, N. (2013). Vestibular activation & differentially modulates human early visual cortex and V5/MT excitability and response entropy. *Cerebral Cortex, 23*, 12-19.

Senkowski, D., Schneider, T. R., Foxe, J. J., & Engel, A. K. (2008). Crossmodal binding through neural coherence: Implications for multisensory processing. *Trends in Neurosciences, 31*(8), 401-409.

Senkowski, D., Talsma, D., Grigutsch, M., Herrmann, C. S., & Woldorff, M. G. (2007). Good times for multisensory integration: effects of the precision of temporal synchrony as revealed by gamma-band oscillations. *Neuropsychologia, 45*(3), 561-571.

Senkowski, D., Talsma, D., Herrmann, C. S., & Woldorff, M. G. (2005). Multisensory processing and oscillatory gamma responses: effects of spatial selective attention. *Experimental Brain Research, 166*(3-4), 411-426.

Shams, L., Kamitani, Y., & Shimojo, S. (2000). What you see is what you hear. *Nature, 408*(6814), 788-788.

Shattuck, D. W., Chiang, M. C., Barysheva, M., McMahon, K. L., De Zubicaray, G. I., Meredith, M., ... & Thompson, P. M. (2008, September). Visualization tools for high angular resolution diffusion imaging. In International conference on medical image computing and computer-assisted intervention (pp. 298-305). Springer, Berlin, Heidelberg.

Shayman, C. S., Seo, J. H., Oh, Y., Lewis, R. F., Peterka, R. J., & Hullar, T. E. (2018). Relationship between vestibular sensitivity and multisensory temporal integration. *Journal of Neurophysiology*, *120*(4), 1572-1577.

Shedden, J.M., Grundy, J.G. & Mohrenschildt, M.v. (September 2012). Measuring ERPs in an immersive virtual reality motion simulator: Tracking visual targets correlated with self-motion. Cognitive Seminar, McMaster University.

Sheppard, J. P., Raposo, D., & Churchland, A. K. (2013). Dynamic weighting of multisensory stimuli shapes decision-making in rats and humans. *Journal of Vision*, *13*(6), 4-4.

Shim, D. B., Song, M. H., & Park, H. J. (2018). Typical sensory organization test findings and clinical implication in acute vestibular neuritis. *Auris Nasus Larynx, 45*(5), 916-921.

Shin, J. (2010). Passive rotation-induced theta rhythm and orientation homeostasis response. *Synapse, 64*(5), 409-415.

Siegel, M., Donner, T. H., & Engel, A. K. (2012). Spectral fingerprints of large-scale neuronal interactions. *Nature Reviews Neuroscience, 13*(2), 121.

Singer, W., & Gray, C. M. (1995). Visual feature integration and the temporal correlation hypothesis. *Annual Review of Neuroscience, 18*(1), 555-586.

Smedal, H., Rogers, T., Duane, T., Holden, G., & Smith, J. (1963). The physiological limitations of performance during acceleration. *Aerospace Medicine, 34*, 48-55.

Sochůrková, D., Rektor, I., Jurák, P., & Stančák, A. (2006). Intracerebral recording of cortical activity related to self-paced voluntary movements: a Bereitschaftspotential and event-related desynchronization/synchronization. SEEG study. *Experimental Brain Research, 173*(4), 637-649.

Solis-Escalante, T., Müller-Putz, G. R., Pfurtscheller, G., & Neuper, C. (2012). Cue-induced beta rebound during withholding of overt and covert foot movement. *Clinical Neurophysiology, 123*(6), 1182-1190.

Souman, J. L., Frissen, I., Sreenivasa, M. N., & Ernst, M. O. (2009). Walking straight into circles. *Current Biology, 19*(18), 1538-1542.

Spence, C. (2002). Multisensory attention and tactile information-processing. *Behavioural Brain Research, 135*(1-2), 57-64.

Spence, C., Baddeley, R., Zampini, M., James, R., & Shore, D. I. (2003). Multisensory temporal order judgments: When two locations are better than one. *Perception & Psychophysics, 65*(2), 318-328.

Spence, C., & Driver, J. (2000). Attracting attention to the illusory location of a sound: reflexive crossmodal orienting and ventriloquism. *Neuroreport, 11*(9), 2057-2061.

Spence, C., & Santangelo, V. (2009). Capturing spatial attention with multisensory cues: A review. *Hearing research, 258*(1-2), 134-142.

Spinks, R. L., Kraskov, A., Brochier, T., Umilta, M. A., & Lemon, R. N. (2008). Selectivity for grasp in local field potential and single neuron activity recorded simultaneously from M1 and F5 in the awake macaque monkey. *Journal of Neuroscience, 28*(43), 10961-10971.

Srinivasan, R., Nunez, P. L., Tucker, D. M., Silberstein, R. B., & Cadusch, P. J. (1996). Spatial sampling and filtering of EEG with spline laplacians to estimate cortical potentials. *Brain Topography, 8*(4), 355-366.

St. George, R. J., & Fitzpatrick, R. C. (2011). The sense of self-motion, orientation and balance explored by vestibular stimulation. *The Journal of Physiology, 589*(4), 807-813.

Stančák Jr, A., Feige, B., Lücking, C. H., & Kristeva-Feige, R. (2000). Oscillatory cortical activity and movement-related potentials in proximal and distal movements. *Clinical Neurophysiology, 111*(4), 636-650.

Stancák Jr, A., & Pfurtscheller, G. (1995). Desynchronization and recovery of β rhythms during brisk and slow self-paced finger movements in man. *Neuroscience Letters, 196*(1-2), 21-24.

Stancák Jr, A., & Pfurtscheller, G. (1996). Event-related desynchronisation of central beta-rhythms during brisk and slow self-paced finger movements of dominant and nondominant hand. *Cognitive Brain Research, 4*(3), 171-183.

Stanford, T. R., & Stein, B. E. (2007). Superadditivity in multisensory integration: putting the computation in context. *Neuroreport, 18*(8), 787-792.

Stephan, T., Deutschländer, A., Nolte, A., Schneider, E., Wiesmann, M., Brandt, T., & Dieterich, M. (2005). Functional MRI of galvanic vestibular stimulation with alternating currents at different frequencies. *Neuroimage, 26*(3), 721-732.

Sterman, M. B., & Egner, T. (2006). Foundation and practice of neurofeedback for the treatment of epilepsy. *Applied Psychophysiology and Biofeedback, 31*(1), 21.

Storzer, L., Butz, M., Hirschmann, J., Abbasi, O., Gratkowski, M., Saupe, D., ... & Dalal, S. S. (2016). Bicycling and walking are associated with different cortical oscillatory dynamics. *Frontiers in Human Neuroscience, 10*, 61.

Suzuki, M., Kitano, H., Ito, R., Kitanishi, T., Yazawa, Y., Ogawa, T., ... & Kitajima, K. (2001). Cortical and subcortical vestibular response to caloric stimulation detected by functional magnetic resonance imaging. *Cognitive Brain Research, 12*(3), 441-449.

Szurhaj, W., Derambure, P., Labyt, E., Cassim, F., Bourriez, J. L., Isnard, J., ... & Mauguière, F. (2003). Basic mechanisms of central rhythms reactivity to preparation and execution of a voluntary movement: a stereoelectroencephalographic study. *Clinical Neurophysiology, 114*(1), 107-119.

Takahashi, K., Saleh, M., Penn, R. D., & Hatsopoulos, N. (2011). Propagating waves in human motor cortex. *Frontiers in Human Neuroscience, 5*, 40.

Tallon-Baudry, C., & Bertrand, O. (1999). Oscillatory gamma activity in humans and its role in object representation. *Trends in Cognitive Sciences, 3*(4), 151-162.

Tallon-Baudry, C., Bertrand, O., Delpuech, C., & Pernier, J. (1997). Oscillatory γ-band (30–70 Hz) activity induced by a visual search task in humans. *Journal of Neuroscience, 17*(2), 722-734.

Talsma, D., Doty, T. J., & Woldorff, M. G. (2007). Selective attention and audiovisual integration: is attending to both modalities a prerequisite for early integration?. *Cerebral Cortex, 17*(3), 679-690.

Talsma, D., Senkowski, D., Soto-Faraco, S., & Woldorff, M. G. (2010). The multifaceted interplay between attention and multisensory integration. *Trends in Cognitive Sciences, 14*(9), 400-410.

Talsma, D., & Woldorff, M. G. (2005). Selective attention and multisensory integration: multiple phases of effects on the evoked brain activity. *Journal of Cognitive Neuroscience, 17*(7), 1098-1114.

Tang, X., Wu, J., & Shen, Y. (2016). The interactions of multisensory integration with endogenous and exogenous attention. *Neuroscience & Biobehavioral Reviews, 61*, 208-224.

Telford, L., Seidman, S.H, & Paige, G.D. (1997). Dynamics of squirrel monkey linear vestibuloocular reflex and interactions with fixation distance. *Journal of Neurophysiology, 78*, 1775-1790.

Tiitinen, H. T., Sinkkonen, J., Reinikainen, K., Alho, K., Lavikainen, J., & Näätänen, R. (1993). Selective attention enhances the auditory 40-Hz transient response in humans. *Nature, 364*(6432), 59-60.

Todd, N. P. M., Rosengren, S. M., & Colebatch, J. G. (2008). A source analysis of short-latency vestibular evoked potentials produced by air-and bone-conducted sound. *Clinical Neurophysiology, 119*(8), 1881-1894.

Tokumaru, O., Kaida, K., Ashida, H., Yoneda, I., & Tatsuno, J. (1999). EEG topographical analysis of spatial disorientation. *Aviation, Space, and Environmental Medicine, 70*(3 Pt 1), 256-263.

Tolman, E. C. (1948). Cognitive maps in rats and men. *Psychological Review, 55*(4), 189.

Tombini, M., Zappasodi, F., Zollo, L., Pellegrino, G., Cavallo, G., Tecchio, F., ... & Rossini, P. M. (2009). Brain activity preceding a 2D manual catching task. *Neuroimage, 47*(4), 1735-1746.

Toth, K., Freund, T. F., & Miles, R. (1997). Disinhibition of rat hippocampal pyramidal cells by GABAergic afferents from the septum. *The Journal of Physiology, 500*(2), 463-474.

Town, S. M., Brimijoin, W. O., & Bizley, J. K. (2017). Egocentric and allocentric representations in auditory cortex. *PLoS Biology, 15*(6), e2001878.

Townsend, B., Legere, J.K., Mohrenschildt, M. V., & Shedden, J.M. (2022). Beta-band power is an index of multisensory weighting during self-motion perception. *NeuroImage: Reports, 2*, 100102.

Townsend, B., Legere, J. K., O'Malley, S., Mohrenschildt, M. V., & Shedden, J. M. (2019). Attention modulates event-related spectral power in multisensory self-motion perception. *NeuroImage, 191*, 68-80.

Townsend, B., O'Malley, S., Legere, J., v. Mohrenschildt, M., & Shedden, J.M. (2015, June). Electrophysiological correlates of self-motion perception. In J.R. Schoenherr (chair), *Cognition and Applications I*. Symposium conducted at the 25th Annual Meeting of Canadian Society for Brain, Behaviour, and Cognitive Science.

Treisman, A., & Geffen, G. (1967). Selective attention: Perception or response?. Quarterly *Journal of Experimental Psychology, 19*(1), 1-17.

Treisman, A. M., & Gelade, G. (1980). A feature-integration theory of attention. *Cognitive Psychology, 12*(1), 97-136.

Tremblay, L., Elliott, D., & Starkes, J. L. (2004). Gender differences in perception of self-orientation: Software or hardware?. *Perception, 33*(3), 329-337.

Tuladhar, A. M., Huurne, N. T., Schoffelen, J. M., Maris, E., Oostenveld, R., & Jensen, O. (2007). Parieto-occipital sources account for the increase in alpha activity with working memory load. *Human Brain Mapping, 28*(8), 785-792.

Turton, A. J., Dewar, S. J., Lievesley, A., O'Leary, K., Gabb, J., & Gilchrist, I. D. (2009). Walking and wheelchair navigation in patients with left visual neglect. *Neuropsychological rehabilitation, 19*(2), 274-290.

Tzagarakis, C., Ince, N. F., Leuthold, A. C., & Pellizzer, G. (2010). Beta-band activity during motor planning reflects response uncertainty. *Journal of Neuroscience, 30*(34), 11270-11277.

Valerio, S., & Taube, J. S. (2012). Path integration: how the head direction signal maintains and corrects spatial orientation. *Nature Neuroscience, 15*(10), 1445-1453.

Vallar, G., Guariglia, C., & Rusconi, M. L. (1997). *Modulation of the neglect syndrome by sensory stimulation*. In P. Thier & H.-O. Karnath (Eds.), Parietal lobe contributions to orientation in 3D space (pp. 555–578). Heidelberg: Springer-Verlag

Vallar, G., Lobel, E., Galati, G., Berthoz, A., Pizzamiglio, L., & Le Bihan, D. (1999). A fronto-parietal system for computing the egocentric spatial frame of reference in humans. *Experimental Brain Research, 124*(3), 281-286.

Van Elk, M., Van Schie, H. T., Van Den Heuvel, R., & Bekkering, H. (2010). Semantics in the motor system: motor-cortical beta oscillations reflect semantic knowledge of end-postures for object use. *Frontiers in Human Neuroscience, 4*, 8.

Van Kerkoerle, T., Self, M. W., Dagnino, B., Gariel-Mathis, M. A., Poort, J., Van Der Togt, C., & Roelfsema, P. R. (2014). Alpha and gamma oscillations characterize feedback and feedforward processing in monkey visual cortex. *Proceedings of the National Academy of Sciences, 111*(40), 14332-14341.

Varghese, J. P., Marlin, A., Beyer, K. B., Staines, W. R., Mochizuki, G., & McIlroy, W. E. (2014). Frequency characteristics of cortical activity associated with perturbations to upright stability. *Neuroscience letters*, *578*, 33-38.

Varghese, J. P., McIlroy, R. E., & Barnett-Cowan, M. (2017). Perturbation-evoked potentials: Significance and application in balance control research. *Neuroscience & Biobehavioral Reviews*, *83*, 267-280.

Vass, L. K., & Epstein, R. A. (2013). Abstract representations of location and facing direction in the human brain. *Journal of Neuroscience, 33*(14), 6133-6142.

Vertes, R. P., & Kocsis, B. (1997). Brainstem-diencephalo-septohippocampal systems controlling the theta rhythm of the hippocampus. *Neuroscience, 81*(4), 893-926.

Vibell, J., Klinge, C., Zampini, M., Spence, C., & Nobre, A. C. (2007). Temporal order is coded temporally in the brain: early event-related potential latency shifts underlying prior entry in a cross-modal temporal order judgment task. *Journal of Cognitive Neuroscience, 19*(1), 109-120.

Vilhelmsen, K., van der Weel, F.R., & van der Meer, A.L.H. (2015). A high-density EEG study of differences between three high speeds of simulated forward motion from optic flow in adult participants. *Frontiers in Systems Neuroscience.*

von Stein, A., Chiang, C., & König, P. (2000). Top-down processing mediated by interareal synchronization. *Proceedings of the National Academy of Sciences, 97*(26), 14748-14753.

Wagner, A. R., Akinsola, O., Chaudhari, A. M., Bigelow, K. E., & Merfeld, D. M. (2021). Measuring vestibular contributions to age-related balance impairment: A review. *Frontiers in Neurology, 12*, 99.

Walker, S., Monto, S., Piirainen, J. M., Avela, J., Tarkka, I. M., Parviainen, T. M., & Piitulainen, H. (2020). Older age increases the amplitude of muscle stretch-induced cortical beta-band suppression but does not affect rebound strength. *Frontiers in Aging Neuroscience, 12*, 117.

Wall, M. B., & Smith, A. T. (2008). The representation of egomotion in the human brain. *Current biology, 18*(3), 191-194.

Warren, W., & Kurtz, K. (1992). The role of central and peripheral vision in perceiving the direction of self-motion. *Perception & Psychophysics, 51*, 443-454.

Watson, S. R., Brizuela, A. E., Curthoys, I. S., Colebatch, J. G., MacDougall, H. G., & Halmagyi, G. M. (1998). Maintained ocular torsion produced by bilateral and unilateral galvanic (DC) vestibular stimulation in humans. *Experimental Brain Research, 122*(4), 453-458.

Welday, A. C., Shlifer, I. G., Bloom, M. L., Zhang, K., & Blair, H. T. (2011). Cosine directional tuning of theta cell burst frequencies: evidence for spatial coding by oscillatory interference. *Journal of Neuroscience, 31*(45), 16157-16176.

Welgampola, M. S., Ramsay, E., Gleeson, M. J., & Day, B. L. (2013). Asymmetry of balance responses to monaural galvanic vestibular stimulation in subjects with vestibular schwannoma. *Clinical Neurophysiology, 124*(9), 1835-1839.

Wheaton, L., Fridman, E., Bohlhalter, S., Vorbach, S., & Hallett, M. (2009). Left parietal activation related to planning, executing and suppressing praxis hand movements. *Clinical Neurophysiology, 120*(5), 980-986.

Wilson, V., & Melvill Jones, G. (1979). *Mammalian Vestibular Physiology*. New York, USA: Premium Press.

Wong, S. C. P., & Frost, B. J. (1978). Subjective motion and acceleration induced by the movement of the observer's entire visual field. *Perception & Psychophysics, 24*, 115-120.

Woolrich, M., Mullinger, K. J., Francis, S. T., Brookes, M. J., Quinn, A. J., Fry, A., & Pakenham, D. O. (2019). Post-stimulus beta responses are modulated by task duration. *NeuroImage*, 206.

Wu, J., Li, Q., Bai, O., & Touge, T. (2009). Multisensory interactions elicited by audiovisual stimuli presented peripherally in a visual attention task: a behavioral and event-related potential study in humans. *Journal of Clinical Neurophysiology, 26*(6), 407-413.

Wu, J., Yang, J., Yu, Y., Li, Q., Nakamura, N., Shen, Y., ... & Abe, K. (2012). Delayed audiovisual integration of patients with mild cognitive impairment and Alzheimer's disease compared with normal aged controls. *Journal of Alzheimer's Disease, 32*(2), 317-328.

Yao, D., Wang, L., Arendt-Nielsen, L., & Chen, A. C. (2007). The effect of reference choices on the spatio-temporal analysis of brain evoked potentials: the use of infinite reference. *Computers in Biology and Medicine, 37*(11), 1529-1538.

Yakubovich, S., Israeli-Korn, S., Halperin, O., Yahalom, G., Hassin-Baer, S., & Zaidel, A. (2020). Visual self-motion cues are impaired yet overweighted during visual–vestibular integration in Parkinson's disease. *Brain Communications, 2*(1).

Yordanova, J., Kolev, V., & Polich, J. (2001). P300 and alpha event-related desynchronization (ERD). *Psychophysiology, 38*(1), 143-152.

Young, L. R., & Oman, C. M. (1969). Model for vestibular adaptation to horizontal rotation. *Aerospace Medicine, 40*(10), 1076-1080.

Zaitsev, M., Akin, B., LeVan, P., & Knowles, B. R. (2017). Prospective motion correction in functional MRI. *Neuroimage, 154*, 33-42.

Zhu, H., Tang, X., Wei, W., Mustain, W., Xu, Y., & Zhou, W. (2011). Click-evoked responses in vestibular afferents in rats. *Journal of Neurophysiology, 106*(2), 754-763.